IN THE UNITED STATES PATENT AND TRADEMARK OFFICE

Applicant.
Serial No ·
Filing Date:
For:

Docket No.:
Group Art Unit:
Examiner:

DECLARATION OF SHERMAN FONG, Ph.D. UNDER 37 C.F.R. § 1.132

Commissioner for Patents
P.O. Box 1450
Alexandria, VA 22313-1450

Sir:

I, Sherman Fong, Ph.D. declare and say as follows: -

1. I am an inventor of the above-identified patent application.

2. I was awarded a Ph.D. in Microbiology by the University of California at Davis, CA in 1975.

3. After postdoctoral training and holding various research positions at Scripps Clinic and Research Foundation, La Jolla, CA, I joined Genentech, Inc., South San Francisco, CA in 1987. I am currently a Senior Scientist at the Department of Immunology/Discovery Research of Genentech, Inc.

4. My scientific Curriculum Vitae is attached to and forms part of this Declaration.

5. I am familiar with the skin vascular permeability assay (Assay #64), which has been used by me and others under my supervision, to test the activities of novel polypeptides discovered in Genentech's Secreted Protein Discovery Initiative project.

6. The skin vascular permeability assay, is also known in the art as the Miles assay and was first described by Miles and Miles in 1952 when they studied vascular responses to histamine (Miles A.A., and Miles E.M., J. Physiol., 1952, 118: 228-257, see **Exhibit A**). Since then it has been reliably used for identifying proinflammatory molecules.

7. Proinflammatory molecules can directly or indirectly cause vascular permeability by causing immune cells to exit from the blood stream and move to the site of injury or infection. These proinflammatory molecules recruit cells like leukocytes which includes monocytes, macrophages,

basophils, and eosinophils. These cells secrete a range of cytokines which further recruit and activate other inflammatory cells to the site of injury or infection. How leukocytes exit the vasculature and move to their appropriate destination of injury or infection is critical and is tightly regulated. Leukocytes move from the blood vessel to injured or inflamed tissues by rolling along the endothelial cells of the blood vessel wall and then extravasate through the vessel wall and into the tissues (see **Exhibit B**). This diapedesis and extravasation step involves cell activation and a stable leukocyte-endothelial cell interaction

8. Hence, proinflammatory molecules are useful in treating infections, as local administration of the proinflammatory polypeptide would stimulate immune cells already present at the site of infection and induce more immune cells to migrate to the site, thus removing the infection at a faster rate. Examples of proinflammatory molecules that induce neutrophils to extravasate are MIP-1 and MIP-2. Other proinflammatory may be able to activate immune cells, as shown with the CXC chemokines activation of neutrophils, and the non-CXC chemokines which are chemotactic for T lymphocytes (Baggiolini *et al.*, Adv Immunology 1994; 55-97-179 see **Exhibit C**).

Inappropriate expression of proinflammatory molecules may cause an abnormal immune cell reponse and lead tissue destruction. Examples of such abnormal immune reponses include at least the following conditions: psoriasis, inflammatory bowel disease, renal disease, arthritis, immune-mediated alopecia, stroke, encephalitis, Multiple Sclerosis, hepatitis, and others. Therefore, inhibitors of such proinflammatory molecules find use in the treatment of these conditions. Further, proinflammatory molecules with angiostatic properties are useful in the inhibition of angiogenesis during abnormal wound healing or abnormal inflammation during infection. Further, proinflammatory molecules that are also angiostatic are useful in treating tumors, by inhibiting the neovascularization that accompanies tumor growth (Strieter RM. *et al.*, J. Biol. Chem. 1995; 270: 27348-27357 see **Exhibit D**). Administration of the proinflammatory polypeptide, either alone or in combination with another angiostatic factor such as anti-VEGF, would be useful for limiting or reducing tumor growth.

9. The Skin Vascular Permeability Assay was used to identify such proinflammatory and immune related molecules. Miles and Miles described this assay initially in 1952, in their work on vascular response to histamine (Miles A.A., and Miles E.M., J. Physiol. 1952; (118) 228-257 *supra*). Miles and Miles solved the critical variables in the assay, such as performing the intradermal injection, where to inject, effects of temperature, effects of dosage, and effects of anesthetic used. Using this assay, Miles and Miles proved that histamine increased the capillary permeability in the skin, thus allowing cells to exit the vasculature. The assay was used qualitatively until other investigators quantitated it by

extracting the amount of accumulated marker dye and measuring its absorbance at 620 nm (Udaka et al., Proc Soc Exp Biol Med 1970; (133) 1384-1387 see **Exhibit E**).

10. The Skin Vascular permeability assay was used in the clinic in determining if blood coagulation factor XIII (FXIII) could be used in treating Shonlein Henoch Purpura (SHP) (Hirahara K., et al., Thrombosis Res 1993; 71(2) 139-148 see **Exhibit F**). SHP is an immunovascular disease, characterized by hemorrhagic skin lesions, gastro-intestinal bleeding and hematuria. The physiology of SHP was undetermined, but destruction of FXIII by leukocytes that migrated into the area and secreted destructive proteases was believed to play a role. This hypothesis was tested by using antibodies raised to guinea pig endothelial cells. These antibodies were specific for endothelial cells and not for fibroblasts, and when injected into the skin of a guinea pig, caused increased vascular permeability. When FXIII was mixed with this antibody and injected, the marker dye showed less spreading, indicating that FXIII was suppressing the vascular permeability and did so in a dose dependant manner. The conclusion was that FXIII was stabilizing the microvasculature, leading to less permeability, and therefore FXIII may be useful in the treatment of SHP.

11. The Skin Vascular Permeability assay has been confirmed by alternate experimental methods. Senger et al., used the Skin Vascular Permeability assay as described by Miles and determined that a secreted factor they called VPF (later determined to be VEGF), caused vascular permeability (Senger D.R., et al., Science 1983; (219) 983-985 see **Exhibit G**). In these experiments VPF was subjected to the Skin Vascular Permeability assay, the sites of injection were analyzed by light and electron microscopy and VPF caused vascular permeability without damaging endothelial cells or causing mast cell degranulation.

12. Yeo et al., confirmed the viability of the Skin Vascular Permeability assay by correlating it with disassociation enhanced lanthanide fluoroimmunoassay (DELFIA) results (Yeo K.T., Clin. Chem 1992; (38) 71-75 see **Exhibit H**). VPF (VEGF) was first measured using the Skin Vascular Permeability assay by quantifiying the amount of accumulated dye in the skin as described in Udaka et al., (supra). Anti-VPF antibodies were used to quantitate the amount of VPF in the DELFIA. This assay has increased sensitivity as the result is read by a fluorometer, instead of dye absorbance. The investigators found that the sensitivity of the DELFIA was greater than the Skin Vascular Permeability assay, but there was an excellent linear correlation (r^2= 0.94) between the two assays.

13. The Applicant's Skin Vascular Permeability assay was conducted using anesthetized Hairless guinea pigs. A sample of a purified PRO polypeptide or a conditioned media test sample was injected intradermally onto the backs of the test animals with 100 µL per injection site. It was possible to have up to about 24 injection sites per animal. One mL of Evans Blue dye (1% in physiologic buffered saline), was injected intracardially as the marker dye. Blemishes at the injection sites were then measured (mm diameter) after 1 hr, 6 hrs and 24 hrs post injection. Animals were sacrificed at the appropriate time after injection, and each skin injection site was biopsied and fixed in paraformaldehyde. The biopsies were then prepared for histopathalogic evaluation. Each site was evaluated for inflammatory cell infiltration into the skin. Sites with visible inflammatory cell inflammation were scored as positive. Polypeptides tested stimulated an immune response and induced mononuclear cell, eosinophil and PMN infiltration at the site of injection of the animal. Perivascular infiltrate at the injection site was scored as positive; no infiltrate at the site of injection is scored as negative.

An example of a positive reaction is shown in **Exhibit I**. The top row is injected with Interleukin-8 (IL-8) control and shows no increased vascular permeability. The 2nd row from the top is VEGF as a positive control. The 2 bottom rows show a positive result from a PRO polypeptide, performed in duplicate.

14. It is my opinion that the PRO polypeptide that shows activity in the Skin Vascular permeability assay has specific, substantial and credible utilities. In the experiments performed in the instant application, the results of the skin vascular permeability assay were further analyzed by histopathological examination to rule out inflammation due to endothelial cell damage or mast cell degranulation. Hence, the vascular permeability observed was not due to histamine release or endothelial cell damage. Examples of utilities include, enhancing immune cell recruitment to sites of injury or infection, or inhibitors to treat autoimmune diseases such as psoriasis etc. as discussed above. Furthermore, the angiogenic or angiostatic properties of proinflammatory molecules would also find practical utility in controlling tumorigenesis.

15. I declare further that all statements made in this Declaration of my own knowledge are true and that all statements made on information and belief are believed to be true and further, that these statements are made with the knowledge that willful statements and the like so made are punishable by fine or imprisonment, or both, under Section 1001 of Title 18 of the United States Code and that such willful false statements may jeopardize the validity of the application or any patent granted thereon.

Date: 8/27/04

By: Sherman Fong

Sherman Fong, Ph.D.

Sherman Fong, Ph.D.

Senior Scientist
Department of Immunology
Genentech Inc.
1 DNA Way.
South San Francisco, California 94080-4990

19 Basinside Way
Alameda, California 94502

Work Telephone: (650) 225-2783
Home Telephone: (510) 522-5411
FAX: (650) 225-8221

Education:

1978 - 1980 Postdoctoral Fellow in Immunology, Research Institute of Scripps Clinic, Scripps Clinic and Research Foundation, La Jolla, California

1975 - 1978 Postdoctoral Fellow in Immunology, University of California at San Francisco, San Franciso, California

1970 - 1975 Ph.D. in Microbiology, University of California at Davis, California

1966 - 1970 B.A. in Biology/Microbiology, San Francisco State University, San Francisco, California

Professional Positions:
Currently: Senior Scientist, Department of Immunology/Discovery Research, Genentech, Inc., South San Francisco, California

8/00-8/01 Acting Director, Department of Immunology, Genentech, Inc. South San Francisco, California

10/89 Senior Scientist in the Department of Immunology/Discovery Research, Genentech, Inc. South San Francisco, California

3/89 - 10/89 Senior Scientist and Immunobiology Group Leader, Department of Pharmacological Sciences, Immunobiology Section/Medical Research and Development, Genentech, Inc., S. San Francisco, California

9/87 - 3/89 Scientist, Department of Pharmacological Sciences, Immunopharmacology Section/Medical Research and Development, Genentech, Inc., S. San Francisco, California

1/82 - 9/87 Assistant Member (eq. Assistant Professor level), Department of Basic and Clinical Research, Division of Clinical Immunology, Scripps Clinic and Research Foundation, La Jolla, California

6/80 - 12/81 Scientific Associate in the Department of Clinical Research, Division of Clinical Immunology, Scripps Clinic and Research Foundation, La Jolla, California

7/78 - 6/80 Postdoctoral training in the laboratory of Dr. J. H. Vaughan, Chairman, Department of Clinical Research, Division of Clinical Immunology, Scripps Clinic and Research Foundation, La Jolla, California

2/75 - 6/78 Postdoctoral training in the laboratory of Dr. J. W. Goodman, Department of Microbiology and Immunology, School of Medicine, University of California, San Francisco, California

7/71 - 12/74 Research Assistant and Graduate Student, Department of Medical Microbiology, School of Medicine, University of California, Davis, California, under Dr. E. Benjamini

Awards:
Recipient: National Institutes of Health Postdoctoral Fellowship Award (1975).

Recipient: Special Research Award, (New Investigator Award), National Institute of Health (1980).

Recipient: P.I., Research Grant Award, National Institute of Health (1984).

Recipient: Research Career Development Award (R01), National Institutes of Health (1985).

Recipient: P.I., Multi-Purpose Arthritis Center Resarch Grant, NIH (1985)

Recipient: P.I., Resarch Grant Award, (R01 Renewal), National Institute of Health (1987).

Scientific Associations:

Sigma Xi, University of California, Davis, California Chapter

Member, The American Association of Immunologists

Committee Service and Professional Activities:

Member of the Immunological Sciences Study Section, National Institutes of Health Research Grant Review Commitee, (1988-1992).

Advisory Committee, Scientific Review Committee for Veteran's Administration High Priority Program on Aging, 1983.

Ad Hoc member of Immunological Sciences Study Section, National Institutes of Health, 1988.

Ad Hoc Reviewer: Journal of Clinical Investigations, Journal of Immunology, Arthritis and Rheumatism, International Immunology, Molecular Cell Biology, and Gastroenterology

Biotechnology Experience

Established at Genentech in 1987-1989 within the Immunobiology Laboratory, in the Department of Pharmcological Sciences, group to study the immunogenicity of recombinant hGH (Protropin®) in hGH transgenic mice.

Served as Immunologist on the **Biochemical Subteam for Protropin® Project** team.

Served as Immunologist on the **Met-less hGH and Dnase project teams**, two FDA approved biological drugs: second generation hGH Nutropin® and Pulmozyme® (DNase).

Served immunologist in1989-1990 on the **CD4-IgG project team** carrying out in vitro immunopharmacological studies of the effects of CD4-IgG on the in vitro human immune responses to mitogens and antigens and on neutrophil responses in support of the filing of IND to FDA in 1990 for use of CD4-IgG in the prevention of HIV infection. Product was dropped.

In 1989-1991, initiated and carried research and development work on antibodies to CD11b and CD18 chains of the leukocyte β2 integrins. Provided preclinical scientific data to **Anti-CD18 project team**

supporting the advancement of humanized anti-CD18 antibody as anti-inflammatory in the acute setting. IND filed in 1996 and currently under clinical evaluation.

1993-1997, **Research Project Team leader** for small molecule $\alpha4\beta1$ integrin antagonist project. Leader for collaborative multidisciplinary team (N=11) composed of immunologists, molecular/cell biologists, protein engineers, pathologists, medicinal chemists, pharmacologists, pharmaceutical chemists, and clinical scientists targeting immune-mediated chronic inflammatory diseases. Responsible for research project plans and execution of strategy to identify lead molecules, assessment of biological activities, preclinical evaluation in experimental animals, and identification of potential clinical targets. Responsible for identification, hiring, and working with outside scientific consultants for project. Helped established and responsible for maintaining current research collaboration with Roche-Nutley. Project transfered to Roche-Nutley.

1998-present, worked with Business Development to identify and create joint development opportunity with LeukoSite (currently Millennium) for monoclonal antibody against $\alpha4\beta7$ intergin (LDP-02) for therapeutic treatment for inflammatory bowel disease (UC and Crohn';s disease). Currently, working as scientific advisor to the core team for phase II clinical trials for LDP-02.

Currently, **Research Project Team Biology Leader** (1996-present) for small molecule antagonists for $\alpha4\beta7$/MAdCAM-1 targeting the treatment of human inflammatory bowel diseases and diseases of the gastrointestinal tract. Responsible for leading collaborative team (N=12) from Departments of Immunology, Pathology, Analytical Technology, Antibody Technology, and Bio-Organic Chemistry to identify and evaluate lead drug candidates for the treatment of gastrointestinal inflammatory diseases.

Served for nearly fifteen years as **Ad Hoc reveiwer** on Genentech Internal Research Review Committee, Product Development Review Committee, and Pharmacological Sciences Review Committee.

Worked as Scientific advisor with staff of the **Business Development** Office on numerous occasions at Genentech, Inc. to evaluate the science of potential in-licensing of novel technologies and products.

2000-2001 Served as Research Discovery representative on Genentech Therapeutic Area Teams (Immunology/Endocrine, Pulmonary/Respiratory Disease Task Force)

Invited Symposium Lectures:

Session Chairperson and speaker, American Aging Association 12th Annual National Meeting, San Francisco, California, 1982.

Invited Lecturer, International Symposium, Mediators of Immune Regulation and Immunotherapy, University of Western Ontario, London, Ontario, Canada, 1985.

Invited Lecturer, workshop on Human IgG Subclasses, Rheumatoid Factors, and Complement. American Association of Clinical Chemistry, San Francisco, California, 1987.

Plenary Lecturer, First International Waaler Conference on Rheumatoid Factors, Bergen, Norway, 1987.

Invited Lecturer, Course in Immunorheumatology at the Universite aux Marseilles, Marseilles, France, 1988.

Plenary Lecturer, 5th Mediterranean Congress of Rheumatology, Istanbul, Turkey, 1988.

Invited Lecturer, Second Annual meeting of the Society of Chinese Bioscientist of America, University of California, Berkeley, California, 1988.

Lecturer at the inaugural meeting of the Immunology by the Bay sponsored by The Bay Area Bioscience Center. The β2 Integrins in Acute Inflammation, July 14, 1992.

Lecturer, "Research and Development -- An Anatomy of a Biotechnology Company", University of California, Berkeley, Extension Course, given twice a year--March 9, 1995 to June 24, 1997.

Lecturer, "The Drug Development Process – Biologic Research - Genomics", University of California, Berkeley Extension, April 21, 1999, October, 1999, April 2000, October, 2000.

Lecturer, "The Drug Development Process – Future Trends/Impact of Pharmacogenomics", University of California Berkeley Extension, April 2001, October 2001, April 2002.

Invited Speaker, "Targeting of Lymphocyte Integrin α4β7 Attentuates Inflammatory Bowel Diseases", in Sympoium on "Nutrient effects on Gene Expression" at the Institute of Food Technology Symposium, June, 2002.

Patents:

Dennis A. Carson, Sherman Fong, Pojen P. Chen.
U.S. Patent Number 5,068,177: Anti-idiotype Antibodies induced by Synthetic Polypeptides, Nov. 26, 1991

Sherman Fong, Caroline A. Hebert, Kyung Jin Kim and Steven R. Leong.
U.S. Patent Number 5,677,426: Anti-IL-8 Antibody Fragments, Oct. 14, 1997

Claire M. Doerschuk, Sherman Fong, Caroline A. Hebert, Kyung Jin Kim, Steven R. Leong. U.S. Patent Number 5,686,070: Methods for Treating Bacterial Pneumonia, Nov. 11, 1997

Claire M. Doerschuk, Sherman Fong, Caroline A. Hebert, Kyung Jin Kim, Steven R. Leong. U.S. Patent 5,702,946: Anti-IL-8 Monoclonal Antibodies for the Treatment of Inflammatory Disorders, Dec. 30, 1997

Sherman Fong, Caroline A. Hebert, Kyung Jin Kim, Steven R. Leong.
U.S. Patent Number 5,707,622: Methods for Treating Ulcerative Colits, Jan. 13, 1998

Sherman Fong, Napoleone Ferrara, Audrey Goddard, Paul Godowski, Austin Gurney, Kenneth Hillan, and Mickey Williams. U.S. Patent Number 6,074,873: Nucleic acids encoding NL-3, June 13, 2000

Sherman Fong, Napoleone Ferrara, Audrey Goddard, Paul Godowski, Austin Gurney, Kenneth Hillan, and Mickey Williams. U.S. Patent Number 6,348,351 B1: The Receptor Tyrosine Kinase Ligand Homologues. February 19, 2002

Patent Applications:

Sherman Fong, Kenneth Hillan, Toni Klassen
U.S. Patent Application: "Diagnosis and Treatment of Hepatic Disorders"

Sherman Fong, Audrey Goddard, Austin Gurney, Daniel Tumas, William Wood
U.S. Patent Application: Compositions and Methods for the Treatment of Immune Related Diseases.

Sherman Fong, Mary Gerritsen, Audrey Goddard, Austin Gurney, Kenneth Hillan, Mickey Williams, William Wood . U.S. Patent Application: Promotion or Inhibition of Cardiovasculogenesis and Angiogenesis

Avi Ashkenazi, Sherman Fong, Audrey Goddard, Austin Gurney, Mary Napier, Daniel Tumas, William Wood. US Patent Application: Compounds, Compositions and Methods for the Treatment of Diseases Characterized by A33-Related Antigens

Chen, Filvaroff, Fong, Goddard, Godowski, Grimaldi, Gurney, Hillan, Tumas, Vandlen, Van Lookeren, Watanabe, Williams, Wood, Yansura
US Patent Application: IL-17 Homologous Polypeptides and Therapeutic Uses Thereof

Ashkenazi, Botstein, Desnoyers, Eaton, Ferrara, Filvaroff, Fong, Gao, Gerber, Gerritsen, Goddard, Godowski, Grimaldi, Gurney, Hillan, Kljavin, Mather, Pan, Paoni, Roy, Stewart, Tumas, Williams, Wood
US Patent Application: Secreted And Transmembrane Polypeptides And Nucleic Acids Encoding The Same

Publications:

1. Scibienski R, Fong S, Benjamini E: Cross tolerance between serologically non-cross reacting forms of egg white lysozyme. J Exp Med 136:1308-1312, 1972.

2. Scibienski R, Harris M, Fong S, Benjamini E: Active and inactive states of immunological unresponsiveness. J Immunol 113:45-50, 1974.

3. Fong S: Studies on the relationship between the immune response and tumor growth. Ph D Thesis, 1975.

4. Benjamini E, Theilen G, Torten M, Fong S, Crow S, Henness AM: Tumor vaccines for immunotherapy of canine lymphosarcoma. Ann NY Acad Sci 277:305, 1976.

5. Benjamini E, Fong S, Erickson C, Leung CY, Rennick D, Scibienski RJ: Immunity to lymphoid tumors induced in syngeneic mice by immunization with mitomycin C treated cells. J Immunol 118:685-693, 1977.

6. Goodman JW, Fong S, Lewis GK, Kamin R, Nitecki DE, Der Balian G: T lymphocyte activation by immunogenic determinants. Adv Exp Biol Med 98:143, 1978.

7. Goodman JW, Fong S, Lewis GK, Kamin R, Nitecki DE, Der Balian G: Antigen structure and lymphocyte activation. Immunol Rev 39:36, 1978.

8. Fong S, Nitecki DE, Cook RM, Goodman JW: Spatial requirements of haptenic and carrier determinants for T-dependent antibody responses. J Exp Med 148:817, 1978.

9. Fong S, Chen PP, Nitecki DE, Goodman JW: Macrophage-T cell interaction mediated by immunogenic and nonimmunogenic forms of a monofunctional antigen. Mol Cell Biochem 25:131, 1979.

10. Tsoukas CD, Carson DA, Fong S, Pasquali J-L, Vaughan JH: Cellular requirements for pokeweed mitogen induced autoantibody production in rheumatoid arthritis. J Immunol 125:1125-1129, 1980.

11. Pasquali J-L, Fong S, Tsoukas CD, Vaughan JH, Carson DA: Inheritance of IgM rheumatoid factor idiotypes. J Clin Invest 66:863-866, 1980.

12. Fong S, Pasquali J-L, Tsoukas CD, Vaughan JH, Carson DA: Age-related restriction of the light chain heterogeneity of anti-IgG antibodies induced by Epstein-Barr virus stimulation of human lymphocytes in vitro. Clin Immunol Immunopathol 18:344, 1981.

13. Fong S, Tsoukas CD, Frincke LA, Lawrance SK, Holbrook TL, Vaughan JH, Carson DA: Age-associated changes in Epstein-Barr virus induced human lymphocyte autoantibody responses. J Immunol 126:910-914, 1981.

14. Tsoukas CD, Fox RI, Slovin SF, Carson DA, Pellegrino M, Fong S, Pasquali J-L, Ferrone S, Kung P, Vaughan JH: T lymphocyte-mediated cytotoxicity against autologous EBV-genome-bearing B cells. J Immunol 126:1742-1746, 1981.

15. Fong S, Tsoukas CD, Pasquali J-L, Fox RI, Rose JE, Raiklen D, Carson DA, Vaughan JH: Fractionation of human lymphocyte subpopulations on immunoglobulin coated petri dishes. J Immunol Methods 44:171-182, 1981.

16. Pasquali J-L, Tsoukas CD, Fong S, Carson DA, Vaughan JH: Effect of Levamisole on pokeweed mitogen stimulation of immunoglobulin production in vitro. Immunopharmacology 3:289-298, 1981.

17. Pasquali J-L, Fong S, Tsoukas CD, Hench PK, Vaughan JH, Carson DA: Selective lymphocyte deficiency in seronegative rheumatoid arthritis. Arthritis Rheum 24:770-773, 1981.

18. Fong S, Fox RI, Rose JE, Liu J, Tsoukas CD, Carson DA, Vaughan JH: Solid- phase selection of human T lymphocyte subpopulations using monoclonal antibodies. J Immunol Methods 46:153-163, 1981.

19. Pasquali J-L, Fong S, Tsoukas CD, Slovin SF, Vaughan JH, Carson DA: Different populations of rheumatoid factor idiotypes induced by two polyclonal B cell activators, pokeweed mitogen and Epstein-Barr virus. Clin Immunol Immunopathol 21:184-189, 1981.

20. Carson DA, Pasquali J-L, Tsoukas CD, Fong S, Slovin SF, Lawrance SK, Slaughter L, Vaughan JH: Physiology and pathology of rheumatoid factors. Springer Semin Immunopathol 4:161-179, 1981.

21. Fox RI, Fong S, Sabharwal N, Carstens SA, Kung PC, Vaughan JH: Synovial fluid lymphocytes differ from peripheral blood lymphocytes in patients with rheumatoid arthritis. J Immunol 128:351-354, 1982.

22. Seybold M, Tsoukas CD, Lindstrom J, Fong S, Vaughan JH: Acetylcholine receptor antibody production during leukoplasmapheresis for Myasthenia Gravis. Arch Neurol 39:433-435, 1982.

23. Tsoukas CD, Fox RI, Carson DA, Fong S, Vaughan JH: Molecular interactions in human T-cell-mediated cytotoxicity to Epstein-Barr virus. I. Blocking of effector cell function by monoclonal antibody OKT3. Cell Immunol 69:113-121, 1982.

24. Sabharwal UK, Vaughan JH, Fong S, Bennett P, Carson DA, Curd JG: Activation of the classical pathway of complement by rheumatoid factors: Assessment by radioimmunoassay for C4. Arthritis Rheum 25:161-167, 1982.

25. Fox RI, Carstens SA, Fong S, Robinson CA, Howell F, Vaughan JH: Use of monoclonal antibodies to analyze peripheral blood and salivary gland lymphocyte subsets in Sjogren's Syndrome. Arthritis Rheum 25:419, 1982.

26. Fong S, Miller JJIII, Moore TL, Tsoukas CD, Vaughan JH, Carson DA: Frequencies of Epstein-Barr virus inducible IgM anti-IgG B lymphocytes in normal children and in children with Juvenile Rheumatoid Arthritis. Arthritis Rheum 25:959-965, 1982.

27. Goodman JW, Nitecki DE, Fong S, Kaymakcalan Z: Antigen bridging in the interaction of T helper cells and B cells. Adv Exp Med Biol 150:219-225, 1982.

28. Goodman JW, Nitecki DE, Fong S, Kaymakcalan Z: Antigen bridging in T cell-B cell interaction: Facts or fiction. In: Protein Conformation as Immunologic Signal. EMBO Workshop, Portonenere, Italy, 1982.

29. Tsoukas CD, Carson DA, Fong S, Slovin SF, Fox RI, Vaughan JH: Lysis of autologous Epstein-Barr virus infected B cells by cytotoxic T lymphocytes of rheumatoid arthritis patients. Clin Immunol Immunopathol 24:8-14, 1982.

30. Fong S, Vaughan JH, Tsoukas CD, Carson DA: Selective induction of autoantibody secretion in human bone marrow by Epstein-Barr virus. J Immunol 129:1941-1945, 1982.

31. Sabharwal UK, Fong S, Hoch S, Cook RD, Vaughan JH, Curd JG: Complement activation by antibodies to Sm in systemic lupus erythematosus. Clin Exp Immunol 51:317-324, 1983.

32. Tsoukas CD, Carson DA, Fong S, Vaughan JH: Molecular interactions in human T cell mediated cytotoxicity to EBV. II. Monoclonal antibody OKT3 inhibits a post-killer-target recognition/adhesion step. J Immunol 129:1421-1425, 1982.

33. Welch MJ, Fong S, Vaughan JH, Carson DA: Increased frequency of rheumatoid factor precursor B lymphocytes after immunization of normal adults with tetanus toxoid. Clin Exp Immunol 51:299-305, 1983.

34. Fong S, Vaughan JH, Carson DA: Two different rheumatoid-factor producing cell populations distinguished by the mouse erythrocyte receptor and responsiveness to polyclonal B cell activators. J Immunol 130:162-164, 1983.

35. Fox RI, Hueniken M, Fong S, Behar S, Royston I, Singhal SK, Thompson L: A novel cell surface antigen (T305) found in increased frequency on acute leukemia cells and in autoimmune disease states. J Immunol 131:762-767, 1983.

36. Fong S: Solid-phase panning for the fractionation of lymphoid cells. In: Cell separation: methods and selected applications. Pretlow TG, Pretlow TP (eds.) pp. 203-219. Academic Press, New York, 1983.

37. Carson DA, Fong S: A common idiotype on human rheumatoid factors identified by a hybridoma antibody. Mol Immunol 20:1081-1087, 1983.

38. Fong S, Gilbertson TA, Carson DA: The internal image of IgG in cross- reactive anti-idiotypic antibodies against human rheumatoid factors.
J Immunol 131:719-724, 1983.

39. Fox RI, Adamson TC, Fong S, Young C, Howell FV: Characterization of the phenotype and function of lymphocytes infiltrating the salivary gland in patients with primary Sjogren syndrome. Diagn Immunol 1:233-239, 1983.

40. Fox RI, Adamson III TC, Fong S, Robinson CA, Morgan EL, Robb JA, Howell FV: Lymphocyte phenotype and function in pseudolymphoma associated with Sjogren's syndrome. J Clin Invest 72:52-62, 1983.

41. Fong S, Gilbertson TA, Chen PP, Vaughan JH, Carson DA: Modulation of human rheumatoid factor-specific lymphocyte responses with a cross- reactive anti-idiotype bearing the internal image of antigen. J Immunol 132:1183-1189, 1984.

42. Chen PP, Houghten RA, Fong S, Rhodes GH, Gilbertson TA, Vaughan JH, Lerner RA, Carson DA: Anti-hypervariable region antibody induced by a defined peptide. A new approach for studying the structural correlates of idiotypes. Proc Natl Acad Sci USA 81:1784-1788, 1984.

43. Fox RI, Fong S, Tsoukas CD, Vaughan JH: Characterization of recirculating lymphocytes in rheumatoid arthritis patients: Selective deficiency of natural killer cells in thoracic duct lymph. J Immunol 132:2883-2887, 1984.

44. Chen PP, Fong S, Normansell D, Houghten RA, Karras JG, Vaughan JH, Carson DA: Delineation of a cross-reactive idiotype on human autoantibodies with antibody against a synthetic peptide. J Exp Med 159:1502-1511, 1984.

45. Fong S, Carson DA, Vaughan JH: Rheumatoid factor. In: Immunology of Rheumatic Diseases. Gupta S, Talal N (eds.): Chapter 6. pp. 167-196. Plenum Publishing Corp., New York, 1985.

46. Fong S: Immunochemistry. In: Immunology as applied to Otolaryngology. Ryan AF, Poliquis JF, Harris A (eds.): pp. 23-53. College Hill Press, San Diego, 1985.

47. Fong S, Chen PP, Vaughan JH, Carson DA: Origin and age-associated changes in the expression of a physiologic autoantibody. Gerontology 31:236-250, 1985.

48. Chen PP, Fong S, Houghten RA, Carson DA: Characterization of an epibody: An anti-idiotype which reacts with both the idiotype of rheumatoid factors (RF) and the antigen recognized by RFs. J Exp Med 161:323, 1985.

49. Chen PP, Goni F, Fong S, Jirik F, Vaughan JH, Frangione B, Carson DA: The majority of human monoclonal IgM rheumatoid factors express a primary structure-dependent cross-reactive idiotype. J Immunol 134:3281-3285, 1985.

50. Lotz M, Tsoukas CD, Fong S, Carson DA, Vaughan JH: Regulation of Epstein- Barr virus infections by recombinant interferon. Selected sensitivity to interferon-gamma. Eur J Immunol 15:520-525, 1985.

51. Chen PP, Kabat EA, Wu TT, Fong S, Carson DA: Possible involvement of human D-minigenes in the first complementarity-determining region of kappa light chains. Proc Natl Acad Sci USA 82:2125-2127, 1985.

52. Goldfien RD, Chen PP, Fong S, Carson DA: Synthetic peptides corresponding to third hypervariable region of human monoclonal IgM rheumatoid factor heavy chains define an immunodominant idiotype. J Exp Med 162:756-761, 1985.

53. Fong S, Chen PP, Gilbertson TA, Fox RI, Vaughan JH, Carson DA: Structural similarities in the kappa light chains of human rheumatoid factor paraproteins and serum immunoglobulins bearing a cross-reactive idiotype. J Immunol 135:1955-1960, 1985.

54. Chen PP, Goni F, Houghten RA, Fong S, Goldfien RD, Vaughan JH, Frangione B, Carson DA: Characterization of human rheumatoid factors with seven antiidiotypes induced by synthetic hypervariable-region peptides. J Exp Med 162:487-500, 1985.

55. Fong S, Gilbertson TA, Hueniken RJ, Singhal SK, Vaughan JH, Carson DA: IgM rheumatoid factor autoantibody and immunoglobulin producing precursor cells in the bone marrow of humans. Cell Immunol 95:157-172, 1985.

56. Fong S, Chen PP, Goldfien RD, Jirik F, Silverman G, Carson DA: Recurrent idiotypes of human anti-IgG autoantibodies: their potential use for immunotherapy. In: Mediators of Immune Regulation and Immunotherapy. Singhal SK, Delovitch TL (eds.): pp. 232-243. Elsevier Science Publishing Co., New York, 1986.

57. Fox RI, Chen PP, Carson DA, Fong S: Expression of a cross reactive idiotype on rheumatoid factor in patients with Sjogren's syndrome. J Immunol 136:477-483, 1986.

58. Jirik FR, Sorge J, Fong S, Heitzmann JG, Curd JG, Chen PP, Goldfien R, Carson DA: Cloning and sequence determination of a human rheumatoid factor light-chain gene. Proc Natl Acad Sci USA, 83:2195-2199, 1986.

59. Lotz M, Tsoukas CD, Fong S, Dinarello CA, Carson DA, Vaughan JH: Release of lymphokines following Epstein-Barr virus infection in vitro. I. The sources and kinetics of production of interferons and interleukins in normal humans. J Immunol, 136:3636-3642, 1986.

60. Lotz M, Tsoukas CD, Fong S, Dinarello CA, Carson DA, Vaughan JH: Release of lymphokines following infection with Epstein-Barr virus in vitro. II. A monocyte dependent inhibitor of interleukin-1 downregulates the production of interleukin-2 and gamma interferon in rheumatoid arthritis. J Immunol, 136:3643-3648, 1986.

61. Fong S, Chen PP, Gilbertson TA, Weber JR, Fox RI, Carson DA: Expression of three cross reactive idiotypes on rheumatoid factor autoantibodies from patients with autoimmune diseases and seropositive adults. J Immunol, 137:122-128, 1986.

62. Fong S, Gilbertson TA, Chen PP, Karras JG, Vaughan JH, Carson DA: The common occurrence of internal image type anti-idiotypic antibodies in rabbits immunized with monoclonal and polyclonal human IgM rheumatoid factors. Clin Exp Immunol, 64:570-580, 1986.

63. Fox RI, Carson DA, Chen P, Fong S: Characterization of a cross reactive idiotype in Sjogren's syndrome. Scand J Rheum S61:83-88, 1986.

64. Silverman GJ, Carson DA, Solomon A, Fong S: Human kappa light chain subgroup analysis with synthetic peptide-induced antisera. J Immunol Methods 95:249-257, 1987.

65. Goldfien R, Chen P, Kipps TJ, Starkebaum G, Heitzmann JG, Radoux V, Fong S, Carson DA: Genetic analysis of human B cell hybridomas expressing a rheumatoid factor-associated cross-reactive idiotype. J Immunol 138:940- 944, 1987.

66. Carson DA, Chen PP, Fox RI, Kipps TJ, Jirik F, Goldfien RD, Silverman G, Radoux V, Fong S: Rheumatoid factors and immune networks. Annu Rev Immunol 5:109-126, 1987.

67. Kipps TJ, Fong S, Tomhave E, Chen PP, Goldfien RD, Carson DA: High frequency expression of a conserved kappa variable region gene in chronic lymphocytic leukemia. Proc Natl Acad Sci USA 84:2916-2920, 1987

68. Fong S, Chen PP, Fox RI, Goldfien RD, Silverman GJ, Radoux V, Jirik F, Vaughan JH, Carson DA: Rheumatoid factors in human autoimmune disease: Their origin, development and function. Path Immunopath Res 5:407-449, 1987.

69. Goldfien RD, Fong S, Chen P, Carson DA: Structure and function of rheumatoid factor: Implications for its role in the pathogenesis of mixed cryoglobulinemia. In: Antiglobulins, cryoglobulins and glomerulonephritis, Proceedings of 2nd International Milano Meeting of Nephrology. Ponticelli C, Minetti L, D'Amico G (eds.) Martinus Nijhoff, Dordrecht pp. 17-27, 1986.

70. Silverman GJ, Carson DA, Patrick K, Vaughan JH, Fong S: Expression of a germline human kappa chain associated cross reactive idiotype after in vitro and in vivo infection with Epstein-Barr virus. Clin Immunol Immunopathol 43:403-411, 1987.

71. Silverman GJ, Fong S, Chen PP, Carson DA: Clinical update: Cross reactive idiotype and the genetic origin of rheumatoid factors. J Clin Lab Anal, 1:129-135, 1987.

72. Chen PP, Fong S, Carson DA: Molecular basis of reactivity of epibodies. In: Elicitation and use of anti-idiotypic antibodies and their biological applications. Bona C (ed.), CRC Press, Boca Raton, Fla, in press.

73. Fong S, Chen PP, Carson DA, Fox, RI: Rheumatoid factor in Sjogren's syndrome. In: Sjogren's Syndrome: Clinical and Immunological Aspects. Talal N, Moutsopoulos HM, Kassan SS (eds.), Springer-Verlag, New York, pp. 203-217, 1987.

74. Chen PP, Fong S, Carson DA: The use of defined peptides in characterizing idiotypes. Int Rev Immunol 2:419-432, 1987.

75. Chen PP, Fong S, Goni F, Houghten RA, Frangione B, Liu F, Carson DA: Analyses of human rheumatoid factors with anti-idiotypes induced by synthetic peptides. Monogr Allergy 22:12-23, 1987.

76. Carson DA, Chen PP, Radoux V, Jirik F, Goldfien RD, Silverman GJ, Fong S: Molecular basis for the cross-reactive idiotypes on human anti-IgG autoantibodies (rheumatoid factors) In: Autoimmunity and Autoimmune Disease. Ciba Foundation Symposium 129 pp. 123-130, 1987.

77. Radoux V, Fong S, Chen PP, Carson DA: Rheumatoid factors: current concepts. In: Advances in Inflammation Research. Lewis, A. (Ed), Raven Press, New York, pp.295-304, 1987.

78. Kipps TJ, Fong S, Chen PP, Miller WE, Piro LD, Carson DA: Immunoglobulin V gene utilization in CLL. In: Chronic lymphocytic leukemia: recent progress and future direction, Alan R Liss, Inc., New York, pp. 115-126, 1987.

79. Fong S, Chen PP, Fox RI, Goldfien RD, Radoux V, Silverman GJ, Crowley JJ, Roudier J, Carson DA: The diversity and idiotypic pattern of human rheumatoid factors in disease. Concepts in Immunopath 5: 168-191, 1988.

80. Fox RI, Fong S, Chen PP, Kipps TJ: Autoantibody production in Sjogren's syndrome: a hypothesis regarding defects in somatic diversification of germline encoded genes. In Vivo 2: 47-56, 1988.

81. Chen PP, Fong S, Goni F, Silverman GJ, Fox RI, Liu M-K, Frangione B, Carson DA: Cross-reacting idiotypes on cryoprecipitating rheumatoid factor. Springer Seminar Series in Immunopath 10: 35-55, 1988.

82. Chen PP, Fong S, Carson DA: Rheumatoid factor. Rheumatic Diseases of North America 13:545-568, 1987.

83. Carson DA, Chen PP, Kipps TJ, Radoux V, Jirik FR, Goldfien RD, Fox RI, Silverman GJ, Fong S. Idioytpic and genetic studies of human rheumatoid factors. Arthritis Rheum 30: 1321-1325, 1987.

84. Fong S, Chen PP, Crowley JJ, Silverman GJ, Carson DA: Idiotypic characteristics of rheumatoid factors. Scand J Rheumatol, Suppl. 75: 58-65, 1988.

85. Crowley JJ, Goldfien RD, Schrohenloher RE, Spiegelberg HL, Silverman GJ, Mageed RA, Jefferis R, Koopman WJ, Carson DA, Fong S: Incidence of three cross reactive idiotypes on human rheumatoid factor paraproteins. J Immunol 140: 3411-3418, 1988.

86. Fong S, Chen PP, Crowley JJ, Silverman GJ, Carson DA: Idiotypes and the structural diversity of human rheumatoid factors. Springer Seminar Series in Immunopath 10: 189-201, 1988.

87. Silverman GJ, Goldfien, Chen PP, Mageed RA, Jefferis R, Goni F, Frangione B, Fong S, Carson DA. Idiotypic and subgroup analysis of human monoclonal rheumatoid factors: implications for structural and genetic basis of autoantibodies in humans. J Clin Invest 82: 469-475, 1988.

88. Fox RI, Chan E, Benton L, Fong S, Friedlander M. Treatment of primary Sjogren' syndrome with hydroxychloroquine. American Journal of Medicine 85 (suppl 4A): 62-67, 1988.

89. Fong S. La Diversite Structurale Des Facteurs Rhumatoides Humains. In Immunorhumatologie. Roux H, Luxembourg A, Roudier J, (Eds.). Solal, editeurs, Marseille, pp 162-166, 1989.

90. Fu, Y., Arkin, S., Fuh, G., Cunningham, B.C., Wells, J.A., Fong, S., Cronin, M., Dantzer, R., Kelley, K. Growth hormone augments superoxide anion secretion of human neutrophils by binding to the prolactin receptor. J. Clin. Invest 89: 451-457, 1992.

91. Weber, J.R., Nelson, C., Cunningham, B.C., Wells, J.A., Fong, S. Immunodominant structures of human growth hormone identified by homolog-scanning mutagenesis. Mol. Immunol. 29: 1081-1088, 1992.

92. Bushell, G., Nelson, C., Chiu, H., Grimley, C., Henzel, W., Burnier, J., Fong, S. The role of cathepsin B in the generation of T cell antigenic epitopes of human growth hormone. Mol. Immunol. 30:587-591, 1993.

93. Bednarczyk, J.L., Wygant, J.N., Szabo, M.C., Molinari-Storey, L., Renz, M., Fong, S., McIntyre, B.W. Homotypic leukocyte aggregation triggered by a monoclonal antibody specific for novel epitope expressed by the integrin $\beta1$ subunit: Conversion of non-responsive cells by transferring human $\alpha4$ subunit cDNA. J. Cell. Biochem. 51: 465-478, 1993.

94. Berman, P.W., Nakamura, G., Riddle, L., Chiu, H., Fisher, K., Champe, M., Gray, A., Ward, P., Fong, S. Biosynthesis and function of membrane bound and secreted forms of recombinant Mac-1. J. Cell. Biochem. 52:183-195, 1993.

95. Crowe, D.T., Chiu, H., Fong, S., Weissman, I.L. Regulation of the avidity of integrin $\alpha4\beta7$ by the $\beta7$ cytoplasmic domain. J. Biol. Chem. 269:14411-14418, 1994.

96. Renz, M.E., Chiu, H.H., Jones, S., West, C., Fox, J., Kim, J.K., Presta, L.G., Fong, S. Structural requirements for adhesion of soluble recombinant murine VCAM-1 to $\alpha4\beta1$. J. Cell Biol. 125:1395-1406, 1994.

97. Chiu, H. H., Crowe, D. T., Renz, M. E., Presta, L. G., Jones, S., Weissman, I. L., and Fong, S. Similar but non-identical amino acid residues on vascular cell adhesion molecule-1 are involved in the interaction with $\alpha4\beta1$ and $\alpha4\beta7$ under different activity states. J. Immunol. 155:5257-5267, 1995.

98. Viney, J. L., Jones, S., Chiu, H., Lagrimas, B., Renz, M., Presta, L., Jackson, D., Hillan, K., Fong, S. Mucosal Addressin Cell Adhesion Molecule-1. A structural and functional analysis demarcates the integrin binding motif. J. Immunol. 157: 2488-2497, 1996.

99. Fong, S., Jones, S., Renz, M.E., Chiu, H.H., Ryan, A.M., Presta, L. G., and Jackson, D. Mucosal Addressin Cell Adhesion Molecule-1 (MAdCAM-1)--Its binding motif for $\alpha4\beta7$ and role in experimental colitis. Immunologic Research 16: 299-311, 1997.

100. Jackson, D.Y., Quan, C., Artis, D.R., Rawson, T., Blackburn, B., Struble, M., Fitzgerald, G., Chan K., Mullin, S., Burnier, J.P., Fairbrother, W.J., Clark, K., Beresini, M., Chiu, H., Renz, M., Jones, S., and Fong, S. Potent $\alpha4\beta1$ Peptide Antagonists as Potential Anti-Inflammatory Agents. J. Med. Chem. 40: 3359-3368, 1997.

101. Viney, J.L. and Fong, S. $\beta7$ Integrins and Their Ligands in Lymphocyte Migration to the Gut. Chemical Immunology: 'Mucosal T Cells' . Chemical Immunology 71;64-76, 1998.

102. Bradley, L.M., Malo, M.E., Fong, S., Tonkonogy, S.L., and Watson, S.R. Blockade of both L-selectin and $\alpha4$ Integrins Abrogate Naïve CD4 Cell Trafficking and Responses in Gut-Associated Lymphoid Organs. International Immunology 10, 961-968, 1998.

103. Quan, C., Skelton, N., Clark, K., Jackson, D.Y., Renz, M., Chiu, H.H., Keating, S.M., Beresini, M.H., Fong, S., and Artis D.R. Transfer of a Protein Binding Epitope to a Minimal Designed Peptide. Bioploymers (Peptide Science);47,265-275, 1998.

104. Hillan, K.J., Hagler, K.E., MacSween, R.N.M., Ryan, A.M., Renz, M.E., Chiu, H.H., Ferrier, R.K., Bird, G.L., Dhillon, A.P., Ferrell, L.D., Fong, S. Expression of the Mucosal Vascular Addressin, MAdCAM-1, in Inflammatory Liver Disease. Liver 19, 509-518, 1999

105. Pender, S.L.F., Salmela, M.T., Monteleone, G., Schnapps, D., McKenzie, C., Spencer, J., Fong, S., Saarialho-Kere, U., and MacDonald, T.T. Ligation of alpha 4 beta 1 integrin on human intestinal mucosal mesenchymal cells selectively upregulates membrane type-1 matrix metalloproteinase and confers a migratory phenotype. American Journal of Pathology 157, 1955-1962, 2000.

106. Liang, T.W., DeMarco, R., Gurney, A., Hooley, J., Huang, A., Klassen, T., Mrsny, R., Tumas, D., Wright, B.D., and Fong, S. Characterization of Human Junctional Adhesion Molecule (huJAM): Evidence for involvement in cell-cell contact and tight junction regulation. American Journal of Physiology; Cell Physiology 279, C1733-C1743, 2000.

107. Liang, T.W., Chiu, H.H., Gurney, A., Sidle, A., Tumas, D.B., Schow, P., Foster, J., Klassen, T., Dennis, K., DeMarco, RA.., Pham T., Frantz, G., Fong, S. VE-JAM/JAM 2 interacts with T, NK, and dendritic cells through JAM 3. J.Immunology 168, 1618-1626, 2002.

107. Dupree,N., Artis, D.R., Castanedo, G., Marsters, J., Sutherlin, D., Caris, L., Clark, K., Keating, S.,Beresini, M., Chiu, H., Fong, S., Lowman, H., Skeleton, N., and Jackson, D. Selective $\alpha4\beta7$ Antagonists and Their Potential as Anti-Inflammatory Agents. J. Med. Chem. 45, 3451-3457, 2002.

108. Castanedo, G.M., Sailes, F.C., Dubree, N., Nicholas, J., Caris, L., Keating, S., Chiu, H., Fong, S., Marsters, J., Jackson, D.Y., Sutherlin, D.P. The Solid Phase Synthesis of Dual $\alpha4\beta1/\alpha4\beta7$ Antagonists: Two Scaffolds with Overlapping Pharmacophores. Bioorganic and Medicinal Chemistry Letters 12, 2913-2917, 2002.

J. Physiol. (1952) 118, 228–257

VASCULAR REACTIONS TO HISTAMINE, HISTAMINE-LIBERATOR AND LEUKOTAXINE IN THE SKIN OF GUINEA-PIGS

By A. A. MILES and E. M. MILES

From the National Institute for Medical Research, Mill Hill, London

(*Received* 3 *April* 1952)

A substantial increase in capillary permeability is a feature of acute inflammation in bacterial infections. The present investigation is part of an attempt to prove an old hypothesis, namely, that this increase in permeability is mediated by histamine. A comparative study was made of histamine, of the histamine-liberator 48/80, a condensation product of *p*-methoxyphenylethylmethylamine and formaldehyde (Baltzly, Buck, de Beer & Webb, 1949), and of leukotaxine (Menkin, 1936, 1938*a*, *b*).

In animals with a recently injected vital dye in their blood, the intradermal injection of substances that increase permeability of the blood vessels is followed by an accumulation of dye at the site of injection, presumably due to the passage of an excess of dye-stained plasma into the tissue spaces. When the blood flow and the vascular bed of the skin are relatively constant, differences in the size and intensity of stained areas of skin reflect differences in vascular permeability, and may be used to investigate the properties of substances that increase permeability in this way. Our work was confined to the skin of guinea-pigs, partly because much is already known about skin reactions to toxins and other inflammatory agents, and partly because it is a tissue readily studied in the intact and unanaesthetized animal—an important consideration with phenomena which, like the passage of dye through vascular endothelium, are peculiarly dependent on the state of the blood vessels in the tissue under test.

MATERIALS AND METHODS

Albino guinea-pigs, 300–450 g in weight, were used throughout. The skin of the trunk was depilated, after clipping away the hair, by a paste consisting of wheat flour, 350 g; talcum powder, 350 g; barium sulphide, 250 g; Castile soap powder, 50 g; and water. The depilated area was thoroughly washed with warm water.

Detection of increased permeability. Neither the intradermal injection nor the pricking-in of histamine or 48/80 produce in the depilated skin any measurable reaction indicating change in

vascular permeability; and there is no trace of the wheal that characterizes the reaction of human skin to histamine. In the skin of animals with circulating dye, however, both substances induce remarkably constant effects. A 5% solution of pontamine sky blue 6X ('pontamine blue') was used, given intravenously in the leg in doses of 65–75 mg/kg body weight. Animals so injected are referred to below as 'blued'. A few minutes after the injection of the dye the sites of wounds, of too-long application of depilating paste, and of recent careless or even firm manipulation of the skin, become blue. Though traumatic blueing of this kind commonly results from depilation, with nice judgement it is possible to depilate cleanly without damage to the skin. Owing to the sensitivity to trauma of blued animals, injections cannot be made into the skin pinched into a fold between thumb and finger; the skin must be steadied by gentle stretching over the underlying tissue.

In the absence of further interference, the skin of a blued animal becomes generally and maximally stained in 10 hr or more; but up to 6 hr after the intravenous dye, the intradermal injection of a substance that increases permeability results in a local increase in the intensity of blueing. The best contrasts were obtained within 1 hr of giving the dye. Unless otherwise stated, all our injections were given into the skin of the trunk posterior to the shoulder blade and anterior to the knee joint in the sitting animal, and omitting the thin skin about 30–40 mm on each side of the ventral mid-line; all solutions for injection were made up in 0·85% saline, which by itself induces no blueing. The volume injected was usually 0·1 ml., which initially raises a bleb 9–11 mm in diameter. With short-bevel no. 26 gauge needles, a small area of traumatic blueing 1–3 mm in diameter develops at the centre of the bleb.

Skin reactions in the ears of blued animals were induced either by free-hand intradermal injections with a no. 28 needle, or by injections with a mechanically manipulated glass micro-needle into animals under light bromethol (avertin) anaesthesia. The micro-injections were either intradermal or made directly into the lymphatic plexus of the ear, which is readily entered via one of the numerous anastomosing lymphatic channels at the margin of the ear. The ears were transilluminated and observed under ×20 and ×40 magnification.

Materials. The acid phosphate of histamine was used; amounts are cited as the weight of the base. The specimen of 48/80 (Wellcome Research Laboratories, U.S.A.) was probably in the form of the dimer, trimer and tetramer (Paton, 1951), with an average molecular weight of about 540 The leukotaxine was a single batch prepared by Dr J. H. Humphrey, by a combination of the methods of Cullumbine & Rydon (1946) and Spector (1951), and corresponded to the fractions described by Spector as active in inducing capillary permeability, containing eight to fourteen amino-acid residues. On this basis its molecular weight is of the order of 1500.

RESULTS

The mechanics of intradermal injection

The behaviour of injected drugs is determined in part by the mechanics of intradermal injection. The skin of the trunk moves loosely over the underlying abdominal and thoracic muscles. For our purpose this movable skin may be described as three layers of about equal thickness (Text-fig. 1*a*). (*A*) Epidermis and dermis which together are about 1·0 mm thick, appearing on cross-section as a dense whitish layer, whiter in the deeper part; the dermis contains an extensive plexus of blood vessels (*sp*) round the main bodies of the glands and hair follicles, and a fine plexus of lymphatic channels, detectable when indian ink is injected into this region by a micro-needle. (*B*) A looser connective tissue about 1·0 mm thick, appearing on cross-section as a grey gelatinous layer; at its base, immediately above *C*, the panniculus carnosus, is a plexus

of blood vessels (dp) and a coarse scanty plexus of lymphatic channels, each joined to the corresponding upper plexus in A by relatively few vessels. (C) The panniculus carnosus, a muscle layer about 1·0 mm thick.

In making an intradermal injection, the depth of the needle-tip to some extent determines the depth at which the bulk of the injected fluid will spread, but not as completely as is generally supposed. The fluid spreads outwards, upwards and downwards to form a lenticular mass of wet tissue (Text-fig. 1*b*). When the needle tip is as low as the deepest part of B, the swelling of the skin

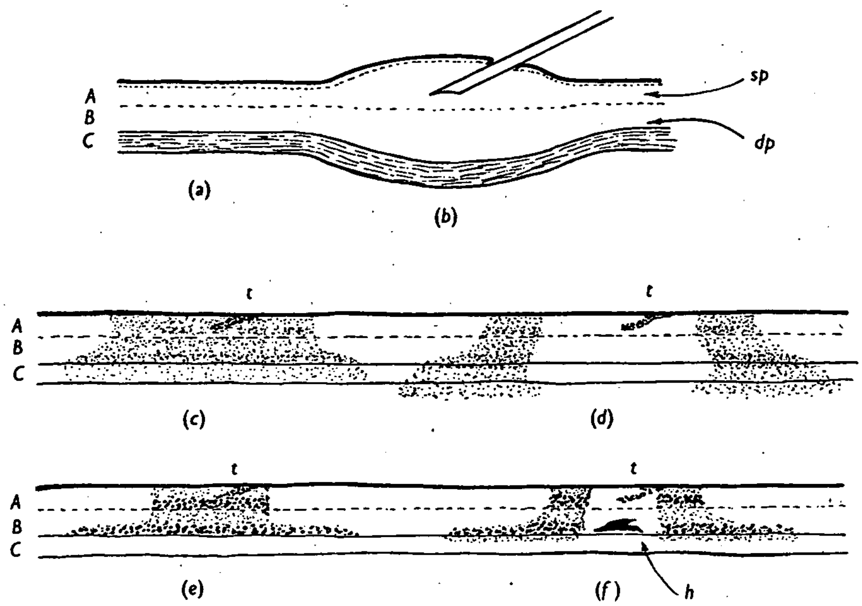

Text-fig. 1. Schematic sections of guinea-pig skin. (*a*) normal; (*b*) intradermal injection bleb; (*c*) blueing with low dose of histamine, showing traumatic blueing *t*, due to needle; (*d*) blueing with high dose of histamine showing central inhibition; (*e*) blueing with low dose of 48/80; (*f*) blueing with high dose of 48/80, showing central inhibition, and haemorrhage, *h*. *sp*, *dp* = superficial and deep plexus of blood vessels. For definition of layers A, B and C, see p. 229.

is due mainly to the distension of that layer, but when it lies in the middle of B, or in the dermis, both B and the dermis are equally permeated by the injection fluid. The initial diameter of the bleb is a simple function of volume injected; being linearly related to log. volume (Text-fig. 3*a*–*d*).

The initially domed injection-bleb of saline is scarcely visible after 3–4 hr. Some of the fluid is doubtless taken into the blood stream and some into the lymphatic channels; though, judging by the results of intradermal injection of dyes and indian ink, only a very small proportion of the injected substances escapes by the lymphatic channels during the first 2 hr. Other forces must be at work to account for the gradual disappearance of the bleb, which both decreases in thickness and spreads outwards. The diameter of a 0·1 ml. bleb,

measured under illumination by a very oblique beam of light, grows linearly with respect to log. time (Text-fig. 2); and on the average, blebs starting at 10·5 mm are 19·5 mm in diameter after 2 hr and 20·5 mm after 4 hr. The rate of spread is much the same in freshly killed animals. The decrease in thickness is partly due to seepage through the muscle layer into the subcutaneous tissue, which becomes noticeably wet; and partly to the outward spread of the fluid. Of the forces responsible for the outward spread, diffusion is unlikely to play any large part, because the intradermal invasion of diffusible substances applied to the cut edge fo normal skin is small and slow (e.g. the enzyme hyaluronidase, Hechter, 1946). Spread probably takes place by mass movement of the fluid either by reason of the hydrostatic pressures engendered in the tissue during injection or because the tissue has an affinity for water, which moves therefore from the hydrated bleb to the surrounding less hydrated tissue.

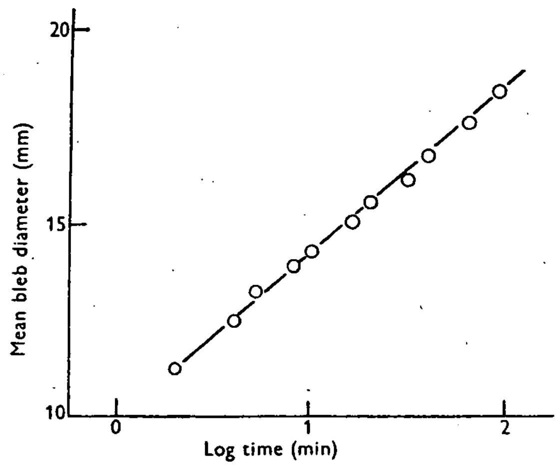

Text-fig. 2. Growth of an intradermal bleb in the guinea-pig formed by 0·1 ml. saline. Each point the mean of three blebs.

Large syringe pressures are required to initiate an intradermal bleb. In a series of measurements on ten guinea-pigs, this pressure varied between 80 and 140 cm Hg; once the bleb was begun, it increased rapidly in size under syringe pressures of 60–100 cm Hg. Only 1–2 cm Hg were required to expel fluid rapidly from the unimpeded syringe needle. The tissues do not, however, store the energy to a degree represented by these pressures, because when the bleb is cut vertically across its middle, fluid oozes only very slowly from the cut surface. Indeed, the pressure within the bleb soon after it is made cannot be higher than that in the small vessels involved, because exudation from the vessels takes place in blebs only 3 min old (see p. 236). At this time the maximum pressure must therefore be less than that in the largest vessels from which exudation takes place; and probably does not exceed 1–2 cm Hg. That the occlusion of the vessels during injection is only short-lived can be seen when

the formation of an intradermal bleb is watched under low-power magnification in a transilluminated hyperaemic ear. The hyperaemia is apparently restored after a few seconds. In arteries 0·4–0·8 mm in diameter, the flow returns in 5–10 sec; and in veins 0·5–2 mm in diameter flow returns in 30–120 sec, and initial diameter is restored in under 3 min. The high injection pressures are apparently needed only to tear apart the tissues at the advancing edge of the bleb.

Fluid may be expressed more rapidly by gently pinching the cut edge of a bleb between finger and thumb. A great deal of the fluid therefore cannot be held by hydration of the tissues. It is presumably held in innumerable small, distended, interconnecting loculi in the connective tissues, and is forced outwards to the periphery of the bleb by contraction of the distended tissue fibres. Hydration, however, may well account for the retention of some of the fluid in a cut bleb, as the following experiment shows. The average water content of pieces of muscle-free, intact skin from the trunk was about 50 %; i.e. one part of dry matter holds about one part of water. Pieces of fresh guinea-pig skin were cut into 10 μ slices on a freezing microtome, washed in saline to remove damaged cells and the contents of the cells cut open during section, and the washed slices allowed to imbibe water from 0·85 % saline for 30 min at 32° C. They were then deposited as a hard cake by centrifugation, and excess fluid removed from the deposit by firm pressing between sheets of filter-paper. The average water content of these masses was about 70 %, i.e. one part of dry matter can hold 70/30 = 2·3 parts water. A 0·1 ml. bleb occupies about 160 mg of intact skin, which, if it attained the same degree of hydration as the sliced skin, could hold $80 \times 2{\cdot}3 = 184$ mg water; i.e. not only the 80 mg of natural water, but the injected 100 mg as well.

The dosage-response to intradermally injected substances

The distribution in the skin of an intradermally injected substance will depend on its concentration and the rate at which it is adsorbed or 'fixed' by the tissues during the outward flow of injection fluid from the needle. A substance that was adsorbed very little would spread with the injection fluid, and, according to the evidence in Text-fig. 2, would eventually produce lesions whose diameter was directly proportional to the diameter of the injection bleb; i.e. to the volume of fluid injected. Most substances, however, are adsorbed in some degree, and accumulate at and around the centre of the bleb. The relation of the bleb-diameter to lesion-diameter with different drugs can be used to characterize their adsorption to the tissues. It was explored for histamine, 48/80 and leukotaxine by two methods of injection in blued animals: (*a*) graded concentrations in a constant injection-volume, and (*b*) graded injection-volumes containing a constant dose.

'Constant-volume' measurements. Four doses of the substance under test in

0·1 ml., were randomized in a 4 × 4 Latin square on the trunk, two rows on each side of the spinal mid-line. Histamine, 48/80 and leukotaxine all produced round blue lesions in the skin and in each case the lesion-diameters measured 30 min after injection were linearly related to the log. dose (cf. Text-fig. 5*a*, *b*). The responses were subjected to analysis of variance, with the results exemplified in Table 1, which records a titration of histamine in three blued animals. The departure from linearity of the regression line of lesion-diameter on log. dose is insignificant. The variation between columns and rows is also insignificant, so that for practical purposes the skin of the more dorsal

TABLE 1. Analysis of variance of a titration of histamine in a 4-fold Latin square in three blued guinea-pigs

	Degrees of freedom	Sum of squares	Mean square	Variance ratio	*P*
Between animals	2	3·2279	1·61395	1·66	>0·05
Between columns	3	3·1275	1·0425	1·07	>0·05
Between rows	3	2·0174	0·6725	—	—
Between doses	3	312·7425	104·2475	107·46	<0·001
Linearity	1	72·8017	72·8017	75·05	<0·001
Curvature	1	3·2939	3·2939	3·40	>0·05
Response	1	235·8784	235·8784	243·15	<0·001
Error	36	34·9239	0·9701	—	—
Total	47	356·0392	—	—	—

Tested placement of injections dorsal v. ventral

part of the guinea-pig's trunk may be considered homogeneous in its sensitivity to histamine. (This is not true of the thinner ventral skin, where lesions tend to be larger.) Each animal yields a mean of four responses per dose. The error term for inter-animal variation is large, but reliable comparisons between various treatments were obtained in other tests by using four to six animals per group. This linear relationship differs from that found by Bain (1949) in the human skin, where *area* of histamine whealing was proportional to log. dose. Linearity of diameter against log. dose holds for many substances in guinea-pig skin: diphtheria toxin (Miles, 1949), tuberculin in tuberculous animals (Wadley, 1949) and appears to hold for other bacterial antigens in hypersensitive animals, and for the lesions produced in the blued animals by various toxins such as the exotoxins of *Clostridium welchii*, *Cl. oedematiens* and *Staphylococcus aureus*, and for cobra venom (unpublished work). The difference in Bain's titration may lie in the modification of histamine spread or of wheal-diameter, by the copious exudation during whealing that occurs in man but not in the guinea-pig.

Full 4 × 4 Latin-square titrations were usually made only when the significance of a result was in doubt; in most of the tests fewer replications of doses were used, partially randomized among three to six animals per group. In these titrations, 48/80 and leukotaxine differed from histamine mainly in the slope of the dosage-response lines. Slopes varied with each experiment, and particularly with the amount of dye injected. Moreover, since the concentration of circulating dye falls rapidly during the first 2 hr, slope decreases with lapse of

time between blueing the animal and the intradermal titration. In guinea-pigs receiving 65 mg/kg tested soon after its injection, the slopes for histamine lay between 2·8 and 3·5, for 48/80 between 1·5 and 2·0 and for leukotaxine between 1·5 and 4·0. The shallow slope of 48/80, which indicates an increase of only 1·5–2·0 mm in lesion-diameter for a 10-fold increase in concentration, suggests that, compared with histamine, it is strongly adsorbed to the tissues. It should be noted that the susceptibility of this linear dosage-response to statistical analysis makes possible an accurate though not very precise measure of the potency of each of the three substances. The method is too insensitive for routine assay, but was well adapted to our investigations of skin reactions. Thus where parallel regression lines can be fitted to two sets of log. dose-diameter responses, the horizontal distance between the two lines is the log. ratio of drug potency; and, for a given specimen of a drug, it is the log. inverse ratio of sensitivity to the drug. For example, in Text-fig. 5*b*, 3 mg neoantergan has shifted the slope to the right by 0·43 = antilog. 2·7. That is, the neoantergan has decreased the 48/80-sensitivity of the animals 2·7-fold, since 2·7 × the dose in normal animals is required to produce the same effect in the treated animal.

'*Constant-amount' measurements*. In this method a fixed amount of the drug was injected in volumes of 0·05, 0·1, 0·2 and 0·4 ml.; i.e. the concentration of the drug is varied. The diameter of the blebs, measured immediately after the injections, was linear with respect to log. volume (Text-fig. 3*a*, *A*); and, according to the data in Text-fig. 2, after a given period (e.g. 30 min, Text-fig. 3*a*, *B*) the expanded bleb-diameters would be linear, on a line parallel to that for the immediate bleb-diameters (Text-fig. 3*a*, *B*). The slope of the initial bleb-diameters, irrespective of any lesion produced by the drug injected, is relatively constant in the region of 9·0. When the drug has acted the resulting lesion-diameters are also linear with respect to log. injection volume. Text-fig. 3*a*, *C* and *D*, records results with 12·5 and 50 μg pontamine blue in unblued animals. The 'lesion' here is the area of skin coloured by the injected dye. The slope of lesion-diameter is not parallel to that for initial bleb-diameter, which would have indicated no adsorption during injection. Nor is it horizontal, which would have indicated an adsorption so strong that it was independent of concentration within the range tested. The slope of *C* and *D* is in fact 5·5, compared with 9·7 for the initial bleb-diameter. Pontamine blue has a good affinity for skin tissue (Evans, Miles & Niven, 1948), and we would therefore expect slopes like *C* and *D*, which show that as the solutions are forced outwards during injection, adsorption decreases with decreasing concentration of the injection fluid. The magnitude of the slope, compared with that for the initial bleb, is a reasonable inverse indicator of the affinity of the tissues for the drug. Text-fig. 3*b*–*d*, and Table 2 summarize similar titrations on histamine, 48/80 and leukotaxine; the slopes indicate that the tissue affinity is least for histamine, and greatest for leukotaxine.

The relative position of the two slopes is also informative. In Text-fig. 3*a*, the 50 μg line *D* crosses *A* at about 10 mm, i.e. the skin occupied by the initial bleb from 0·1 ml. just adsorbs the dye. The 50 μg of dye is clearly insufficient

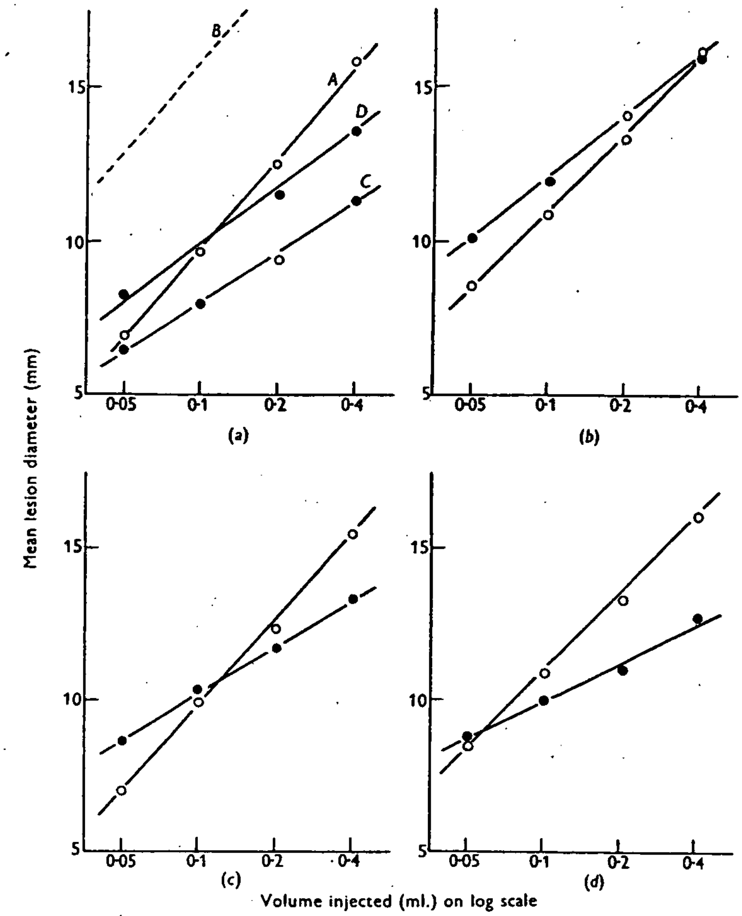

Text-fig. 3. Constant-dose intradermal titrations. Lesion-diameters plotted against log. volume injected. Each point the mean of twelve to sixteen lesions. In all the graphs, ○ — ○, mean diameter of the initial blebs raised by the *fluid* injected; ● — ●, diameter of lesion produced by the *substances* injected. (*a*) pontamine blue: *A*, initial bleb-diameter; *B*, bleb-diameter after 30 min calculated from data in Text-fig. 2. *C* and *D*, lesion-diameters of 12·5 and 50 μg dye. (*b*) Histamine, 8 μg; (*c*) 48/80, 13 μg; and (*d*) leukotaxine, 40 μg, in blued animals (see pp. 234–6 and Table 2).

to fill the 0·2 ml. bleb. It oversaturates the 0·05 ml. bleb so that as the fluid spreads outwards from the region initially filled by the injection, the excess of dye is carried some way with it; at 30 min, when the reading was taken, the dye has spread over 8 mm and the fluid (line *B*) over 12·5 mm. The intersect of initial bleb-diameters and lesion-diameters is thus a convenient measure of the

adsorbing power of the skin for a given dose of drug, though clearly it can give no information about the concentration gradient of the drug within the bleb. It is the volume in which the adsorption of the drug is so balanced that the minimal effective concentration is produced at the edge of the initial bleb; and may be called the critical volume. In Text-fig. 3*a*, the critical volume for 50 μg of pontamine blue is 0·105 ml.

TABLE 2. Slopes and critical volumes in 'constant-amount' titrations of histamine, 48/80 and leukotaxine

Substance	Approx. equimolar dose (μg)	Slope mean diameter		Critical volume (ml.)
		Initial bleb	Lesion	
Histamine	8	8·6	6·6	0·400
48/80	13	9·3	5·2	0·012
Leukotaxine	40	8·6	4·1	0·058
(Pontamine blue	—	9·8	6·2	0·105)

For a valid comparison, the critical volumes of equimolar concentrations of histamine, 48/80 and leukotaxine were determined from the data in Text-fig. 3*c–e* (Table 2). 8 μg of histamine was tested, and the approximate molecular equivalent, 13 μg, of 48/80. The result for an equimolar amount of leukotaxine (40 μg) was extrapolated from the slope for 20 μg using the value 4·0 for the slope of a constant-volume titration. The values both for slope and critical volume must be regarded as very approximate. Histamine (Table 2) has a high 'constant-amount' slope, and a high critical volume; it is thus relatively poorly adsorbed during injection, and the skin is relatively poor in adsorbing sites. Both 48/80 and leukotaxine are more strongly adsorbed, and the skin is richer in adsorbing sites.

Skin reactions to histamine

Histamine even as strong as 1·6% will not induce blueing in dyed animals when applied to undamaged skin. When the skin of blued animals is damaged by rubbing (cf. Matolsty & Matolsty, 1951) or scratching sufficient to produce patches of traumatic blueing, the application of 1% histamine will increase the size and intensity of such blueing, presumably because the drug, having penetrated the damaged skin, diffuses inwards from the damaged area. It is also possible to induce blueing by the electrophoresis of 1% histamine; the histamine is not however driven in uniformly, but produces irregular patches of blueing. In none of these tests was whealing ever observed.

Intradermal injection in the trunk. Histamine injected intradermally into blued animals produces a round area of blueing that appears in 3–5 min and increases slightly in diameter and intensity during the next 7 min. In a volume of 0·1 ml., as little as 0·1–0·2 μg is effective; with increasing dose the blue increases in intensity and area. With amounts greater than 1–3 μg the colour first appears at the edge of the bleb, but gradually fills the centre. With doses

of 4 μg and more, the centre remains uncoloured except for the traumatic blueing round the site of needle-entry, and colour develops at the edge. More than 10–20 μg produces only a narrow band of very faint blue at the edge of the bleb.

On section after 10 min, a 1 μg histamine lesion is seen to be uniformly stained at the skin surface, more widely stained in layer *B* (Text-fig. 1*c*), and feebly stained in the muscle. Occasionally the staining is slightly deeper in the region of the two plexuses of blood vessels. With stronger doses of histamine (Text-fig. 1*d*), the drug has in 10 min spread downwards and outwards so that there is blue exudate in the underlying subcutaneous tissues, and the abdominal and thoracic muscles may be stained. The other feature of the stronger dose, the central inhibition of blueing, is also evident in cross-section, where the colourless zone reaches down to the muscle layer.

The linear response, lesion diameter on log. dose, holds with histamine for diameters between 5 and 17 mm: below 4 mm histamine blueing may be confused with traumatic blueing. In reading the diameters, inhibition of blueing at the centre is ignored even though with the higher concentrations of the drug only faint, thin rings of blue may be produced. The lesion-diameters measured on the under-surface of flayed skin are larger than those on the upper surface, by about 40%. This ratio is approximately constant. There is, however, no advantage in the measurement, because the lesions are less well defined and, with the bigger doses, obscured by subcutaneous blue exudate.

Intradermal injections in the ear. Blueing of the ear, as in the trunk (see below), was partly inhibited by bromethol anaesthesia; but under light anaesthesia it was sufficiently strong for a number of useful observations, though lesion diameters were not such a consistent guide to drug-sensitivity. The ear was found to be less sensitive to histamine than the skin of the trunk. In unblued animals, concentrations of 5–1000 μg/ml. caused immediate flushing of the skin of the bleb, which lasted about 10 min. Stronger histamine, up to 10,000 μg/ml. also caused immediate flush, and after $1\frac{1}{2}$ min an intense vasoconstriction, lasting 3–5 min, of the arteries traversing the bleb area.

In blued animals, the permeability effect is visible in $1\frac{1}{2}$ min. The minimal blueing concentration was about 0·5 μg/ml. Central inhibition of blueing occurred at 50 μg/ml., lasting only 3 min, after which the centre of the bleb became blue. At 1000 μg/ml. it lasted about 16 min, unlike the central inhibition by 50 μg/ml. in the skin of the trunk, which persisted for several hours. The results in Table 6 were obtained from blebs of 3 mm initial diameter; the injection volume was not measured exactly.

With concentrations of 100 μg/ml. the area of blueing of a 3 mm bleb was 10 mm in diameter after 10 min. Histamine in stronger concentrations, 1000–10,000 μg, leaked into the lymphatic plexus, spread both distally and proximally through the freely anastomosing channels, passing back into the

tissues to produce an oedematous wedge-shaped area of intense blueing with its apex at the base of the ear where the main lymphatic ducts leave the ear (Pl. 1A, B). This is a characteristic lymphatic spread of strong histamine in the ear, and is also produced by strong histamine injected directly into the lymphatic plexus. It is evident therefore, that histamine readily passes both ways through lymphatic endothelium.

Factors that change skin-reactivity to histamine in the trunk

Temperature. Depilated animals held at 10° C react poorly to histamine; those at 20° C react well; and those at 37° C poorly and irregularly. Thus, the mean lesion-diameters for 3, 9 and 27 μg histamine were 6·7, 8·3 and 9·6 mm at 20° C, and 4·7, 5·7 and 5·9 mm in animals held at 37° C. The intensity of blueing was considerably less at 37° C. In this reaction to heat the guinea-pig is similar to man in his whealing reaction to histamine (Lewis & Grant, 1924).

Anaesthesia. Under ether, chloroform, chloralose, bromethol, pentobarbitone and urethane anaesthesia, blueing is greatly diminished or even abolished. In general, the deeper the anaesthesia, the greater the inhibition of blueing. After a short period of anaesthesia with ether, bromethol or chloroform, reactivity is sometimes restored on recovery. Loss of reactivity is accompanied by a decline in the pressure of the central arteries of the ear, measured by a modified Grant's capsule (Miles & Niven, 1950), from 40 to 70 mm in the unanaesthetized state, to 20–40 mm Hg. This suggests that in the skin of the trunk also there is in anaesthesia a decline in blood pressure to the point where dye is no longer forced out into the tissues, though the permeability of the vessels may be increased by the histamine. However, in many recovered animals, in which the blood pressures in the ear have returned to normal, the skin of the trunk remains unresponsive; either the anaesthetic has modified histamine-sensitivity, or the circulation is in these areas restored less quickly than in the ear.

Shock. In guinea-pigs given sublethal shocking doses of *Proteus vulgaris* and *Bacterium coli* endotoxins, of adenosine-triphosphate, insulin or intraperitoneal hypertonic glucose, reactivity to histamine is diminished; and, as in anaesthesia, the loss is associated with low blood pressure in the ear, and with low skin temperature (Miles & Niven, 1950). In shocked or anaesthetized blued animals, whose skin does not respond to histamine, it is possible to demonstrate an increase in capillary permeability by indirectly raising the intracapillary pressure. When a suction cup is applied to the skin of these animals, substantial blueing of a histamine-treated area is produced within 5 min, by a suction of 10 mm Hg applied intermittently for 2–3 sec every 10 sec.

Infection and malnutrition. Guinea-pigs suffering from spontaneous chronic infective abscesses, or in poor health because of heavy infection with B.C.G.

(Bacillus of Calmette and Guérin) or as a result of long-term partial deficiency of vitamin C, react poorly to histamine.

Cortisone, preparations of adrenocorticotrophic hormone (ACTH) and posterior pituitary lobe extract (P.P.E.). In an attempt to relate the anti-allergic effect of cortisone and ACTH to an effect on histamine sensitivity, histamine was titrated in blued animals, 2–3 hr after doses of cortisone (2 mg) or ACTH (1 i.u.). These doses had proved effective in diminishing tuberculin allergy in the guinea-pig (Long & Miles, 1950). The cortisone had no effect. The diameters of the lesions were not substantially changed by the ACTH, but intensity of staining was greatly diminished. At this time, the skin of the ACTH-treated animals was slightly colder than those of controls. Nearly all current preparations of ACTH contain some posterior lobe extractives, and these may have been responsible for the ACTH effect we observed. Certainly both 2 and 0·2 i.u. P.P.E., given subcutaneously $2\frac{1}{2}$ hr before the titration, diminished reactivity to histamine (Text-fig. 4); and here again the diminution was probably due to poor blood supply, because the skin was cooler than that of the controls.

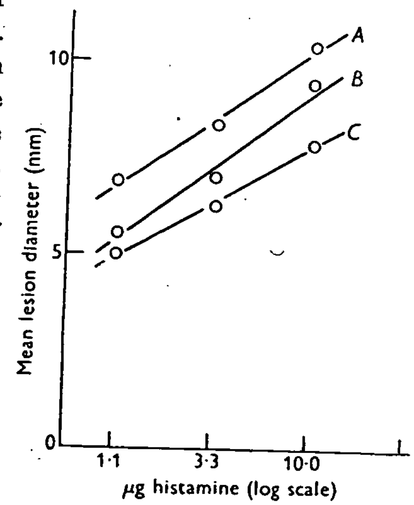

Text-fig. 4. The depressant effect of intramuscular posterior pituitary extract (P.P.E.) on histamine blueing in the guinea-pig. Each point the mean of twelve lesions. *A*, untreated animals; *B*, 0·2 i.u. P.P.E., 2·5 hr earlier; *C*, 2·0 i.u. P.P.E., 2·5 hr earlier.

Neoantergan. 20 μg neoantergan (mepyramine maleate) given intradermally in 0·1 ml. itself induced slight blueing of the skin; 5 μg histamine induced intense blueing 11 mm in diameter; and 20 μg neoantergan mixed with 5 μg histamine gave a pale blue area 10 mm in diameter. Local neutralization by neoantergan is therefore possible, but not very effective. Intravenous neoantergan, on the other hand, is most effective; 0·1 mg/kg almost abolished histamine blueing, and 0·02 mg/kg diminished the efficacy of intradermal histamine about 9-fold (Text-fig. 5*a*).

Excepting inhibition in animals held at high atmospheric temperatures, and by intravenous neoantergan, most of the effects on blueing described above can be attributed to a decline of intravascular pressure, rather than to insensitivity to histamine. The insensitivity of an abnormally warm skin may be due, as Lewis & Grant (1924) suggested for the human subject, to the more rapid removal of histamine in the more physiologically active tissue. The variety of the states in which there is inhibition of blueing is a warning that

absence of local blueing cannot safely be interpreted as absence of increase in capillary permeability unless there is good reason to believe that the blood supply to the skin and the state of the skin vessels have not been altered by the experimental procedure. On the other hand, it is reasonable to assume that a substance like histamine, which rapidly induces a deep blueing in healthy animals held at an atmospheric temperature of about 20° C, does so by an abnormal increase in capillary permeability. Histamine can act as vasodilator, but it is unlikely that the increased blueing in the guinea-pig is due to increased flow and exudation of dye as a result simply of vasodilatation, as suggested by Dekanski (1949). The rate of histamine blueing is too rapid to be attributable to this cause. Histamine induces in 3 min an intensity of blueing reached by untreated skin in 10 hr or more; i.e. the rate of accumulation of the dye is increased by over 200-fold.

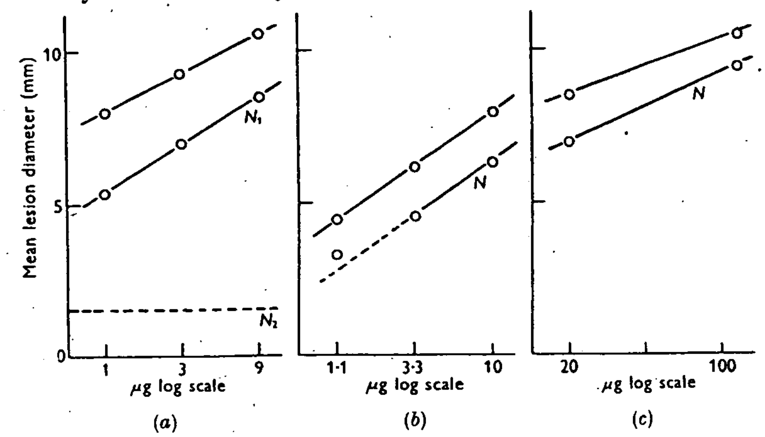

Text-fig. 5. The effect of neoantergan (N) on blueing in the guinea-pig. Each point the mean of twelve or sixteen lesions. (a) Histamine, $N_1 = 0{\cdot}02$ mg/kg, N_2 = average diameter of lesion with 0·1 mg/kg; (b) 48/80, $N = 8$ mg/kg; (c) leukotaxine, $N = 3$ mg/kg.

The time-course of the histamine effect

The rate of 'fixation' of histamine. The 'constant-amount' titration of histamine (Text-fig. 3b, Table 2), measuring the blue area developing in 10 min, shows that during injection the drug is lightly adsorbed. Within 5 min, however, some reaction with tissue must have occurred, because the increased permeability is by that time almost fully developed. The rate of that reaction may be estimated by the technique of superinjection (Miles, 1949) in which a substance is injected through a needle painted with a trace of indian ink so that the site of needle entry is exactly marked; and after an interval an injection of saline made into the same site. If any of the injected substance is free, it will be displaced outwards by the superinjected saline beyond the periphery of the initial bleb, with a consequent increase in the size of the lesion; if there is no increase, the injected substance has already been held fixed or destroyed by the tissues.

In applying the method to histamine and histamine-liberators the evidence from increase in lesion-diameter is not unambiguous because the superinjected saline may push, not free histamine, but already-formed blue exudate, beyond its original confines. The ambiguity may be resolved in part by determining the rate at which 'exudate' is fixed to the tissues. To this end, guinea-pig serum was coloured with pontamine blue so that in an unblued animal 0·1 ml. stained the skin to the intensity produced by 3 μg histamine in 0·1 ml. injected into a blued animal. Into the sites of injection of this fluid, 0·2 ml. saline were superinjected after graded intervals of time. The results were variable but indicated that some of the dyed serum was fixed within 3–4 min and the rest could be dislodged by superinjection up to 20 min. later. The best that can be

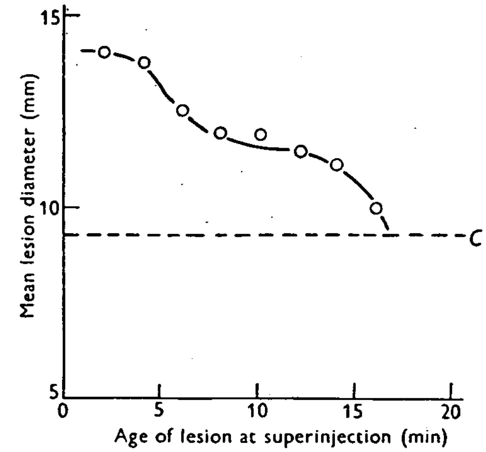

Text-fig. 6. The fixation of 3 μg histamine by guinea-pig skin. Superinjection of histamine lesions by 0·2 ml. saline. C = average diameter of control lesions. Each point the mean of four lesions.

hoped for from the test is that with time the lesion-diameters decline to a steady value, but this will not necessarily be the same as the diameter of lesions left to develop without superinjection. When saline was superinjected into blebs made in blued animals with 3 μg histamine (Text-fig. 6) little was fixed in 3–4 min, a period corresponding to the latent period before blue exudation starts, the greater part was fixed in 4–12 min, and nearly all was fixed in 16 min old lesions. If we allow 3 min for the fixation of the blue exudate, then all the histamine may be fixed in as little as 13 min, and most of it is fixed, as might be expected, during the period when the histamine-induced exudation is taking place.

Duration of increased permeability. The duration of the histamine effect was measured by injecting 2 μg in 0·1 ml. at regular intervals for 30 min in an animal, and giving the dye intravenously immediately after the last intradermal injection; there are thus lesions varying in age from 1 to 30 min when the dye is injected, and lesions in which the vessels are no longer permeable do

not blue. It is clear from Text-fig. 7*b* that after 10 min the capillaries have recovered; only the traumatic blueing caused by the needle remains. A similar result was obtained in the ear (Text-fig. 7*a*) Here the residual traumatic blueing due to the fine micro-needle is minimal.

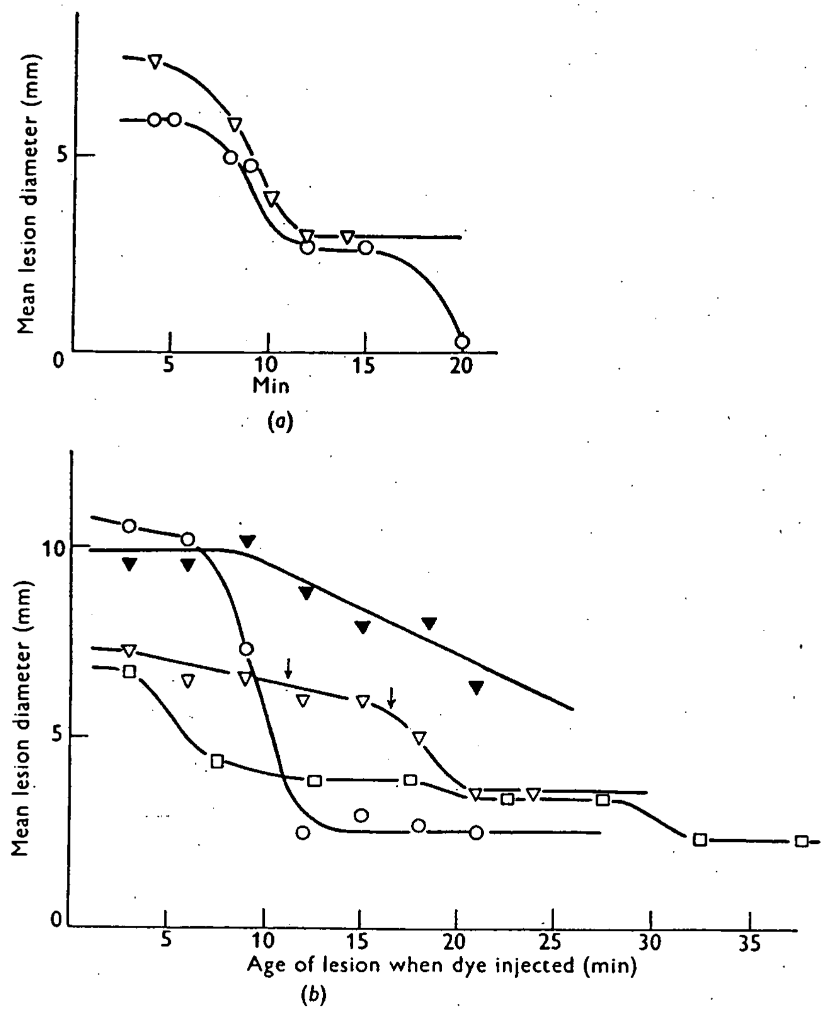

Text-fig. 7. The duration of increased permeability in guinea-pig skin. In each case there is a decline to the level of traumatic blueing induced by the injection needle. (*a*) The ear: histamine, approx. 2 μg in 0·02 ml., ○ — ○; 48/80, 2 μg in 0·02 ml., ▽—▽. (*b*) The trunk: histamine, 1 μg in 0·1 ml., ○ — ○; 48/80, 20 μg in 0·1 ml., ▼—▼; 2 μg in 0·1 ml., ▽—▽; leukotaxine, 10 μg in 0·1 ml., □ — □.

Immunity to histamine. It follows that the site of a histamine injection remains colourless if it is 10–15 min old when dye is given. When more histamine is superinjected into such a site, blueing is either feeble or absent. The

injection site has become refractory—or immune—to further histamine. The immunity is neither solid nor regular in its manifestation; it may take the form of diminished area of feeble staining, as though all the tissue were partly immunized; or of small patches of blue from 1 to 4 mm in diameter, as though the blood vessels in certain areas of the injection site had escaped immunization. This irregularity of response partly spoils measurement of immunity in terms of lesion-diameter, but the differences between immune and non-immune tissues are usually so large that mean lesion-diameters are good enough indices of the change. It is clear, for example, from Table 3, that after 1 hr 9 μg

TABLE 3. Immunizing action of intradermal histamine to injections of histamine made 1 hr later. Means of three lesions

Immunizing dose of histamine (μg)	Mean diameter (mm) and intensity* of reaction to test dose of histamine		
	1 μg	3 μg	9 μg
Nil	8·5 + +	10 + +	11·3 + +
9	0	6 f.	7·8 f.

* f., ±, +, + + = faint, moderate, marked, intense blueing.

induces a solid immunity to 1 μg, and a substantial immunity to 9 μg. A number of similar experiments established that though some immunity is present after 10 min, when the capillaries have recovered from the immunizing dose, it is greatest in lesions 1½–2½ hr old, and is passing off after 4 hr.

Histamine in concentrations of 10–100 μg/ml. immunized the ear vessels to histamine. Immunity was irregular in lesions up to 35 min old, well established after 40 min, maximal at 2–3 hr and lasted up to 5 hr. After 40 min, 50 μg/ml. had immunized to a test dose of 50 μg/ml. so that the diameter and intensity of blueing was reduced from 9 mm + +, in a control area to 4 mm ±, in the immunized area; 20 μg/ml. did not immunize to 50 μg/ml., and the immunity induced by 10 μg/ml., though it protected against 10 μg/ml., lasted only 60 min.

The inhibition of skin-reactivity by high concentrations of histamine

The restriction of blueing to the periphery of blebs containing 4 μg histamine or more may be explained in terms of the recovery of normal impermeability and of immunity, if we also postulate that the histamine at the centre of the bleb was strong enough to induce vasoconstriction of the arterioles for at least 10 min. As a result, the centre of the bleb would not blue during this time because the blood supply is cut off—a state corresponding to the inhibition of whealing in man by pressure-occlusion of the vessels—and by the time the blood supply is re-established, the central capillaries would have recovered from the histamine. Alternatively, the reaction of the vessels with high concentrations of histamine may proceed so rapidly that the immune stage is reached before the preceding stage of permeability can manifest itself by the escape of dye.

Lewis & Grant (1924) inferred that the refractory state was not due to occlusion of the lumen of the vessels by viscous R.B.C. or other material, because it could be induced in a relatively bloodless arm, and because, even though whealing was inhibited, vascular reactions that indicated a fully patent vascular bed could still be elicited. There is no anatomically convenient site in the guinea-pig for occlusion tests as applied by Lewis & Grant, and the dermis is too dense for direct observation of vascular changes. The vessels were proved patent by direct test. Injections of 5 or 10 μg histamine were made at intervals, in the skin over the right scapular region of normal guinea-pigs under urethane anaesthesia. At the end of the series of skin injections, 4 ml. indian ink was put into the right axillary artery. During the preparation of this artery, the blood supply to the skin was interrupted for the last 2–3 min of the experiment. The state of the vascular bed was deduced (*a*) by direct observation of the blackening of the skin; (*b*) from the pattern of the ink-filled vessels seen by low-power microscopy in excised skin areas fixed in 10% formalin, dehydrated and cleared with clove oil; and (*c*) from the distribution of ink in the lumen of capillaries seen in histological section of individual blebs. In tests by these methods on eight animals, there was no evidence of blocked vessels in histamine lesions from 5 to 30 min old.

Skin reactions to 48/80

Intradermal injection in the trunk. In the skin of blued animals, 48/80, like histamine, induces a round area of blueing whose diameter is linearly related to the log. dose injected in a constant volume of 0·1 ml. (Text-Fig. 5*b*). The slope of the dose-response line is much less than that of histamine, varying between 1·5 and 2·0. The blueing develops in 3–5 min and is more intense than that produced by histamine; the minimal effective dose distinguishable from traumatic blueing by the injection needle is about 0·2 μg. With doses of 2–4 μg the blue first appears at the periphery of the bleb and invades the centre. In cross-section of 48/80 lesions the blue area is confined to the two upper layers of the skin (Text-fig. 1*e*). The blueing is not uniform as it is with histamine; it is more intense in the region of the two plexuses of blood vessels, and especially that immediately over the muscle layer. The 48/80 does not spread downwards to the subcutaneous tissues. Even with doses of 30 μg in 0·1 ml., only the upper part of the muscle layer is blued, and there is no blueing of subcutaneous tissues or underlying muscle. This is not due to absence of histamine available for liberation in the muscle or subcutaneous tissues, because direct injection of 48/80 into these sites induced intense localized blueing. This difference in the spread of 48/80 and histamine from the injection site is not likely to be due to the difference in molecular weights, which are of the order of 540 for the trimer of 48/80 and 310 for the acid phosphate of histamine; the difference confirms the conclusions about the greater adsorption of 48/80 derived from the results of the 'constant-amount' titrations (Text-fig. 3*c* and Table 2).

The centre of the 48/80 bleb remains unblued with doses over 5 μg; at most it becomes pink with a purplish tinge, and sometimes there are small patches of haemorrhage (Text-fig. 1*f*). The absence of response may in part be due to temporary vasoconstriction by 48/80 itself or by the histamine it liberates, followed by recovery of normal permeability before the vessels become patent. But it is to a large extent due to a more permanent damage, presumably thrombotic, to the blood vessels, because the pink area remains when the surrounding skin is blackened by intra-arterial injections of indian ink; and the blocking of the vessels is evident in stained sections of the ink-treated skin.

Intradermal injection in the ear. Concentrations of 10 and 100 μg/ml. caused an immediate flushing; with 10 μg/ml. blueing started in 7 min, and with 100 μg/ml. in $1\frac{1}{2}$ min. Blueing in a histamine bleb develops uniformly over the treated area, whereas that due to 48/80 begins at the edge of the bleb and after 5 min, along the course of the large vessels, particularly the arteries, lying under it. These paravascular streaks then coalesce to form a uniformly blue lesion. Above 250 μg/ml. this blueing occurs only at the periphery of the bleb. There is a central area whose size varies with the concentration, in which within $1\frac{1}{2}$ min, the small superficial vessels thrombose without prior constriction. The underlying larger vessels become invisible but refill with circulating blood after about 10 min. By this time there is very slight blueing in the central area, so that by naked eye the lesion is faint purplish pink in the centre surrounded by deep blue (Pl. 2A). This central thrombosis and inhibition persist for over 6 hr.

Though 48/80 spreads outwards to blue an area 50–200 times that of the initial bleb, the resulting lesion is always round. Unlike histamine, 48/80, even at 10,000 μg/ml. does not leak in the lymphatic plexus beyond the confines of the bleb to produce a wedge-shaped blue lesion. Even when 48/80 is injected directly into the plexus, the blue area is approximately round (Pl. 2B). After 15 min or more a blue prolongation towards the base of the ear may develop, but this is observably the coloration of the lymphatic ducts with blue exudate from the bleb; it is not due to an increased permeability of blood vessels adjacent to the channels, as with histamine. These observations confirm the conclusions from the behaviour of 48/80 lesions in the skin of the trunk, that it is fixed firmly and rapidly to the tissue, whereas histamine at first moves freely, and begins to be fixed only after 2–3 min; and that inhibition at the centre is due to thrombosis of the vessels. Moreover, since 48/80 lesions blue as fast as histamine lesions, but no faster, and since the duration of the 48/80 effect is almost identical with that of histamine (Text-fig. 7*a*), it is probable that 48/80 liberates histamine very quickly and its latent period is mainly that of the liberated histamine.

Factors that change the skin-reactivity to 48/80. Blueing by 48/80, like that by histamine, is partly inhibited during anaesthesia and shock, and by

warming the animals in an atmosphere at 37° C. Sickly animals respond poorly to 48/80; this is probably not due to a diminution in the skin of histamine available for liberation, because the same animals are proportionally insensitive to histamine itself. As with histamine, most of the states of apparent insensitivity to 48/80 appear to be due to a poor blood supply to the skin.

Neoantergan intravenously is much less effective with 48/80 than with histamine. The effect of 8 mg/kg body weight 30 min before the injection of 48/80 is shown in Text-fig. 5*b*. Three concentrations of 48/80 and a saline control were titrated in blued animals, the four doses being randomized in a Latin square over sixteen sites. Three animals were used in each group so that each point is the mean of twelve readings. There is a 3-fold decrease in the 48/80 effect. In other tests 6 mg neoantergan/kg decreased the effect 5-fold, and 2 mg decreased it 2·5-fold. In a few animals the neoantergan greatly diminished the intensity but not the area of blueing by 48/80. The relative inefficiency of circulating neoantergan in antagonizing 48/80 suggests that 48/80 may have a more direct action on capillary permeability; histamine activity was reduced 9-fold by 0·02 mg neoantergan/kg, whereas as much as 6 mg/kg was required for a 5-fold decrease of 48/80 activity. Moreover, doses up to 15 mg/kg, which is near the LD 50 of neoantergan, did not abolish the response to 48/80. It is possible that at the centre of the bleb, 48/80 itself is in a sufficiently high concentration to increase capillary permeability by direct action. Nevertheless, since the area of the 48/80 lesion is diminished by neoantergan, the drug in the concentrations obtaining at the edge of the lesion clearly act by liberating histamine. In the centre of the lesion, either the increase in permeability is not wholly due to histamine, or the available neoantergan is overwhelmed by histamine rapidly liberated by the high concentration of 48/80.

Fixation of 48/80. Superinjection of 0·2 ml. saline into lesions of various ages made by 2 μg of 48/80, failed to increase the lesion-diameter after 2–3 min. With larger doses, 48/80 remained free for a longer period, and superinjection increased the lesion-diameter after 10 min or more.

Duration. The increased permeability, as tested by late blueing, induced by a single dose, lasts for 7–10 min, after which it declines, so that after 20–25 min no blueing occurs. In the graph illustrating this recovery (Text-fig. 7*b*), the arrows indicate the period between 12 and 15 min, when the blueing ceases to be intense and becomes relatively feeble; the decrease in lesion-diameter does not fully indicate the recovery of the vessels, which is substantially complete at 12–15 min.

Immunity. The three experiments in Table 4 exemplify the immunity induced by 48/80 to test injection of the same substance. Thus in Expt. I, 2 μg partly, and 10 μg almost wholly, immunize to test doses of 10 μg. In Expt. II, 50 μg immunize to 50 μg to some extent after 30 min and well after 3 hr, whereas after 5 hr the immunity is wearing off. Immunity is maximum

between 1·5 and 3·5 hr (Expt. III). In the ear, a concentration of 20 μg/ml. immunizes well to test doses of the same concentration. Here also, the immunity is at a maximum between 1·5 and 3·5 hr, and then passes off gradually and is gone at 5–6 hr.

TABLE 4. Immunizing action of intradermal 48/80 and histamine. Means of four to six lesions

Expt.	Immunizing agent and dose (μg)		Age of primary lesion (hr)	Mean diameter (mm) and intensity* of reaction to test dose of 48/80 (10 μg)	Histamine (2 μg)
I	48/80	0	2	8·5 + +	7·0 f.
		2	2	2·0 f.	2·0 f.
		10	2	8·0 f.	2·0 f.
II	48/80	50	0·5	9 +	8·5 +
			3	1·5 f.	2·0 f.
			5	4 +	8·0 f.
	Histamine	5	0·5	9 + +	2 ±
			3	9 + +	8 f.
			5	8·5 + +	9 +
	Saline		0·5	10 + +	10 + +
			3	10·5 +	10·5 +
			5	10·5 +	10·5 +
III	48/80	30	0·5	5·2 ±	7·3 +
			1·5	1·8 +	2·0 f.
			2·5	0·0	0·7 ±
			3·5	3·8 ±	5·5 +
			4·5	3·3 +	6·5 +
			5·5	7·2 +	6·7 +
			6·5	6·2 +	6·7 +
	Saline		2·5	8·7 + +	6·7 +

* Intensity: symbols as Table 3.

The site of action of 48/80. The accumulation of blue at the level of the two plexuses of blood vessels in skin treated with 48/80, as compared with the more general blueing with histamine (Text-fig. 1) and the visible development of blueing along the larger vessels of similarly treated ears, suggests strongly that the main reservoirs of histamine available for liberation are closely associated with the smaller arteries and veins. The association of this histamine with blood vessels may also be inferred from the intensity of blueing induced in body skin by the two substances. The amount of histamine that can be extracted from the skin of the trunk is about 3 μg/g (Feldberg & Miles, unpublished work); and a 10 mm lesion occupies about 150 mg skin. The intensity of blueing induced by enough 48/80 to give a lesion-diameter of 10 mm is far greater than that produced by injecting 0·5 μg histamine (the amount that 48/80 presumably liberates) in about 0·35 ml. saline, a volume that will give a 10 mm lesion (see Text-fig. 3*b*). We conclude that after injection a great deal of this dose of histamine is ineffective because it is distributed through relatively non-vascular tissue, and that the endogenous histamine which can be liberated by 48/80 must be concentrated near or in the blood vessels.

Cross-immunity with histamine. As already noted, the lesions developing

after the injection of a substance into an already-injected site are variable and not easily measured. Cross-immunity is nevertheless obvious by reason of a decline in intensity or size or both, of the blued area. Tables 3 and 4 exemplify the results usually obtained. Histamine and 48/80 each induces a good immunity to itself; histamine induces only a fair immunity to 48/80, but 48/80 induces a good immunity to histamine. In the ear, concentrations of 20 μg/ml. of both induced a good though not marked cross-immunity between 48/80 and histamine. It appears, therefore, that 48/80 immunizes both by liberating histamine, which in turn immunizes the susceptible vessels, and either by exhausting the histamine which can be liberated in the skin or by interfering with the mechanism of release of the bound histamine not liberated by the immunizing dose.

Skin reactions to leukotaxine

In most respects, the reaction of the blood vessels to leukotaxine were remarkably similar to those produced by 48/80. The chief difference lay in the very high concentration of leukotaxine required to induce thrombosis of the vessels.

Intradermal injection in the trunk and the ear. Like 48/80, leukotaxine induces in 3–5 min a round area of intense blueing, the diameter of which is in proportion to the log. dose in the constant-volume titration (Text-fig. 3*d*) and to the log. volume in the constant-amount titration (Text-fig. 5*c*). Leukotaxine appears to be strongly adsorbed to the skin tissues (Table 2); minimal blueing dose in 0·1 ml. is about 1 μg; inhibition of blueing at the centre of the bleb may occur with amounts from 10 μg upwards, absent in some animals until 100–500 μg is reached. This inhibition is not permanent; the area blues within 15–25 min. With large doses, 2 mg or more, small areas of permanent inhibition are produced. On cross-section, the blue leukotaxine blebs are like those of 48/80 (Text-fig. 1*e*).

In the ear, concentrations of 200 μg/ml. and over induce a general dilatation of the small vessels within 30 sec, and a rapid blueing that starts first along the small vessels, then the larger veins and finally along the larger arteries within the bleb. When concentrations of 300 μg or more per ml. are placed near one of the larger veins or arteries, a narrow band of vasoconstriction may appear within 1 min, disappearing after 1–2 min. With concentrations above 2·5 mg/ml., thrombosis of the vessels may occur at the centre of the bleb, though it is less severe and less regular in occurrence than that induced by 48/80. The blued areas are always approximately round (cf. Pl. 2B) whether made by intradermal or intralymphatic injection.

Effect of anaesthesia and neoantergan. Blueing is diminished in area and intensity during bromethol and urethane anaesthesia. Intravenous neoantergan, 3–8 mg/kg body weight, diminishes the leukotaxine effect from 1·5- to

3-fold (Text-fig. 5*c*); the degree of neutralization is of the same order as that of 48/80, but rather less marked.

Time-course of the leukotaxine effect. By the superinjection method, putting 0·2 ml. saline into 5 μg lesions, all the leukotaxine appeared to be fixed in 16 min and most of it in the first 5–8 min. The capillaries of the skin treated with 10 μg wholly regained their normal impermeability within 25 min; most of them had recovered after 10 min (Text-fig. 7*a*, *b*).

Immunity. Table 5 typifies the results of several tests of leukotaxine immunity. Three immunizing doses of each substance, histamine, 48/80 and leukotaxine were used, and immunity tested after 2 hr by superinjecting the lowest dose again. As is common in all such tests, immunity is best when the

TABLE 5. Immunity and cross-immunity induced in the skin by leukotaxine. Primary lesions 2 hr old. Means of four lesions

Immunizing agent and dose (μg)		Mean diameter (mm) and intensity* of reaction to test dose of: Histamine (2 μg)	48/80 (5 μg)	Leukotaxine (17 μg)
Histamine	8	7·4±	N.T.	7·0 + +
	4	7·0±	N.T.	6·2 + +
	2	7·1±	7·0±	7·4 + +
	0	10·0 +	7·8 + +	7·6 + +
48/80	20	N.T.	3·4±	2·0 +
	10	N.T.	3·5±	2·2 +
	5	8·0±	4·6±	5·0 +
	0	9·0 +	7·2 + +	8·0 + +
Leukotaxine	67	N.T.	N.T.	4·0±
	33	N.T.	N.T.	3·4±
	17	9·0±	7·1 +	4·8±
	0	9·5 +	7·8 + +	7·4 + +

* Intensity: symbols as in Table 3.
N.T. = No test.

immunizing dose is 4–10 times greater than the test dose. In this example immunity must be judged as much by decrease in intensity as by decrease in diameter of the blueing. Leukotaxine immunizes well to itself but only moderately to histamine and 48/80. Histamine immunizes moderately to itself and 48/80, and slightly to leukotaxine; whereas 48/80, though immunizing only moderately to histamine, immunizes well to itself and leukotaxine. Leukotaxine immunity is maximal in 1–2 hr, and has passed off by the 4th hr.

DISCUSSION

The study of increased permeability in the skin of the trunk of blued guinea-pigs has shown that after a latent period of 1½–3 min, injected histamine induces a gross increase in capillary permeability, which is maximum within the next 5 min. In concentrations of from 1 to 100 μg/ml. it can be characterized by the response of blued animal to varied doses in constant injection-volume

and to constant doses in varied injection-volume. By the superinjection of saline into histamine lesions of varying ages, and by the intravenous injection of dye at varying periods after the intradermal histamine, it can be shown that from 3 to 10 min free histamine is disappearing from the lesion, and the capillaries are recovering their normal low permeability. By the superinjection of histamine into recovered histamine-treated areas, it can be shown that as they recover, the vessels become partly immune to histamine; the immunity increases up to 2 hr, and declines after 4 hr. This immunity is not due to any interruption of the blood supply to the immunized tissues. With concentrations above 100 μg/ml. no blueing due to increased permeability is detectable.

In the ear, the outstanding peculiarity is the high concentration required to produce even a 15 min inhibition of blueing at the centre of the lesion, and the transience of the effect with lower concentrations (p. 237 and Table 6).

TABLE 6. Comparison of the approximate minimal effective concentrations of histamine, 48/80 and leukotaxine in the skin of the trunk (10 mm blebs) and the ear (3 mm blebs)

		Minimal effective concentration in μg/ml.	
Effect	Drug	Trunk	Ear
Blueing	Histamine	1–2	0·5
	48/80	2	5·0
	Leukotaxine	10	—
Temporary inhibition of blueing, and arterial constriction*	Histamine	10–30	50
	48/80	10–30	250
	Leukotaxine	100	300
Thrombosis of blood vessels	48/80	30–50	250
	Leukotaxine	2500	5000
Leak of free drug into surrounding lymphatic plexus	Histamine	—	1000
	48/80	—	>10000
	Leukotaxine	—	>10000

* Presumed in trunk, demonstrable in ear.

In the skin of the trunk inhibition lasts for hours. For this relative permanence we postulated an arterial vasoconstriction, and therefore an absence of exudation, for periods longer than the duration of increased permeability. This relation does not hold in the ear because vasoconstriction is visibly relaxed within 3–7 min, and increased permeability lasts up to 8 min and may persist, though feebly, for 12–15 min. The relative insensitivity of the ear to this inhibitory effect may be a reflexion of its greater vascularity; either the injected histamine is swept away by the blood and lymph streams more quickly or much of the injected histamine is taken up by receptors in the numerous small vessels, so that on reaching the underlying larger vessels its concentration is too low for vasoconstriction. As Table 6 shows, the ear displays the same relative insensitivity towards 48/80 and leukotaxine, and presumably for the same reasons.

The action of 48/80 in many ways resembles that of histamine. Both substances have a latent period of about 3 min. When blueing starts they become 'fixed' to the tissues; as blueing proceeds, the vessels recover their normal low permeability and are apparently normal at the end of 10–20 min. They are at this time partly immune to second doses of the same size, and the immunity increases for 2 hr; and after 4 hr it begins to decline. But there are marked differences, which raise the question how far the release of histamine accounts fully for the action of 48/80 on capillary permeability? First, the distribution of blueing by histamine is general, but that produced by 48/80 is concentrated in the region of the arteries and veins in both the skin of the trunk and the ear, suggesting that bound histamine is localized in or near these larger vessels. Secondly, whereas high concentrations of histamine inhibit blueing by altering the immunity of the vessels, high concentrations of 48/80 do so by damaging the vessels so that thrombosis occurs. Thirdly, the two substances differ in their susceptibility to circulating neoantergan; we have to assume either that 48/80 has a direct action on capillaries, or that the histamine it releases is less sensitive than injected histamine to neoantergan. Since 48/80 is well established as a potent histamine-liberator (Feldberg & Paton, 1951; Paton, 1951; Paton & Schachter, 1951) the second assumption is the more justified, particularly because insensitivity to antihistaminics is displayed by other known histamine-liberators (MacIntosh & Paton, 1949). Although in our experiments complete extinction of 48/80 blueing by neoantergan was impossible, partial neutralization was achieved by 200 times the dose required to neutralize histamine to the same extent. The parallelism of dosage-response in untreated and neoantergan-treated animals (Text-fig. 5*b*) is consistent with a true neutralization, and with the hypothesis that the unneutralized blueing is due to some 'pharmacological inaccessibility' of the liberated histamine rather than to a direct action of 48/80 on the capillaries. This inaccessibility may result from the ready adsorption of 48/80 to the tissues, and the concentration of the depots of available histamine near the blood vessels. This histamine is perhaps 'intrinsic' in Dale's (1948) sense that it is released from the cells on which it acts. Our observations are not exact enough to decide this point. But whatever reason for the relative inefficacy of neoantergan with 48/80, the fact indicates that we need not demand of a presumed histamine-liberator that its susceptibility to inhibition by neoantergan shall be of the same order as that of histamine.

Our observations on 48/80 provide a pattern of the intradermal behaviour of a histamine-liberator, for comparison with substances like leukotaxine, whose capacity to liberate histamine is in doubt. Menkin (1936, 1938*a*, *b*) isolated leukotaxine from sterile inflammatory exudates, and described its capacity to increase capillary permeability. Later work (Duthie & Chain, 1939; Spector, 1951) proved it to be a family of positively chemotactic

polypeptides, of which the larger members have this action on the capillaries. Rocha e Silva & Dragstedt (1941) postulated that leukotaxine acted via histamine, and Dekanski (1949) showed that on intradermal injection it increased the histamine equivalent in cat's skin, and that its 'blueing' action was neutralized by neoantergan. Menkin (1936, 1938*a*), and Cullumbine & Rydon (1946) deny the mediation of histamine because leukotaxine does not cause contraction in isolated smooth muscle, and the blueing is not antagonized by neoantergan (Cullumbine, 1947). We shall not, however, expect a histamine-liberator to cause isolated smooth muscle to contract. Menkin (1938*a*) showed that leukotaxine did not do so; but neither does 48/80 (Paton, 1951). Nor is Cullumbine's failure to detect a neoantergan effect by roughly quantitative tests unexpected. Leukotaxine in the skin can have a very shallow dosage-response slope, so that as much as a 10-fold drop in potency might diminish the diameter of the lesion by as little as 2 mm. Unless the neutralization test is made at several dose-levels in several animals, a genuine though small neutralization effect might well be missed. The relative insusceptibility of leukotaxine to neoantergan may well be determined by factors responsible for the similar behaviour of 48/80 and other liberators. Leukotaxine differs from histamine in spreading less readily through the tissues after local injection, as first recorded by Menkin, and in failing to induce inhibition at the centre of injection blebs, except in high concentrations. If it acts solely by histamine-liberation, inhibition of blueing may be impossible because there is not enough histamine to reach required concentration, even though it is localized round the vessels upon which it ultimately acts. An inhibiting dose of histamine, say 5 μg, produces a lesion about 8 mm in diameter, involving about 60 mg of skin. Ignoring spread to adjacent tissues, we arrive at an average inhibiting concentration of 83 μg histamine/g skin; whereas the normal content of extractable histamine in the skin of the trunk is of the order of 3 μg/g (W. Feldberg & A. A. Miles, unpublished work). This histamine is presumably all available for liberation. Leukotaxine, except for its inability to induce thrombosis in moderate concentrations, behaves in most respects like 48/80. Both these substances resemble histamine in several respects, notably the similarity of the time-course of blueing (the lag period and duration of permeability) and in the induction and duration of immunity.

We can attach weight to these likenesses as a proof that leukotaxine acts through histamine if the effects are peculiar to histamine. This may well be so, but it should be noted that the time-course of blueing, and duration of permeability is shared by a large number of blueing substances besides 48/80, e.g. neoarsphenamine, stilbamidine, acetylcholine, peptone and hypotonic saline (unpublished work); and though some of these substances are probably histamine-liberators, the time course of their effect may reflect very general properties of vascular endothelium. The evidence obtained from the cross-

immunization tests, which are summarized in Table 7, may be misleading for a similar reason, that in the endothelium there is only one kind of site which is affected, and made resistant, by a wide variety of substances. In addition, cross-immunity between substances other than histamine does not necessarily imply the same site of action. Cross-immunity between histamine and another substance may well be an expression of true histamine immunity; but cross-immunity between two presumed histamine-liberators may be due either to exhaustion of the available histamine, to the immunization of vessels by liberated histamine or to an inhibition of the mechanism of histamine release.

TABLE 7. Summary of tests of immunity and cross-immunity to increased capillary permeability in the skin

	Immunity		
	Tested with		
Induced by	Histamine	48/80	Leukotaxine
Histamine	+ +	+	+
48/80	+ + +	+ + +	+ + +
Leukotaxine	+ +	+	+ + +

+, + +, + + + = moderate, good and marked immunity.

It should be noted here that we have used the very general terms 'immunity' and 'immunization' in this connexion, rather than 'refractoriness' or 'refractory state' because we have applied them generally to drug-resistance induced in the skin by substances other than histamine. The terms can legitimately be extended to cover these phenomena; and though our histamine 'immunity' may be the same phenomenon as Lewis & Grant's (1924) refractoriness to histamine whealing in man, we are not in a position to equate them. The two phenomena have much in common; whealing was inhibited in man by occlusion of the blood supply for 10 min and our blueing is inhibited by withholding the circulating dye for 10 min. Both were relative, never demonstrably absolute. But whereas in man the refractory state lasts 5–10 min, the immune state lasts several hours in the guinea-pig. The immunity induced by histamine, leukotaxine and 48/80 in some respects resembles the immunity to whealing of nervous origin described by Grant, Pearson & Comeau (1935). In both cases it lasts for several hours, and both are explicable in terms of an exhaustion of a substance like histamine or H-substance increasing capillary permeability.

The cross-immunity we demonstrated was never very solid. This may have been due to deviations from the exact superposition of the test injection on the region of immunized tissue, and to the different degrees of tissue affinity of the three substances tested. It may, however, reflect a distinction between the modes of action; though as regards leukotaxine, it is probably significant that the histamine-liberator 48/80 immunized well against leukotaxine. Although cross-immunity should not be accepted as a sufficient single criterion

of similarity of action, in conjunction with other evidence it is strongly suggestive.

Our various tests of the increase of capillary permeability in the skin by the three substances, do not constitute a rigorous proof that the effect of 48/80 and leukotaxine on the capillary endothelium of the skin is mediated by histamine. Nevertheless, taking the evidence as a whole, our observations on these three substances are all consistent with the view that leukotaxine acts as a histamine-liberator in inflammatory lesions. The question whether histamine, through leukotaxine or some other endogenous liberator, is the *sole* mediator of the increased capillary permeability in inflammation, is less easy to answer. A given blood vessel made permeable by histamine or leukotaxine becomes substantially immune to the further action of the drugs within 20 min. The 'perpetuation of increased vessel permeability due to the gradual accumulation of peptides in the tissues' postulated by Spector (1951) in the natural course of inflammation must therefore be produced either by partial stimulation, and consequently only a partial immunization, of some parts of the vessel, leaving other parts for later stimulation; or, what is more consistent with the observed expansion of most progressive inflammatory lesions, by a gradual outward spread of leukotaxine to as yet unaffected vessels, leaving impermeable those already affected. But even with these refinements, the major role of leukotaxine is not necessarily established in inflammation, particularly infective inflammation. For example, the time-course of blueing by several clostridial exotoxins is quite different from that of leukotaxine (unpublished work); blueing may take an hour to develop and permeability persist for several hours; and cross-immunity with histamine and histamine-liberators is difficult to demonstrate. The behaviour of *Cl. oedematiens* exotoxin is singular, because the increased capillary permeability induced by a single dose persists for more than 30 hr. This observation probably has some bearing on the extensive oedema which accompanies infection by this microbe, but in this context it is chiefly interesting as indicating the existence of substances of pathological importance which appear to alter capillary permeability in a manner quite different from that of histamine or histamine-liberators.

SUMMARY

1. The increase in capillary permeability in the skin of the trunk, and ear of guinea-pigs was measured by the size and intensity of the blue lesion induced by the intradermal injection of histamine, the histamine-liberator 48/80, and leukotaxine, in animals with pontamine sky blue 6X in their circulation. In the trunk, the mean lesion-diameter from graded doses of these drugs in a constant volume is proportional to the log. dose; and for a constant dose in graded injection-volumes it is proportional to the log. volume.

other evidence it is strongly

·ermeability in the skin by the
proof that the effect of 48/80
of the skin is mediated by
a whole, our observations on
ιe view that leukotaxine acts
ons. The question whether
dogenous liberator, is the *sole*
in inflammation, is less easy
by histamine or leukotaxine
›n of the drugs within 20 min.
γ due to the gradual accumu-
·pector (1951) in the natural
ed either by partial stimula-
ıtion, of some parts of the
or, what is more consistent
inflammatory lesions, by a
unaffected vessels, leaving
vith these refinements, the
tablished in inflammation,
, the time-course of blueing
; from that of leukotaxine
› develop and permeability
ı histamine and histamine-
of *Cl. oedematiens* exotoxin
ıbility induced by a single
probably has some bearing
:on by this microbe, but in
: existence of substances of
ɩpillary permeability in a
istamine-liberators.

in of the trunk, and ear of
ɔf the blue lesion induced
mine-liberator 48/80, and
ᛕ in their circulation. In
loses of these drugs in a
ıd for a constant dose in
;. volume.

2. The linear dosage-response to histamine, 48/80 and leukotaxine forms the basis of an assay method in the 'constant-volume' titration; 'constant-dose' measurements can be used to measure the affinity of skin tissue for the three substances.

3. Histamine has a relatively low, and 48/80 and leukotaxine a relatively high, affinity for skin tissue. Injected histamine spreads readily with the injection fluid to the subcutaneous tissues and lymphatic channels, whereas 48/80 and leukotaxine tend to remain in the skin.

4. All three substances increase capillary permeability within 3–5 min of injection, and their action is mostly finished in 10–15 min, and wholly so in 30 min. Between 15 and 30 min after the injection, the capillaries not only begin to recover their normal low permeability, but become immune to further doses of the drug. The immunity is greatest from 1–3 hr and declines after 4–5 hr.

5. Histamine blueing is general throughout the depth of the skin; 48/80 blueing is most intense in the region of arterioles, venules and the smaller arteries and veins, suggesting that the histamine available for liberation is located in these regions.

6. High local concentrations of histamine inhibit blueing by inducing severe local vasoconstriction during the period of increased permeability, so that by the time the constriction is relaxed the vessel walls have recovered their normal low permeability. High local concentrations of 48/80 inhibit blueing by thrombosing the blood vessels.

7. Anaesthesia, shock and chilling decrease blueing. The effect appears to be secondary to a decline in local intravascular pressures, and not to resistance of the capillaries to permeability-inducing substances.

8. Circulating neoantergan strongly antagonizes histamine blueing. It is over 200 times less effective with 48/80 and leukotaxine, but a definite antagonism to both substances is demonstrable.

9. The three substances induce a substantial cross-immunity to one another. The cross-immunity to histamine is presumably due to histamine liberated by 48/80 and leukotaxine. Cross-immunity between histamine-liberators may be due either to histamine immunization of the blood vessels, exhaustion of histamine or inhibition of the mechanism of histamine release.

10. The similarities in the time-course and duration of the permeability effect, and in the induction of cross-immunity, give strong support to the view that leukotaxine increases capillary permeability by liberating histamine. In all the tests made, the differences between leukotaxine and histamine were paralleled by differences between 48/80 and histamine, excepting the thrombosing effect of strong 48/80. Since 48/80 is an established histamine-liberator, these differences are not good evidence that substances displaying them do not liberate histamine.

We are greatly indebted to Dr E. J. de Beer at the Wellcome Research Laboratories, Tuckahoe, U.S.A., for a generous gift of the compound 48/80, and to our colleague Dr J. H. Humphrey for leukotaxine.

REFERENCES

Bain, W. H. (1949). The quantitative comparison of histamine antagonists in man. *Proc. R. Soc. Med.* **42**, 615–623.

Baltzly, R., Buck, J. S., de Beer, E. J. & Webb, F. J. (1949). A family of long-acting depressors. *J. Amer. chem. Soc.* **71**, 1301–1305.

Cullumbine, H. (1947). Leukotaxine and histamine. *Nature, Lond.*, **159**, 841–842.

Cullumbine, H. & Rydon, H. N. (1946). A study of the formation, properties and partial purification of leukotaxine. *Brit. J. exp. Path.* **27**, 33–46.

Dale, H. H. (1948). Antihistamine substances. *Brit. med. J.* ii, 281–283.

Dekanski, J. (1949). The effect of protein hydrolysates (leukotaxine) on skin-histamine in cats. *J. Physiol.* **108**, 233–245.

Duthie, E. S. & Chain, E. (1939). A polypeptide responsible for some of the phenomena of acute inflammation. *Brit. J. exp. Path.* **20**, 417–429.

Evans, D. G., Miles, A. A. & Niven, J. S. F. (1948). The enhancement of bacterial infections by adrenaline. *Brit. J. exp. Path.* **29**, 20–39.

Feldberg, W. & Paton, W. D. M. (1951). Release of histamine from skin and muscle in the cat by opium alkaloids and other histamine liberators. *J. Physiol.* **114**, 490–509.

Grant, R. T., Pearson, R. S. B. & Comeau, W. J. (1935). Observations on urticaria provoked by emotion, by exercise and by warming the body. *Clin. Sci.* **2**, 253–272.

Hechter, O. (1946). Mechanism of hyaluronidase action in skin. *Science*, **104**, 409–411.

Lewis, T. & Grant, R. T. (1924). Vascular reactions of the skin to injury. II. The liberation of a histamine-like substance in injured skin; the underlying cause of factitious urticaria and of wheals produced by burning; and observations upon the nervous control of certain skin reactions. *Heart*, **11**, 209–265.

Long, D. A. & Miles, A. A. (1950). Opposite actions of thyroid and adrenal hormones in allergic hypersensitivity. *Lancet*, i, 492–495.

MacIntosh, F. C. & Paton, W. D. M. (1949). The liberation of histamine by certain organic bases. *J. Physiol.* **109**, 190–219.

Matolsty, A. G. & Matolsty, M. (1951). The action of histamine and anti-histaminic substances on the endothelial cells of the small capillaries in the skin. *J. Pharmacol.* **102**, 237–249.

Menkin, V. (1936). Studies on inflammation. XII. Mechanism of increased capillary permeability. A critique of the histamine hypothesis. *J. exp. Med.* **64**, 485–502.

Menkin, V. (1938*a*). Studies on inflammation. XIV. Isolation of the factor concerned with increased capillary permeability in injury. *J. exp. Med.* **67**, 129–144.

Menkin, V. (1938*b*). Studies on inflammation. XV. Concerning the mechanism of cell migration. *J. exp. Med.* **67**, 145–152.

Miles, A. A. (1949). The fixation of diphtheria toxin to skin tissue with special reference to the action of circulating antitoxin. *Brit. J. exp. Path.* **30**, 319–344.

Miles, A. A. & Niven, J. S. F. (1950). The enhancement of infection during shock produced by bacterial toxins and other agents. *Brit. J. exp. Path.* **31**, 73–95.

Paton, W. D. M. (1951). Compound 48/80: a potent histamine liberator. *Brit. J. Pharmacol.* **6**, 499–508.

Paton, W. D. M. & Schachter, M. (1951). The influence of an antihistamine drug on the release of histamine in the unanaesthetized dog. *Brit. J. Pharmacol.* **6**, 509–513.

Rocha e Silva, M. & Dragstedt, C. A. (1941). Observations on the trypan blue capillary permeability test in rabbits. *J. Pharmacol.* **73**, 405–411.

Spector, W. G. (1951). The role of some higher peptides in inflammation. *J. Path. Bact.* **63**, 93–110.

Wadley, F. M. (1949). The use of biometric methods in comparisons of acid-fast allergens. *Amer. Rev. Tuberc.* **60**, 131–139.

LES
earch Laboratories, Tuckahoe,
eague Dr J. H. Humphrey for

igonists in man. *Proc. R. Soc.*
. family of long-acting depres-
d., **159**, 841–842.
, properties and partial purifi-
1–283.
ie) on skin-histamine in cats.
ie of the phenomena of acute
ent of bacterial infections by
m skin and muscle in the cat
114, 490–509.
ations on urticaria provoked
, 253–272.
cience, **104**, 409–411.
njury. II. The liberation of
of factitious urticaria and
vous control of certain skin
adrenal hormones in allergic
stamine by certain organic
anti-histaminic substances
harmacol. **102**, 237–249.
ased capillary permeability.
e factor concerned with in-
14.
echanism of cell migration.
ith special reference to the
during shock produced by
or. *Brit. J. Pharmacol.* **6**,
amine drug on the release
09–513.
he trypan blue capillary
ation. *J. Path. Bact.* **63**,
ns of acid-fast allergens.

A

B

A

B

VASCU

A. Untreated ear of blued
due to the relative th
B. The same ear as in A a
phatic plexus. The inc
of intense blueing is ap

A. Ear of a blued guinea-p
at the centre of the le
B. Ear of a blued guinea
phatic plexus. The op
ear. The area of inter

EXPLANATION OF PLATES

Plate 1

A. Untreated ear of blued guinea-pig, showing the degree of initial opacity near the main vessels, due to the relative thickness of the ear in that region. ×5.

B. The same ear as in A after injection of strong histamine (1000 μg/ml.) directly into the lymphatic plexus. The indian-ink stain on the skin at the top marks the injection site. The area of intense blueing is approximately wedge shaped, with the apex at the base of the ear. ×5.

Plate 2

A. Ear of a blued guinea-pig injected with strong 48/80 (500 μg/ml.). There is inhibition of blueing at the centre of the lesion, with the thrombosed superficial vessels in sharp focus. ×5.

B. Ear of a blued guinea-pig after injection of strong 48/80 (150 μg/ml.) directly into the lymphatic plexus. The opacity round the main vessels on the left is due to the thickness of the ear. The area of intense blueing is approximately circular. ×5.

Annu. Rev. Immunol. 1997. 15:675–705

HUMAN CHEMOKINES: An Update

Marco Baggiolini, Beatrice Dewald, and Bernhard Moser
Theodor Kocher Institute, University of Bern, CH 3000 Bern 9, Switzerland;
e-mail: baggiolini@tki.unibe.ch

KEY WORDS: structure, structure-activity relations, receptors, leukocyte migration, pathophysiology, HIV

ABSTRACT

Interleukin 8, the first chemokine to be characterized, was discovered nearly ten years ago. Today, more than 30 human chemokines are known. They are often upregulated in inflammation and act mainly on leukocytes inducing migration and release responses. The present review deals largely with the new developments of the last three years. Several structural studies have shown that most chemokines form dimers. The dimers, however, dissociate upon dilution, and the monomers constitute the biologically active form. Chemokine activities are mediated by seven-transmembrane-domain, G protein coupled receptors, five of which were discovered in the past three years. The primary receptor-binding domain of all chemokines is near the NH_2 terminus, and antagonists can be obtained by truncation or substitutions in this region. Major progress has been made in the understanding of chemokine actions on T lymphocytes that respond to several CC chemokines but also to IP10 and Mig, two CXC chemokines that selectively attract Tcells via a novel receptor. Effects of chemokines on angiogenesis and tumor growth have been reported, but the data are still contradictory and the mechanisms unknown. Of considerable interest is the recent discovery that some chemokines function as HIV-suppressive factors by interacting with chemokine receptors which, together with CD4, were recognized as the binding sites for HIV-1.

INTRODUCTION

Chemokines constitute a large family of small cytokines with four conserved cysteines linked by disulfide bonds (Figure 1). Two subfamilies, CXC and CC chemokines, are distinguished according to the position of the first two cysteines, which are separated by one amino acid or are adjacent. Most chemokine sequences were derived from cDNAs encoding proteins of 92 to 125 amino acids with leader sequences of 20 to 25 amino acids. In humans, the genes of the CXC chemokines are clustered on chromosome 4, and those of the CC

0732-0582/97/0410-0675$08.00

Table 1 Ligand selectivity of chemokine receptors

Receptors	New	Old nomenclature	Ligands[a]
CXC chemokines	CXCR1	IL-8R1 (type A)	IL-8
	CXCR2	IL-8R2 (type B)	IL-8, GROα,β,γ, NAP-2, ENA78, GCP-2
	CXCR3	IP10/MigR	IP10, Mig
	CXCR4	LESTR, HUMSTR	SDF-1
CC chemokines	CCR1	RANTES/MIP-1αR	RANTES, MIP-1α, MCP-2, MCP-3
	CCR2a/b	MCP-1RA/B	MCP-1, MCP-2, MCP-3, MCP-4
	CCR3	EotaxinR, CC CKR3	eotaxin, RANTES, MCP-3, MCP-4
	CCR4	CC CKR4	RANTES, MIP-1α, MCP-1
	CCR5	CC CKR5	RANTES, MIP-1α, MIP-1β

[a]K_d of 0.1 to 10 nM or Ca^{2+} mobilization at <10 nM.

chemokines on chromosome 17. As indicated by the rapidly expanding literature, chemokines are increasingly studied because of their actions on leukocytes and their role in inflammation and immunity. Additional interest is arising from the recent discovery of a function of chemokines and chemokine receptors in HIV infection. Because of space limitations, we shall concentrate on new, biologically important findings on human chemokines reported during the past three years. For older reports, the reader may turn to our last, comprehensive review, which appeared at the beginning of 1994 and covered the literature up to the middle of 1993 (1). Several other reviews that have appeared since 1994 may also be consulted (2–4). The new, simplified nomenclature for chemokine receptors, which was elaborated at the 1996 Gordon Research Conference on "Chemotactic Cytokines" (Table 1), will be used.

CHEMOKINE STRUCTURE

Three-Dimensional Structure of CXC and CC Chemokines

The first chemokines for which the three-dimensional structure was determined are PF4 and IL-8. Their monomeric structures are very similar and comprise a NH_2-terminal loop, three antiparallel β-strands connected by loops, and a COOH-terminal α-helix. IL-8 forms globular dimers in solution consisting of a six stranded antiparallel β-sheet (made up of the three β-strands of each subunit) and two antiparallel helices lying across the β-sheet. The axis of symmetry is located between residues 26 and 26′ at the center of strands $\beta 1$ and $\beta 1'$ (5–7). PF4 forms an asymmetric tetramer by the dimerization of dimers of the IL-8 type (8). The structures of GROα and NAP-2 are similar to that of IL-8, at both the monomer and dimer level (9–12). GROα differs from IL-8 in the NH_2-terminal region containing the ELR motif, the NH_2-terminal loop extending between residues 12 and 23, and the turn between residues 31 and 36,

which is linked to the NH_2-terminal region through the 9 to 35 disulfide bond. These regions are involved in receptor interaction (13), and the differences could determine receptor specificity.

The three-dimensional structure of MIP-1β (14) and RANTES (15, 16) consists of dimers formed by interaction of the NH_2-terminal regions of the monomers yielding an elongated, cylindrical shape. The axis of symmetry is located between residues 10 and 10′ in MIP-1β and 9 and 9′ in RANTES. These residues are part of an additional, short antiparallel β-sheet formed by the strands $\beta 0$ and $\beta 0'$. The distribution of surface hydrophobicity differs markedly between CXC and CC chemokines (17), and this is believed to be the reason for the different mode of dimerization (7, 17). The core hydrophobicity clusters of CXC and CC chemokines, by contrast, are at equivalent positions, in agreement with the similarity of the three-dimensional structure of the monomers.

Monomers and Dimers

Because most chemokines dimerize in solution, the dimer was generally assumed to be the biologically relevant form. Although the biological activities are observed at nanomolar concentrations, while the dissociation constants are mostly in the micromolar range (18, 19), this remained the prevailing view until proof was provided that IL-8 can function as a monomer (20). For this purpose an IL-8 analog was synthesized with N-methyl-Leu instead of Leu at position 25 to disrupt hydrogen bonding between the monomers. The methylated analog remains monomeric even at millimolar concentration and has nonetheless full activity on neutrophils (20). Its three-dimensional structure is similar to that of the subunits of the IL-8 dimer, indicating that the constraints imposed by dimer formation are not critical for the tertiary fold (21). Among the CC chemokines, monomeric forms of MIP-1α were studied extensively and found to be biologically active (22–24). Data obtained by size exclusion HPLC, analytical ultracentrifugation, chemical cross-linking, and titration microcalorimetry support the conclusion that IL-8 and MCP-1, at physiological concentrations, occur predominantly as monomers (18, 25). Platelet basic protein (PBP) and its congeners including NAP-2 appear to behave in a similar manner (10). A different view was presented for MCP-1 based on the observations that chemically cross-linked dimers were active at nanomolar concentrations and that an antagonist obtained by NH_2-terminal truncation formed a heterodimer with wild-type MCP-1 acting as a dominant negative inhibitor (26).

NEW CHEMOKINES AND CHEMOKINE ACTIONS

Many new human chemokines have been discovered in the past few years, and considerable new information has been gathered about their activities on

different types of leukocytes. Several of the more than 30 gene products, however, are known just by the cDNA-deduced amino acid sequence, and little information is available on biological effects. The dendrogram in Figure 1 presents all human chemokines described to date. Although the number has grown considerably, CXC and CC chemokines still fall into completely separate branches. Most new chemokines belong to the CC subfamily. They include: (i) eotaxin (27) and MCP-4 (28), which are structurally closely related to MCP-1; (ii) HCC-1 and a newly identified alternative splicing variant HCC-3, which are similar to MIP-1α (29); (iii) TARC (thymus and activation-regulated chemokine), obtained from thymus-derived RNA, and reported to be chemotactic for T cell lines but not for blood T lymphocytes, monocytes, or neutrophils (30); and (iv) HCC-2, a CC chemokine with six instead of four cysteines located at identical positions as in the murine chemokines C10 (31), CCF18 (32), MRP-2 (33), and MIP-1γ (34). Several new chemokine cDNAs were isolated from human tissues within a large-scale cDNA sequencing program (Human Genome Sciences Ltd, Rockville, MD), and the mature proteins were expressed in insect cells (Figure 1). Some of the new CC chemokines are virtually inactive on granulocytes, monocytes, and lymphocytes, suggesting that they may stimulate precursor cells or other targets. It is important to realize, however, that the actual NH_2 terminus of these chemokines is unknown and that lack of activity may result from incorrect processing upon expression in insect cells.

The following subsections describe several newly discovered chemokines and some known ones for which interesting new properties were found. The chemokine receptors, to which reference is made, are described in a later section and Table 1.

The Monocyte Chemotactic Proteins

MCP-1 was the first CC chemokine to be characterized biologically and shown to attract monocytes but not neutrophils (1). Two related proteins, MCP-2 (HC-14) and MCP-3, were subsequently identified (35), and MCP-4 was described only recently (28). The MCPs share a pyroglutamate proline NH_2-terminal motif and are structurally closely related to each other and to eotaxin (56% to 71% amino acid sequence identity) (Figure 1). They have a broad spectrum of activity and attract monocytes (28, 36), T lymphocytes (37–39), and basophil leukocytes (1, 40–42). MCP-2, MCP-3, and MCP-4, in contrast to MCP-1, are also active on eosinophil leukocytes (28, 40, 42). These patterns can be explained with a minimum of three receptors: CCR1 recognizing RANTES, MCP-2, and MCP-3; CCR2 recognizing all MCPs; and CCR3 recognizing RANTES, MCP-3, MCP-4, and eotaxin. Monocytes and presumably also basophils express CCR1 and CCR2, and eosinophils express CCR1 and CCR3

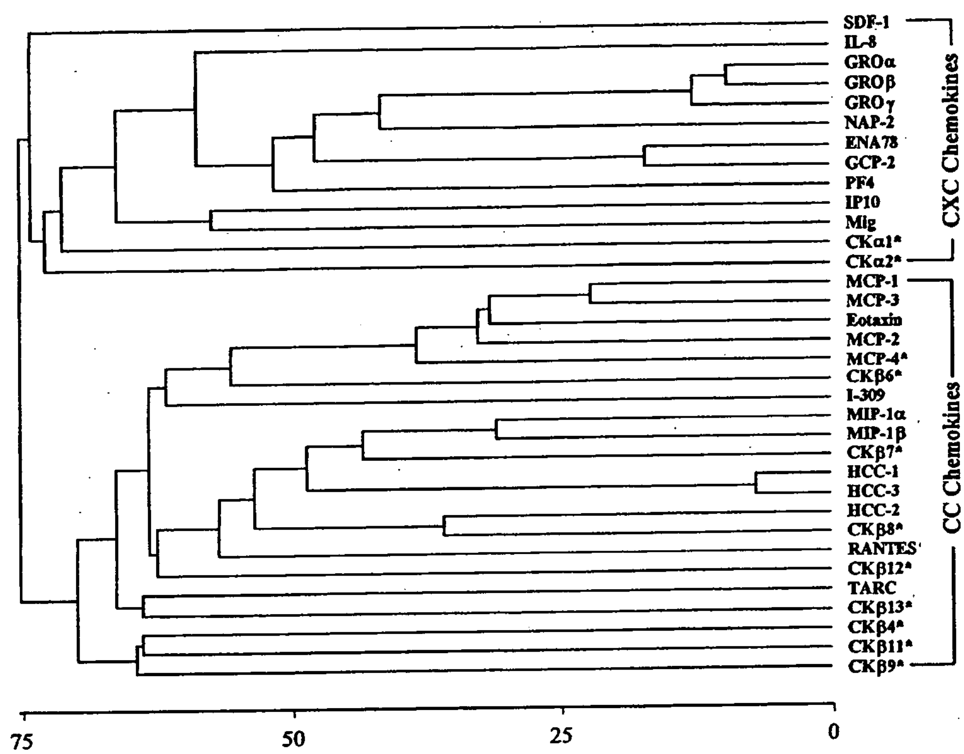

Figure 1 Structure similarity diagram of human CXC and CC chemokines. Similarity scores of the proteins were determined by the average linkage cluster analysis (181). The gap penalty, window size, filtering level, and K-tuple size parameters for pairwise alignments were set at 3, 10, 2.5 and 1, respectively. Distance to the branching points indicates the percent of sequence divergence. Highest pairwise similarity (7.5% divergence) is obtained for the CC chemokines HCC-1 and HCC-3, which differ only in the NH_2-terminal region preceding the adjacent cysteines. Overall similarity between the two subfamilies of chemokines is 24.5% (75.5% divergence). Chemokines from Human Genome Sciences Ltd. are listed by their laboratory abbreviation, CKα or CKβ (for CXC and CC chemokines, respectively) followed by a number. GeneBank accession numbers for the sequences are (from top to bottom): U16752, M17017, J03561, M36820, M36821, M54995, L37036, P80162, M20901, X02530, X72755, X14768, X72308, U18941, P80075, M57502, X03754, J04130, Z49270, Z70293, Z70292, M21121, and D43767. The accession numbers for the chemokines marked with an asterisk are not available.

(2, 3, 43, 44). The picture may become more complex when CCR4 and CCR5 are considered, but the distribution of these receptors and their selectivity must first be studied in more detail. In basophils, MCP-1 is highly effective as a stimulus of histamine and peptido-leukotriene release, but it has only moderate chemotactic activity, whereas RANTES is a strong chemoattractant and a weak inducer of mediator release. This suggests that CCR1 and CCR2 are functionally different, and indeed, maximum migration and release are obtained with MCP-3 that binds to both receptors (2).

Of particular interest are the effects of the MCPs on lymphocytes. Studies on human $CD4^+$ or $CD8^+$ T cell clones (28, 37) and human blood lymphocytes (38, 39) show that all four MCPs are potent attractants for activated T lymphocytes. Under similar conditions, MCP-1, MCP-3, and MCP-4 attract more cells than do RANTES, MIP-1α, and MIP-1β across bare or endothelial cell-coated filters. All MCPs also induce a transient *B. pertussis* toxin–sensitive rise in the cytosolic free Ca^{2+} concentration ($[Ca^{2+}]_i$) in $CD4^+$ and $CD8^+$ T cells (28, 37). Conditioning with IL-2 markedly enhances the expression of CCR1 and CCR2 and the chemotactic responsiveness to RANTES and MCP-1 (45) (see *Lymphocyte Recruitment*). Similar migration responses are observed for natural killer (NK) cells (46) and dendritic cells (47), and the MCPs were also found to induce $[Ca^{2+}]_i$ changes and exocytosis of granzyme A and N-acetyl-β-glucosaminidase in cloned human NK cells (48). In addition, several CC chemokines including the MCPs were reported to enhance target cell lysis by blood-derived NK cells (49).

Eotaxin

A CC chemokine acting on eosinophils and termed *eotaxin* was originally isolated from the bronchoalveolar fluid of allergic guinea-pigs (50). Murine (51) and human homologs (27) were subsequently cloned. They share over 60% sequence identity with guinea-pig eotaxin and are equally selective for eosinophils. Human eosinophils express high numbers of a receptor for eotaxin, CCR3, which was cloned by three independent groups (43, 44, 52). Binding studies have shown that eotaxin as well as RANTES and MCP-3 recognize this receptor (43), in agreement with their ability to attract CCR3-transfected cells (44). In addition, cross-desensitization experiments with eosinophils suggest that CCR3 recognizes MCP-4 as well (27, 28). MCP-4 is very active on eosinophils and is equivalent to eotaxin as chemoattractant and superior to MCP-3 in desensitizing eosinophils toward eotaxin (28). In contrast to other CC chemokines, eotaxin has a high degree of selectivity for its receptor. It is inactive on neutrophils and monocytes, which do not appear to express CCR3 (44, 52, 53) but has weak-to-moderate chemotactic activity toward IL-2-conditioned T lymphocytes (28). Eotaxin exclusively attracts eosinophils when

applied in vivo (27), and its expression is enhanced in animal models of allergic inflammation (50, 54) and in tissue cells at sites of eosinophil accumulation in humans (27). Northern blot analysis showed constitutive expression of eotaxin in human small intestine, colon, heart, kidney, and pancreas; major amounts of this chemokine are believed to be produced by epithelial and endothelial cells as well as eosinophil leukocytes (53). Due to its preferential, powerful action on eosinophils and its occurrence in different species, eotaxin is considered a most relevant chemokine in the pathophysiology of allergic conditions and asthma (55).

IP10 and Mig

IP10 is a CXC chemokine that was identified several years ago as the product of a gene induced by interferon-γ (IFNγ), which was found to be expressed in delayed-type hypersensitivity reactions of the skin (56, 57). For a long time the biological activity of this chemokine remained unclear. Another IFNγ-induced human CXC chemokine, Mig, was later described (58). IP10 was reported to attract human monocytes, T lymphocytes, and NK cells (49, 59), and Mig was shown to attract tumor-infiltrating T lymphocytes (60). A receptor that is specific for IP10 and Mig, CXCR3, was recently cloned (see *CXC Chemokine Receptors*) and found to be selectively expressed on activated T lymphocytes that appear to be the only target cell for the two IFNγ-inducible chemokines (61). The restricted expression and the selectivity for a single receptor on T cells suggest that IP10 and Mig are involved in the regulation of lymphocyte recruitment and the formation of the lymphoid infiltrates observed in autoimmune inflammatory lesions, delayed-type hypersensitivity, some viral infections, and certain tumors.

SDF-1

The CXC chemokine SDF-1 (stromal cell–derived factor 1) occurs in two alternative splicing variants, SDF-1α and SDF-1β, that were cloned from mouse bone marrow stromal cell lines (62, 63). SDF-1α stimulates the proliferation of B cell progenitors and was also termed PBSF (pre-B cell growth stimulating factor (63). Murine SDF-1α was purified as a lymphocyte chemoattractant from a stromal cell culture supernatant (64). A homologous gene of human origin coding for both SDF forms was later characterized, and SDF-1α was shown to be the more abundant variant (64a). Mature human and murine SDF-1α consist of 68 amino acids and differ only at position 18 (valine in the human and isoleucine in the murine protein). Subsequent studies showed that synthetic human SDF-1 stimulates monocytes, neutrophils, and peripheral blood lymphocytes, as is indicated by $[Ca^{2+}]_i$ changes and chemotaxis (64, 65). SDF-1 binds to CXCR4, a former orphan receptor cloned in several laboratories (66–70), (see

CXC Chemokine Receptors), and induces Ca^{2+} mobilization in CHO cells that stably express this receptor (65, 71). No cross-desensitization is observed with other chemokines, which underlines the selectivity of CXCR4. In transfected cell lines coexpressing CXCR4 and CD4 and in blood lymphocytes, SDF-1 is a powerful HIV-suppressive factor (see *HIV Replication*). Mice lacking the SDF-1 gene die perinatally and present multiple defects of development, including a severe reduction of B cell and myeloid progenitors in the bone marrow, in addition to a septal defect in the heart. These findings suggest that SDF-1 may display additional functions that are not typical for chemokines (72).

CHEMOKINE RECEPTORS

Chemokines act via seven-transmembrane-domain (7TM) receptors (1, 3), which form a distinct group of structurally related proteins within the superfamily of receptors that signal through heterotrimeric GTP-binding proteins (Table 1). More than by the overall sequence identity, relatedness is manifested by a number of conserved structural motifs mainly found within the transmembrane domains. The most important of these motifs are: TD(X)YLLNLA (X2)DLLF(X2)TLP(X)W in TM 2, the NH_2- and COOH-terminal extensions of the DRYLAIVHA-motif in TM 3 and the second intracellular loop, PLL(X) M(X2)CY in TM 5, W(X)PYN in TM 6, and HCC(X)NP(X)IYAF(X)G(X2)FR in TM 7. In addition, all chemokine receptors have two conserved cysteines, one in the NH_2-terminal domain and the other in the third extracellular loop (Cys^{30} and Cys^{277} in CXCR1) that are assumed to form a disulfide bond critical for the conformation of the ligand-binding pocket. On the basis of the overall sequence identity, two subgroups can be recognized: CXC chemokine receptors with 36–77% and CC chemokine receptors with 46–89% identical amino acids (Figures 2 and 3).

CXC Chemokine Receptors

Two receptors for IL-8, CXCR1 (IL-8RA/R1) and CXCR2 (IL-8RB/R2), are expressed on neutrophils. They share 77% identical amino acids, and their genes are colocalized on chromosome 2q35 (73, 74). One receptor, CXCR2, has high affinity for IL-8 and all other CXC chemokines that attract neutrophils (e.g. the GRO proteins, NAP-2, etc.), while the other, CXCR1, has high affinity for IL-8 only (1). IL-8 receptors are also found on monocytes, basophils, and eosinophils, but the responses of these cells to IL-8 are much weaker than those of neutrophils (1). In T lymphocytes, expression of both IL-8 receptors is revealed by RT-PCR but not by Northern blotting (75, 76), suggesting that the numbers are low. Using monoclonal antibodies and FACS analysis, it was observed that CXCR1 and CXCR2 are present on all neutrophils and monocytes,

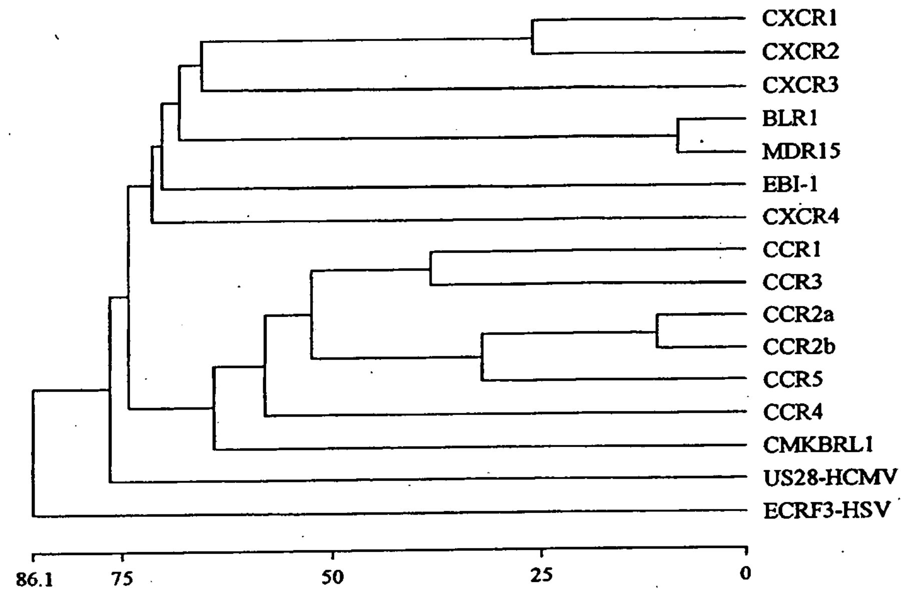

Figure 2 Structure similarity diagram of human chemokine receptors. Similarity scores were determined as described for Figure 1. The highest degree of divergence (86.1%) with respect to all the other receptors is observed for herpesvirus saimiri ECRF3 and the highest pairwise similarity (8.3% divergence) for BLR1 and MDR15. GeneBank accession numbers for the sequences are (from top to bottom): M68932, M73969, X95876, X68149, X68829, L08176, X71635, L10918, U51241, U03882, U03905, X91492, X85740, U28934, L20501, and S76368.

but only on a minority of lymphocytes. They are found in low numbers on NK and CD8$^+$ T cells, with high donor-to-donor variation, but they are absent in CD4$^+$ T cells or B cells (77, 78). Interestingly, while both receptors are present in similar numbers on neutrophils, CXCR2 appears to prevail on other leukocytes (78). Analysis of transendothelial migration shows that MCP-1 attracts CD26$^+$ T cells while the cells responding to IL-8 are CD26-negative (77). Expression of CXCR1 and CXCR2, as assessed by immunocytochemistry or RT-PCR, was also reported in cultured melanocytes and fibroblasts (75), epithelial cells in inflamed skin (79), and fibroblasts and smooth muscle cells of burn lesions (80). There is no evidence for a functional role of the expressed receptors, however.

Chimerae between the rabbit CXCR1 and the human CXCR2 were used to show that the NH_2-terminal domain determines, to a large extent, ligand selectivity (81, 82). Receptors carrying the NH_2-terminal domain of CXCR1 are selective for IL-8, whereas those carrying the NH_2-terminal domain of CXCR2 have high affinity for other CXC chemokines as well. Alanine scanning

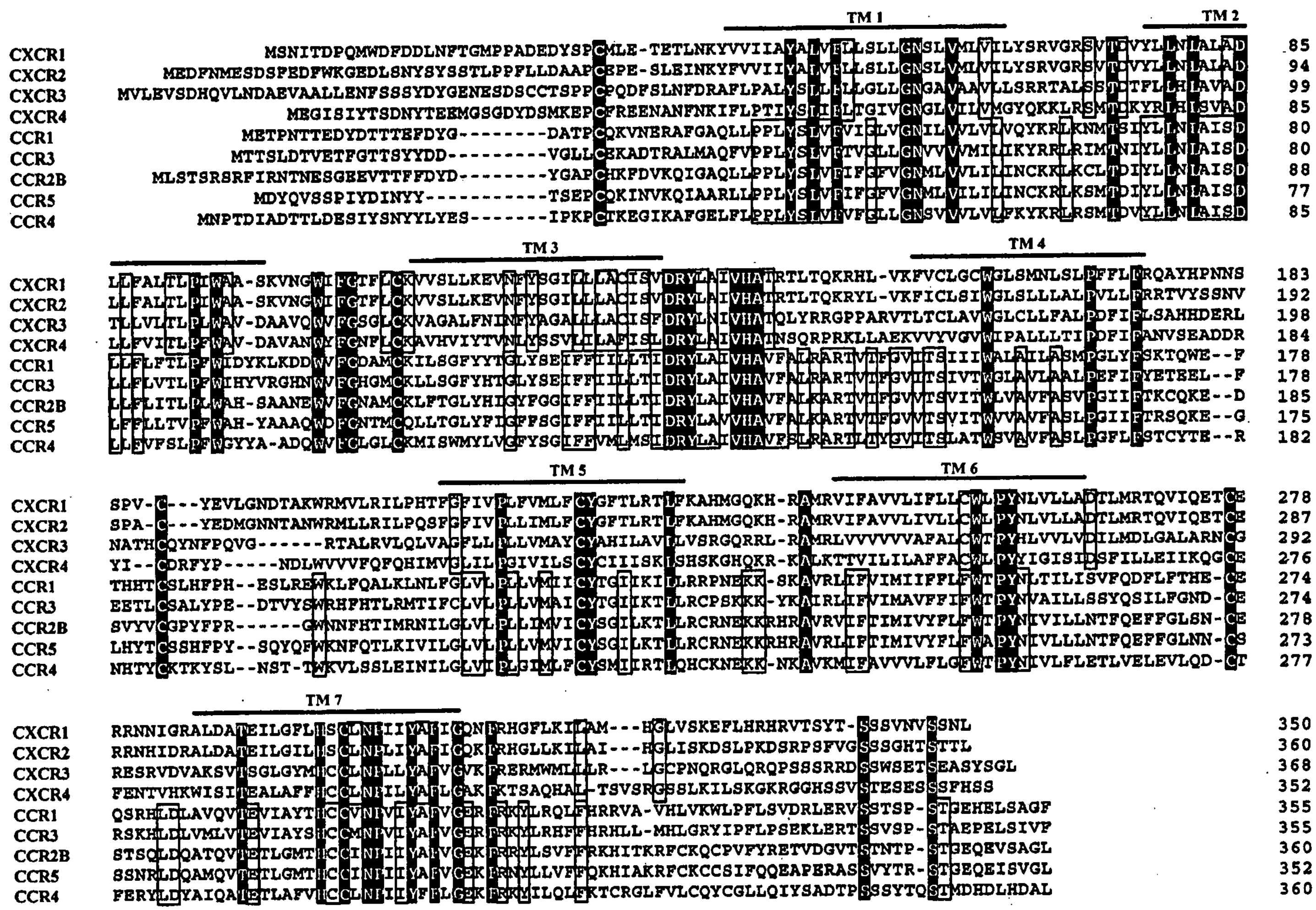
TM 1
TM 2
TM 3
TM 4
TM 5
TM 6
TM 7
CXCR1
CXCR2
CXCR3
CXCR4
CCR1
CCR3
CCR2B
CCR5
CCR4

was cloned from a cDNA library derived from an Epstein-Barr virus–infected Burkitt's lymphoma, and shown to be expressed exclusively in B and T cell lines (103). Another receptor, CMKBRL1 (chemokine beta receptor-like 1) shows interesting similarities with chemokine receptors. Its gene is located on chromosome 3p21 together with other CC chemokine receptors, and transcripts are found in leukocytes as well as in lymphoid and neural tissues (104, 105).

Some chemokine receptors may mediate functions that are unrelated to cell migration, as is exemplified by two receptors of viral origin. US28 consists of 354 amino acids and is encoded by human cytomegalovirus. It recognizes several CC chemokines, including MCP-1, RANTES, MIP-1α, and MIP-1β (87, 106). Conversely, ECRF3, a 321 amino acid protein encoded by herpesvirus saimiri, recognizes IL-8, GROα, and NAP-2, but not CC chemokines (107). It is interesting that these viral receptors discriminate between CXC and CC chemokines although they share less than 30% identical amino acids with the human chemokine receptors. In human fibroblasts, cytomegalovirus induces the expression of IL-8 receptors and shows enhanced replication in receptor-expressing cells that are exposed to IL-8 (108). This suggests that the expression of chemokine receptors in infected cells may be of advantage for the replication of some viruses (3, 108).

Receptor Function and Signal Transduction

Our review of this topic is largely restricted to neutrophils and cell lines transfected with the IL-8 receptors, which were studied more extensively. Signaling by chemokine receptors depends on coupling to *Bordetella pertussis* toxin-sensitive G-proteins. Experiments with COS-7 cells in which IL-8 receptors were cotransfected with different G-proteins have shown that CXCR1 and CXCR2 couple to $G\alpha_{i2}$, $G\alpha_{i3}$, $G\alpha_{14}$, $G\alpha_{15}$, and $G\alpha_{16}$ but not to $G\alpha_q$ or $G\alpha_{11}$ (109). Studies on CC chemokine receptors are less advanced. CCR1 was shown to couple to $G\alpha_{14}$ but not $G\alpha_{16}$, while CCR2b couples to both G-proteins. No coupling to these G-proteins was observed for CCR2a, however, suggesting differences in G-protein usage (90).

The function of CXCR1 and CXCR2 was studied in Jurkat cells stably transfected with one or the other cDNA. CXCR1-expressing cells bind IL-8 with high affinity, and GROα and NAP-2 with low affinity, while CXCR2-expressing cells have high affinity for all three ligands. Both types of transfectants respond equally well to IL-8, as shown by $[Ca^{2+}]_i$ changes and chemotaxis, and no difference is observed in the function of CXCR2 after stimulation with IL-8, GROα, or NAP-2. CXCR1-transfected cells migrate in response to GROα and NAP-2, which bind with low affinity, provided that high concentrations are used (110). Similar experiments show that both receptors activate the p42/p44 MAP kinase (111). These results indicate that CXCR1 and CXCR2 signal and

function independently of each other. Monoclonal antibodies that selectively block CXCR1 or CXCR2 were used to study the function of the individual receptors in neutrophils. Both IL-8 receptors trigger $[Ca^{2+}]_i$ changes, chemotaxis and granule exocytosis, whereas phospholipase D activation and the respiratory burst are only observed after stimulation of CXCR1 (112). These observations are in agreement with a study showing that in human neutrophils phospholipase D is activated by stimulation with IL-8, but not with GROα or NAP-2 (113). All three chemokines, on the other hand, induce similar $[Ca^{2+}]_i$ changes and patterns of phosphorylation. Activation of p42/44 MAP kinase is also observed in cells transfected with CCR2 cDNA after stimulation with MCP-1 (114).

There is strong evidence for a role of phosphatidylinositol 3-kinase (PI3K) in chemokine-mediated signal transduction (115, 116). PI3K isoforms may become activated directly by interaction with the G-protein $\beta\gamma$ subunit or by small GTPases, Src-related tyrosine kinases, or phosphotyrosines that bind to the SH2 domain of PI3K. Phosphatidylinositol lipids phosphorylated at the 3-OH position are supposed to trigger a variety of cellular responses (117). A study on murine pre-B cells transfected with CXCR1 showed that the small GTPase Rho is implicated in IL-8-mediated adhesion to fibrinogen (118), suggesting that IL-8 receptors can activate small GTPases, which in turn regulate cytoskeletal rearrangement, phospholipase D activation, and induction of the respiratory burst (117). Leukocyte responses to chemokines are characteristically transient, and the receptors become rapidly desensitized. Phosphorylation of serines and threonines in the COOH-terminal region of CXCR1 and CXCR2 correlates with homologous desensitization after stimulation with IL-8 or GROα, respectively (1, 119, 120). Rat basophilic leukemia cells (RBL-2H3) cotransfected with CXCR1 and the C5a receptor were used to show that heterologous desensitization correlates with COOH-terminal phosphorylation of the receptors (121).

STRUCTURE-ACTIVITY RELATIONS

CXC Chemokines

The short sequence Glu-Leu-Arg (ELR motif), which precedes the first cysteine in all CXC chemokines that act on neutrophils is essential for binding and activation of both IL-8 receptors (CXCR1 and CXCR2). Additional structural domains, however, are required because short peptides containing the ELR motif are inactive, and neither IP10 nor MCP-1 can be converted into neutrophil-activating chemokines by introduction of the ELR motif (1). Active CXC chemokines have a short NH_2-terminal domain, and it has been suggested that if the sequence is extended, it can fold over the ELR motif and prevent its recognition by the receptor (10). Studies with IL-8 have shown that the arginine

adjacent to the first cysteine is very sensitive to substitution (1). It is interesting to note that three CXC chemokines, IP10, Mig, and SDF-1, that were recently shown to act via novel CXC chemokine receptors (61, 65) have a conserved arginine before the first cysteine. The Arg-Cys-X-Cys motif may be a general requirement for the binding to CXC chemokine receptors.

Several attempts have been made to define the structural elements for high-affinity binding to the IL-8 receptors. Studies with synthetic IL-8 analogs with single or double amino acid substitutions and hybrids between IL-8 and the inactive IP 10 have been performed to establish the minimal requirements for activity (13, 122). In addition to the disulfide bridges and the ELR motif, the NH_2-terminal loop region (residues 10–17) and the Gly^{31}-Pro^{32} motif in the β-turn containing the third cysteine (residues 30–35) were found to be of primary importance (13, 19). Single residue mutations and chimeric proteins between IL-8 and CXC chemokines with low affinity for CXCR1, were used to identify the structural determinants for recognition of CXCR1 and CXCR2 (123–127). Of particular interest is the NH_2-terminal loop (residues 10-17 in IL-8), since structural analysis reveals significant differences in this region between monomeric IL-8 and monomeric GROα or NAP-2 (9, 11, 12). Mutations of human and rabbit IL-8 highlight the importance of Tyr^{13} and Lys^{15} for high affinity binding to CXCR1 (123). Mutants of IL-8 and GROα with reversed receptor selectivity were obtained by exchanging the NH_2-terminal loops of the two chemokines (residues 10–17 of IL-8 and 12–18 of GROα) and residues preceding the fourth cysteine (Glu^{48} and Leu^{49} of IL-8, and Ala^{50} of GROα) (127).

The substitution of Tyr^{28} and Arg^{30} in MCP-1 by the corresponding residues in IL-8, Leu and Val, was reported to lower the activity toward monocytes and to confer neutrophil chemotactic activity to the CC chemokine (128). Conversely, replacement of Leu^{25} and Val^{27} in IL-8 by tyrosines, the corresponding residues of RANTES (129), or substitution of Leu^{25} by a modified cysteine were reported to yield mutants with CC chemokine activity (130). Using synthetic mutants, we were unable to confirm the results obtained by substitutions with natural amino acids (128, 129), and we found that the weak activity that IL-8 normally has on monocytes (131) was not affected by the substitutions (I Clark-Lewis, B Dewald, unpublished observation).

CC Chemokines

The NH_2-terminal region of MCP-1 is of critical importance for receptor recognition and activation. The situation is similar to that of IL-8 and its analogs that activate neutrophils, but the structural requirements are more strict because the entire sequence of 10 residues preceding the first cysteine is required for full activity (19, 132). Truncation or elongation of the NH_2-terminal sequence leads to considerable loss of activity, but the NH_2-terminal pyroglutamate can

be replaced by several other noncyclic amino acids. This is particularly interesting because MCP-2, MCP-3, and MCP-4 share with MCP-1 the NH_2-terminal pyroglutamate and high affinity for CCR2.

The role of the NH_2-terminal domain for MCP-1 activity was studied with a series of NH_2-terminally truncated analogs, MCP-1(2–76) to MCP-1(10–76), of the full-length form of 76 residues. Deletion of the NH_2-terminal pyroglutamate, yielding MCP-1(2–76), results in a marked, at least 50-fold decrease in activity on monocytes (132) and basophils (133), and deletion of the next residue leads to total loss of activity. Analogs with deletions of 3 or 4 residues, MCP-1(4-76) and MCP-1(5-76), are active again on both cells, while all further truncation analogs, MCP-1(6-76) through MCP-1(10-76), are inactive. A surprising observation was that MCP-1(2–76), the analog without NH_2-terminal pyroglutamate, is a powerful stimulus for eosinophil leukocytes, which do not express CCR2 and do not respond to full-length MCP-1 (133). On further truncation, the activity on eosinophils changes in the same way as in monocytes and basophils. It can be assumed that the effects on eosinophils are mediated via CCR3, and it is remarkable that MCP-1 acquires activity on these cells only after NH_2-terminal deletion, whereas MCP-2, MCP-3, and MCP-4, which share the NH_2- terminus with MCP-1, are potent attractants in their full-length form.

Several of the truncated MCP-1 analogs, MCP-1(9–76) and MCP-1(10–76) in particular, act as antagonists presumably by blocking CCR2, and they prevent the responses to MCP-1, MCP-2, and MCP-3, but not to RANTES, MIP-1α, or MIP-1β (132). Analogous studies performed with RANTES and MCP-3 yielded antagonists for multiple CC chemokine receptors (95). RANTES(9–68) and MCP-3(10–76) inhibit receptor binding and functional activities of MCP-1, MCP-3, and RANTES. The decreased selectivity of the truncated analogs, RANTES in particular, suggests that receptor specificity is dictated by residues within the NH_2-terminal domain, which are lost upon truncation, while other structural determinants assure the interaction with multiple receptors. Two additional CC chemokine antagonists were reportedly obtained by NH_2-terminal elongation: MCP-3 with three additional residues, Arg-Glu-Phe, which blocks the activity of MCP-3 (134), and RANTES with an additional methionine, which blocks the activity of RANTES and MIP-1α, but not of MCP-1 or IL-8 (135).

These observations demonstrate the critical role of the sequence preceding the first cysteine for the binding and function of MCP-1, MCP-3, and RANTES, and, together with former evidence on CXC chemokines (1), emphasize the overall importance of the NH_2-terminal domain for the biological activity of all chemokines. Interesting differences are nevertheless apparent between CXC and CC chemokines. Minimal modifications of the NH_2 terminus can drastically reduce or even qualitatively change the activity of CC chemokines, while

truncation up to the ELR motif progressively enhances the potency of IL-8 and other CXC chemokines (1). In both cases, elimination of most residues in the short NH_2-terminal stretch or modification of recognition motifs yields derivatives that still recognize the receptor but do not induce functional responses and thus act as antagonists.

PERSPECTIVES

We conclude by highlighting some new developments and concepts of potential interest. For areas where progress has been slow and areas that were reviewed recently, only a few indicative references will be given. Research on chemokines has provided considerable insight into the mechanism of diapedesis, and the ability of endothelial cells to generate attractant chemokines has been recognized as a fundamental process. Outstanding reviews have been published on this subject (136–138). Of interest is the potential activity of chemokines on myeloid progenitor cells. MIP-1α was described early on as a regulator of hematopoiesis (139) and inhibitor of stem cell proliferation (140). Although the disruption of the MIP-1α gene in mice does not appear to cause cellular abnormalities in the bone marrow or blood (141), chemokines are still considered as potential stimuli of leukocyte production and release from the bone marrow. Another major subject is the role of chemokines in tumors. It is well documented that transformed cell lines produce high amounts of different chemokines for which anti-tumor as well as tumor-promoting activities have been suggested (1). The role of chemokines in tumor growth is still unclear, and some new evidence for angiogenic and angiostatic effects will be discussed (see *Angiogenesis*).

Selectivity

Collectively, chemokines and chemokine receptors form a sophisticated system for the regulation of leukocyte and lymphocyte traffic across different compartments from the tissue of origin and the blood to sites of homing, host defense, or disposal. Substantial new information has been obtained about the selectivity and the complexity of the system, and some simplifications are no longer justified. The concept, for instance, that CXC chemokines act primarily on neutrophils, whereas CC chemokines act on the other types of leukocytes must be revised in view of the recent identification of new CXC chemokine receptors, CXCR3 and CXCR4, that mediate lymphocyte recruitment (61, 65, 71). When considering the ligands of the four CXC and five CC chemokine receptors (Table 1), an interesting difference becomes apparent: CXC chemokines have high affinity for single receptors (IL-8 which binds to CXCR1 and CXCR2 is the only exception), whereas most CC chemokines recognize two or more receptors

that differ in ligand specificity and cellular distribution. MCP-1 and eotaxin, which act via CCR2 and CCR3, respectively, are the only CC chemokines with restricted receptor usage. It is conceivable that CXC chemokines elicit more selective leukocyte responses than CC chemokines.

Tissue-Bound Chemokines

The early observation that IL-8 is effective for several hours after intradermal application (142) suggested that chemokines can associate in active form with the tissue matrix. In vitro, IL-8 binds to glycosaminoglycans through its COOH-terminal α-helix and remains active when complexed to heparin or heparan sulfate (143). To some degree, this interaction appears to be selective since IL-8, GROα, NAP-2, and PF4 differ in their binding to heparin subfractions as shown by affinity co-electrophoresis (144). MIP-1β and RANTES also retain activity when bound to the tissue matrix and induce adherence of T cells (145, 146). Together these observations suggest that interaction with matrix glycosaminoglycans may help to confine chemokines within the site of their formation and so support the concept that the migration of leukocytes could be directed by a solid, rather than fluid, chemokine gradient. In situ binding of IL-8 and RANTES, but not of MIP-1α, was observed in venular endothelial cells of the skin, and IL-8 was shown to bind to endothelia of mucosal and serosal sites, but not of parenchymatous tissues (147). It is possible that chemokines bound to the surface of endothelial cells direct diapedesis. The evidence for this attractive hypothesis, however, is still weak because only a few chemokines have been shown to bind, and the binding is restricted to some microvascular beds. In addition, chemokines, like other cationic proteins, can impair the activity of growth factors by competition for their binding sites on heparan sulfate (148, 149), a process that may explain some antiproliferative and angiostatic activities.

Most chemokines associate with the so-called Duffy antigen on erythrocytes (1). The "Duffy antigen receptor for chemokines" (DARC) was cloned and shown to consist of 338 amino acids and to comprise seven putative transmembrane domains. DARC has less than 20% amino acid identity with CXC and CC chemokine receptors and does not signal (150, 151). DARC is also expressed in some B and T cells, the endothelial cells of postcapillary venules and the Purkinje cells in the cerebellum (152). It is not clear, however, whether this promiscuous receptor is functionally relevant on endothelial cells and has a role in chemokine-dependent diapedesis because experiments with erythrocytes have shown that IL-8 is inactive toward neutrophils when bound to DARC (153).

Lymphocyte Recruitment

Chemokines are now generally recognized as the long-sought mediators of lymphocyte recruitment. A first hint came from the early studies on IP10, which is

expressed at sites of lymphocyte accumulation in delayed-type hypersensitivity. Subsequent studies suggested a role for IL-8, but the evidence has repeatedly been questioned, and although papers in support of this concept are still being published, the CC chemokines have emerged as a major force in lymphocyte trafficking. RANTES, MIP-1α, and MIP-1β were shown several years ago to attract T lymphocytes, and, more recently, the monocyte chemotactic proteins were found to perform similar functions (see *The Monocyte Chemotactic Proteins*).

To define conditions for lymphocyte responsiveness, the migration induced by RANTES, MCP-1, and other CC chemokines was studied in relation to the expression of two main receptors, CCR1 and CCR2, in CD45RO$^+$ blood lymphocytes cultured under different stimulatory conditions (45). A close correlation between receptor expression and chemotaxis was observed and found to depend strictly on pretreatment of the cells with IL-2. Receptor expression and responsiveness are rapidly downregulated when IL-2 is withdrawn and are fully restored when IL-2 is supplied again. IL-2 can be substituted partially by IL-4, IL-10, or IL-12, but not by IL-13, IFNγ, IL-1β, or TNFα. Interestingly, treatment with anti-CD3 alone or in combination with anti-CD28 rapidly downregulates receptors and migration. Receptor upregulation by IL-2 and downregulation by other stimuli of activation and proliferation suggest that T cells become responsive to chemokines after IL-2-mediated expansion and not during the early stages of antigen-dependent activation. Other studies showed that phytohemagglutinin-treated lymphocytes do not express CCR1 (88) and that human T cell clones lose migratory capacity after treatment with anti-CD3 (37). The opposite effect, however, was also reported (154).

The CC chemokines that attract lymphocytes are also chemotactic for monocytes, basophils, and eosinophils (2, 36), suggesting that the action of CC chemokines on lymphocytes is not selective. The role of MCP-1 in mononuclear cell recruitment was shown in a model of delayed-type hypersensitivity in rats (155) as well as in mice with *Cryptococcus neoformans* lung infection (156), where neutralizing antibodies against MCP-1 markedly decreased the local infiltration by monocytes and T lymphocytes.

A more selective recruitment of lymphocytes is likely to occur in response to IP10 and Mig, which bind to CXCR3, a receptor that does not recognize other chemokines and is confined to IL-2-activated T cells. Upon viral infection, for instance, IP10 and Mig are upregulated by locally produced IFNγ and thus become available for the recruitment of effector lymphocytes as part of the antiviral response. The potential role of IFNγ-induced chemoattractants in lymphocyte migration is highlighted by a comparison of the influx of radiolabeled neutrophils and lymphocytes in sheep after intradermal injection of chemoattractants and cytokines (157). The ratio of neutrophils to lymphocytes

was 45:1 after injection of IL-8 or C5a, about 5:1 after injection of TNFα or IL-1α, and only 0.1:1 after injection of IFNγ. Lymphotactin, a protein with only two cysteines and some structural similarity to chemokines, was also described as a selective attractant for lymphocytes (158). Such activities, however, have not been confirmed. Recombinant lymphotactin and two synthetic variants were extensively tested on human thymocytes and several preparations of T cells, including T cell clones, monocytes, and neutrophils, but no chemotactic activity nor $[Ca^{2+}]_i$ changes were observed (159).

Angiogenesis

The study of the formation of new blood vessels was greatly encouraged by the recognition of the role of angiogenesis for tumor growth, and the effects of growth factors on endothelial cells (160). Popular models of angiogenesis are the neovascularization of the cornea or the chick chorioallantoic membrane. Angiogenic factors are applied locally in an adsorptive pellet, and angiostatic substances are either added to the pellet or injected systemically. Enhancement or inhibition of endothelial cell proliferation and/or in vitro migration are considered as predictive of angiogenic or angiostatic activity, respectively.

A possible involvement of chemokines in the regulation of angiogenesis was originally suggested by studies showing that PF4 has angiostatic (161) and potential anti-tumor activity (162). Similar effects were observed with other cationic proteins, and recently it was shown that PF4 and IP10 share binding sites on heparan sulfate and inhibit the proliferation of endothelial cells presumably by displacing growth factors (163). The opposite effect, angiogenesis, was reported for IL-8 and several other CXC chemokines with the NH_2-terminal ELR motif (164, 165). Modification of the ELR motif reportedly confers angiostatic properties to IL-8, and introduction of the ELR motif converts the chemokine Mig from angiostatic to angiogenic. The mechanism of these phenomena has not been studied, and no receptors for angiogenic chemokines were described. It is unlikely that angiogenesis depends on neutrophil recruitment because some of the ELR-containing proteins studied, like platelet basic protein and connective tissue-activating peptide III, are inactive on neutrophils (1). In a later study the effects of IL-8 on human umbilical vein and dermal microvascular endothelial cells were examined, but no IL-8 binding nor IL-8-dependent $[Ca^{2+}]_i$ changes were observed, and no CXCR1 or CXCR2 transcripts were detected by PCR (166).

Angiostatic rather than angiogenic activity by CXC chemokines was reported by Cao et al (167) who compared the GRO proteins. They found that GROα, GROβ, and PF4 inhibit the proliferation of capillary endothelial cells stimulated with basic fibroblast growth factor, whereas GROγ was inactive. In vivo GROβ inhibited the neovascularization of the chorioallantoic membrane

and the mouse cornea, and it depressed the growth of murine Lewis lung carcinoma. Most recently, however, an anti-tumor effect was reported in SCID mice bearing human non–small cell lung cancer by neutralizing IL-8 with an antiserum (168). A tumor-promoting effect of IL-8 may also be inferred from the correlation between IL-8 expression and metastatic potential of melanoma cell lines in mice (169). On the other hand, IL-8 inhibits the proliferation of non-small cell cancer lines (170) and reduces tumorigenicity by recruitment of neutrophils in nude mice receiving tumor cells that express the human IL-8 gene (171). Anti-tumor activity was formerly observed in mice inoculated with tumor cells engineered to produce high levels of IP10, and the activity was found to depend on the recruitment of T lymphocytes and other white cells (172). Similar experiments were done with cells overexpressing murine MCP-1 (1). Furthermore, angiogenic properties were reported for soluble E-selectin and VCAM-1, which may be shed from the endothelial surface by enzymes released from adhering leukocytes (173). These and other observations emphasize the complexity of the pathophysiological process and suggest that, in many instances, the angiogenic effects of chemokines may be mediated by products released from the accumulating phagocytes.

HIV Replication

A most exciting new development came from the discovery that some chemokines function as HIV-1-suppressive factors. While searching for factors that delay the outbreak of AIDS, Cocchi et al (174) found that RANTES, MIP-1α, and MIP-1β produced by CD8$^+$ T cell lines are potent inhibitors of infection by monocyte/macrophage-tropic HIV-1 strains. These observations indicated that chemokines may determine the susceptibility to HIV infection and disease progression, and they suggested that chemokine receptors could in some way be involved in the recognition of HIV-1. Shortly thereafter, Feng et al (86) identified by expression cloning a 7TM receptor (termed fusin) that complements CD4 in a cell-fusion model of lymphocyte-tropic HIV-1 infection. Fusin is identical to CXCR4, and its ligand, SDF-1, was found to be a potent inhibitor of infection by lymphocyte-tropic HIV-1 strains in cell lines that coexpress CXCR4 and CD4 and in blood lymphocytes (65, 71). The HIV-suppressive factors RANTES, MIP-1α, and MIP-1β do not prevent the infection of cells expressing CXCR4. Unlike SDF-1, they interact with several receptors (see *CC Chemokine Receptors*) and one of them, CCR5, was shown by several groups to be the main coreceptor for entry of monocyte/macrophage-tropic HIV-1 strains (175–179). CCR3 and CCR2b have similar functions (176–178), but their role as HIV coreceptors is less prominent, suggesting that viral Env proteins have lower affinity for these receptors.

The repertoire of chemokine receptors in CD4$^+$ cells is likely to influence viral tropism, and it will be important to study the regulation of receptor

expression, particularly in T lymphocytes, macrophages, and dendritic cells. Viral entry is assumed to begin with the interaction of the highly variable viral Env protein, gp120, with CD4 and a chemokine receptor. Mutational changes of gp120 could lead to a switch in recognition from CCR5/CCR3 to CXCR4, and a shift from monocyte/macrophage-tropic to lymphocyte-tropic, syncytium-inducing strains. Recognition of CXCR4, which is widely expressed in blood leukocytes (66–70), could contribute to a spreading of the infection. There is already some evidence for a protective role of RANTES, MIP-1α, and MIP-1β in individuals who remain uninfected despite high-risk exposure to HIV (180), and the therapeutic application of chemokines to prevent infection may be considered. Of particular interest is the possibility that SDF-1 in combination with CC chemokines could help to decrease virus load and prevent the emergence of the syncytium-inducing viruses characteristic for the progression to AIDS.

ACKNOWLEDGMENTS

We thank Dr. Mariagrazia Uguccioni and Dr. Marlene Wolf for critical reading of the manuscript. This work was supported by Grant 31-039744.93 to M Baggiolini and B Moser from the Swiss National Science Foundation. B Moser is recipient of a career development award from the Prof. Max Cloetta Foundation.

Literature Cited

1. Baggiolini M, Dewald B, Moser B. 1994. Interleukin-8 and related chemotactic cytokines—CXC and CC chemokines. *Adv. Immunol.* 55:97–179
2. Baggiolini M, Dahinden CA. 1994. CC chemokines in allergic inflammation. *Immunol. Today* 15:127–33
3. Murphy PM. 1994. The molecular biology of leukocyte chemoattractant receptors. *Annu. Rev. Immunol.* 12:593–633
4. Schall TJ, Bacon KB. 1994. Chemokines, leukocyte trafficking, and inflammation. *Curr. Opin. Immunol.* 6:865–73
5. Clore GM, Appella E, Yamada M, Matsushima K, Gronenborn AM. 1990. Three-dimensional structure of interleukin 8 in solution. *Biochemistry* 29:1689–96
6. Baldwin ET, Weber IT, St. Charles R, Xuan J-C, Appella E, Yamada M, Matsushima K, Edwards BFP, Clore GM, Gronenborn AM, Wlodawer A. 1991. Crystal structure of interleukin 8: symbiosis of NMR and crystallography. *Proc. Natl. Acad. Sci. USA* 88:502–6
7. Clore GM, Gronenborn AM. 1995. Three-dimensional structures of α and β chemokines. *FASEB. J.* 9:57–62
8. St. Charles R, Walz DA, Edwards BF. 1989. The three-dimensional structure of bovine platelet factor 4 at 3.0-Å resolution. *J. Biol. Chem.* 264:2092–99
9. Fairbrother WJ, Reilly D, Colby TJ, Hesselgesser J, Horuk R. 1994. The solution structure of melanoma growth stimulating activity. *J. Mol. Biol.* 242:252–70
10. Yang Y, Mayo KH, Daly TJ, Barry JK, La Rosa GJ. 1994. Subunit association and structural analysis of platelet basic protein and related proteins investigated by ^{1}H NMR spectroscopy and circular dichroism. *J. Biol. Chem.* 269:20,110–18
11. Kim K-S, Clark-Lewis I, Sykes BD. 1994. Solution structure of GRO/melanoma

growth stimulatory activity determined by [1]H NMR spectroscopy. *J. Biol. Chem.* 269:32,909–15
12. Malkowski MG, Wu JY, Lazar JB, Johnson PH, Edwards BFP. 1995. The crystal structure of recombinant human neutrophil-activating peptide-2 (M6L) at 1.9-Å resolution. *J. Biol. Chem.* 270: 7077–87
13. Clark-Lewis I, Dewald B, Loetscher M, Moser B, Baggiolini M. 1994. Structural requirements for interleukin-8 function identified by design of analogs and CXC chemokine hybrids. *J. Biol. Chem.* 269:16,075–81
14. Lodi PJ, Garrett DS, Kuszewski J, Tsang ML-S, Weatherbee JA, Leonard WJ, Gronenborn AM, Clore GM. 1994. High-resolution solution structure of the β chemokine hMIP-1β by multidimensional NMR. *Science* 263:1762–67
15. Skelton NJ, Aspiras F, Ogez J, Schall TJ. 1995. Proton NMR assignments and solution conformation of RANTES, a chemokine of the C-C type. *Biochemistry* 34:5329–42
16. Chung C, Cooke RM, Proudfoot AEI, Wells TNC. 1995. The three-dimensional solution structure of RANTES. *Biochemistry* 34:9307–14
17. Covell DG, Smythers GW, Gronenborn AM, Clore GM. 1994. Analysis of hydrophobicity in the α and β chemokine families and its relevance to dimerization. *Protein Sci.* 3:2064–72
18. Burrows SD, Doyle ML, Murphy KP, Franklin SG, White JR, Brooks I, McNulty DE, Scott MO, Knutson JR, Porter D, Young PR, Hensley P. 1994. Determination of the monomer-dimer equilibrium of interleukin-8 reveals it is a monomer at physiological concentrations. *Biochemistry* 33:12,741–45
19. Clark-Lewis I, Kim K-S, Rajarathnam K, Gong J-H, Dewald B, Moser B, Baggiolini M, Sykes BD. 1995. Structure-activity relationships of chemokines. *J. Leuk. Biol.* 57:703–11
20. Rajarathnam K, Sykes BD, Kay CM, Dewald B, Geiser T, Baggiolini M, Clark-Lewis I. 1994. Neutrophil activation by monomeric interleukin-8. *Science* 264:90–92
21. Rajarathnam K, Clark-Lewis I, Sykes BD. 1995. [1]H NMR solution structure of an active monomeric interleukin-8. *Biochemistry* 34:12,983–90
22. Mantel C, Kim YJ, Cooper S, Kwon B, Broxmeyer HE. 1993. Polymerization of murine macrophage inflammatory protein 1α inactivates its myelosuppressive effects in vitro: the active form is a monomer. *Proc. Natl. Acad. Sci. USA* 90:2232–36
23. Avalos BR, Bartynski KJ, Elder PJ, Kotur MS, Burton WG, Wilkie NM. 1994. The active monomeric form of macrophage inflammatory protein-1α interacts with high- and low-affinity classes of receptors on human hematopoietic cells. *Blood* 84:1790–801
24. Lord BI. 1995. MIP-1α increases the self-renewal capacity of the hemopoietic spleen-colony-forming cells following hydroxyurea treatment in vivo. *Growth Factors* 12:145–49
25. Paolini JF, Willard D, Consler T, Luther M, Krangel MS. 1994. The chemokines IL-8, monocyte chemoattractant protein-1, and I-309 are monomers at physiologically relevant concentrations. *J. Immunol.* 153:2704–17
26. Zhang Y, Rollins BJ. 1995. A dominant negative inhibitor indicates that monocyte chemoattractant protein 1 functions as a dimer. *Mol. Cell. Biol.* 15:4851–55
27. Ponath PD, Qin SX, Ringler DJ, Clark-Lewis I, Wang J, Kassam N, Smith H, Shi XJ, Gonzalo JA, Newman W, Gutierrez-Ramos JC, Mackay CR. 1996. Cloning of the human eosinophil chemoattractant, eotaxin—expression, receptor binding, and functional properties suggest a mechanism for the selective recruitment of eosinophils. *J. Clin. Invest.* 97:604–12
28. Uguccioni M, Loetscher P, Forssmann U, Dewald B, Li HD, Lima SH, Li YL, Kreider B, Garotta G, Thelen M, Baggiolini M. 1996. Monocyte chemotactic protein 4 (MCP-4), a novel structural and functional analogue of MCP-3 and eotaxin. *J. Exp. Med.* 183:2379–84
29. Schulz-Knappe P, Mägert HJ, Dewald B, Meyer M, Cetin Y, Kubbies M, Tomeczkowski J, Kirchhoff K, Raida M, Adermann K, Kist A, Reinecke M, Sillard R, Pardigol A, Uguccioni M, Baggiolini M, Forssmann WG. 1996. HCC-1, a novel chemokine from human plasma. *J. Exp. Med.* 183:295–99
30. Imai T, Yoshida T, Baba M, Nishimura M, Kakizaki M, Yoshie O. 1996. Molecular cloning of a novel T cell-directed CC chemokine expressed in thymus by signal sequence trap using Epstein-Barr virus vector. *J. Biol. Chem.* 271:21,514–21
31. Orlofsky A, Berger MS, Prystowsky MB. 1991. Novel expression pattern of a new member of the MIP-1 family of cytokine-like genes. *Cell. Regulat.* 2:403–12

32. Hara T, Bacon KB, Cho LC, Yoshimura A, Morikawa Y, Copeland NG, Gilbert DJ, Jenkins NA, Schall TJ, Miyajima A. 1995. Molecular cloning and functional characterization of a novel member of the C-C chemokine family. *J. Immunol.* 155:5352–58
33. Youn B-S, Jang I-K, Broxmeyer HE, Cooper S, Jenkins NA, Gilbert DJ, Copeland NG, Elick TA, Fraser MJ Jr, Kwon BS. 1995. A novel chemokine, macrophage inflammatory protein-related protein-2, inhibits colony formation of bone marrow myeloid progenitors. *J. Immunol.* 155:2661–67
34. Poltorak AN, Bazzoni F, Smirnova II, Alejos E, Thompson P, Luheshi G, Rothwell N, Beutler B. 1995. MIP-1gamma: molecular cloning, expression, and biological activities of a novel CC chemokine that is constitutively secreted in vivo. *J. Inflamm.* 45:207–19
35. Van Damme J, Proost P, Lenaerts J-P, Opdenakker G. 1992. Structural and functional identification of two human, tumor-derived monocyte chemotactic proteins (MCP-2 and MCP-3) belonging to the chemokine family. *J. Exp. Med.* 176:59–65
36. Uguccioni M, D'Apuzzo M, Loetscher M, Dewald B, Baggiolini M. 1995. Actions of the chemotactic cytokines MCP-1, MCP-2, MCP-3, RANTES, MIP-1α and MIP-1β on human monocytes. *Eur. J. Immunol.* 25:64–68
37. Loetscher P, Seitz M, Clark-Lewis I, Baggiolini M, Moser B. 1994. The monocyte chemotactic proteins, MCP-1, MCP-2 and MCP-3, are major attractants for human CD4$^+$ and CD8$^+$ T lymphocytes. *FASEB. J.* 8:1055–60
38. Carr MW, Roth SJ, Luther E, Rose SS, Springer TA. 1994. Monocyte chemoattractant protein 1 acts as a T-lymphocyte chemoattractant. *Proc. Natl. Acad. Sci. USA* 91:3652–56
39. Roth SJ, Carr MW, Springer TA. 1995. C-C chemokines, but not the C-X-C chemokines interleukin-8 and interferon-γ inducible protein-10, stimulate transendothelial chemotaxis of T lymphocytes. *Eur. J. Immunol.* 25:3482–88
40. Dahinden CA, Geiser T, Brunner T, von Tscharner V, Caput D, Ferrara P, Minty A, Baggiolini M. 1994. Monocyte chemotactic protein 3 is a most effective basophil- and eosinophil-activating chemokine. *J. Exp. Med.* 179:751–56
41. Alam R, Forsythe P, Stafford S, Heinrich J, Bravo R, Proost P, Van Damme J. 1994. Monocyte chemotactic protein-2, monocyte chemotactic protein-3, and fibroblast-induced cytokine: Three new chemokines induce chemotaxis and activation of basophils. *J. Immunol.* 153:3155–59
42. Weber M, Uguccioni M, Ochensberger B, Baggiolini M, Clark-Lewis I, Dahinden CA. 1995. Monocyte chemotactic protein MCP-2 activates human basophil and eosinophil leukocytes similar to MCP-3. *J. Immunol.* 154:4166–72
43. Daugherty BL, Siciliano SJ, DeMartino JA, Malkowitz L, Sirotina A, Springer MS. 1996. Cloning, expression, and characterization of the human eosinophil eotaxin receptor. *J. Exp. Med.* 183:2349–54
44. Ponath PD, Qin SX, Post TW, Wang J, Wu L, Gerard NP, Newman W, Gerard C, Mackay CR. 1996. Molecular cloning and characterization of a human eotaxin receptor expressed selectively on eosinophils. *J. Exp. Med.* 183:2437–48
45. Loetscher P, Seitz M, Baggiolini M, Moser B. 1996. Interleukin-2 regulates CC chemokine receptor expression and chemotactic responsiveness in T lymphocytes. *J. Exp. Med.* 184:569–77
46. Allavena P, Bianchi G, Zhou D, Van Damme J, Jìlek P, Sozzani S, Mantovani A. 1994. Induction of natural killer cell migration by monocyte chemotactic protein-1, -2 and -3. *Eur. J. Immunol.* 24:3233–36
47. Sozzani S, Sallusto F, Luini W, Zhou D, Piemonti L, Allavena P, Van Damme J, Valitutti S, Lanzavecchia A, Mantovani A. 1995. Migration of dendritic cells in response to formyl peptides, C5a, and a distinct set of chemokines. *J. Immunol.* 155:3292–95
48. Loetscher P, Seitz M, Clark-Lewis I, Baggiolini M, Moser B. 1996. Activation of NK cells by CC chemokines—chemotaxis, Ca^{2+} mobilization, and enzyme release. *J. Immunol.* 156:322–27
49. Taub DD, Sayers TJ, Carter CRD, Ortaldo JR. 1995. α and β chemokines induce NK cell migration and enhance NK-mediated cytolysis. *J. Immunol.* 155:3877–88
50. Jose PJ, Griffiths-Johnson DA, Collins PD, Walsh DT, Moqbel R, Totty NF, Truong O, Hsuan JJ, Williams TJ. 1994. Eotaxin: a potent eosinophil chemoattractant cytokine detected in a guinea pig model of allergic airways inflammation. *J. Exp. Med.* 179:881–87
51. Rothenberg ME, Luster AD, Leder P. 1995. Murine eotaxin: an eosinophil chemoattractant inducible in endothelial

cells and in interleukin 4-induced tumor suppression. *Proc. Natl. Acad. Sci. USA* 92:8960–64

52. Combadiere C, Ahuja SK, Murphy PM. 1995. Cloning and functional expression of a human eosinophil CC chemokine receptor. *J. Biol. Chem.* 270:16,491–94; correction: *J. Biol. Chem.* 270:30,235
53. Garcia-Zepeda EA, Rothenberg ME, Ownbey RT, Celestin J, Leder P, Luster AD. 1996. Human eotaxin is a specific chemoattractant for eosinophil cells and provides a new mechanism to explain tissue eosinophilia. *Nature. Med.* 2:449–56
54. Collins PD, Marleau S, Griffiths-Johnson DA, Jose PJ, Williams TJ. 1995. Cooperation between interleukin-5 and the chemokine eotaxin to induce eosinophil accumulation in vivo. *J. Exp. Med.* 182:1169–74
55. Baggiolini M. 1996. Eotaxin: a VIC (very important chemokine) of allergic inflammation? *J. Clin. Invest.* 97:587
56. Luster AD, Ravetch JV. 1987. Biochemical characterization of a γ interferon-inducible cytokine (IP-10). *J. Exp. Med.* 166:1084–97
57. Kaplan G, Luster AD, Hancock G, Cohn ZA. 1987. The expression of a γ interferon-induced protein (IP-10) in delayed immune responses in human skin. *J. Exp. Med.* 166:1098–108
58. Farber JM. 1993. HuMIG: a new human member of the chemokine family of cytokines. *Biochem. Biophys. Res. Commun.* 192:223–30
59. Taub DD, Lloyd AR, Conlon K, Wang JM, Ortaldo JR, Harada A, Matsushima K, Kelvin DJ, Oppenheim JJ. 1993. Recombinant human interferon-inducible protein 10 is a chemoattractant for human monocytes and T lymphocytes and promotes T cell adhesion to endothelial cells. *J. Exp. Med.* 177:1809–14
60. Liao F, Rabin RL, Yannelli JR, Koniaris LG, Vanguri P, Farber JM. 1995. Human mig chemokine: biochemical and functional characterization. *J. Exp. Med.* 182:1301–14
61. Loetscher M, Gerber B, Loetscher P, Jones SA, Piali L, Clark-Lewis I, Baggiolini M, Moser B. 1996. Chemokine receptor specific for IP10 and Mig: structure, function and expression in activated T lymphocytes. *J. Exp. Med.* 184:963–69
62. Tashiro K, Tada H, Heilker R, Shirozu M, Nakano T, Honjo T. 1993. Signal sequence trap: a cloning strategy for secreted proteins and type I membrane proteins. *Science* 261:600–3
63. Nagasawa T, Kikutani H, Kishimoto T. 1994. Molecular cloning and structure of a pre-B-cell growth-stimulating factor. *Proc. Natl. Acad. Sci. USA* 91:2305–9
64. Bleul CC, Fuhlbrigge RC, Casasnovas JM, Aiuti A, Springer TA. 1996. A highly efficacious lymphocyte chemoattractant, stromal cell-derived factor 1 (SDF-1). *J. Exp. Med.* 184:1101–9

64a. Shirozu M, Nakano T, Inazawa J, Tashiro K, Tada H, Shino hara T, Honjo T. 1995. Structure and chromosomal localization of the human stromal cell-derived factor 1 (SDF-1) gene. *Genomics* 28:495–500

65. Oberlin E, Amara A, Bachelerie F, Bessia C, Virelizier JL, Arenzana-Seisdedos F, Schwartz O, Heard JM, Clark-Lewis I, Legler DF, Loetscher M, Baggiolini M, Moser B. 1996. The CXC chemokine SDF-1 is the ligand for LESTR/fusin and prevents infection by T-cell-line-adapted HIV-1. *Nature.* 382:833–35
66. Loetscher M, Geiser T, O'Reilly T, Zwahlen R, Baggiolini M, Moser B. 1994. Cloning of a human seven-transmembrane domain receptor, LESTR, that is highly expressed in leukocytes. *J. Biol. Chem.* 269:232–37
67. Federsppiel B, Melhado IG, Duncan AMV, Delaney A, Schappert K, Clark-Lewis I, Jirik FR. 1993. Molecular cloning of the cDNA and chromosomal localization of the gene for a putative seven-transmembrane segment (7-TMS) receptor isolated from human spleen. *Genomics* 16:707–12
68. Nomura H, Nielsen BW, Matsushima K. 1993. Molecular cloning of cDNAs encoding a LD78 receptor and putative leukocyte chemotactic peptide receptors. *Int. Immunol.* 5:1239–49
69. Herzog H, Hort YJ, Shine J, Selbie LA. 1993. Molecular cloning, characterization, and localization of the human homolog to the reported bovine NPY Y3 receptor: lack of NPY binding and activation. *DNA Cell. Biol.* 12:465–71
70. Jazin EE, Yoo H, Blomqvist AG, Yee F, Weng G, Walker MW, Salon J, Larhammar D, Wahlestedt C. 1993. A proposed bovine neuropeptide Y (NPY) receptor cDNA clone, or its human homologue, confers neither NPY binding sites nor NPY responsiveness on transfected cells. *Regul. Pept.* 47:247–58
71. Bleul CC, Farzan M, Choe H, Parolin C, Clark-Lewis I, Sodroski J, Springer T. 1996. The lymphocyte chemoattractant SDF-1 is a ligand for LESTR/fusin and blocks HIV-1 entry. *Nature.* 382:829–33
72. Nagasawa T, Hirota S, Tachibana K, Takakura N, Nishikawa S, Kitamura Y,

Yoshida N, Kikutani H, Kishimoto T. 1996. Defects of B-cell lymphopoiesis and bone marrow myelopoiesis in mice lacking the CXC chemokine PBSF/SDF-1. *Nature*. 382:635–38
73. Holmes WE, Lee J, Kuang W-J, Rice GC, Wood WI. 1991. Structure and functional expression of a human interleukin-8 receptor. *Science* 253:1278–80
74. Murphy PM, Tiffany HL. 1991. Cloning of complementary DNA encoding a functional human interleukin-8 receptor. *Science* 253:1280–83
75. Moser B, Barella L, Mattei S, Schumacher C, Boulay F, Colombo MP, Baggiolini M. 1993. Expression of transcripts for two interleukin 8 receptors in human phagocytes, lymphocytes and melanoma cells. *Biochem. J.* 294:285–92
76. Xu L, Kelvin DJ, Ye GQ, Taub DD, Ben-Baruch A, Oppenheim JJ, Wang JM. 1995. Modulation of IL-8 receptor expression on purified human T lymphocytes is associated with changed chemotactic responses to IL-8. *J. Leukocyte. Biol.* 57:335–42
77. Qin SX, LaRosa G, Campbell JJ, Smith-Heath H, Kassam N, Shi XJ, Zeng L, Butcher EC, Mackay CR. 1996. Expression of monocyte chemoattractant protein-1 and interleukin-8 receptors on subsets of T cells: correlation with transendothelial chemotactic potential. *Eur. J. Immunol.* 26:640–47
78. Chuntharapai A, Lee J, Hébert CA, Kim KJ. 1994. Monoclonal antibodies detect different distribution patterns of IL-8 receptor A and IL-8 receptor B on human peripheral blood leukocytes. *J. Immunol.* 153:5682–88
79. Schulz BS, Michel G, Wagner S, Süss R, Beetz A, Peter RU, Kemény L, Ruzicka T. 1993. Increased expression of epidermal IL-8 receptor in psoriasis: down-regulation by FK-506 in vitro. *J. Immunol.* 151:4399–406
80. Nanney LB, Mueller SG, Bueno R, Peiper SC, Richmond A. 1995. Distributions of melanoma growth stimulatory activity or growth-regulated gene and the interleukin-8 receptor B in human wound repair. *Am. J. Pathol.* 147:1248–60
81. LaRosa GJ, Thomas KM, Kaufmann ME, Mark R, White M, Taylor L, Gray G, Witt D, Navarro J. 1992. Amino terminus of the interleukin-8 receptor is a major determinant of receptor subtype specificity. *J. Biol. Chem.* 267:25,402–6
82. Gayle RB III, Sleath PR, Srinivason S, Birks CW, Weerawarna KS, Cerretti DP, Kozlosky CJ, Nelson N, Vanden Bos T, Beckmann MP. 1993. Importance of the amino terminus of the interleukin-8 receptor in ligand interactions. *J. Biol. Chem.* 268:7283–89
83. Hébert CA, Chuntharapai A, Smith M, Colby T, Kim J, Horuk R. 1993. Partial functional mapping of the human interleukin-8 type A receptor. Identification of a major ligand binding domain. *J. Biol. Chem.* 268:18,549–53
84. Leong SR, Kabakoff RC, Hébert CA. 1994. Complete mutagenesis of the extracellular domain of interleukin-8 (IL-8) type A receptor identifies charged residues mediating IL-8 binding and signal transduction. *J. Biol. Chem.* 269:19,343–48
85. Ahuja SK, Lee JC, Murphy PM. 1996. CXC chemokines bind to unique sets of selectivity determinants that can function independently and are broadly distributed on multiple domains of human interleukin-8 receptor B—determinants of high affinity binding and receptor activation are distinct. *J. Biol. Chem.* 271:225–32
86. Feng Y, Broder CC, Kennedy PE, Berger EA. 1996. HIV-1 entry cofactor: functional cDNA cloning of a seven-transmembrane, G protein-coupled receptor. *Science* 272:872–77
87. Neote K, DiGregorio D, Mak JY, Horuk R, Schall TJ. 1993. Molecular cloning, functional expression, and signaling characteristics of a C-C chemokine receptor. *Cell* 72:415–25
88. Gao J-L, Kuhns DB, Tiffany HL, McDermott D, Li X, Francke U, Murphy PM. 1993. Structure and functional expression of the human macrophage inflammatory protein 1α/RANTES receptor. *J. Exp. Med.* 177:1421–27
89. Charo IF, Myers SJ, Herman A, Franci C, Connolly AJ, Coughlin SR. 1994. Molecular cloning and functional expression of two monocyte chemoattractant protein 1 receptors reveals alternative splicing of the carboxyl-terminal tails. *Proc. Natl. Acad. Sci. USA* 91:2752–56
90. Kuang YN, Wu YP, Jiang HP, Wu DQ. 1996. Selective G protein coupling by C-C chemokine receptors. *J. Biol. Chem.* 271:3975–78
91. Raport CJ, Schweickart VL, Chantry D, Eddy RL Jr, Shows TB, Godiska R, Gray PW. 1996. New members of the chemokine receptor gene family. *J. Leuk. Biol.* 59:18–23
92. Franci C, Wong LM, Van Damme J, Proost P, Charo IF. 1995. Monocyte chemoattractant protein-3, but not mono-

cyte chemoattractant protein-2, is a functional ligand of the human monocyte chemoattractant protein-1 receptor. *J. Immunol.* 154:6511–17

93. Ben-Baruch A, Xu LL, Young PR, Bengali K, Oppenheim JJ, Wang JM. 1995. Monocyte chemotactic protein-3 (MCP3) interacts with multiple leukocyte receptors—C-C CKR1, a receptor for macrophage inflammatory protein-1α/Rantes, is also a functional receptor for MCP3. *J. Biol. Chem.* 270:22,123–28
94. Combadiere C, Ahuja SK, Van Damme J, Tiffany HL, Gao JL, Murphy PM. 1995. Monocyte chemoattractant protein-3 is a functional ligand for CC chemokine receptors 1 and 2B. *J. Biol. Chem.* 270:29671–75
95. Gong JH, Uguccioni M, Dewald B, Baggiolini M, Clark-Lewis I. 1996. RANTES and MCP-3 antagonists bind multiple chemokine receptors. *J. Biol. Chem.* 271:10,521–27
96. Power CA, Meyer A, Nemeth K, Bacon KB, Hoogewerf AJ, Proudfoot AEI, Wells TNC. 1995. Molecular cloning and functional expression of a novel CC chemokine receptor cDNA from a human basophilic cell line. *J. Biol. Chem.* 270:19495–500
97. Hoogewerf AJ, Black D, Proudfoot AEI, Wells TNC, Power CA. 1996. Molecular cloning of murine CC CKR-4 and high affinity binding of chemokines to murine and human CC CKR-4. *Biochem. Biophys. Res. Commun.* 218:337–43
98. Samson M, Labbe O, Mollereau C, Vassart G, Parmentier M. 1996. Molecular cloning and functional expression of a new human CC-chemokine receptor gene. *Biochemistry* 35:3362–67
99. Dobner T, Wolf I, Emrich T, Lipp M. 1992. Differentiation-specific expression of a novel G protein-coupled receptor from Burkitt's lymphoma. *Eur. J. Immunol.* 22:2795–99
100. Kaiser E, Förster R, Wolf I, Ebensperger C, Kuehl WM, Lipp M. 1993. The G protein-coupled receptor BLR1 is involved in murine B cell differentiation and is also expressed in neuronal tissues. *Eur. J. Immunol.* 23:2532–39
101. Förster R, Emrich T, Kremmer E, Lipp M. 1994. Expression of the G-protein-coupled receptor BLR1 defines mature, recirculating B cells and a subset of T-helper memory cells. *Blood* 84:830–40
102. Barella L, Loetscher M, Tobler A, Baggiolini M, Moser B. 1995. Sequence variation of a novel heptahelical leucocyte receptor through alternative transcript formation. *Biochem. J.* 309:773–79
103. Birkenbach M, Josefsen K, Yalamanchili R, Lenoir G, Kieff E. 1993. Epstein-Barr virus-induced genes: first lymphocyte-specific G protein-coupled peptide receptors. *J. Virol.* 67:2209–20
104. Combadiere C, Ahuja SK, Murphy PM. 1995. Cloning, chromosomal localization, and RNA expression of a human β chemokine receptor-like gene. *DNA Cell. Biol.* 14:673–80
105. Raport CJ, Schweickart VL, Eddy RL Jr, Shows TB, Gray PW. 1995. The orphan G-protein-coupled receptor-encoding gene V28 is closely related to genes for chemokine receptors and is expressed in lymphoid and neural tissues. *Gene* 163:295–99
106. Gao J-L, Murphy PM. 1994. Human cytomegalovirus open reading frame US28 encodes a functional β chemokine receptor. *J. Biol. Chem.* 269:28539–42
107. Ahuja SK, Murphy PM. 1993. Molecular piracy of mammalian interleukin-8 receptor type B by herpesvirus saimiri. *J. Biol. Chem.* 268:20,691–94
108. Murayama T, Kuno K, Jisaki F, Obuchi M, Sakamuro D, Furukawa T, Mukaida N, Matsushima K. 1994. Enhancement of human cytomegalovirus replication in a human lung fibroblast cell line by interleukin-8. *J. Virol.* 68:7582–85
109. Wu D, LaRosa GJ, Simon MI. 1993. G protein-coupled signal transduction pathways for interleukin-8. *Science* 261:101–3
110. Loetscher P, Seitz M, Clark-Lewis I, Baggiolini M, Moser B. 1994. Both interleukin-8 receptors independently mediate chemotaxis. Jurkat cells transfected with IL-8R1 or IL-8R2 migrate in response to IL-8, GROα and NAP-2. *FEBS Lett.* 341:187–92
111. Jones SA, Moser B, Thelen M. 1995. A comparison of post-receptor signal transduction events in Jurkat cells transfected with either IL-8R1 or IL-8R2: chemokine mediated activation of p42/p44 MAP-kinase (ERK-2). *FEBS Lett.* 364:211–14
112. Jones SA, Wolf M, Qin S, Mackay CR, Baggiolini M. 1996. Different functions for the interleukin 8 receptors of human neutrophil leukocytes. NADPH oxidase and phospholipase D are activated through IL-8R1 but not IL-8R2. *Proc. Natl. Acad. Sci. USA* 93:6682–86
113. L'Heureux GP, Bourgoin S, Jean N, McColl SR, Naccache PH. 1995. Diverging signal transduction pathways activated by interleukin-8 and related chemokines in

human neutrophils: interleukin-8, but not NAP-2 or GROα, stimulates phospholipase D activity. *Blood* 85:522–31
114. Dubois PM, Palmer D, Webb ML, Ledbetter JA, Shapiro RA. 1996. Early signal transduction by the receptor to the chemokine monocyte chemotactic protein-1 in a murine T cell hybrid. *J. Immunol.* 156:1356–61
115. Thelen M, Uguccioni M, Bösiger J. 1995. PI 3-kinase-dependent and independent chemotaxis of human neutrophil leukocytes. *Biochem. Biophys. Res. Commun.* 217:1255–62
116. Turner L, Ward SG, Westwick J. 1995. RANTES-activated human T lymphocytes: a role for phosphoinositide 3-kinase. *J. Immunol.* 155:2437–44
117. Bokoch GM. 1995. Chemoattractant signaling and leukocyte activation. *Blood* 86:1649–60
118. Laudanna C, Campbell JJ, Butcher EC. 1996. Role of Rho in chemoattractant-activated leukocyte adhesion through integrins. *Science* 271:981–83
119. Mueller SG, Schraw WP, Richmond A. 1994. Melanoma growth stimulatory activity enhances the phosphorylation of the class II interleukin-8 receptor in non-hematopoietic cells. *J. Biol. Chem.* 269:1973–80
120. Richardson RM, DuBose RA, Ali H, Tomhave ED, Haribabu B, Snyderman R. 1995. Regulation of human interleukin-8 receptor A: identification of a phosphorylation site involved in modulating receptor functions. *Biochemistry* 34:14193–201
121. Richardon RM, Ali H, Tomhave ED, Haribabu B, Snyderman R. 1995. Cross-desensitization of chemoattractant receptors occurs at multiple levels—evidence for a role for inhibition of phospholipase C activity. *J. Biol. Chem.* 270:27829–33
122. Rajarathnam K, Clark-Lewis I, Sykes BD. 1994. ^{1}H NMR studies of interleukin 8 analogs: characterization of the domains essential for function. *Biochemistry* 33:6623–30
123. Schraufstätter IU, Ma M, Oades ZG, Barritt DS, Cochrane CG. 1995. The role of Tyr^{13} and Lys^{15} of interleukin-8 in the high affinity interaction with the interleukin-8 receptor type A. *J. Biol. Chem.* 270:10428–31
124. Heinrich JN, Bravo R. 1995. N51 competes ^{125}I-interleukin (IL)-8 binding to IL-8Rβ but not IL-8Rα—structure-function analysis using N51/IL-8 chimeric molecules. *J. Biol. Chem.* 270:28,014–17
125. Hammond MEW, Shyamala V, Siani MA, Gallegos CA, Feucht PH, Abbott J, Lapointe GR, Moghadam M, Khoja H, Zakel J, Tekamp-Olson P. 1996. Receptor recognition and specificity of interleukin-8 is determined by residues that cluster near a surface-accessible hydrophobic pocket. *J. Biol. Chem.* 271:8228–35
126. Williams G, Borkakoti N, Bottomley GA, Cowan I, Fallowfield AG, Jones PS, Kirtland SJ, Price GJ, Price L. 1996. Mutagenesis studies of interleukin-8—identification of a second epitope involved in receptor binding. *J. Biol. Chem.* 271:9579–86
127. Lowman HB, Slagle PH, DeForge LE, Wirth CM, Gillece-Castro BL, Bourell JH, Fairbrother WJ. 1996. Exchanging interleukin-8 and melanoma growth-stimulating activity receptor binding specificities. *J. Biol. Chem.* 271:14,344–52
128. Beall CJ, Mahajan S, Kolattukudy PE. 1992. Conversion of monocyte chemoattractant protein-1 into a neutrophil attractant by substitution of two amino acids. *J. Biol. Chem.* 267:3455–59
129. Lusti-Narasimhan M, Power CA, Allet B, Alouani S, Bacon KB, Mermod J-J, Proudfoot AEI, Wells TNC. 1995. Mutation of Leu^{25} and Val^{27} introduces CC chemokine activity into interleukin-8. *J. Biol. Chem.* 270:2716–21
130. Lusti-Narasimhan M, Chollet A, Power CA, Allet B, Proudfoot AEI, Wells TNC. 1996. A molecular switch of chemokine receptor selectivity—chemical modification of the interleukin-8 Leu25⟶Cys mutant. *J. Biol. Chem.* 271:3148–53
131. Walz A, Meloni F, Clark-Lewis I, von Tscharner V, Baggiolini M. 1991. $[Ca^{2+}]_i$ changes and respiratory burst in human neutrophils and monocytes induced by NAP-1/interleukin-8, NAP-2, and gro/MGSA. *J. Leuk. Biol.* 50:279–86
132. Gong J-H, Clark-Lewis I. 1995. Antagonists of monocyte chemoattractant protein 1 identified by modification of functionally critical NH_2-terminal residues. *J. Exp. Med.* 181:631–40
133. Weber M, Uguccioni M, Baggiolini M, Clark-Lewis I, Dahinden CA. 1996. Deletion of the NH_2-terminal residue converts monocyte chemotactic protein 1 from an activator of basophil mediator release to an eosinophil chemoattractant. *J. Exp. Med.* 183:681–85
134. Masure S, Paemen L, Proost P, Van Damme J, Opdenakker G. 1995. Expression of a human mutant monocyte chemotactic protein 3 in *Pichia pastoris* and characterization as an MCP-3

receptor antagonist. *J. Interferon Cytokine Res.* 15:955–63
135. Proudfoot AEI, Power CA, Hoogewerf AJ, Montjovent MO, Borlat F, Offord RE, Wells TNC. 1996. Extension of recombinant human RANTES by the retention of the initiating methionine produces a potent antagonist. *J. Biol. Chem.* 271:2599–603
136. Springer TA. 1995. Traffic signals on endothelium for lymphocyte recirculation and leukocyte emigration. *Annu. Rev. Physiol.* 57:827–72
137. Butcher EC, Picker LJ. 1996. Lymphocyte homing and homeostasis. *Science* 272:60–66
138. Luscinskas FW, Gimbrone MA Jr. 1996. Endothelial-dependent mechanisms in chronic inflammatory leukocyte recruitment. *Annu. Rev. Med.* 47:413–21
139. Broxmeyer HE, Sherry B, Lu L, Cooper S, Carow C, Wolpe SD, Cerami A. 1989. Myelopoietic enhancing effects of murine macrophage inflammatory proteins 1 and 2 on colony formation in vitro by murine and human bone marrow granulocyte/macrophage progenitor cells. *J. Exp. Med.* 170:1583–94
140. Graham GJ, Wright EG, Hewick R, Wolpe SD, Wilkie NM, Donaldson D, Lorimore S, Pragnell IB. 1990. Identification and characterization of an inhibitor of haemopoietic stem cell proliferation. *Nature* 344:442–44
141. Cook DN. 1996. The role of MIP-1α in inflammation and hematopoiesis. *J. Leuk. Biol.* 59:61–66
142. Colditz IG, Zwahlen RD, Baggiolini M. 1990. Neutrophil accumulation and plasma leakage induced in vivo by neutrophil-activating peptide-1. *J. Leukocyte. Biol.* 48:129–37
143. Webb LMC, Ehrengruber MU, Clark-Lewis I, Baggiolini M, Rot A. 1993. Binding to heparan sulfate or heparin enhances neutrophil responses to interleukin 8. *Proc. Natl. Acad. Sci. USA* 90:7158–62
144. Witt DP, Lander AD. 1994. Differential binding of chemokines to glycosaminoglycan subpopulations. *Curr. Biol.* 4:394–400
145. Tanaka Y, Adams DH, Shaw S. 1993. Proteoglycans on endothelial cells present adhesion-inducing cytokines to leukocytes. *Immunol. Today* 14:111–15
146. Gilat D, Hershkoviz R, Mekori YA, Vlodavsky I, Lider O. 1994. Regulation of adhesion of $CD4^+$ T lymphocytes to intact or heparinase-treated subendothelial extracellular matrix by diffusible or anchored RANTES and MIP-1β. *J. Immunol.* 153:4899–4906
147. Rot A, Hub E, Middleton J, Pons F, Rabeck C, Thierer K, Wintle J, Wolff B, Zsak M, Dukor P. 1996. Some aspects of IL-8 pathophysiology. 3. Chemokine interaction with endothelial cells. *J. Leuk. Biol.* 59:39–44
148. Watson JB, Getzler SB, Mosher DF. 1994. Platelet factor 4 modulates the mitogenic activity of basic fibroblast growth factor. *J. Clin. Invest.* 94:261–68
149. Brown KJ, Parish CR. 1994. Histidine-rich glycoprotein and platelet factor 4 mask heparan sulfate proteoglycans recognized by acidic and basic fibroblast growth factor. *Biochemistry* 33:13,918–27
150. Chaudhuri A, Polyakova J, Zbrzezna V, Williams K, Gulati S, Pogo AO. 1993. Cloning of glycoprotein D cDNA, which encodes the major subunit of the Duffy blood group system and the receptor for the *Plasmodium vivax* malaria parasite. *Proc. Natl. Acad. Sci. USA* 90:10793–97
151. Horuk R, Chitnis CE, Darbonne WC, Colby TJ, Rybicki A, Hadley TJ, Miller LH. 1993. A receptor for the malarial parasite *Plasmodium vivax*: the erythrocyte chemokine receptor. *Science* 261:1182–84
152. Horuk R, Martin A, Hesselgesser J, Hadley T, Lu ZH, Wang ZX, Peiper SC. 1996. The Duffy antigen receptor for chemokines: structural analysis and expression in the brain. *J. Leuk. Biol.* 59:29–38
153. Darbonne WC, Rice GC, Mohler MA, Apple T, Hébert CA, Valente AJ, Baker JB. 1991. Red blood cells are a sink for interleukin 8, a leukocyte chemotaxin. *J. Clin. Invest.* 88:1362–69
154. Taub DD, Conlon K, Lloyd AR, Oppenheim JJ, Kelvin DJ. 1993. Preferential migration of activated $CD4^+$ and $CD8^+$ T cells in response to MIP-1α and MIP-1β. *Science* 260:355–58
155. Rand ML, Warren JS, Mansour MK, Newman W, Ringler DJ. 1996. Inhibition of T cell recruitment and cutaneous delayed-type hypersensitivity-induced inflammation with antibodies to monocyte chemoattractant protein-1. *Am. J. Pathol.* 148:855–64
156. Huffnagle GB, Strieter RM, Standiford TJ, McDonald RA, Burdick MD, Kunkel SL, Toews GB. 1995. The role of monocyte chemotactic protein-1 (MCP-1) in the recruitment of monocytes and $CD4^+$ T cells during a pulmonary

Cryptococcus neoformans infection. *J. Immunol.* 155:4790–97

157. Colditz IG, Watson DL. 1992. The effect of cytokines and chemotactic agonists on the migration of T lymphocytes into skin. *Immunology* 76:272–78
158. Kennedy J, Kelner GS, Kleyensteuber S, Schall TJ, Weiss MC, Yssel H, Schneider PV, Cocks BG, Bacon KB, Zlotnik A. 1995. Molecular cloning and functional characterization of human lymphotactin. *J. Immunol.* 155:203–9
159. Müller S, Dorner B, Korthäuer U, Mages HW, D'Apuzzo M, Senger G, Kroczek RA. 1995. Cloning of ATAC, an activation-induced, chemokine-related molecule exclusively expressed in CD8+ T lymphocytes. *Eur. J. Immunol.* 25:1744–48
160. Leek RD, Harris AL, Lewis CE. 1994. Cytokine networks in solid human tumors: regulation of angiogenesis. *J. Leuk. Biol.* 56:423–35
161. Maione TE, Gray GS, Petro J, Hunt AJ, Donner AL, Bauer SI, Carson HF, Sharpe RJ. 1990. Inhibition of angiogenesis by recombinant human platelet factor-4 and related peptides. *Science* 247:77–79
162. Sharpe RJ, Byers HR, Scott CF, Bauer SI, Maione TE. 1990. Growth inhibition of murine melanoma and human colon carcinoma by recombinant human platelet factor 4. *J. Natl. Cancer. Inst.* 82:848–53
163. Luster AD, Greenberg SM, Leder P. 1995. The IP-10 chemokine binds to a specific cell surface heparan sulfate site shared with platelet factor 4 and inhibits endothelial cell proliferation. *J. Exp. Med.* 182:219–31
164. Koch AE, Polverini PJ, Kunkel SL, Harlow LA, DiPietro LA, Elner VM, Elner SG, Strieter RM. 1992. Interleukin-8 as a macrophage-derived mediator of angiogenesis. *Science* 258:1798–801
165. Strieter RM, Polverini PJ, Kunkel SL, Arenberg DA, Burdick MD, Kasper J, Dzuiba J, Van Damme J, Walz A, Marriott D, Chan SY, Roczniak S, Shanafelt AB. 1995. The functional role of the ELR motif in CXC chemokine-mediated angiogenesis. *J. Biol. Chem.* 270:27348–57
166. Petzelbauer P, Watson CA, Pfau SE, Pober JS. 1995. IL-8 and angiogenesis: evidence that human endothelial cells lack receptors and do not respond to IL-8 in vitro. *Cytokine* 7:267–72
167. Cao YH, Chen C, Weatherbee JA, Tsang M, Folkman J. 1995. gro-β, a -C-X-C- chemokine, is an angiogenesis inhibitor that suppresses the growth of Lewis lung carcinoma in mice. *J. Exp. Med.* 182:2069–77
168. Arenberg DA, Kunkel SL, Polverini PJ, Glass M, Burdick MD, Strieter RM. 1996. Inhibition of interleukin-8 reduces tumorigenesis of human non-small cell lung cancer in SCID mice. *J. Clin. Invest.* 97:2792–802
169. Singh RK, Gutman M, Radinsky R, Bucana CD, Fidler IJ. 1994. Expression of interleukin 8 correlates with the metastatic potential of human melanoma cells in nude mice. *Cancer. Res.* 54:3242–47
170. Wang JY, Huang M, Lee P, Komanduri K, Sharma S, Chen G, Dubinett SM. 1996. Interleukin-8 inhibits non-small cell lung cancer proliferation: a possible role for regulation of tumor growth by autocrine and paracrine pathways. *J. Interferon Cytokine Res.* 16:53–60
171. Hirose K, Hakozaki M, Nyunoya Y, Kobayashi Y, Matsushita K, Takenouchi T, Mikata A, Mukaida N, Matsushima K. 1995. Chemokine gene transfection into tumour cells reduced tumorigenicity in nude mice in association with neutrophilic infiltration. *Br. J. Cancer* 72:708–14
172. Luster AD, Leder P. 1993. IP-10, a -C-X-C- chemokine, elicits a potent thymus-dependent antitumor response in vivo. *J. Exp. Med.* 178:1057–65
173. Koch AE, Halloran MM, Haskell CJ, Shah MR, Polverini PJ. 1995. Angiogenesis mediated by soluble forms of E-selectin and vascular cell adhesion molecule-1. *Nature* 376:517–19
174. Cocchi F, DeVico AL, Garzino-Demo A, Arya SK, Gallo RC, Lusso P. 1995. Identification of RANTES, MIP-1α, and MIP-1β as the major HIV-suppressive factors produced by CD8+ T cells. *Science* 270:1811–15
175. Dragic T, Litwin V, Allaway GP, Martin SR, Huang YX, Nagashima KA, Cayanan C, Maddon PJ, Koup RA, Moore JP, Paxton WA. 1996. HIV-1 entry into CD4+ cells is mediated by the chemokine receptor CC-CKR-5. *Nature* 381:667–73
176. Deng HK, Liu R, Ellmeier W, Choe S, Unutmaz D, Burkhart M, Di Marzio P, Marmon S, Sutton RE, Hill CM, Davis CB, Peiper SC, Schall TJ, Littman DR, Landau NR. 1996. Identification of a major co-receptor for primary isolates of HIV-1. *Nature* 381:661–66
177. Choe H, Farzan M, Sun Y, Sullivan N, Rollins B, Ponath PD, Wu L, Mackay CR, LaRosa G, Newman W, Gerard N, Gerard C, Sodroski J. 1996. The β-chemokine

receptors CCR3 and CCR5 facilitate infection by primary HIV-1 isolates. *Cell* 85:1135–48

178. Doranz BJ, Rucker J, Yi Y, Smyth RJ, Samson M, Peiper SC, Parmentier M, Collman RG, Doms RW. 1996. A dual-tropic primary HIV-1 isolate that uses fusin and the β-chemokine receptors CKR-5, CKR-3, and CKR-2b as fusion cofactors. *Cell* 85:1149–58
179. Alkhatib G, Combadiere C, Broder CC, Feng Y, Kennedy PE, Murphy PM, Berger EA. 1996. CC CKR5: A RANTES, MIP-1α, MIP-1β receptor as a fusion cofactor for macrophage-tropic HIV-1. *Science* 272:1955–58
180. Paxton WA, Martin SR, Tse D, O'Brien TR, Skurnick J, VanDevanter NL, Padian N, Braun JF, Kotler DP, Wolinsky SM, Koup RA. 1996. Relative resistance to HIV-1 infection of CD4 lymphocytes from persons who remain uninfected despite multiple high-risk sexual exposures. *Nature Med.* 2:412–17
181. Sneath PHA, Sokal RR. 1973. *Numerical Taxonomy*. New York: Freeman

THE JOURNAL OF BIOLOGICAL CHEMISTRY

Vol. 270, No. 45, Issue of November 10, pp. 27348–27357, 1995
Printed in U.S.A.

The Functional Role of the ELR Motif in CXC Chemokine-mediated Angiogenesis*

(Received for publication, July 7, 1995, and in revised form, August 11, 1995)

Robert M. Strieter‡§, Peter J. Polverini¶, Steven L. Kunkel‖, Douglas A. Arenberg‡, Marie D. Burdick‡, James Kasper**, Judith Dzuiba‡‡, Jo Van Damme§§, Alfred Walz¶¶, David Marriott‖‖, Sham-Yuen Chan‖‖, Steven Roczniak**, and Armen B. Shanafelt**

*From the Departments of ‡Internal Medicine (Division of Pulmonary and Critical Medicine) and ‖Pathology, the University of Michigan Medical School, Ann Arbor, Michigan 48109-0360, the ¶University of Michigan Dental School, Section of Oral Pathology, Ann Arbor, Michigan 48109, the §§Rega Institute, University of Leuven, B-3000 Leuven, Belgium, the ¶¶Theodor Kocher Institut, University of Bern, CH-3000, Bern 9, Switzerland, the **Institute of Molecular Biologicals and ‡‡Institute of Research Technologies, Bayer Corporation, West Haven, Connecticut 06516, and the ‖‖Department of Molecular and Cellular Biology, Bayer Corporation, Berkeley, California 94701*

In this study, we demonstrate that the CXC family of chemokines displays disparate angiogenic activity depending upon the presence or absence of the ELR motif. CXC chemokines containing the ELR motif (ELR-CXC chemokines) were found to be potent angiogenic factors, inducing both *in vitro* endothelial chemotaxis and *in vivo* corneal neovascularization. In contrast, the CXC chemokines lacking the ELR motif, platelet factor 4, interferon γ-inducible protein 10, and monokine induced by γ-interferon, not only failed to induce significant *in vitro* endothelial cell chemotaxis or *in vivo* corneal neovacularization but were found to be potent angiostatic factors in the presence of either ELR-CXC chemokines or the unrelated angiogenic factor, basic fibroblast growth factor. Additionally, mutant interleukin-8 proteins lacking the ELR motif demonstrated potent angiostatic effects in the presence of either ELR-CXC chemokines or basic fibroblast growth factor. In contrast, a mutant of monokine induced by γ-interferon containing the ELR motif was found to induce *in vivo* angiogenic activity. These findings suggest a functional role of the ELR motif in determining the angiogenic or angiostatic potential of CXC chemokines, supporting the hypothesis that the net biological balance between angiogenic and angiostatic CXC chemokines may play an important role in regulating overall angiogenesis.

Angiogenesis, characterized by the neoformation of blood vessels, is an essential biological event encountered in a number of physiological and pathological processes, such as embryonic development, the formation of inflammatory granulation tissue during wound healing, chronic inflammation, and the growth of malignant solid tumors (1–5). Neovascularization can be rapidly induced in response to diverse pathophysiologic stimuli. Under conditions of homeostasis, the rate of capillary endothelial cell turn-over is typically measured in months or years (6, 7). However, the process of angiogenesis during normal wound repair is rapid, transient, and tightly controlled. During neovascularization, normally quiescent endothelial cells are stimulated, degrade their basement membrane and proximal extracellular matrix, migrate directionally, divide, and organize into new functioning capillaries invested by a basal lamina (1–5). The abrupt termination of angiogenesis that accompanies the resolution of the wound repair suggests two possible mechanisms of control: a marked reduction in angiogenic mediators coupled with a simultaneous increase in the level of angiostatic factors that inhibit new vessel growth (8). In contrast to neovascularization of normal wound repair, tumorigenesis is associated with exaggerated angiogenesis, suggesting the existence of augmented angiogenic and reduced levels of angiostatic mediators (3, 9). Although most investigations studying angiogenesis have focused on the identification and mechanism of action of angiogenic factors, recent evidence suggests that angiostatic factors may play an equally important role in the control of neovascularization (8, 10–26).

Recently, platelet factor 4 (PF4),[1] a member of the CXC chemokine family, has been found to be an inhibitor of angiogenesis (27). In contrast, interleukin-8 (IL-8), another member of the CXC chemokine family, has been shown to have potent angiogenic properties (28–30). Although these CXC chemokines have significant homology on the amino acid level, one of the major differences between IL-8 and PF4 is the presence in IL-8 of the sequence Glu-Leu-Arg (the ELR motif), which is not found in PF4 (31–34). These three amino acids appear to be important in ligand/receptor interactions on neutrophils (35, 36) and are highly conserved in all members of the CXC chemokine family that demonstrate biological activation of neutrophils (35, 36).

In this study, we demonstrate that members of the CXC chemokine family that contain the ELR motif, as compared with members that lack these three amino acids, are potent inducers of angiogenic activity. In addition, we show that CXC chemokines that lack the ELR motif, PF4, interferon γ-inducible protein 10 (IP-10), and monokine induced by γ-interferon (MIG) are potent inhibitors of both CXC (ELR) chemokine and

* This work was supported, in part, by National Institutes of Health Grants HL50057, CA66180, and 1P50HL46487 (to R. M. S.), HL39926 (to P. J. P.), and HL31693 and HL35276 (to S. L. K.) and by the General Savings and Retirement Fund (ASLK) Cancer Foundation, Belgium (to J. V. D.). The costs of publication of this article were defrayed in part by the payment of page charges. This article must therefore be hereby marked "*advertisement*" in accordance with 18 U.S.C. Section 1734 solely to indicate this fact.

§ To whom correspondence should be addressed: Dept. of Internal Medicine, Div. of Pulmonary and Critical Care, Box 0360, University of Michigan Medical Center, 3916 Taubman Dr., Ann Arbor, MI 48109-0360. Tel.: 313-764-4554; Fax: 313-764-4556.

[1] The abbreviations used are: PF4, platelet factor 4; IL-8, interleukin-8; IP-10, interferon γ-inducible protein 10; MIG, monokine induced by γ-interferon; bFGF, basic fibroblast growth factorbasic fibroblast growth factor; PAGE, polyacrylamide gel electrophoresis; GRO, growth-related oncogene; ENA-78, epithelial neutrophil activating protein-78; GCP-2, granulocyte chemotactic protein-2; PBS, phosphate-buffered saline; GST, glutathione *S*-transferase; HPF, high power field(s); IFN, interferon.

basic fibroblast growth factor (bFGF)-induced angiogenesis. Moreover, substitution of the ELR motif in IL-8 generated proteins that antagonized the angiogenic effects of ELR-CXC chemokines and bFGF, while a mutant of MIG containing the ELR motif was angiogenic. These results suggest that the presence or absence of the ELR motif in CXC chemokines functionally defines the angiogenic (ELR containing) or angiostatic (non-ELR) characteristics of these proteins. These findings support the notion that CXC chemokines play an important role in the regulation of angiogenesis by acting as either angiogenic or angiostatic factors.

MATERIALS AND METHODS

Reagents—Human recombinant IP-10 (lyophilized protein with no additives) was purchased from Pepro Tech Inc. (Rocky Hill, NJ). IP-10 was >98% pure by SDS-PAGE analysis. Human recombinant bFGF (lyophilized protein with no additives) was purchased from R&D Systems Inc. (Minneapolis, MN). bFGF was >97% pure, as determined by NH_2 terminus analysis and SDS-PAGE. Recombinant human PF4, natural NH_2-terminal truncated forms of platelet basic protein (connective tissue activating protein-III, β-thromboglobulin, and neutrophil-activating protein-2), recombinant IL-8 (72 amino acids), recombinant human growth-related oncogene (GRO-α), recombinant human GRO-β, recombinant human GRO-γ, and recombinant human epithelial neutrophil activating protein-78 (ENA-78) were provided by A. Walz. These chemokines were lyophilized proteins with no additives and were >97% pure, as determined by NH_2 terminus analysis and SDS-PAGE. Natural granulocyte chemotactic protein-2 (GCP-2; Ref. 34) was provided by J. Van Damme and was >98% pure, as determined by NH_2 terminus analysis and SDS-PAGE. Endotoxin levels were less than 0.1 ng/μg for the above cytokines. The proteins were either reconstituted in Dulbecco's modified Eagle's medium with 0.1% bovine serum albumin for analysis in endothelial cell chemotaxis assays, Hanks' balanced salt solution with calcium/magnesium for analysis in neutrophil cell chemotaxis assays, or 1 × PBS for the corneal micropocket model of angiogenesis.

Bacterial Host Strains and Vectors—The *Escherichia coli* K12 strain DH5αF′ (Life Technologies, Inc.) was used as host for the propagation and maintenance of M13 DNA, and for expression of IL-8 and MIG proteins. Strain CJ236 was used to prepare uracil-DNA for use in site-directed mutagenesis (37). pGEX 4T-1 (Pharmacia Biotech Inc.) was used as the expression vector for all MIG cDNAs (38). pMAL-c2 (New England BioLabs) was used as the expression vector for all IL-8 cDNAs.

Mutagenesis, Recombinant DNA, and Sequencing Protocols—Site-directed mutagenesis was followed the protocol described by Kunkel *et al.* (37). Individual clones were sequenced using the dideoxynucleotide method (39) with modifications described in the Sequenase® (U. S. Biochemical Corp.) protocol. M13 (replicative form) DNA (40) containing confirmed MIG mutations was cleaved with *Bam*HI and *Xba*I (New England Biolabs) and subcloned into pGEX 4T-1. A 197-base pair *Sac* I (New England Biolabs) fragment from pMAL.hIL-8 (maltose binding protein-Ile-Glu-Gly-Arg-human IL-8 fusion protein expression vector) containing the coding sequence for the NH_2-terminal 49 amino acids of the 72-amino acid form of human IL-8 sequence was subcloned to pUC118 (ATCC) digested with *Sac*I for site-directed mutagenesis. Clones containing confirmed IL-8 mutations were cleaved with *Sac*I and subcloned into pMAL.hIL-8 digested with *Sac*I.

Cloning, Expression, and Purification of Human MIG—The open reading frame of human MIG (38) was amplified from cDNA generated from interferon γ-stimulated (1000 units/ml for 16 h) THP-1 cells by polymerase chain reaction. The 5′-primer used, 5′-CAAGGTGGATCCATGAAGAAAAGTGGTGTTC-3′, encodes a *Bam*HI restricition site immediately upstream of the ATG start site. The 3′-primer, 5′-GCAAGCTCTAGATTATGTAGTCTTCTTTTGACGAGAACG-3′, encodes a *Xba*I restriction site immediately downstream of the TAA stop codon. The 402-base pair fragment was subcloned to M13mp19 and was confirmed as the human MIG open reading frame by sequencing. Thr^{23} of the open reading frame sequence is the predicted NH_4-terminal amino acid of the mature, secreted MIG protein (38) and will be referred to here as amino acid position 1. Amino acids Lys^6 and Gly^7 were modified to Glu and Leu, respectively, by site-directed mutagenesis, generating the MIG mutein ELR-MIG. A *Bam*HI restriction site was introduced overlapping Gly^{-1} and Thr^1 by site-directed mutagenesis (37), resulting in mutein MIG or ELR-MIG cDNAs encoding a Thr^1 to Ser substitution. 324-base pair fragments obtained from correct M13 RF clones digested with *Bam*HI/*Xba*I were subcloned to pGEX 4T-1 to generate glutathione *S*-transferase-MIG fusion DNAs (GST-MIG or GST-ELR-MIG). The sequence encoded by these DNAs contains the thrombin recognition sequence LVPRGS between the GST and MIG sequences. Digestion of GST-MIG fusion protein with thrombin is predicted to release MIG protein having an NH_4-terminal sequence Gly-Ser-Pro, *versus* the predicted nonmodified NH_4-terminal sequence Thr-Pro.

Cultures of *E. coli* strain DH5αF′ harboring GST-MIG or GST-ELR-MIG plasmid were grown in 1 liter of LB media containing 50 μg/ml ampicillin to A_{600} ~ 0.5 at 22 °C with aeration, and protein expression was induced by the addition of 0.1 mM final isopropyl-1-thio-β-D-galactoside and continued incubation at 22 °C for 5–6 h. After induction, the cells were harvested by centrifuging at 6,000 × *g* for 10 min and the pellet was washed once in ice-cold PBS and resuspended in 10 ml of ice-cold 10 mM HEPES, 30 mM NaCl, 10 mM EDTA, 10 mM EGTA, 0.25% Tween 20, 1 mM phenylmethylsulfonyl fluoride (added fresh), pH 7.5 (lysis buffer). The resulting suspension was quick-frozen in liquid nitrogen. After thawing, phenylmethylsulfonyl fluoride was again added to yield a final concentration of 2 mM. The suspension was sonicated using a Branson Sonifier 250 equipped with a microtip for 2 min at output setting 5 with a 40% duty cycle. Triton X-100 was added to a final concentration of 1%, and the lysate was mutated for 30 min at room temperature to aid in the solubilization of the fusion protein. The lysate was then centrifuged at 34,500 × *g* for 10 min, and the supernatant was transferred to a fresh tube.

The GST-MIG protein was purified using the Pharmacia GST purification module (Pharmacia) essentially as described in the manufac-

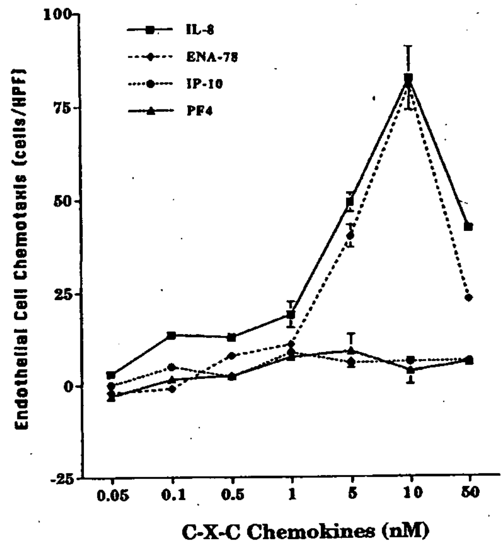

FIG. 1. **Endothelial cell chemotaxis in response to CXC chemokines (50 pM to 50 nM).** To demonstrate specific migration, background (unstimulated control) migration (cells/HPF) was subtracted.

TABLE I
Endothelial cell chemotaxis in response to CXC chemokines
Experimental n = 3.

Condition (10 nM)	Increase over control
	-fold
IL-8	5.1 ± 0.7
ENA-78	6.5 ± 0.8
GCP2	6.2 ± 0.4
GRO-α	5.3 ± 0.3
GRO-β	3.5 ± 0.2
GRO-γ	4.5 ± 0.5
PBP	3.4 ± 0.1
CTAP-III	5.2 ± 0.3
β-TG	1.6 ± 0.2
NAP-2	3.9 ± 0.1
IP-10	0.1 ± 0.1
PF4	0.1 ± 0.0
MIG	0.1 ± 0.0

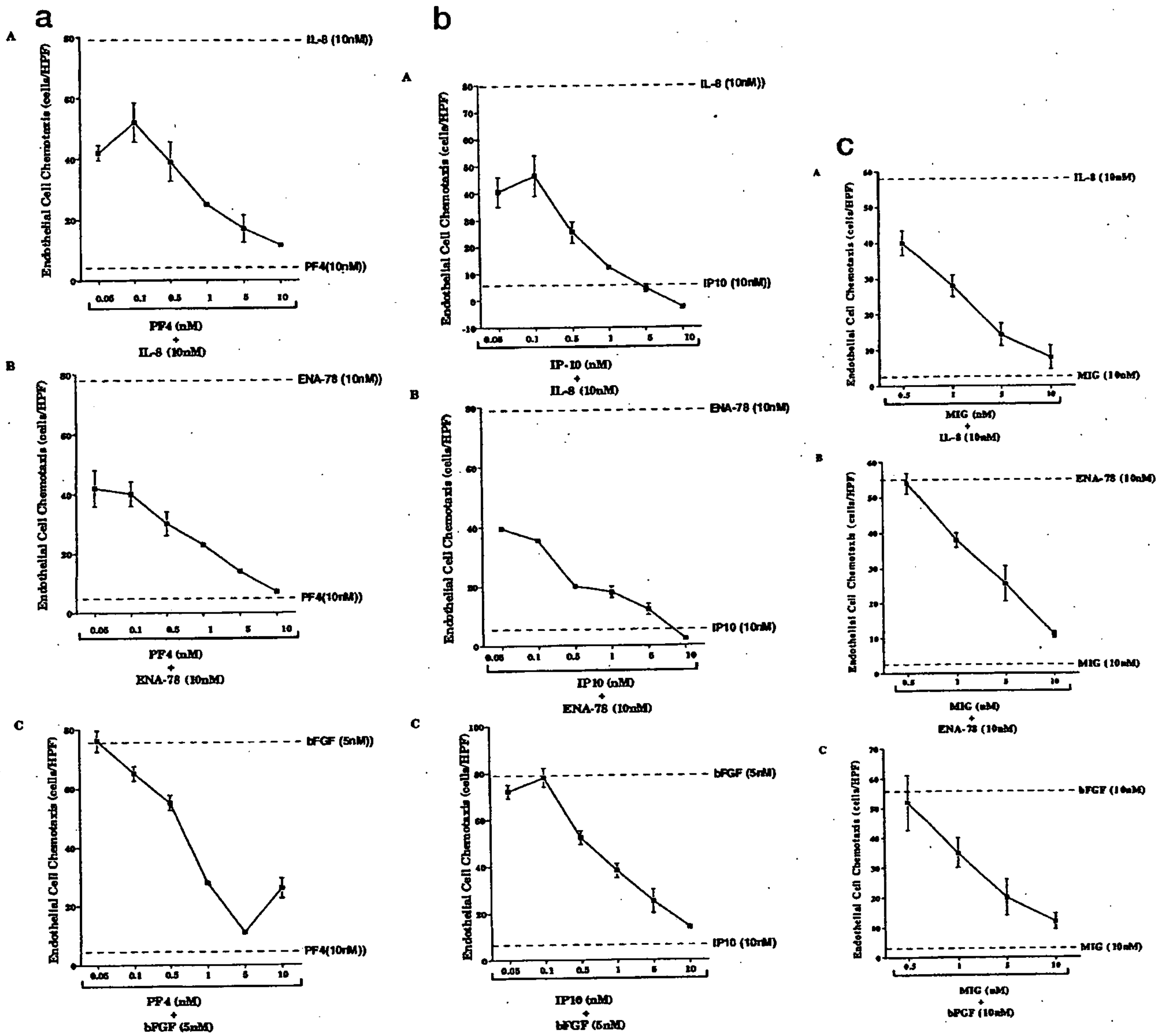

FIG. 2. **Endothelial cell chemotaxis in response to IL-8 (10 nM), ENA-78 (10 nM), and bFGF (5 nM) in the presence of varying concentrations PF4 (50 pM to 10 nM; *part a*), IP-10 (50 pM to 10 nM; *part b*), and MIG (500 pM to 10 nM; *part c*).** To demonstrate specific migration, background (unstimulated control) migration (cells/HPF) was subtracted.

turer's protocol. GST-fusion protein sonicate was passed over a 2-ml glutathione-Sepharose 4B column equilibrated in PBS. After washing with PBS, the GST-fusion protein was eluted with 3 column volumes of 10 mM reduced glutathione, 50 mM Tris-HCL, pH 8.0. 10 units of thrombin/A_{280} unit of fusion protein was added to the eluted GST-MIG or GST-ELR-MIG fusion protein and incubated at room temperature with occasional gentle mixing for 2–3 h. MIG or ELR-MIG protein was ≥95% cleaved from the GST protein under these conditions as monitered by SDS-PAGE (41). The pH of the MIG-containing solution was adjusted to 4.0 using 0.5 M sodium acetate, pH 4.0, filtered through a cellulose acetate 0.45-μm filter (Costar) and passed over a Mono S column (Pharmacia) equilibrated with 20 mM sodium acetate, pH 4.0. MIG protein was eluted as a single peak using a 0–2 M NaCl gradient, and dialyzed against 0.5 mM $NaPO_4$, 20 mM NaCl, pH 7.0. Purified MIG and ELR-MIG was obtained endotoxin-free (<1.0 enzyme units/ml; QCL-1000 test, BioWhittaker), and yields ranged from 100–200 μg/liter (quantitated by amino acid analysis) with a purity of >95% (determined by SDS-PAGE, with apparent molecular mass of 16 kDa; amino acid analysis accuracy > 90%). Mass spectrometry of the purified MIG and ELR-MIG proteins confirmed their predicted mass.

Cloning, Expression, and Purification of Human IL-8—The 72-amino acid mature form of IL-8 was amplified using polymerase chain reaction from an IL-8 cDNA in pET3a (kindly provided by I. U. Schraufstatter, Scripps Clinic). The 5′-primer used, 5′-AGTGCTAAAGAACTTAGATG-3′, encodes the beginning reading frame of IL-8, and the 3′ primer, 5′-GGGATCCTCATGAATTCTC-3′, contains a *Bam*HI restriction site immediately after the stop codon. The 220-base pair PCR product was purified by gel electrophoresis, digested with *Bam*HI (New England Biolabs), subcloned into pMal-c2 previously digested with *Xmn*I and *Bam*HI (New England Biolabs) to generate pMal.hIL-8. Clones containing inserts were confirmed by sequencing. Site-directed mutagenesis was used to modify amino acids Glu[4]-Leu[5]-Arg[6] to Thr-Val-Arg or Asp-Leu-Gln, generating TVR-IL-8 or DLQ-IL-8, respectively. Correct clones were identified by sequencing and subcloned as *Sac*I fragments from pUC118 into pMal.hIL-8 digested with *Sac*I.

Cultures of *E. coli* strain DH5αF′ harboring pMal.hIL-8, pMal.TVR-IL-8, or pMal.DLQ-IL-8 were grown in 1-liter LB media containing 50 μg/ml ampicilin to A_{600} ~ 0.5 at 37 °C with aeration, and protein expression was induced by the addition of 0.3 mM final isopropyl-1-thio-β-D-galactoside and continued incubation at 37 °C for 2 h. Cells were harvested by centrifuging at 5800 × *g* for 10 min and the pellet was washed once in ice-cold PBS and resuspended in 10 ml of ice-cold lysis buffer. The resulting suspension was quick-frozen in liquid nitrogen.

After thawing, the suspension was sonicated using a Branson Soni-

TABLE II
The IC50 of PF4, IP-10, and MIG for the inhibition of the agonists IL-8, ENA-78, and bFGF

Experimental $n = 3$.

Agonist	IL-8 (10 nM)	ENA78 (10 nM)	bFGF (5 nM)
	M	M	M
PF4	5×10^{-11}	5×10^{-11}	1×10^{-9}
IP-10	5×10^{-11}	5×10^{-11}	1×10^{-9}
MIG	5×10^{-10}	5×10^{-9}	1×10^{-9}

TABLE III
Neutrophil chemotaxis in response to CXC chemokines. Control is media alone

Experimental $n = 3$.

Condition (10 nM)	Cells/HPF
Control	18.4 ± 1.8
IP10	20.7 ± 4.2
MIG	8.6 ± 1.5
IL-8	96.4 ± 6.5
IL-8 + IP10	94.1 ± 9.3
IL-8 + MIG	78.6 ± 10.5

fier 250 equipped with a microtip for 2 min at output setting 5 with a 40% duty cycle. The suspension was clarified by centrifugation at 9000 × *g*, the supernatant was diluted 5-fold in 10 mM $NaPO_4$, 500 mM NaCl, 1 mM EGTA, 0.25% Tween 20, pH 7.0 (column buffer), and loaded onto a 10-ml amylose resin (New England Biolabs) affinity column. After extensive washing with column buffer, the maltose binding protein fusion protein was eluted with column buffer containing 10 mM maltose. Mutein or wild-type IL-8 proteins were released by incubation with 1 μg of Factor Xa (New England Biolabs)/A_{280} maltose binding protein fusion protein at room temperature overnight and were then passed over a Mono S column (Pharmacia) equilibrated in 10 mM $NaPO_4$, pH 6.2, and eluted in a 0–1 M NaCl gradient. 1 ml of amylose resin was added to fractions containing mutant or wild-type IL-8 protein to remove residual free maltose binding protein by incubation for 30 min at room temperature with gentle shaking. The resin was removed by centrifugation, and the supernatant was dialyzed against 0.5 mM $NaPO_4$, 20 mM NaCl, pH 7.5. Yields were ranged from 0.2 to 3.5 mg for wild-type or mutant IL-8 proteins and were ≥95% pure as assessed by SDS-PAGE and endotoxin-free (<1.0 enzyme units/ml). Proteins were quantitated by amino acid analysis, and had accuracies between 88–93%.

Endothelial Cell Chemotaxis—Endothelial cell chemotaxis was performed in 48-well chemotaxis chambers (Nucleopore Corp.) as described previously (28, 42). Briefly, bovine adrenal gland capillary endothelial cells were suspended at a concentration of 10^6 cells/ml in Dulbecco's modified Eagle's medium with 0.1% bovine serum albumin and placed into each of the bottom wells (25 μl). Nucleopore chemotaxis membranes (5-μm pore size) were coated with 0.1 mg/ml gelatin. The membranes were placed over the wells and the chambers were sealed, inverted, and incubated for 2 h to allow cells to adhere to the membrane. The chambers were then reinverted; 50 μl of sample (containing media alone, ELR-CXC chemokines, non-ELR-CXC chemokines, bFGF, or combinations of ELR-CXC and non-ELR-CXC chemokines or non-ELR-CXC chemokines and bFGF) was dispensed into the top wells and reincubated for an additional 2 h. Membranes were then fixed and stained with Diff-Quik staining kit (American Scientific Products), and cells that had migrated through the membrane were counted in 10 high power fields (HPF; 400×). Results were expressed as the number of endothelial cells that migrated per HPF after subtracting the background (unstimulated control) to demonstrate specific migration. Each sample was assessed in triplicate. Experiments were repeated at least three times.

Neutrophil Chemotaxis—Heparinized venous blood was collected from healthy volunteers and mixed 1:1 with 0.9% saline, and mononuclear cells were separated by Ficoll-Hypaque density gradient centrifugation. Human neutrophils were then isolated by sedimentation in 5% dextran, 0.9% saline (Sigma) and separated from erythrocytes by hypotonic lysis. After washing twice, neutrophils were suspended in Hanks' balanced salt solution with calcium/magnesium (Life Technologies, Inc.) at a concentration of 2×10^6 cells/ml. Neutrophils were >95% viable as determined by trypan blue exclusion. Neutrophil chemotaxis was performed as described previously (43, 44). 150 μl of sample (ELR-CXC, non-ELR-CXC, or combination of ELR-CXC and non-ELR-CXC chemokines), 1×10^{-7} M formylmethionyleucylphenylalanine (Sigma), or Hanks' balanced salt solution (Life Technologies, Inc., Grand Island, NY) alone were placed in duplicate bottom wells of a blind well chemotaxis chamber. A 3-μm pore size polycarbonate filter (polyvinylpyrrolidone-free, Nucleopore Corp.) was placed in the assembly, and 250 μl of human neutrophil was suspension placed in each of the top wells. Chemotaxis chamber assemblies were incubated at 37 °C in humidified 95% air, 5% CO_2 for 60 min. The filters were removed, fixed in absolute methanol, and stained with 2% toluidine blue (Sigma). Neutrophils that had migrated through to the bottom of the filter were counted in 10 HPF (400×) using a Javelin chromachip camera (Javelin Electronics, Japan) attached to a Olympus BH-2 microscope interfaced with a MacIntosh II computer containing an Image Capture 1000 frame grabber (Scion Corp., Walkersville, MD) and NIH Image, version 1.40 software (National Institutes of Health Public Software, Bethesda, MD). Each sample was assessed in triplicate. Experiments were repeated at least three times.

Corneal Micropocket Model of Angiogenesis—*In vivo* angiogenic activity was assayed in the avascular cornea of Long Evans rat eyes, as described previously (28, 29, 42). Briefly, cytokines were combined with sterile Hydron (Interferon Sciences Inc.) casting solution, and 5-μl aliquots were air-dried on the surface of polypropylene tubes. Prior to implantation, pellets were rehydrated with normal saline. Animals were anesthetized with an intraperitoneal injection of ketamine (150 mg/kg) and atropine (250 μg/kg). Rat corneas were anesthetized with 0.5% proparacaine hydrochloride ophthalmic solution followed by implantation of the Hydron pellet into an intracorneal pocket (1–2 mm from the limbus). 6 days after implantation, animals were pretreated intraperitoneally with 1000 units of heparin (Elkins-Sinn, Inc., Cherry Hill, NJ), anesthetized with ketamine (150 mg/Kg), and perfused with 10 ml of colloidal carbon via the left ventricle. Corneas were then harvested and photographed. No inflammatory response was observed in any of the corneas treated with the above cytokines. Positive neovascularization responses were recorded only if sustained directional ingrowth of capillary sprouts and hairpin loops toward the implant were observed. Negative responses were recorded when either no growth was observed or when only an occasional sprout or hairpin loop displaying no evidence of sustained growth was detected.

Statistical Analysis—Data were analyzed by a Macintosh IIfx computer using the Statview II statistical package (Abacus Concepts, Inc., Berkeley, CA). Data were expressed as mean ± S.E. and compared using the nonparametric analysis with the Wilcoxon signed rank test. Data were considered statistically significant if p values were ≤0.05.

RESULTS

CXC Chemokines Display Disparate Angiogenic Activity—Endothelial cell chemotaxis was performed in the presence or absence of IL-8, ENA-78, PF4, and IP-10 at concentrations of 50 pM to 50 nM. Both IL-8 and ENA-78 demonstrated a dose-dependent increase in endothelial migration that was significantly greater ($p < 0.05$) than control (background) at concentrations equal to or above 0.1 and 1 nM, respectively, with evidence of a "bell-shape" curve seen with other chemotactic factors (Fig. 1). In contrast, neither PF4 nor IP-10 induced significant ($p > 0.05$) endothelial cell chemotaxis (Fig. 1). Similar findings were also observed using either human umbilical or dermal microvascular endothelial cells (data not shown). The migration seen in response to IL-8 or ENA-78 was due to chemotaxis, not chemokinesis, as checkerboard analysis demonstrated directed, not random, migration (data not shown). Other CXC chemokines were tested for their ability to induce endothelial cell chemotaxis, including ELR-CXC chemokines IL-8, ENA-78, GCP-2, GRO-α, GRO-β, GRO-γ, platelet basic protein, connective tissue activating protein-III, and neutrophil-activating protein-2 or the non-ELR CXC chemokines IP-10, PF4, and MIG (Table I). In a similar fashion to IL-8 or ENA-78, all of the ELR-CXC chemokines tested demonstrated significant ($p < 0.05$) endothelial cell chemotactic activity over the background control, whereas the endothelial cell chemotactic activity induced by MIG was either similar to background control or to the endothelial cell chemotactic activity seen with either PF4 or IP-10. These findings suggested that CXC chemokines could be divided into two groups with defined biolog-

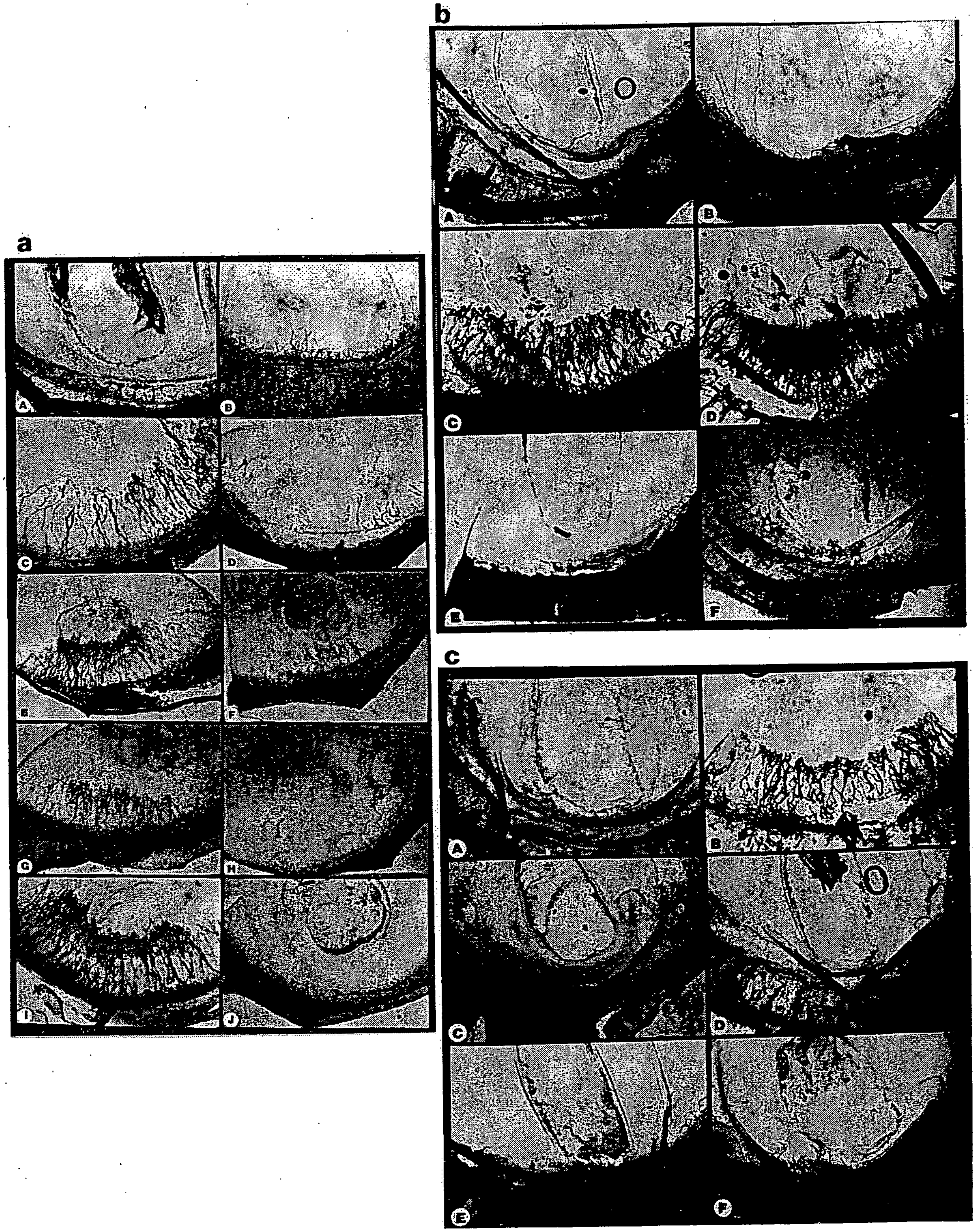

FIG. 3. **Rat cornea neovascularization in response to ELR-CXC chemokines, non-ELR-CXC chemokines, bFGF, or combinations of these cytokines.** *Part a, panels A, B, C, E, G,* and *I*, respectively, represent the corneal neovascular response to a hydron pellet alone (vehicle control), IP-10 (10 nM), IL-8 (10 nM), ENA-78 (10 nM), GRO-α (10 nM), or GCP-2 (10 nM); *part a, panels D, F, H,* and *J*, respectively, represent the combination of IL-8 with IP-10, ENA-78 with IP-10, GRO-α with IP-10, or GCP-2 with IP-10. *Part b, panels A–D*, respectively, represent the corneal neovascular response to a hydron pellet alone (vehicle control), MIG (10 nM), IL-8 (10 nM), or ENA-78 (10 nM); *part b, panels E* and *F*, respectively,

ical activities, one that contains the ELR motif and is chemotactic for endothelial cells and the other that lacks the ELR motif and does not induce endothelial chemotaxis.

PF4, IP-10, or MIG Inhibit IL-8-, ENA-78-, or bFGF-induced Angiogenic Activity—While the above experiments suggested that PF4, IP-10, and MIG were not significant chemotactic factors for endothelial cells, we postulated that these CXC chemokines may be potent inhibitors of angiogenesis. To test this hypothesis, endothelial cell chemotaxis was performed in the presence or absence of IL-8 (10 nM), ENA-78 (10 nM), or bFGF (5 nM) with or without varying concentrations of PF4, IP-10, or MIG from 0 to 10 nM (Fig. 2, *a–c*, respectively). Endothelial cell migration in response to either IL-8, ENA-78, or bFGF was significantly inhibited by PF4, IP-10, or MIG in a dose-dependent manner (Fig. 2). PF4 and IP-10 in a concentration of 50 pM inhibited either IL-8- or ENA-78-induced endothelial chemotaxis by 50%, whereas, PF4 and IP-10 in a concentration of 1 nM attenuated the response to bFGF by 50% (Fig. 2, *a* and *b*, and Table II). MIG at a concentration of 1, 5, and 1 nM inhibited the endothelial cell chemotactic response to IL-8, ENA-78, and bFGF, respectively, by 50% (Fig. 2*c* and Table II). Interestingly, while IP-10 and MIG inhibited IL-8-induced endothelial cell chemotactic activity, neither IP-10 nor MIG were effective in attenuating IL-8-induced neutrophil chemotactic activity ($p > 0.05$) (Table III).

The rat corneal micropocket model of neovascularization was used to determine whether IP-10 or MIG could inhibit the angiogenic activity of either the ELR-containing CXC chemokines or bFGF *in vivo*. Hydron pellets alone, pellets containing IL-8, ENA-78, GRO-α, GCP-2, IP-10, MIG, or bFGF in a concentration of 10 nM, or pellets containing combinations of 10 nM each of IL-8 + IP-10, ENA-78 + IP-10, GRO-α + IP-10, GCP-2 + IP-10, IL-8 + MIG, ENA-78 + MIG, bFGF + IP10, or bFGF + MIG were embedded into the normally avascular rat cornea and assessed for a neovascular response (Fig. 3, *a–c*). The CXC chemokines (IL-8, ENA-78, GRO-α, or GCP-2) or bFGF-induced positive corneal angiogenic responses in six of six corneas, without evidence for significant leukocyte infiltration (assessed by light microscopy). In contrast, hydron pellets alone ($n = 6$ corneas) or pellets containing either IP-10 or MIG (10 nM) ($n = 6$ corneas for each chemokine) only resulted in a positive neovascular response in less than one of six corneas tested for each variable. When IP-10 was added in combination with the ELR-CXC chemokines (IL-8, ENA-78, GRO-α, or GCP-2) or bFGF (Fig. 3, *a* and *c*, respectively), IP-10 significantly abrogated the ELR-CXC chemokine and bFGF-induced angiogenic activity in five of six corneas ($n = 6$ corneas for each manipulation). In addition, MIG inhibited IL-8, ENA-78, and bFGF-induced corneal angiogenic activity in a similar manner to IP-10 (Fig. 3, *b* and *c*).

ELR Muteins of IL-8 and MIG Generate Angiostatic and Angiogenic Proteins, Respectively—Muteins of IL-8 lacking the ELR motif and a mutant of MIG containing the ELR motif were generated to delineate its functional role in CXC chemokine-induced angiogenesis. The ELR motif in wild-type IL-8 was mutated to either TVR (TVR-IL-8; corresponding IP-10 sequence) or DLQ (DLQ-IL-8; corresponding to PF4 sequence) by site-directed mutagenesis and expressed in *E. coli*. TVR-IL-8 and DLQ-IL-8 alone failed to induce endothelial cell chemotactic activity (Fig. 4, *A* and *B*, respectively), yet these muteins inhibited the maximal endothelial chemotactic activity of wild-type IL-8 by 83 and 88% ($p < 0.05$), respectively (Fig. 4, *A* and *B*). Endothelial cell viability, as determined by the exclusion of trypan blue, was unchanged in the presence or absence of either of the IL-8 muteins (data not shown). Neither TVR-IL-8 nor DLQ-IL-8 induced neutrophil chemotaxis, nor were they effective in attenuating neutrophil chemotaxis in response to IL-8 (data not shown).

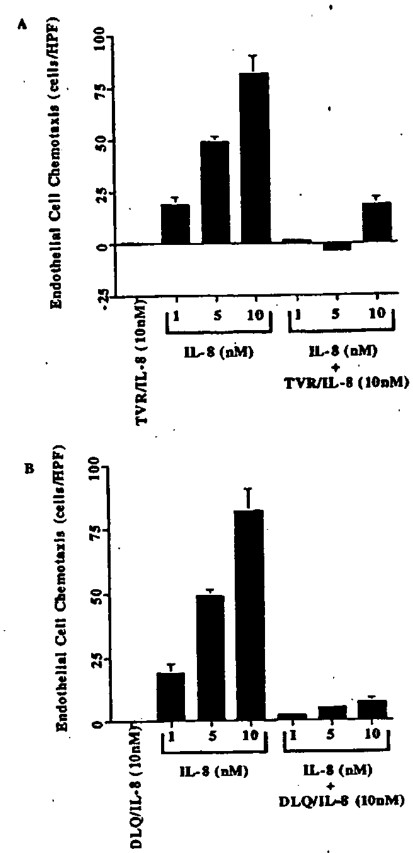

FIG. 4. **Endothelial cell chemotaxis in response to the presence or absence of varying concentrations of IL-8 and IL-8 muteins, TVR-IL-8, and DLQ-IL-8.** *Panel A* is endothelial cell chemotaxis in response to the presence or absence of varying concentrations of IL-8 (1–10 nM), TVR-IL-8 (10 nM), or in combination of varying concentrations of IL-8 with TVR-IL-8 (10 nM). *Panel B* is endothelial cell chemotaxis in response to the presence or absence of varying concentrations of IL-8 (1–10 nM), DLQ-IL-8 (10 nM), or in combination of varying concentrations of IL-8 with DLQ-IL-8 (10 nM). To demonstrate specific migration, background (unstimulated control) migration (cells/HPF) was subtracted.

Using the *in vivo* rat cornea micropocket model of neovascularization, TVR-IL-8 (10 nM) alone did not induce a positive neovascular response in any of the six corneas tested. However, TVR-IL-8 (10 nM) in combination with either IL-8 (10 nM) or ENA-78 (10 nM) resulted in 83% reduction (only one of six corneas positive) in the ability of either IL-8 or ENA-78 to induce cornea neovascularization, as compared with 100% (six of six) of the corneas positive in the presence of either IL-8 or ENA-78 alone (Fig. 5). Moreover, the angiostatic activity of the IL-8 muteins was not only unique to inhibition of ELR-CXC chemokine-induced angiogenic activity, as TVR-IL-8 (10 nM)

represents the corneal neovascular response to the combination of IL-8 with MIG or ENA-78 with MIG. *Part c, panels A–D*, respectively, represents the corneal neovascular response to a hydron pellet alone (vehicle control), bFGF (5 nM), MIG (10 nM), or IP-10 (10 nM); *part c, panels E* and *F*, respectively, represents the corneal neovascular response to the combination of bFGF with MIG or bFGF and IP-10. All panels are at 25× magnification.

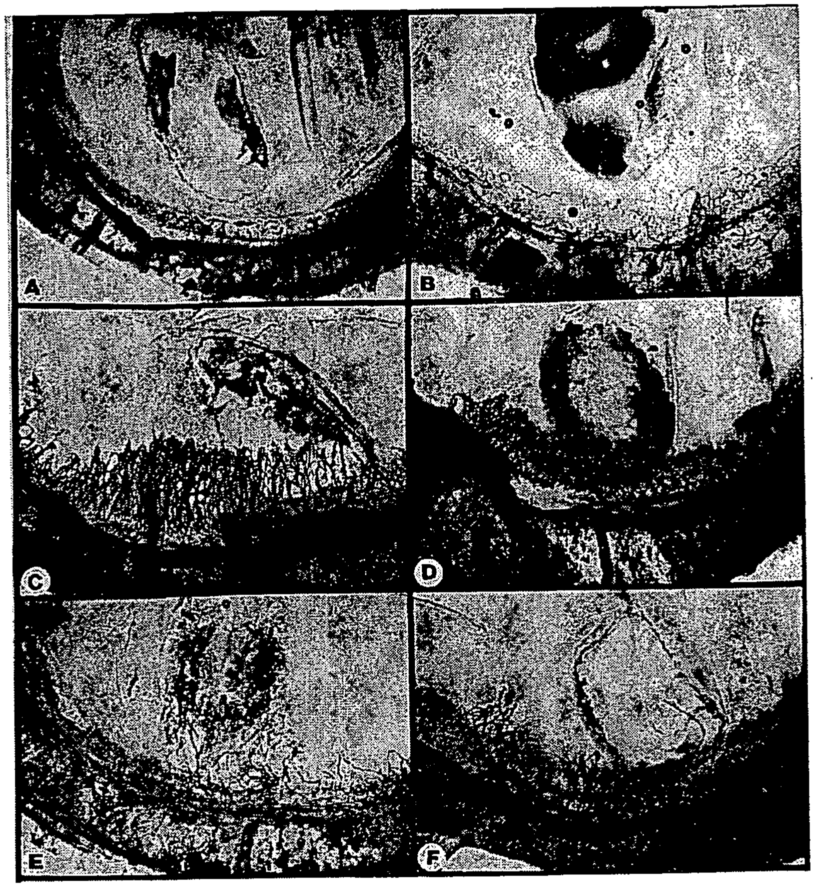

FIG. 5. **Rat cornea neovascularization in response to the IL-8, ENA-78, the IL-8 mutein (TVR-IL-8), and combinations of ENA-78 and TVR-IL-8 or IL-8 and TVR-IL-8.** *Panels A–D* represent a hydron pellet alone, TVR-IL-8 (10 nM), ENA-78 (10 nM), and IL-8 (10 nM), respectively. *Panels E* and *F* represent the combination of ENA-78 and TVR-IL-8 and of IL-8 and TVR-IL-8, respectively. All panels are at 25× magnification.

inhibited both bFGF-induced (10 nM) maximal endothelial cell chemotaxis by 65% ($p < 0.05$) (Fig. 6*a*) and corneal neovascularization (five of six corneas; $n = 6$ corneas for each cytokine) (Fig. 6*b*). Endothelial cell viability, as determined by the exclusion of trypan blue, was unchanged in the presence or absence of the TVR-IL-8 mutant (data not shown). In addition, ELR-MIG (10 nM) induced angiogenic responses in 8 of 10 corneas, as compared with wild-type MIG, which induced an angiogenic response in only 1 of 7 corneas (Fig. 7, *A–D*). Interestingly, MIG (10 nM) inhibited the angiogenic response of ELR-MIG in five of six corneas (Fig. 7, *E* and *F*). These data further support the importance of the ELR motif as a domain for mediating angiogenic activity. Similar to the synthetic ELR-IP-10 (36), ELR-MIG in a concentration of 10 pM to 100 nM failed to induce neutrophil chemotaxis (data not shown).

DISCUSSION

The CXC chemokine family of chemotactic cytokines are polypeptide molecules that appear, in general, to have proinflammatory activities. In monomeric forms, they range from 7 to 10 kDa and are characteristically basic heparin-binding proteins. They display four highly conserved cysteine amino acid residues with the first two cysteines separated by a nonconserved amino acid residue (the CXC cysteine motif). The CXC chemokines are all clustered on human chromosome 4 (q12-q21), and exhibit between 20 and 50% homology on the amino acid level (31–34). Over the last 2 decades, several human CXC chemokines have been identified, including PF4, NH_2-terminal truncated forms of platelet basic protein (connective tissue activating protein-III, β-thromboglobulin, neutrophil-activating protein-2), IL-8, GRO-α, GRO-β, GRO-γ, ENA-78, GCP-2, IP-10, and MIG (31–34, 38). The ubiquitous nature of CXC chemokine production by a variety of cells suggest that these cytokines may play a role in mediating biological events other than leukocyte chemotaxis.

We hypothesized that members of the CXC chemokine family may exert disparate effects in mediating angiogenesis as a function of the presence or absence of the ELR motif for primarily four reasons. First, members of the CXC chemokine family that display binding and activation of neutrophils share the highly conserved ELR motif that immediately precedes the first cysteine amino acid residue, whereas, PF4, IP-10, and MIG lack this motif (35, 36). Second, IL-8 (contains ELR motif) mediates both endothelial cell chemotactic and proliferative activity *in vitro* and angiogenic activity *in vivo* (28), and, in addition, endogenous IL-8 has been found to represent a major angiogenic factor that mediates net angiogenic activity of human nonsmall cell lung cancer (42). In contrast, PF4 (lacking the ELR motif) has been shown to have angiostatic properties (27), and attenuates growth of tumors *in vivo* (45). Third, the interferons (IFN-α, IFN-β, and IFN-γ) are all known inhibitors of wound repair, especially angiogenesis (18, 46–49). These cytokines, however, up-regulate IP-10 and MIG from a number of cells, including keratinocytes, fibroblasts, endothelial cells, and mononuclear phagocytes (38, 50). Finally, we and others have found that IFN-α, IFN-β, and IFN-γ are potent inhibitors of the production of monocyte-derived IL-8, GRO-α, and ENA-78 (51, 52), supporting the notion that IFN-α, IFN-β, and IFN-γ may shift the biological balance of ELR- and non-ELR-CXC chemokines toward a preponderance of angiostatic (non-ELR) CXC chemokines.

In this study, we demonstrated that the members of the CXC chemokine family behave as either angiogenic or angiostatic

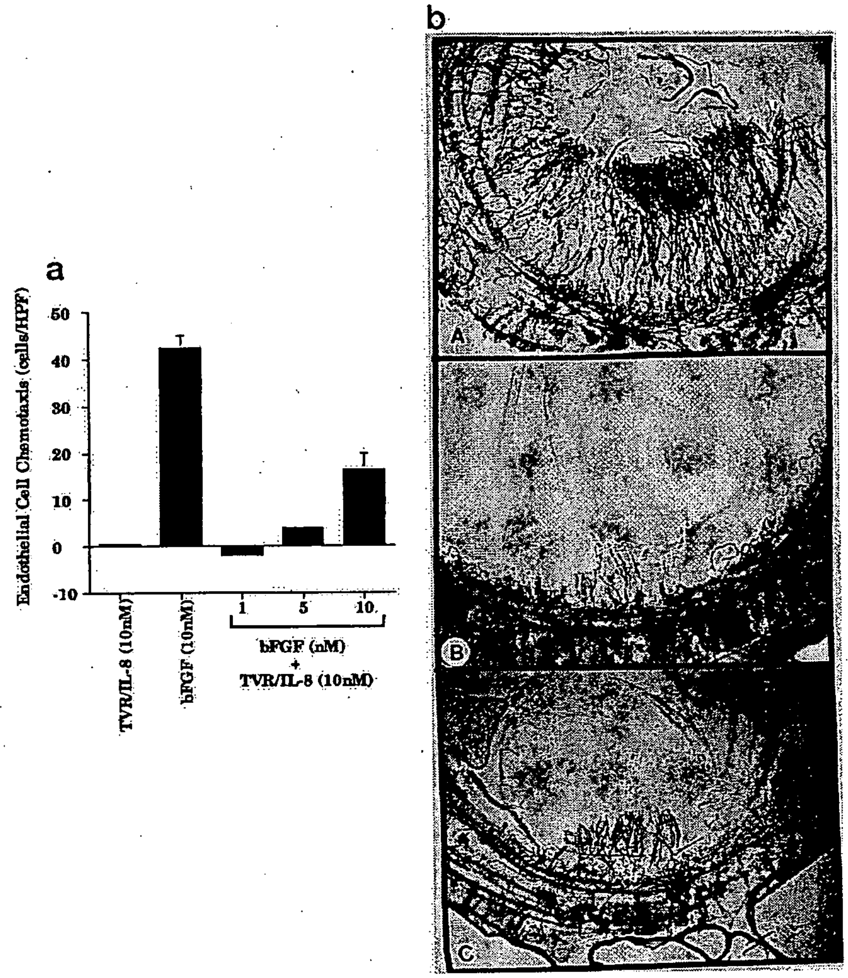

FIG. 6. **Endothelial chemotaxis (*part a*) and rat cornea neovascularization (*part b*) in response to the presence or absence of varying concentrations of bFGF and the IL-8 mutein, TVR-IL-8 (10 nM).** *Part a* is the endothelial chemotaxis in response to the presence or absence of varying concentrations of bFGF (1–10 nM), TVR-IL-8 (10 nM), or in combination of varying concentrations of IL-8 with TVR-IL-8 (10 nM). To demonstrate specific migration, background (unstimulated control) migration (cells/HPF) was subtracted. *Part b, panels A–C* is rat cornea neovascularization in response to bFGF (10 nM), TVR-IL-8 (10 nM), and the combination of bFGF and TVR-IL-8 at 25× magnification, respectively.

factors, depending upon the presence or absence of the ELR motif, respectively. This was supported using both *in vitro* (endothelial cell chemotaxis) and *in vivo* (rat cornea neovascularization) analyses. The evidence *in vitro* of directed (chemotaxis not chemokinesis by checkerboard analysis) migration in response to varying concentrations of ELR-CXC chemokines, IL-8, ENA-78, and the MIG mutein ELR-MIG, and the absence *in vivo* of leukocyte infiltration in the rat cornea during ELR-CXC chemokine-induced neovascularization, supports the direct role ELR-containing CXC chemokines play in mediating angiogenic activity. In contrast, CXC chemokines lacking the ELR motif, PF4, IP-10, MIG, and the two IL-8 muteins DLQ-IL-8 and TVR-IL-8, behave as potent angiostatic regulators of neovascularization, inhibiting not only the angiogenic activity of ELR-CXC chemokines, but also the structurally unrelated angiogenic factor, bFGF. Thus, the ELR motif appears to be essential for dictating the angiogenic activity of the CXC chemokines.

These findings are compatible with the ability of ELR-containing CXC chemokines to bind to both endothelial cells and neutrophils. However, the non-ELR muteins of wild-type IL-8, as well as IP-10 and MIG, inhibited ELR-CXC chemokine-induced angiogenesis but not neutrophil chemotaxis. The finding that IP-10 and MIG block other ELR-CXC chemokine-induced functions, *i.e.* angiogenesis, is unprecedented (53). Moreover, the muteins of wild-type IL-8, as well as IP-10 and MIG, also inhibited the angiogenic activity of the unrelated cytokine, bFGF, suggesting that a receptor system(s) other than the IL-8 receptor may be operative on endothelial cells, which allows the angiostatic CXC chemokines to regulate both ELR-CXC chemokine and bFGF-induced angiogenic activity. This contention is further supported with the evidence that equimolar concentrations of mutant and wild-type IL-8 do not result in a 50% restoration of the endothelial cell chemotactic effect. This response is most likely due to the use of another "receptor" by the angiostatic CXC chemokines. While the Duffy antigen receptor for chemokines has been identified on post-capillary venule endothelial cells (54), this receptor binds not only ELR-CXC chemokines, but also MCP-1 and RANTES (55). We have found that these latter two CC chemokines are not chemotactic for endothelial cells (data not shown).

While the NH_2-terminal ELR motif appears to be essential for angiogenic activity of CXC chemokines, it is uncertain whether the angiostatic properties of the non-ELR-CXC chemokines tested are due to the absence of the ELR motif. In particular, bFGF binds to low affinity cell surface receptors on endothelia that appear to be sulfate proteoglycans (47, 56), and IL-8 specific binding to endothelial cells can be inhibited by preincubation with either heparin or heparan sulfate (57). One can speculate that, in the absence of the ELR motif, a potential mechanism exists by which another amino acid domain, perhaps within the COOH terminus of PF4, IP-10, MIG, TVR-IL-8, and DLQ-IL-8 may compete with either ELR-CXC chemokines or bFGF for proteoglycan binding sites and thus prevent endothelial cell activation and angiogenesis. It also possible, however, that the angiostatic effects of CXC chemokines lacking

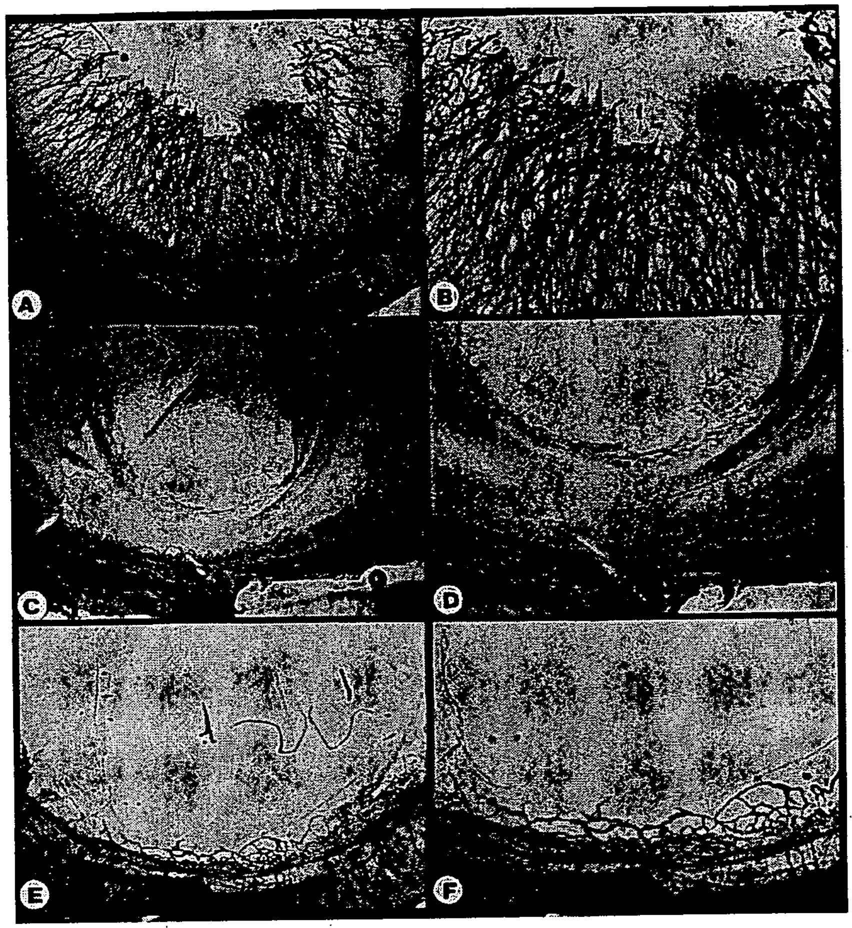

FIG. 7. **Rat cornea neovascularization in response to the MIG mutein, ELR-MIG, MIG, and the combination of ELR-MIG and MIG.** *Panels A* and *B* represents the cornea neovascular response to ELR-MIG (10 nM) at 25 and 50×, respectively. *Panels C* and *D* represent the cornea neovascular response to MIG (10 nM) at 25 and 50× magnification, respectively. *Panels E* and *F* represent the cornea neovascular response to the combination of ELR-MIG and MIG at 25 and 50× magnification, respectively.

the ELR motif are not directly competitive in nature, but are rather mediated through an independent receptor system. Studies in our laboratories are currently addressing these issues.

The interferons have been shown to inhibit wound repair and tumorigenesis through a presumed antiproliferative and angiostatic mechanism (46–49). While the expression of IL-8, GRO-α, and ENA-78 can be induced by a variety of factors, including TNF and IL-1, these chemokines are down-regulated by IFN-γ (51, 52). In contrast, IP-10 and MIG expression is up-regulated by IFN-γ (38, 50). This suggests that the disparate activity of the CXC chemokines as angiogenic or angiostatic factors may be physiologically relevant. The finding that IP-10 and MIG are potent angiostatic factors suggests that IFN-γ, in part, may mediate its angiostatic activity through the local stimulation of production of IP-10 and MIG and by down-regulation of the expression of the angiogenic CXC chemokines, such as IL-8 and ENA-78. This suggests that the magnitude of local IFN-γ expression by mononuclear cells during wound repair, chronic inflammation, or tumorigenesis may be a pivotal event in regulating both angiogenic (through negative feedback) and angiostatic (through positive feedback) CXC chemokine production.

Thus, our findings suggest that the ELR motif is the functional domain that dictates the angiogenic activity of the CXC chemokines, and supports the contention that members of the CXC chemokine family may exert disparate effects in mediating angiogenesis. The magnitude of the expression and relative concentrations of either angiogenic or angiostatic CXC chemokines during neovascularization may thus significantly contribute to the regulation of net angiogenesis during either wound repair, chronic inflammation, or tumorigenesis.

Acknowledgments—We thank Carla Forte (Bayer Corp., West Haven, CT) for technical help during the course of this work and Ghislain Opdenakker (University of Leuven, Leuven, Belgium) for critical review of this manuscript.

REFERENCES

1. Folkman, J., and Cotran, R. (1978) *Int. Rev. Exp. Pathol.* **16,** 207–248
2. Auerbach, R. (1981) *Lymphokines* Vol. IV, Academic Press, New York
3. Folkman, J. (1985) *Adv. Cancer Res.* **43,** 175–203
4. Folkman, J., and Klagsbrun, M. (1987) *Science* **235,** 442–444
5. Leibovich, S. J., and Weisman, D. M. (1988) *Prog. Clin. Biol. Res.* **266,** 131–145
6. Engerman, R. L., Pfaffenenbach, D., and Davis, M. D. (1967) *Lab Invest.* **17,** 738–743
7. Tannock, I. F., and Hayashi, S. (1972) *Cancer Res.* **32,** 77–82
8. Bouck, N. (1990) *Cancer Cells* **2,** 179–85
9. Folkman, J., Watson, K., Ingber, D., and Hanahan, D. (1989) *Nature* **339,** 58–61
10. Brem, H., and Folkman, J. (1975) *J. Exp. Med.* **141,** 427–433
11. Lee, A., and Langer, R. (1983) *Science* **221,** 1185–1187
12. Madri, J. A., Pratt, B. M., and Tucker, A. M. (1988) *J. Cell Biol.* **106,** 1375–1384
13. Ingber, D. E., Madri, J. A., and Folkman, J. (1986) *Endocrinology* **119,** 1768–1775
14. Ingber, D. E., and Folkman, J. (1988) *Lab. Invest.* **59,** 44–51
15. Maragoudakis, M. E., Sarmonika, M., and Panoutscaopoulou, M. (1988) *J. Pharmacol. Exp. Ther.* **244,** 729–733
16. Shapiro, R., and Vallee, B. L. (1987) *Proc. Natl. Acad. Sci. U.S.A.* **84,** 2238–2241
17. Sato, N., Fukuda, K., Nariuchi, H., and Sagara, N. (1987) *J. Natl. Cancer Inst.* **79,** 1383–1391
18. Sidky, Y. A., and Borden, E. C. (1987) *Cancer Res.* **47,** 5155–5161
19. Peterson, H.-I. (1986) *Anticancer Res.* **6,** 251–254
20. Homandberg, G. A., Kramer-Bjerke, J., Grant, D., Christianson, G., and Eisenstein, R. (1986) *Biochim. Biophys. Acta* **874,** 61–71
21. Taylor, S., and Folkman, J. (1982) *Nature* **297,** 307–312
22. Crum, R., Szabo, S., and Folkman, J. (1985) *Science* **230,** 1375–1378
23. Lee, K., Erturk, E., Mayer, R., and Cockett, A. T. K. (1987) *Cancer Res.* **47,**

5021
24. Good, D. J., Polverini, P. J., Rastinejad, F., LeBeau, M. M., Lemons, R. S., Frazier, W. A., and Bouck, N. P. (1990) *Proc. Natl. Acad. Sci. U. S. A.* **87**, 6624–6628
25. O'Reilly, M. S., Holmgren, L., Shing, Y., Chen, C., Rosenthal, R. A., Moses, M., Lane, W. S., Cao, Y., Sage, E. H., and Folkman, J. (1994) *Cell* **79**, 315–328
26. Brooks, P. C., Montgomery, A. M. P., Rosenfeld, M., Reisfeld, R. A., Hu, T., Klier, G., and Cheresh, D. A. (1994) *Cell* **79**, 1157–1164
27. Maione, T. E., Gray, G. S., Petro, J., Hunt, A. J., Donner, A. L., Bauer, S. I., Carson, H. F., and Sharpe, R. J. (1990) *Science* **247**, 77–79
28. Koch, A. E., Polverini, P. J., Kunkel, S. L., Harlow, L. A., DiPietro, L. A., Elner, V. M., Elner, S. G., and Strieter, R. M. (1992) *Science* **258**, 1798–1801
29. Strieter, R. M., Kunkel, S. L., Elner, V. M., Martonyl, C. L., Koch, A. E., Polverini, P. J., and Elner, S. G. (1992) *Am J. Pathol.* **141**, 1279–1284
30. Hu, D. E., Hori, Y., and Fan, T. P. D. (1993) *Inflammation* **17**, 135–143
31. Baggiolini, M., Walz, A., and Kunkel, S. L. (1989) *J. Clin. Invest.* **84**, 1045–1049
32. Miller, M. D., and Krangel, M. S. (1992) *Crit. Rev. Immunol.* **12**, 17–46
33. Baggiolini, M., Dewald, B., and Moser, B. (1994) *Adv. Immunol.* **55**, 97–179
34. Proost, P., De Wolf-Peeters, C., Conings, R., Opdenakker, G., Billiau, A., and Van Damme, J. (1993) *J. Immunol.* **150**, 1000–1010
35. Hebert, C. A., Vitangcol, R. V., and Baker, J. B. (1991) *J. Biol. Chem.* **266**, 18989–18994
36. Clark-Lewis, I., Dewald, B., Geiser, T., Moser, B., and Baggiolini, M. (1993) *Proc. Natl. Acad. Sci. U. S. A.* **90**, 3574–3577
37. Kunkel, T. A., Roberts, J. D., and Zakour, R. A. (1987) *Methods Enzymol.* **154**, 367–382
38. Farber, J. M. (1993) *Biochem. Biophys. Res. Comm.* **192**, 223–230
39. Sanger, F., Nicklen, S., and Coulson, A. R. (1977) *Proc. Natl. Acad. Sci. U. S. A.* **74**, 5463–5467
40. Messing, J. (1983) *Methods Enzymol.* **101**, 20–78
41. Laemmli, U. K. (1970) *Nature* **227**, 680–685
42. Smith, D. R., Polverini, P. J., Kunkel, S. L., Orringer, M. B., Whyte, R. I., Burdick, M. D., Wilke, C. A., and Strieter, R. M. (1994) *J. Exp. Med.* **179**, 1409–1415
43. Strieter, R. M., Kunkel, S. L., Showell, H., Remick, D. G., Phan, S. H., Ward, P. A., and Marks, R. M. (1989) *Science* **243**, 1467–1469
44. Strieter, R. M., Phan, S. H., Showell, H. J., Remick, D. G., Lynch, J. P., Genord, M., Raiford, C., Eskandari, M., Marks, R. M., and Kunkel, S. L. (1989) *J. Biol. Chem.* **264**, 10621–10626
45. Sharpe, R. J., Byers, H. R., Scott, C. F., Bauer, S. I., and Maione, T. E. (1990) *J. Natl. Cancer Inst.* **82**, 848–853
46. Clark, R. A. F. (1993) *J. Dermatol. Surg. Oncol.* **19**, 693–70
47. Klagsbrun, M., and D'Amore, M. (1991) *Annu. Rev. Physiol.* **53**, 217–239
48. Pober, J. S., and Cotran, R. S. (1990) *Pathol. Rev.* **70**, 427–451
49. Stout, A. J., Gresser, I., and Thompson, D. (1993) *Int. J. Exp. Path.* **74**, 79–85
50. Kaplan, G., Luster, A. D., Hancock, G., and Cohn, Z. (1987) *J. Exp. Med.* **166**, 1098–1108
51. Gusella, G. L., Musso, T., Bosco, M. C., Espinoza-Delgado, I., Matsushima, K., and Varesio, L. (1993) *J. Immunol.* **151**, 2725–2732
52. Schnyder-Candrian, S., Strieter, R. M., Kunkel, S. L., and Walz, A. (1995) *J. Leukocyte Biol.* **57**, 929–935
53. Dewald, B., Moser, B., Barella, L., Schumacher, C., Baggiolini, M., and Clark-Lewis, I. (1992) *Immunol. Lett.* **32**, 81–84
54. Hadley, T. J., Lu, Z., Wasniowska, K., Martin, A. W., Peiper, S. C., Hesselgesser, J., and Horuk, R. (1994) *J Clin. Invest.* **94**, 985–991
55. Neote, K., Darbonne, W., Ogez, J., Horuk, R., and Schall, T. (1993) *J. Biol. Chem.* **268**, 12247–12249
56. Moscatelli, D. (1987) *J. Cell. Physiol.* **131**, 123–130
57. Schonbeck, U., Brandt, E., Peterson, F., Flad, H.-D., and Loppnow, H. (1995) *J. Immunol.* **154**, 2375–2383

THROMBOSIS RESEARCH 71; 139–148, 1993
0049-3848/93 $6.00 + .00 Printed in the USA.

SUPPRESSIVE EFFECT OF HUMAN BLOOD COAGULATION FACTOR XIII ON THE VASCULAR PERMEABILITY INDUCED BY ANTI-GUINEA PIG ENDOTHELIAL CELL ANTISERUM IN GUINEA PIGS

Keizo Hirahara, Kazuhiko Shinbo, Mikiko Takahashi
and Tetsuro Matsuishi
Pharma Research Laboratories, Hoechst Japan Limited, 1-3-2,
Minamidai, Kawagoe-shi, Saitama, 350 Japan

(Received 12.11.1992; accepted in revised form 20.4.1993 by Editor A. Takada)

Abstract

We investigated the effect of blood coagulation factor XIII(FXIII) on enhanced permeability induced by anti-endothelial cell antiserum, that was produced by the immunization of guinea pig endothelial cells with adjuvant into rabbits repeatedly. We have found that this antiserum reacts to human and guinea pig endothelial cells but not guinea pig fibroblast cells. The permeability was enhanced by intradermal injection of 400-fold dilution of this antiserum into dorsal skin of guinea pigs. The mixture of equal volume of antiserum and FXIII was intradermally injected into dorsal skin of guinea pig after Evans blue injection, and 15 minutes later the quantity of Evans blue at the each injection site was determined. We recognized the suppressive effect of FXIII on the dye leakage. We also studied the suppressive effect on swelling induced by the antiserum. After the subcutaneous injection of the mixture of antiserum and FXIII into the back of guinea pigs, we measured the thickness of skins at the injection site after day 1, 2 and 3. As a result, FXIII significantly suppressed the swelling. We found that FXIII suppresses the acute and subacute permeability enhancement. These results suggest that FXIII plays an important role on an inflammatory site and that it may exert as an anti-inflammatory protein.

Blood coagulation factor XIII (FXIII), the last enzyme in the

Key words: Factor XIII, anti-endothelial cell antiserum, vascular permeability, anti-inflammatory protein, Schönlein Henoch purpura

blood coagulation cascade, is a transamidase that catalyzes the formation of γ - gultamyl - ε - lysyl peptide crosslinks between polypeptide chains in adjacent fibrin monomers and other plasma proteins(1,2,3). Crosslinks of each fibrin molecule caused a marked increase in the rigidity of the clot network(4). On the other hands, the crosslinks between fibrin and cellular matrix protein such as fibronectin may exert to connect fibrin molecules with the injury sites(5). It is well known that clots play an important role in the prevention of further tissue damage and in subsequent wound healing(6). Schönlein Henoch purpura (SHP) is characterized by hemorrhagic skin lesions, abdominal symptoms including gastro-intestinal bleeding, renal involvement with proteinuria and hematuria and swelling of joints(7). The symptoms are ascribed to generalized inflammation of arterioles and capillaries. That is, the local changes of the coagulation and fibrinolytic system due to immunoreaction were induced in the affected vessels. In 1977, Henriksson and colleagues described a lowering of FXIII activity during the acute phase of this disease(8). The mechanism of the decrease of FXIII activity in the acute phase of SHP has not yet been clarified. Destruction of FXIII molecules by protease derived from leukocytes which migrated into the inflammation sites has been proposed(9). In this connection, Kamitsuji and Fukui et al. reported that the administration of FXIII concentrate may contribute to the improvement of gastro-intestinal complications of SHP patients(10). Recently FXIII concentrate (Fibrogammin P) is used for the treatment of SHP patients(11). According to Matsuoka(12), Bowie et al.(13) and Ito et al.(14), this vasculitis of SHP is regarded as the immunovascular disease that antibody-antigen complexes on the vascular capillary endothelial cells enhances the vascular permeability. Consequently non-thrombocytopenic purpura caused by the injection of anti-endothelial cell antiserum(15). In the present study, we investigated whether or not human FXIII suppresses the enhancement of permeability and swelling induced by anti-endothelial cell antiserum in guinea pigs.

MATERIALS AND METHODS

Materials

Materials were purchased from the following suppliers: Dulbecco phosphate buffer, Dulbecco MEM, FCS(Gibco, USA), ECGS(Calbiochem, USA), Freund's adjuvant(Difco, USA), FITC conjugated anti-rabbit IgG(Cappel, USA), Evans blue, potassium hydroxide(KOH, Kanto Kagaku, Japan), phosphoric acid(Wako Pure Chemical, Japan), Guinea pig complement(Kyokuto, Japan), and Human FXIII(Fibrogammin P, Behringwerke, FRG).

Preparation of anti-guinea pig endothelial cell antiserum
Guinea pig endothelial cells were isolated from the main artery and vena cava(16), then cells were inoculated into tissue culture dishes and incubated for several days with Dulbecco MEM containing 15% FCS and 37.5 µg/ml ECGS till reaching confluency. Confluent monolayer was harvested by a cell scraper. The cells were rinsed twice with Dulbecco phosphate buffered saline(pH 7.2). These cells were used as an antigen for the production of anti-endothelial cell antiserum. The antiserum was obtained from rabbits immunized with emulsion of Freund's complete adjuvant with guinea pig endothelial cells, and boosted with emulsion of Freund's incomplete adjuvant. After several times of boosting, the antibody titer was measured with guinea pig endothelial cells by the methods of cytolysis and indirect immunofluorescence microscopy using FITC conjugated anti-rabbit IgG(17).

Measurement of antibody titer of anti-endothelial cell antiserum
Confluent monolayer of guinea pig endothelial cells in a 96-well plate was incubated with 50 µl of variously diluted antiserum in Dulbecco MEM-15% FCS for 30 min. The medium was then replaced to 50 µl of 5% guinea pig complement in Dulbecco MEM-15% FCS and the cells were further incubated for 30 min. After addition of 10 µl of trypan blue solution, the cell layers were photographed to evaluate the extent of cell lysis. Indirect immunofluorescence microscopy was done as follows. The antiserum was serially diluted two times. The diluted antiserum was then incubated with the main artery at room temperature for 1 hour and rinsed 3 times with Dulbecco phosphate buffer. After washing, 1000-fold dilution of FITC conjugated anti-rabbit IgG was added to the sections, incubated for 30 minutes at room temperature, and washed 3 times with Dulbecco phosphate buffer. All sections were observed by a Nikon microscope equipped with a mercury lamp. The titer was taken as a highest dilution which gave a fluorescent staining just above the background staining of normal serum controls.

Duration of activity of permeability enhancement
Measurement of permeability was studied according to Yamamoto et al.(18). A 100 µl portion of 50-fold diluted antiserum was intradermally injected into the back of a guinea pig before intravenous injection of 0.5 ml of 1 % Evans blue. After 15 minutes of the Evans blue injection, the back skins were harvested and the blue lesions were observed.

Suppressive effect of FXIII on the permeability enhancement
A 100 µl portion of either each diluted antiserum or the mixture of equal volume of FXIII and the diluted antiserum was

intradermally injected into the dorsal skin of guinea pigs after intravenous injection of Evans blue. After 15 minutes, skins were harvested and blue lesions in the skins were observed.

Extraction of Evans blue from guinea pig skins
Evans blue was extracted from skins, soaked with 1 ml of 1 M KOH solution, and incubated at 37°C overnight. After the incubation, 3 ml of 0.6 N phosphoric acid and 3 ml of FRIGEN(Behringwerke, FRG), a defatting agent, was added to each tube and mixed for 30 sec. with a Vortex mixer. Each tube was centrifuged at 3000 rpm for 15 minutes, and the absorbance of the supernatant was measured at 620 nm(19).

Suppressive effect of FXIII on the swelling
One milliliter of equal volume mixture of FXIII and the intact antiserum was subcutaneously injected into the dorsum of guinea pigs. After days 1, 2 and 3, the skins were harvested and the thickness was measured with a slide caliper at injection sites as a marker of swelling. The swelling was shown by the difference of the thicknesses between a injection and a non-injection site.

RESULTS

Characterization of polyclonal anti-guinea pig endothelial cell antiserum
The antibody titer was determined with guinea pig endothelial cells by the methods of cytolysis and indirect immunofluoresence microscopy using FITC conjugated anti-rabbit IgG. As a result, the 50% cytolysis was observed by the 60-fold dilution of antiserum, and the fluorescence was observed by 400-fold dilution. The antiserum exhibited the reactivity with not only guinea pig but also human endothelial cells. However it did not react with guinea pig fibroblasts. When the cryosection of the main artery of a guinea pig was used for the indirect immunofluorescence test, the fluorescence was observed on the inner membrane which was seemed to be endothelial cell. It was also found that the antiserum reacted with the extracellular matrix proteins produced by endothelial cells(data not shown).

Enhanced permeability
First, we studied whether this antiserum induced the permeability in guinea pigs. The variation of permeability after intradermal injection is shown in Fig. 1. The permeability reached the maximum within 5 minutes. This activity for enhancing the permeability almost disappeared within 30 minutes after the injection. This permeability enhancing phenomenon was classified as a short lasting reaction. We next investigated the dose response of this antiserum. As shown in Fig. 2, the activity of

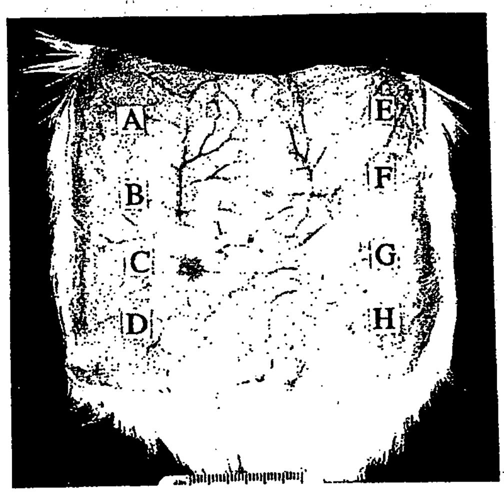

FIG. 1.

Time course of permeability enhancement induced by anti-endothelial cell antiserum. Antiserum was injected into a guinea pig at varying times before intravenous dye injection. Time 0 means an intradermal injection immediately after intravenous dye injection. (A): antiserum, 60 min, (B): antiserum, 30 min, (C): antiserum, 0 min, (D): saline, 30 min, (E): rabbit serum, 60 min, (F): rabbit serum, 30 min, (G): rabbit serum, 0 min, (H): saline, 0 min

enhancing the permeability is recognized by 400-fold dilution of antiserum. The effect of FXIII was examined on the vascular permeability induced by the antiserum. In this experiment, the mixture of antiserum was injected with various concentration of FXIII. As shown in Fig. 3, FXIII shows the suppressive effect on the dye leakage in a dose dependent fashion. We obtained a result that both 200-fold and 400-fold diluted antiserum exhibit the same tendency. Thus the effect of FXIII was examined in 10 guinea pigs and the dye leakage was measured in extravascular space. As shown in Fig. 4, FXIII exhibited the suppressive effect in a dose dependent manner.

Suppressive effect of FXIII on the swelling

When the antiserum was subcutaneously injected into a dorsal skin of guinea pig, edema, in addition to hemorrhage was observed at injection site(20). Thus we examined the suppressive effect of FXIII on the swelling. On injecting the mixture of FXIII and antiserum, the edema was significantly suppressed by FXIII on day 1 and 2(Fig. 5). This result indicates that FXIII suppresses the permeability in the acute and the subacute phase as well.

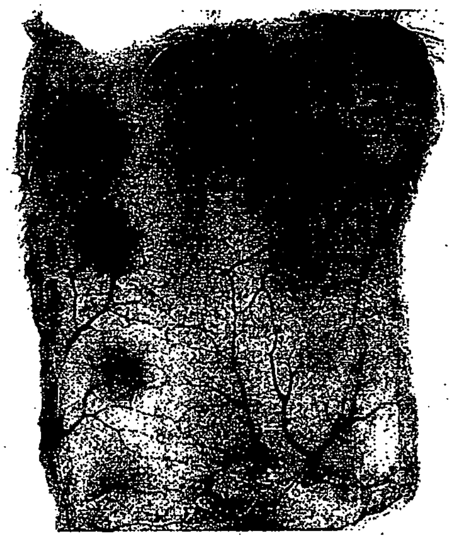

FIG. 2.

Dose response of anti-endothelial cell antiserum in a guinea pig. Each sample was injected immediately after a intravenous dye leakage. NRS: Normal rabbit serum

DISCUSSION

For more than 20 years after its detection of FXIII, many authors have reported that a clotting factor, FXIII, influenced a lot of other systems and thus it was often termed a connective tissue factors (21). The fibrin stabilizing effect is an example of general properties of this factor which crosslinks proteins with suitably configurated ε - lysyl- and γ - glutamyl - residues. Many kinds of proteins are listed as substrates for FXIII, e.g. fibrin(1), collagen(22), fibronectin(5), actin(23) and factor V(24). In this context, the binding of biogenic amines to proteins by FXIII may also participate in the elimination of toxic substances like histamine. FXIII concentrate has been recently used not only for the promotion of the wound healing but also for the treatment of Shönlein Henoch Purpura(SHP)(6,10). The clinical effects of FXIII on SHP are probably due to the stabilization of microvasculature leading to a reduction of the leakage at inflammatory sites. Pilger et al(25) has reported that FXIII shows the suppressive/sealing effect in a screlodermia patient. However none of these reports showed the sealing/suppressive effect on the permeability by FXIII in animal studies. This vasculitis of SHP is regarded as the immunovascular disease that

the vascular permeability is enhanced by the formation of the antigen-antibody complex not with standing ambiguity of trigger which may include drugs, foods, insect bites or bacterial infections(11,12,13,14). Thus we tried to demonstrate the suppressive effect of FXIII on permeability enhancement induced by anti-endothelial cell antiserum. As shown in Figs. 1 and 2, anti-endothelial cell antiserum induces the enhancement of permeability. This phenomenon can be caused by factors such as complement fragments and histamine etc. which are produced by the activation of complement system after complex formation of antiserum with endothelial cells(11,12,13,14). As this phenomenon shows the dose dependent manner by antiserum, condition of SHP patients may be influenced seriously depending on the extent of the antibody generation. SHP patients show the increase of plasma level of IgA and the imbalance of serum IgG subclass and IgM(13,14,26). As shown in Figs. 3, 4 and 5, FXIII suppresses the vascular permeability in acute phase and the edema in subacute phase. These results are supported by some clinical studies. Kamitsuji et al.(10) and Fukui et al.(11) have reported that FXIII shows the suppressive effect on the swelling of joints of SHP patients.

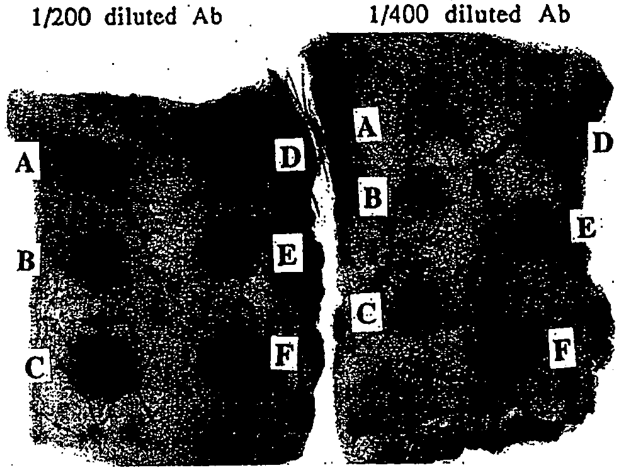

FIG. 3.

Suppressive effect of FXIII on the permeability enhancement induced by anti-endothelial cell antiserum. FXIII was used with the final concentration at a injection site of (A), 3.0 U; (B), 1.5 U; (C), 0.75 U; (D), 0.38 U; (E), medium control. The mixture of FXIII and either 200- or 400- fold diluted antiserum was injected immediately after the intravenous injection of dye.

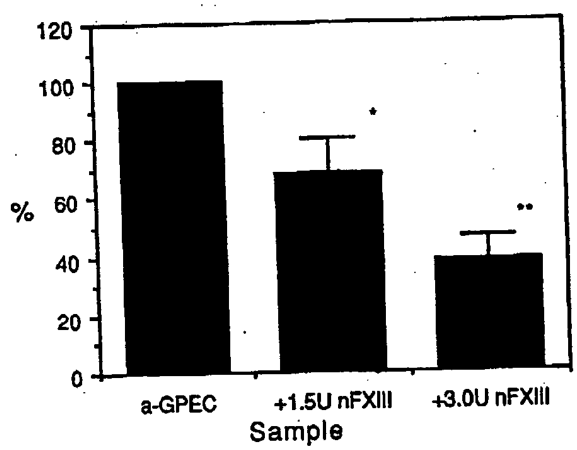

FIG. 4

Suppressive effect of FXIII on the permeability induced by anti-guinea pig endothelial cell antiserum. Extraction of Evans blue at the injection site was according to the materials and methods. n=10, *: p<0.05, **: p<0.01 In this experiment, we used the 300-fold diluted anti-endothelial cell antiserum as a permeability inducer. FXIII was mixed with antiserum, then the mixture was injected intradermally.

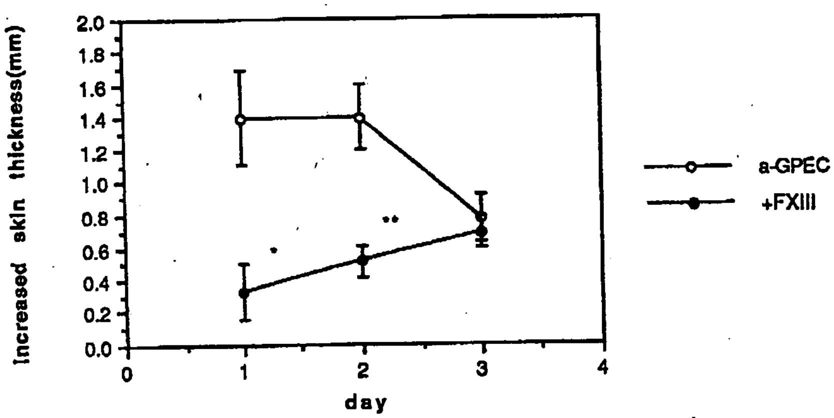

FIG. 5.

Effect of FXIII on the swelling induced by anti-guinea pig endothelial cell antiserum. Open circle (o) denotes the antiserum alone. Closed circle (●) denotes the FXIII plus antiserum. n=5, *: p<0.05, **: p,0.01

Pilger et al.(25) reported that FXIII also shows the suppressive effect on vascular permeability in sclerodermia patients. These results suggest that FXIII may crosslink cellular matrices to prevent the opening of the space between cells(27) and that it may crosslink the enhancing factors for the permeability(21). We have succeeded in demonstrating the suppressive effect of FXIII on vascular permeability in an animal study. This study indicates that FXIII may play a crucial role in an inflammatory site. Consequently it seems that FXIII therapies are necessary for the treatment of some inflammatory diseases (28,29).

REFERENCES

1. ROBBINS, K.C. A study of the comparison of fibrinogen to fibrin. AM. J. Physiol., *142*, 581-588, 1944
2. KESKI-OJA, J., MOSHER, D.F. and VAHERI, A. Crosslinking of a major surface-associated glycoprotein (fibronectin) catalyzed by blood coagulation factor XIII. Cell, *9*, 29-35, 1976
3. ICHINOSE, A., TAMAKI, T. and AOKI, N. FXIII mediated cross-linking of NH2-terminal peptide of alpha-2 plasmin inhibitor to fibrin. FEBS-letter, *153*, 369-371, 1983
4. SHEN, L. and LORAND, L. Contribution of fibrin stabilization to clot strength. J. Clin. Invest., *71*, 1336-1341,1983
5. OKADA, M., BLOMBÄCK, B., DER CHANG, M. and HOROBITZ, B. Fibronectin and fibrinogen structure. J. Biol. Chem., *260*, 1811-1820, 1985
6. MISHIMA, Y., NAGAO, F., ISHIBIKI, K., MATSUDA, M. and NAKAMURA, N. Faktor XIII in der Behandlung postoperativer therapierefraktärer Wundheilungsstorungen. Chirurg, *55*, 803-808, 1984
7. FYE, K.H. and SACK, K.E. Basic and Clinical Immunology, In: *Rheumatic disease*, STITES, D.P., STOBO, J.D., FUDENBERG, H.H. and WELLS, J.V. (eds.), p449, Lange Medical Publications, California, (1982)
8. HENRIKSSON, P., HENDERNER, U. and NILSSON, I.M. Factor XIII (fibrin stabilizing factor) in Henoch-Schönlein's purpura. Acta. Pediatr. Scand., *66*, 273-277, 1977
9. HENRIKSSON, P., NILSSON, I.M., OKLSSON, K. and STENBERG, P. Granulocyte elastase activation and degradation of factor XIII. Thromb. Res., *18*, 343-351, 1980
10. KAMITSUJI, H., TANI, K., YASUI, M., TANIGUCHI, A., TAIRA, K., TSUKADA, S., IIDA, Y., KANNKI, H. and FUKUI, H. Activity of blood coagulation Factor XIII on a prognostic indicator in patients with Henoch-Schönlein purpura. Eur. J. Pediatr., *146*, 519-523, 1987
11. FUKUI, H., KAMITSUJI, H., NAGAO, T., YAMADA, K., AKATSUKA, J., INAGAKI, M., SHIKE, S., KOBAYASHI, Y., YOSHIOKA, K., MAKI, S., SHIRAHATA, A., MIYAZAKI, S., NAKASHIMA, M. and TANAKA, S. Clinical evaluation of a pasteurized factor XIII concentrate administration in Henoch-Schönlein Purpura. Thromb. Res. *56*, 667-675, 1989
12. MATSUOKA, M., Hemorrhagic factors and Thrombosis, In: *Purpura Schönlein-Henoch*, p245-246, Kinbara Shuppan, Tokyo (1981)
13. BOWIE, W.E.J. and OWEN, C.A.Jr Hemostasis and Thrombosis, In: *Non thrombocytopenic vascular disorders*, COLMAN, R.W., HIRSH, J, MARDER, U.J. and SALZMAN, E.W. (eds.), p816-824, Lippincott, Philadelphia, 1987

14. ITO, T. and FUJIMAKI, M. Intergated handbook of internal medicine, In: *Schönlein-Henoch purpura,* IMURA, H., OGATA, E., TAKAKU, S. and TARUI, S.(eds.), p296-300, Nakayama Shupann, Tokyo
15. WILSON, C.B., COLE, E.H., ZANETTI, M. and MAMPASO, F.M. Basic and Clinical Immunology, In: *Renal disease,* STITES, D.P., STOBO, J.D., FUDENBERG, H.H. and WELLS, J.V. (eds.), p557-575, Lange Medical Publication, California (1978)
16. MITSUI, Y. and IMAMURA, J. Isolation and Culture for Functional Cells, In: *Endothelial cells.,* MITSUI, J., TAKAGI, R., ICHIHARA, A., SEKIGUTI, M. and MURAMATSU, T.(eds.) p227-229, Maruzen, Tokyo (1987)
17. WICK, G., BAUNDNER, S. and HERZOG, F. Immunofluorescence, p47-51, Die Medizinishe Verlagsgesellschaft, Marburg (1987)
18. Yamamoto, T., Chemical Mediators of Inflammation and Immunity, In; *Role of Hageman factor in enhancing vascular permeability.,* CHOEN, S., HAYASHI, H., SAITO, K. and TAKADA, A. (eds.), p129-143, Academic Press, New York (1986)
19. KATAYAMA, S., SHIONOYA, H. and OHTAKE, S. A new method for extraction of extravasated dye in the skin and influence of fasting stress on passive cutaneous anaphylaxis in guinea pigs and rats. Microbiol. Immunol. Biol., *22,* 89-101, 1987
20. SHINBO, K., HIRAHARA, K., TAKAHASHI, M. and MATSUISHI, T. Suppressive effect of factor XIII on the hemorrhage induced by anti-endothelial cell antiserum. Int. J. Hematol., *54*(suppl 1), 276, 1991
21. KARGES, H.E. and CLEMENS, R. Factor XIII: Enzymatic and clinical aspects. Behring Inst. Mitt. *82,* 43-58, 1988
22. SORIA, A., SORIA, C. and BOULARD, C. Fibrin stabilizing factor (FXIII) and collagen polymerization. Experientia, *31,* 1355-1357, 1975
23. CHOEN, J., BLANKENBERG, T.A., BORDEN, B., KAHN, D.R. and VEIS, A. Factor XIIIa-catalyzed crosslinking of platelet and muscle. Regulation by nucleotides. Biochem. Biophys. Acta., *628,* 365-375, 1980
24. FRANCIS, R.T., MACDONAGH, J. and MANN, K.G. Factor V is a substrate for the transamidase factor XIIIa. J. Biol. Chem., *261,* 9787-9797, 1986
25. PILGER, E., BERTUCH, H., ULREICH, A. and RAINER, F. Capillary permeability in connective tissue disease.: Influence of Fibrogammin P-therapy, Thromb. Haemostas. *58,* 81, 1987
26, TRYGSTAD, C.W. and STIEHM, E.R. Elevated serum IgA globulin in anaphylactoid purpura. Pediatrics, *47,* 1023-1029, 1971
27. TAKAHASHI, M., SHINBO, K., HIRAHARA, K. and MATSUISHI, T. Effect of activated factor XIII on increase in permeability of human umbilical vein endothelial cell layer. The XXIV Congress of International Society of Hematology in London (abstract), 1992
28. GALOWAY, M.J., MAKIE, M.J. and MACVERRY, B.A. Reduced levels of factor XIII in patients with chronic inflammatory bowel disease. Clin. Lab. Haemat., *5,* 427-428, 1983
29. KURATSUJI, T., OKIMA, T., FUKUMOTO, T., SHIMIZU, S., IWASAKI, Y., TOMITA, Y., MEGURO, T. and YAMADA, K. Factor XIII deficiency in antibiotic-associated pseudomembranous colitis and its treatment with Factor XIII concentrate. Haemostas., *11,* 229-234, 1982

Waterbury, ibid., p. 340; H. Felback, J. Childress, G. Somero, Nature (London) 293, 291 (1981).
15. U. Laemmli, Nature (London) 227, 680 (1970).
16. G. Fairbanks, T. Steck, D. Wallach, Biochemistry 10, 2606 (1971).
17. S. Panyim and R. Chalkley, Arch. Biochem. Biophys. 130, 337 (1969); T. Poole, B. Leach, W. Fish, Anal. Biochem. 60, 596 (1974).
18. Funds for the vessels D.S.R.V. Alvin, R.V. Lulu, and R.V. New Horizon were provided by NSF. Research was supported by NSF grants OCE78-08852 and OCE78-08933 (to J. J. Childress), OCE78-10458 (to J. F. Grassle), and PCM 80-12854 and PCM 78-21784 (to R.C.T.). This work was made possible by the physical and intellectual efforts of many people, including the captains and crews of the vessels named above. We thank B. Smithie and R. Hessler for collection of the East Pacific Rise clam blood and J. J. Childress for supplying the Galápagos Rift Valley clam blood. This article is contribution No. 43 of the Galápagos Rift Biology Expedition.

10 June 1982; revised 12 November 1982

Tumor Cells Secrete a Vascular Permeability Factor That Promotes Accumulation of Ascites Fluid

Abstract. *Tumor ascites fluids from guinea pigs, hamsters, and mice contain activity that rapidly increases microvascular permeability. Similiar activity is also secreted by these tumor cells and a variety of other tumor cell lines in vitro. The permeability-increasing activity purified from either the culture medium or ascites fluid of one tumor, the guinea pig line 10 hepatocarcinoma, is a 34,000- to 42,000-dalton protein distinct from other known permeability factors.*

Abnormal accumulation of fluid commonly accompanies solid and particularly ascites tumor growth (*1*). To investigate the mechanism of tumor ascites formation, we measured the rates of influx and efflux of ^{125}I-labeled human serum albumin (HSA) at various times after the implantation of tumor cells in the peritoneal cavities of guinea pigs. We detected a markedly increased influx of HSA as early as 1 hour after intraperitoneal injection of guinea pig line 10 hepatocarcinoma cells, which provoke a substantial accumulation of ascites fluid (Table 1). In contrast, efflux of HSA from the peritoneal cavities of animals bearing line 10 tumors did not change significantly, even with progressive tumor growth (*2*).

To establish whether the increased influx of fluid induced by tumor cells reflects an alteration in vessel permeability, we injected animals intravenously with colloidal carbon. Examination of the peritoneal cavities of strain 2 guinea pigs, Syrian hamsters, and A/Jax mice bearing syngeneic ascites tumors (line 10, HSV-NIL8, and TA3-St, respectively) revealed that many venules of the peritoneal wall, diaphragm, mesentery, and gastrointestinal serosal surfaces were heavily labeled with colloidal carbon, indicating increased permeability; comparable vessels in control animals were not labeled.

These observations suggest that tumor ascites may be attributable to alterations in the permeability of vessels lining the peritoneum. To investigate the basis for this increased permeability, we used the Miles assay (*3*) to test ascites fluid for the presence of factors that increase vascular permeability (Table 2 and Fig. 1). Ascites fluid from line 10 guinea pig and TA3-St mouse carcinomas and the HSV-NIL8 hamster sarcoma all markedly increased local cutaneous vascular permeability. The increase was evident after 1 minute and maximal within 5 to 10 minutes. By contrast, platelet-poor plasma samples from the same species (Table 2 and Fig. 1) and oil-induced peritoneal exudate fluids (*4*) had little or no activity. The tumor ascites permeability-increasing activity was not inhibited by soybean trypsin inhibitor (1000 μg/ml); therefore, it is not PF/dil (*5*), a permeability factor unmasked when serum is diluted ≥ 1:100 (*6*).

We previously reported that line 10 tumor cells release a vascular permeability-increasing activity in serum-free culture (*7*). This activity is not inhibited by soybean trypsin inhibitor (200 μg/ml), and its production by cells in vitro requires protein synthesis (complete inhibition by 20 μg of cycloheximide per milliliter). Many other tumor cell lines also release permeability-increasing activity in serum-free culture, including guinea pig 104 C1 fibrosarcoma, hamster HSV-NIL8 sarcoma, rat sarcomas B77 Rat 1 and RR 1022, and mouse TA3-St carcinoma, MOPC 21 myeloma, and polyoma BALB/c 3T3 sarcoma. Line 1 guinea pig hepatocarcinoma cells release one-fourth the activity released by line 10 cells, a finding that may explain the relative ability of these cells to promote HSA influx (Table 1) and ascites fluid accumulation (the volume of line 1 ascites fluid was routinely one-fourth that of line 10). Oil-induced guinea pig peritoneal exudate cells (> 70 percent macrophages) neither increase the influx of HSA into the peritoneum (Table 1) nor secrete detectable permeability-increasing activity in vitro. Guinea pig fibroblasts and smooth muscle cells release approximately one-eighth the activity released by comparable numbers of line 10 cells (*8*).

We next purified both the ascites and tissue culture permeability factors from a single tumor, the line 10 guinea pig carcinoma. Permeability-increasing activities from both sources chromatographed identically as single peaks on columns containing Sephadex G-150, heparin-Sepharose, or hydroxylapatite (*9*) and electrophoresed as a single peak with an apparent molecular weight of 34,000 to 42,000 on sodium dodecyl sulfate–polyacrylamide gels (Fig. 2). Using the heparin-Sepharose, hydroxylapatite, and electrophoretic steps in tandem, we purified the permeability-increasing activity approximately 1200-fold from serum-free conditioned medium and approximately 10,000-fold from ascites fluid. As little as 200 ng (5×10^{-12} mole) of the purified material increased vascular permeability to a degree equivalent to that induced by 1.25 μg (4×10^{-9} mole) of histamine.

Rabbits immunized with the purified permeability factor secreted by line 10 cells in vitro produced an immunoglobulin G (IgG) that bound and neutralized virtually all the permeability-increasing activity in undiluted line 10 and line 1 tumor ascites fluids (Table 2) and in line 10 and line 1 culture media. This antibody also blocked the peritoneal influx that follows intraperitoneal injection of line 10 tumor cells (Table 1). In every

Table 1. Peritoneal vessel permeability. Guinea pigs (400 g) were injected intraperitoneally with 3×10^7 line 1 or line 10 tumor cells (*17*) or with peritoneal exudate cells in Hanks balanced salt solution (HBSS) and immediately thereafter were injected intravenously with ^{125}I-labeled HSA (5×10^6 dis/min). One hour later the animals were exsanguinated under ether anesthesia, and peritoneal fluid was collected following intraperitoneal injection of 20 ml of heparinized (10 U/ml) HBSS. For each animal total radioactivity in the ascites fluid was determined and normalized for that in the blood: influx of HSA was computed as the ratio of total disintegrations per minute in peritoneal fluid to those per milliliter of blood. Net influx was determined by subtracting influx values for control animals. Values are means ± standard errors (*N* = 4).

Type of cells injected intraperitoneally	Net peritoneal influx of HSA
Line 1	0.09 ± 0.04
Line 10	0.41 ± 0.08
Line 10 + immune IgG (2 mg)	0.11 ± 0.03
Peritoneal exudate	0

pigs were injected intravenously with ^{125}I-labeled HSA (1.3×10^7 dis/min) in 1 ml of saline containing 0.5 percent Evans Blue dye. Samples to be tested for permeability-increasing activity, in isotonic solution and at neutral *p*H, were injected intradermally in a volume of 0.1 ml. After 20 minutes the animals were exsanguinated under ether anesthesia. Test sites were excised and quantitated for ^{125}I in a gamma counter. The number of net disintegrations per minute extravasated was determined by subtracting values for control sites injected with saline. Each animal also received a series of intradermal histamine injections; these sites served as reference points for the calculation of histamine equivalents. B.L., below limit of quantitation (0.6 μg histamine).

Substance injected intradermally	Net disintegrations per minute ^{125}I-HSA extravasated (mean ± standard error) (N = 3 to 7)	Histamine equivalent* (μg)
Hamster plasma	70 ± 176	B.L.
Hamster ascites (HSV-NIL8)	15,309 ± 1,508	1.3
Guinea pig plasma	1,989 ± 1,070	B.L.
Line 1 ascites	69,609 ± 6,850	5.5
Line 1 ascites + preimmune IgG (80 μg)	70,321 ± 2,567	5.5
Line 1 ascites + immune IgG (80 μg)	3,935 ± 1,568	B.L.
Line 10 ascites	92,472 ± 4,886	10.0
Line 10 ascites + preimmune IgG (80 μg)	93,756 ± 1,171	10.0
Line 10 ascites + immune IgG (80 μg)	7,187 ± 930	B.L.
Line 10 serum-free culture supernatant†		
After 1 hour of culture	1,054 ± 60	B.L.
After 5 hours of culture	3,610 ± 295	0.7
After 24 hours of culture	21,565 ± 617	2.5

*A plot of net disintegrations per minute extravasated in response to histamine versus the logarithm of the number of micrograms of histamine injected generated a straight line (histamine range, 0.6 to 10 μg).
†Derived from cultures containing 2.5×10^6 cells per milliliter.

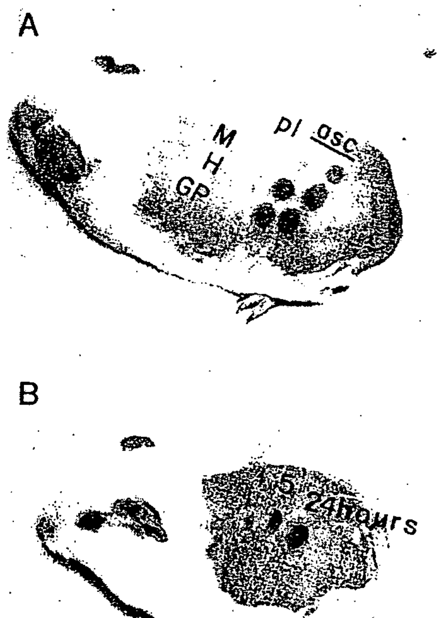

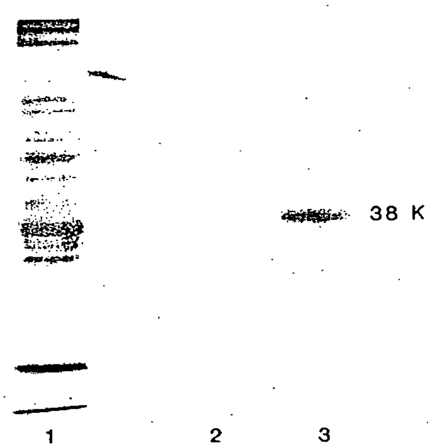

Fig. 1 (left). Miles assay for measuring increased vascular permeability in the skin (see legend to Table 2). Mediators of increased permeability cause bluing at the site of intradermal injection within 5 minutes, whereas control substances such as saline elicit no response. Abbreviations in (A): *pl*, control plasma; *asc*, ascites fluid; *M*, mouse TA3-St tumor; *H*, hamster HSV-NIL8 tumor; and *GP*, guinea pig line 10 tumor. In (B), line 10 cells were cultured (1×10^6 cell/ml) in serum-free Dulbecco's modified Eagle's medium and conditioned media was harvested at 1, 5, and 24 hours as indicated. Fig. 2 (right). Resolution of the permeability-increasing activity on sodium dodecyl sulfate–polyacrylamide slab gels (*16*). Samples were electrophoresed without reduction at 4°C in a 7.5 percent polyacrylamide gel containing 0.1 percent sodium dodecyl sulfate and washed for 1 hour at 4°C in 2.5 percent Triton X-100 and then in phosphate-buffered saline for 1 hour. The gel was sliced, individual slices were extracted, and dialyzed extracts were tested for activity by the Miles assay. Track 1 shows the stained pattern of concentrated line 10 serum-free culture medium. All the activity in track 1 (total recovery was regularly 50 percent) was confined to two adjacent slices (reelectrophoresed in tracks 2 and 3) composing the 34,000 to 42,000 molecular weight region. Line 10 ascites fluid permeability-increasing activity was found to electrophorese identically (molecular weight 34,000 to 42,000) with the activity in line 10 culture medium.

munization (preimmune IgG) was without effect. The IgG from immunized animals (immune IgG) also neutralized the permeability-increasing activity released in culture by an unrelated tumor, the 104 C1 guinea pig fibrosarcoma (*10*), but not the activity of guinea pig PF/dil or the low levels of activity released by guinea pig fibroblasts or smooth muscle cells.

As determined by light and electron microscopy, line 10 permeability factor did not cause endothelial cell damage or mast cell degranulation. Vessels responded equally well to multiple challenges with equivalent doses of line 10 permeability factor administered 30 minutes apart; the effect of a single intradermal injection was rapid (evident within 5 minutes) and transient (little residual increased permeability was detectable 20 minutes after injection), providing further evidence that line 10 permeability factor is not toxic to blood vessels. It does not resemble bradykinin (molecular weight, 1200), plasma kallikrein (108,000), or leukokinins (2500). Leukokinins (*11*) are generated in ascites fluids under nonphysiological conditions (*p*H 3.8 and 37°C for 24 hours) by a mechanism sensitive to 1 μ*M* pepstatin A. Line 10 permeability factor is present in fresh, unmanipulated ascites fluid (*p*H 6.4 to 6.9), and its action is unaffected by 20 μ*M* pepstatin A. Lymphocyte permeability factors with molecular weights of 12,000 (*12*) and 39,000 (*13*) have been reported; however, unlike line 10 permeability factor, the latter increases vascular permeability only after a latent period of 20 minutes. The effects of line 10 permeability factor are not mediated by histamine. Guinea pigs treated with the antihistamines mepyramine (5 μmole/kg, subcutaneously) plus cimetidine (500 μmole/kg) (*14*) responded normally to line 10 permeability factor, although the action of 20 μg of histamine was blocked. It is also unlikely that the effects of this factor are mediated through prostaglandin synthesis. Neither systemic (14 μmole/kg, intraperitoneally) nor local (2 nmole, intradermally) treatment with indomethacin (*15*) affected the response of vessels to the permeability factor.

In conclusion, vessels lining the peritoneal cavities of guinea pigs, hamsters, and mice bearing ascites tumors display markedly greater permeability than do the same vessels in control animals. This increased permeability is apparently due to the presence in ascites fluid of a potent permeability factor not found in normal plasma or serum. The permeability factors found in guinea pig line 10

culture medium or ascites fluids appear to be identical. In addition, they are antigenically related to permeability factors produced by guinea pig line 1 or 104 C1 tumor cells. Secretion of permeability-increasing activity appears to be a common feature of tumor cells, and may contribute to the abnormal accumulation of fluid associated with neoplastic disease.

Note added in proof: The immune IgG raised against line 10 permeability factor also neutralizes the rat dermal vessel permeability-increasing activity released by Walker rat carcinoma cells in culture. Preimmune IgG has no neutralizing effect.

DONALD R. SENGER
STEPHEN J. GALLI
ANN M. DVORAK
CAROLE A. PERRUZZI
V. SUSAN HARVEY
HAROLD F. DVORAK

Departments of Pathology, Beth Israel Hospital, and Harvard Medical School, and Charles A. Dana Research Institute, Beth Israel Hospital, Boston, Massachusetts 02215

References and Notes

1. P. M. Gullino, in *Cancer 3: A Comprehensive Treatise*, F. F. Becker, Ed. (Plenum, New York, 1975), pp. 327–354; M. Green, *Principles of Cancer Treatment* (McGraw-Hill, New York, 1982), pp. 237–243.
2. Clearance of labeled HSA from the peritoneal cavity was not impaired in tumor-bearing animals at any interval. For example, 7 days after intraperitoneal injection of 3×10^7 line 10 tumor cells, 58.4 ± 4.2 percent (mean ± standard error) of the HSA (90 to 95 percent precipitable with trichloroacetic acid) remained in the peritoneal cavities after 2 hours; 56 ± 1.15 percent remained in the controls.
3. A. A. Miles and E. M. Miles, *J. Physiol. (London)* **118**, 228 (1952).
4. M. E. Hammond and H. F. Dvorak, *J. Exp. Med.* **136**, 1518 (1972).
5. A. A. Miles and D. L. Wilhelm, *Br. J. Exp. Pathol.* **36**, 71 (1955).
6. It has been shown that PF/dil is activated Hageman factor (clotting factor XIIa or αHFa) [H. Z. Movat, in *Handbook of Experimental Pharmacology*, vol. 25, *Supplement*, E. G. Erdos, Ed. (Springer-Verlag, Berlin, 1979), p. 1], an activity totally inhibited by 5 μg of soybean trypsin inhibitor per milliliter [A. A. Miles and O. D. Ratnoff, *Br. J. Exp. Pathol.* **45**, 328 (1964)]. We confirmed this finding and therefore conclude that the activity present in undiluted ascites fluid is not PF/dil. However, a ≥ 1:50 dilution of line 10 guinea pig ascites fluid in saline with 0.38 percent sodium citrate in plastic tubes unmasked a second permeability factor activity which, like PF/dil, was inhibited completely by soybean trypsin inhibitor. Because this inhibitable activity was not expressed unless ascites fluid was diluted substantially, we concluded that it was not likely to be responsible for inducing tumor ascites in vivo. Therefore we focused our attention on the permeability-increasing activity in undiluted ascites fluid.
7. H. F. Dvorak *et al.*, *J. Immunol.* **122**, 166 (1979).
8. The cells were cultured in the presence of 10 percent guinea pig serum because protein synthesis by fibroblasts is decreased in the absence of serum.
9. Activities from both ascites fluid and serum-free culture medium bound completely to both heparin-Sepharose and hydroxylapatite. Columns were eluted with linear gradients; ascites and culture medium activities coeluted from heparin-Sepharose as a peak centered at 0.40*M* NaCl–0.01*M* PO_4 (*p*H 7.0) and from hydroxylapatite at 0.25*M* sodium phosphate (*p*H 7.0). To avoid complicating our analysis of diluted ascites fluid fractions with unmasked PF/dil (7), we added soybean trypsin inhibitor (20 μg/ml) to all ascites fluid column fractions before assay.
10. C. H. Evans and J. A. DiPaolo, *Cancer Res.* **35**, 1035 (1975).
11. L. M. Greenbaum, in *Handbook of Experimental Pharmacology*, vol. 25, *Supplement*, E. G. Erdos, Ed. (Springer-Verlag, Berlin, 1979), p. 91.
12. A. Sobel and G. La Grue, in *Lymphokine Reports*, E. Pick, Ed. (Academic Press, New York, 1980), vol. 1, pp. 211–230.
13. J. L. Maillard, E. Pick, J. L. Turk, *Int. Arch. Allergy Appl. Immunol.* **42**, 50 (1972).
14. D. A. A. Owen *et al.*, *Br. J. Pharmacol.* **69**, 615 (1980). Both injections were given 30 minutes before skin testing.
15. J. S. Stoff, R. M. Rosa, P. Silva, F. H. Epstein, *Am. J. Physiol.* **241**, F 231 (1981). Intraperitoneal injections were given 1 and 25 hours before skin testing. For intradermal injections, indomethacin was mixed with test substances.
16. U. K. Laemmli, *Nature (London)* **227**, 680 (1970).
17. B. Zbar, H. T. Wepsic, H. J. Rapp, J. Whang-Peng, T. Borsos, *J. Natl. Cancer Inst.* **43**, 821 (1969); B. Zbar, I. Bernstein, T. Tanaka, H. J. Rapp, *Science* **170**, 1217 (1970).
18. We thank B. Wildi, J. Feder, and R. D. Rosenberg for help and advice, J. Osage for technical assistance, and B. Zbar, R. Hynes, R. Garcia, T. Isomura, and J. Codington for cells. Supported by a grant from the Monsanto Company.

12 October 1982

Yolk Pigments of the Mexican Leaf Frog

Abstract. *Eggs of the Mexican leaf frog contain blue and yellow pigments identified as biliverdin and lutein, respectively. Both pigments are bound to proteins that occur in crystalline form in the yolk platelet. The major blue pigment is biliverdin IX α. The eggs vary in color from brilliant blue to pale yellow-green depending on the amount of each pigment. These pigments may provide protective coloration to the eggs.*

While studying the lipid composition of the eggs and embryos of the Mexican leaf frog, *Agalychnis dacnicolor* (*1*), we observed that their green coloration was due to the presence of two pigments, one blue and one yellow, which together produce blue, blue-green, or yellow-green eggs. We have now identified the major blue pigment as biliverdin IX α and the major yellow pigment as lutein. The presence of the latter pigment is not surprising since lutein is widely distributed among plants and animals (*2*). Biliverdin occurs less often as a pigment, although it has been found in the dog placenta, in the shells of bird eggs, in the skin of fishes and amphibians (*2, 3*), in the eggs and larvae of the tobacco hornworm (*4*), and in the serum and eggs of *Xenopus* (*5*). It seems likely that the utilization of these two pigments by *A. dacnicolor* evolved as a mechanism for producing green eggs. The green coloration of leaf frog eggs, which are laid on green vegetation, may afford camouflage to protect eggs and embryos from predation. However, as far as we can ascertain, there have been no definitive studies on the adaptive value of green eggs, although the ecological implications deriving from a two-pigment system for egg coloration are apparent.

Six different batches of *A. dacnicolor* eggs (100 to 250 eggs) varying in color from brilliant blue to yellow-green were extracted with a 1:1 mixture of chloroform and methanol and a mixture of acetone and hydrochloric acid to obtain the yellow and blue pigments. The pigments were separated by column chromatography on silicic acid. Chloroform eluted the yellow pigment, and acetone eluted the blue pigment. The pigments were further purified by preparative thin-layer chromatography (TLC). The yellow and blue pigments were localized in lipid-rich yolk platelets.

Yolk platelets, which were pale blue-green or pale yellow, were obtained by collagenase treatment of homogenized eggs, followed by differential centrifugation. Analysis by light microscopy of the isolated fresh yolk platelets revealed rounded rectangular platelets of different sizes, and electron microscopy showed that the platelets consisted of closely stacked crystalline arrays about 70 Å thick.

The ultraviolet to visible spectra of the silicic acid column–purified pigments from different eggs are given in Fig. 1, a and b. The blue pigment has major bands at 372 to 376 nm and 640 to 690 nm. The yellow pigments have major bands at 442 to 444 nm and 470 to 471 nm. The relative amount of the yellow and blue pigments in the various eggs was determined by the ratio of the absorbance at 442 nm to that at 650 nm. This ratio was correlated with the color of the egg. The ratio of brilliant blue eggs was 1.15, that of blue eggs was 1.7 to 2.3, that of green eggs was 3.4 to 3.6, and that of yellow-green eggs was 10.4.

The blue pigment has properties consistent with a biliverdin. Both the blue pigment and biliverdin (Sigma) were converted to methyl esters by treatment with methanolic HCl (Supelco). The dimethyl esters were purified by preparative TLC (Merck-Darmstadt silica gel 60 plates) using chloroform and methanol 9:1. Both had identical relative mobility (R_F) values of 0.62, and gave a purple

Molecular Cell, Vol. 4, 915–924, December, 1999, Copyright ©1999 by Cell Press

Selective Requirement for Src Kinases during VEGF-Induced Angiogenesis and Vascular Permeability

Brian P. Eliceiri,* Robert Paul,*
Pamela L. Schwartzberg,† John D. Hood,*
Jie Leng,* and David A. Cheresh*‡
*Departments of Immunology and Vascular Biology
The Scripps Research Institute
10550 North Torrey Pines Road
La Jolla, California 92037
†The National Human Genome Research Institute
National Institutes of Health
Bethesda, Maryland 20892

Summary

Src kinase activity was found to protect endothelial cells from apoptosis during vascular endothelial growth factor (VEGF)–, but not basic fibroblast growth factor (bFGF)–, mediated angiogenesis in chick embryos and mice. In fact, retroviral targeting of kinase-deleted Src to tumor-associated blood vessels suppressed angiogenesis and the growth of a VEGF-producing tumor. Although mice lacking individual Src family kinases (SFKs) showed normal angiogenesis, mice deficient in $pp60^{c\text{-}src}$ or $pp62^{c\text{-}yes}$ showed no VEGF-induced vascular permeability (VP), yet $fyn^{-/-}$ mice displayed normal VP. In contrast, inflammation-mediated VP appeared normal in Src-deficient mice. Therefore, VEGF-, but not bFGF-, mediated angiogenesis requires SFK activity in general, whereas the VP activity of VEGF specifically depends on the SFKs, Src, or Yes.

Introduction

Src Family Kinase

SFKs are important signaling molecules that respond to a wide range of stimuli including growth factors (Twamley-Stein et al., 1993; Broome and Hunter, 1996) and adhesion proteins in the extracellular matrix (Kaplan et al., 1994; Schwartz et al., 1995; Thomas and Brugge, 1997; Klinghoffer et al., 1999). Once activated, SFKs affect a wide range of downstream signaling events including the activation of MAP kinases (Courtneidge et al., 1993). While in vitro studies have elucidated a role for Src in cellular function, due to mechanisms of redundancies and compensation, mice lacking a single SFK (Soriano et al., 1991; Stein et al., 1994) have provided limited insight into the biological function of this important family of nonreceptor tyrosine kinases.

Previous studies have implicated SFKs in vascular cell proliferation. For example, v-Src, an oncogenic variant of Src, is known to promote hemangioma formation in chicks (Stoker et al., 1990), suggesting that under normal circumstances, c-Src or other SFKs may regulate the growth of blood vessels. To initially address this issue, we used avian- or murine-targeted retroviral delivery systems to express mutationally active or inactive forms of Src or intact C-terminal Src kinase (Csk) to disrupt endogenous Src activity within the chick chorioallantoic membrane (CAM) or mouse skin to directly evaluate the general role of Src kinases during angiogenesis. Evidence is provided here that Src kinase is required for VEGF-, but not bFGF-, mediated angiogenesis in both the chick embryo and the mouse. In fact, Src kinase activity was found to be required for endothelial cell survival during VEGF-mediated angiogenesis. While VEGF is an endothelial cell mitogen (Ferrara and Davis-Smyth, 1997), it was originally described for its vascular permeability (VP) activity (Senger et al., 1983; Connolly et al., 1989). In fact, VEGF is unique in this regard, as other growth factors such as bFGF can induce neovascularization but do not induce vascular permeability (Connolly et al., 1989; Murohara et al., 1998). An analysis of mice deficient in specific SFKs demonstrates no decrease in VEGF-dependent neovascularization but a complete ablation of its VP activity in *src*$^{-/-}$ or *yes*$^{-/-}$ mice, while *fyn*$^{-/-}$ mice show no such defect. While mice lacking Src show no VP response to VEGF, they do show a VP response to an inflammatory mediator. Therefore, multiple SFKs can serve as key signaling intermediates involved in VEGF-induced vascular proliferation, while the VP activity of this growth factor depends on Src or Yes in particular.

‡To whom correspondence should be addressed (e-mail: cheresh@scripps.edu).

Results

Src Activity Is Required for VEGF-, but Not bFGF-, Induced Angiogenesis

To establish whether endogenous Src activity was associated with growth factor–mediated angiogenesis, filter disks saturated with either bFGF or VEGF were placed on the CAM of 10-day-old chick embryos. This treatment is known to promote a robust angiogenic response as measured after 48–72 hr (Brooks et al., 1994a). Lysates of these CAMs were evaluated for Src activity by immunoprecipitating Src and measuring its ability to phosphorylate a GST–focal adhesion kinase (FAK) fusion protein in an in vitro kinase assay. At least a 2-fold increase in endogenous Src activity was detected in these lysates 120 min after the addition of either bFGF or VEGF to the CAM tissue (Figure 1A). Importantly, we observed a similar increase in Src activity 15 min after the addition of either growth factor (data not shown). To determine whether Src activity was required for angiogenesis, CAMs stimulated with either bFGF or VEGF were infected with an avian-specific retroviral vector (RCAS) containing a truncation mutant of Src lacking its C-terminal kinase domain (Src 251) (Kaplan et al., 1994). This Src 251 and similar truncation mutants have been shown to function as a dominant negative of multiple SFKs, thereby blocking signaling events downstream of growth factor receptors (Broome and Hunter, 1996; P. L. S., unpublished data). The RCAS retrovirus, when applied to CAM tissues, infects fibroblasts and endothelial cells proximal to the filter disk as determined by infecting CAMs with an RCAS–GFP vector and examination by

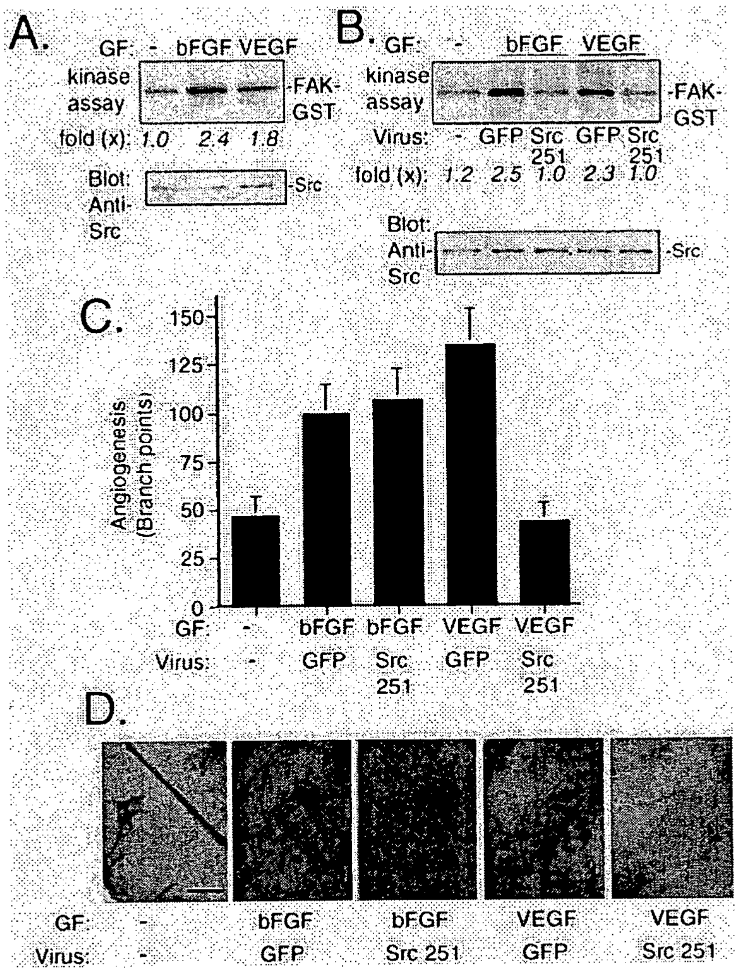

Figure 1. Activation of Endogenous Src Kinase Activity by bFGF and VEGF and the Effect of Kinase-Deleted Src on Angiogenesis In Vivo

(A) Tissue extracts of 10-day-old chick CAMs were exposed to filter paper disks saturated with bFGF or VEGF (2 μg/ml) for 2 hr. Endogenous Src was immunoprecipitated from equivalent amounts of total protein and subjected to an in vitro immune complex kinase assays with a FAK–GST fusion protein as a substrate, electrophoresed, and transferred to nitrocellulose. The relative fold increase in Src activity is indicated in italics. The above kinase assay blot was probed with an anti-Src antibody as a loading control for equivalent Src and IgG content.

(B) Chick CAMs (9 day) were exposed to filter paper disks saturated with RCAS–Src 251 (kinase deleted) or RCAS–GFP containing retroviruses or buffer for 20 hr and then incubated in the presence or absence of bFGF or VEGF for an additional 72 hr. Tissue extracts of these CAMs were examined for endogenous Src activity by in vitro immune complex kinase assay as described above using FAK–GST as a substrate.

(C) The level of angiogenesis was quantified in embryos incubated with RCAS–Src251 or RCAS–GFP followed by stimulation with either bFGF or VEGF as described above. Blood vessels were enumerated by counting blood vessel branch points in a double blinded manner. Each bar represents the mean ± SEM of three replicates.

(D) Micrographs of representative CAMs were taken with an Olympus stereomicroscope. Scale bar, 350 μm.

confocal microscopy (data not shown). Delivery of this kinase-deleted Src completely disrupted endogenous Src kinase activity in these tissues induced with either growth factor (Figure 1B).

To examine the role of Src in angiogenesis, CAMs stimulated with either bFGF or VEGF were infected with the Src 251–containing retrovirus. As shown in Figure 1C, angiogenesis, as measured 72 hr after stimulation with VEGF, was suppressed by delivery of Src 251; however, to our surprise, bFGF-induced angiogenesis was not affected. Importantly, equivalent levels of viral infection were detected in VEGF- and bFGF-stimulated CAMs as measured by epifluorescence and immunoblot analysis of GFP and Src 251, respectively (data not shown). The inhibition of VEGF-induced angiogenesis by kinase-deleted Src was likely due to a direct effect on endothelial cells, since VEGF is a known endothelial cell-specific mitogen. In addition, the failure of Src 251 to disrupt bFGF-induced angiogenesis indicates that the effects on VEGF-mediated angiogenesis are not due to general toxicity. Together, these results demonstrate that, while both bFGF and VEGF can activate Src kinase in these tissues, only VEGF-induced blood vessel formation required this activity. These findings support the recent reports that VEGF and bFGF stimulate distinct pathways of angiogenesis (Friedlander et al., 1995; Ziche et al., 1997).

Suppression of Human Tumor Growth by Targeting the Tumor Vascular Compartment with Retroviral Delivery of Src 251

Tumor growth depends on angiogenesis (Weidner et al., 1991; Folkman and Shing, 1992; Brooks et al., 1994b). In fact, recent reports suggest that tumor growth is susceptible to the antiangiogenic effects of VEGF receptor antagonists (Kim et al., 1993). Therefore, experiments were designed to determine whether suppression of angiogenesis by delivery of kinase-deleted Src 251 would influence the growth of a human medulloblastoma (DAOY), a highly angiogenic tumor known to produce VEGF and very little bFGF (data not shown). This human tumor readily grows on the CAM and produces an active angiogenic response (Figure 2), allowing us to selectively target the tumor vasculature by using the avian-specific RCAS retrovirus, without infecting the human medulloblastoma cells. Delivery of RCAS containing Src 251 to preestablished medulloblastomas resulted in a selective expression of the virus in the tumor-associated

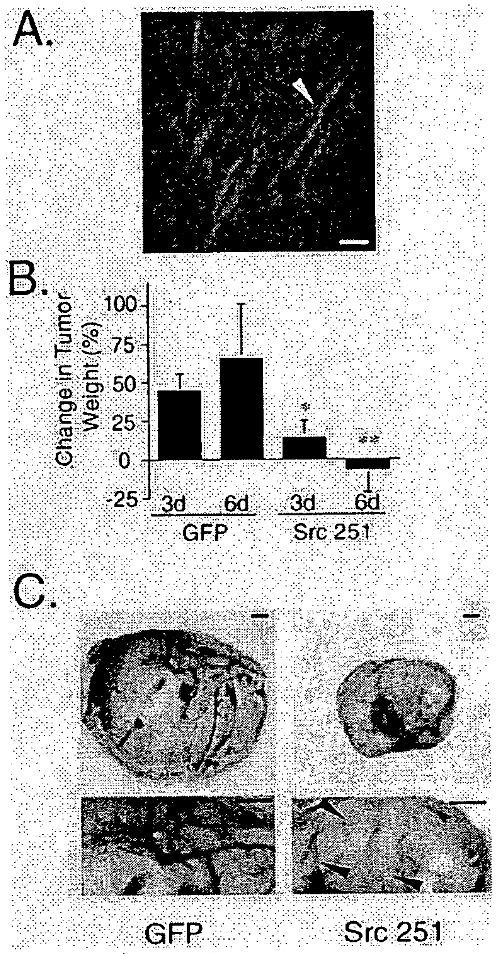

Figure 2. Retroviral Delivery of RCAS–Src 251 to Human Tumors Growing on the Chick CAM Reverses Tumor Growth

(A) Human DAOY medulloblastomas, which express VEGF, were grown on the CAM of chick embryos as described in the Experimental Procedures. Retrovirus containing RCAS–GFP or RCAS–Src 251 was topically applied to preestablished tumors of greater than 50 mg. A representative micrograph of a medulloblastoma tumor fragment infected with RCAS–GFP expressing GFP reveals exclusive expression in the tumor blood vessels (arrowhead) as detected by optical sectioning with a Bio-Rad 1024 laser confocal scanning microscope. Scale bar, 500 μm.

(B) Tumors treated as above were allowed to grow for 3 or 6 days, after which they were resected and wet weights were determined. Data are expressed as the mean change in tumor weight (from the 50 mg tumor starting weight) ± SEM of two replicates. RCAS–Src 251 had a significant impact on tumor growth after 3 days (*$p < 0.002$) and 6 days (**$p < 0.05$).

(C) Representative stereomicrographs of medulloblastoma tumors surgically removed from the embryos were taken with an Olympus stereomicroscope (scale bar, 350 μm). (Lower panel) A high magnification micrograph of each tumor showing the vasculature in detail (scale bar, 350 μm). The arrowhead indicates blood vessel disruption in RCAS–Src 251–treated tumors.

blood vessels (Figure 2A), which led to a complete suppression of tumor growth (Figure 2B). Importantly, the tumor-associated blood vessels in animals treated with virus containing Src 251 were severely disrupted and fewer in number compared to the tumor vessels in control animals (Figure 2C). The fact that RCAS-GFP-infected tumors showed GFP localization only in the tumor vasculature suggests that the antitumor effects observed with retrovirally delivered Src 251 were due to its targeting and antiangiogenic properties.

Src Requirement for Endothelial Cell Survival during VEGF-, but Not bFGF-, Mediated Angiogenesis

Recent evidence suggests that growth factor receptors (Choi and Ballermann, 1995; Satake et al., 1998) and integrins (Meredith et al., 1993; Brooks et al., 1994a) promote survival of angiogenic endothelial cells. The fact that both growth factors and adhesion receptors also regulate Src activity prompted us to examine the role of Src in endothelial cell survival during angiogenesis. Furthermore, the Src 251 mutant has been found to induce apoptosis in selective cell types during bone development (P. L. S., L. Xing, and B. Boyce, unpublished data). CAMs stimulated with either bFGF or VEGF were infected with retrovirus containing Src 251, and cryostat sections of these tissues were examined for the presence of apoptotic cells. As shown in Figure 3A, delivery of Src 251 promoted extensive TUNEL staining among the factor VIII–related antigen (von Willebrand factor [vWf]) positive blood vessels in VEGF-, but not bFGF-, stimulated CAMS. In fact, minimal apoptosis was observed among other cell types in these CAMs (Figure 3), suggesting an endothelial cell-specific requirement for Src kinase activity for cell survival in VEGF-activated blood vessels. In a second series of experiments, retrovirus-infected CAMs stimulated with VEGF or bFGF were subjected to limited collagenase digestion to prepare a single cell suspension. These CAM-derived cells were shown to contain approximately 20%–50% endothelial cells (vWf positive) (Figures 3C and 3D) and analyzed for apoptosis by flow cytometric detection of annexin V–positive cells, an early apoptosis marker. As shown in Figure 3B, cells derived from VEGF-stimulated CAMs infected with Src 251 had significantly increased annexin V staining relative to cells from mock RCAS-GFP-infected CAMs treated with VEGF. In contrast, cells derived from mock-infected CAMs or those infected with RCAS–Src 251 and stimulated with bFGF exhibited little or no annexin V staining (data not shown). In addition, no annexin V staining was detected among cells derived from nonstimulated or bFGF-stimulated CAMs (data not shown). These data demonstrate that Src kinase activity is selectively required for endothelial cell survival during VEGF, but not bFGF-mediated angiogenesis in the CAM.

Selective Requirement for Src Kinase Activity in a Subcutaneous Murine Model of Angiogenesis

To further analyze the role of Src in angiogenesis, a murine model was employed. In this case, angiogenesis was induced by subcutaneous injection of growth factor–depleted Matrigel supplemented with either bFGF (400 ng/ml) or VEGF (400 ng/ml) in athymic wehi (nu/nu) adult mice and analyzed after 5 days (Passaniti et al., 1992). Angiogenesis was quantitated by removing and extracting the angiogenic tissue and then subjecting the

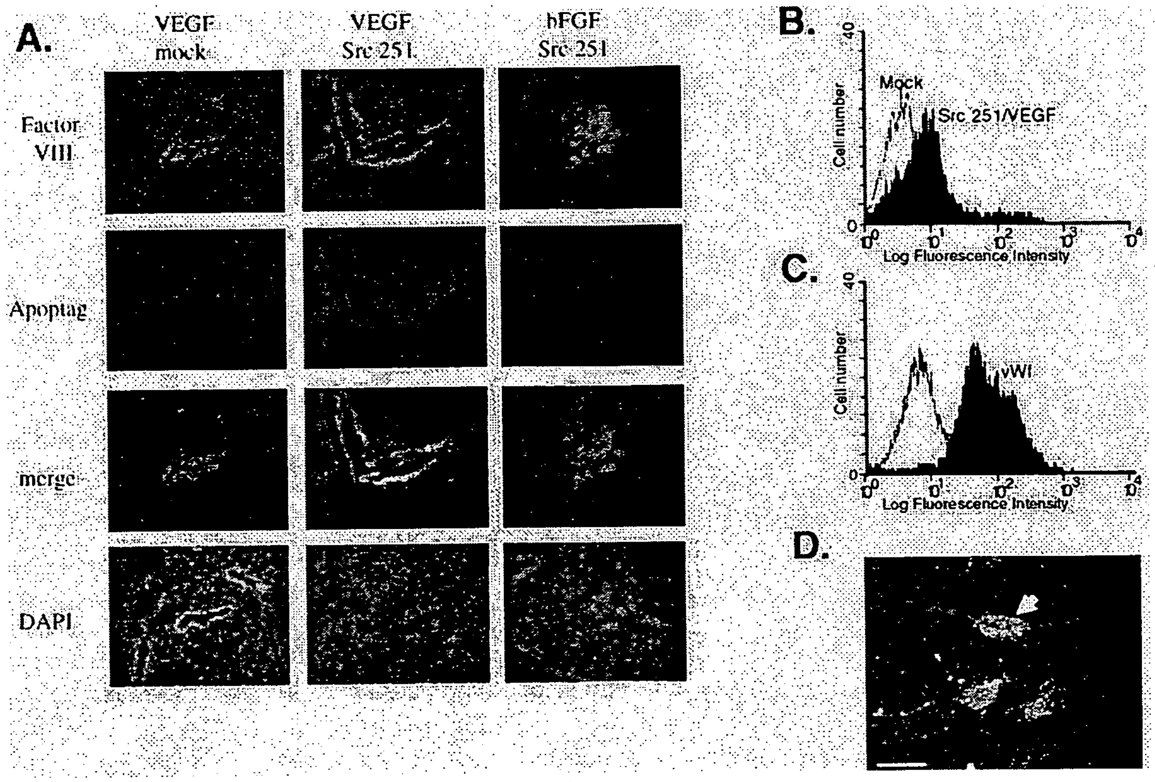

Figure 3. Apoptosis in VEGF-Stimulated Blood Vessels Expressing Src 251

(A) Immunolocalization of factor VIII–related antigen (von Willebrand factor), apoptag immunostaining of apoptotic cells, and nuclear staining with DAPI in cryosections of CAMs expressing RCAS–Src 251 or RCAS–GFP, after stimulation with bFGF or VEGF as described in Figure 1. The merge represents an overlay of the factor VIII staining and apoptag staining. The fluorescence from the GFP was not preserved in the fixation protocol used for the indirect immunofluorescence in these experiments. These micrographs were representative of blood vessel staining in duplicate samples. Scale bar, 50 μm.

(B) Apoptotic cells were identified by annexin V staining of RCAS–Src 251–infected CAMS treated with VEGF and detected by flow cytometry. Collagenase-dissociated cells isolated from RCAS–Src 251– (black) or RCAS-GFP- (mock, white) infected CAMs treated with VEGF, as described in Figure 1, were incubated with annexin V. The fluorescence from the GFP was not detected in these assays, and the FACS profile was similar to untreated controls. The flow cytometry data for each experiment was representative of at least three replicates.

(C) Anti-vWf staining was detected with a FITC-labeled secondary antibody used to identify endothelial cells by flow cytometry, and this was compared to parallel collagenase-dissociated untreated CAM cells incubated without primary antibody.

(D) Immunolocalization of endogenous von Willebrand factor in collagenase-dissociated untreated permeabilized CAM cells (arrowhead) replated on 3 μg/ml collagen and detected with a fluorescent secondary antibody (bar, 10 μm).

lysates to immunoblotting with a VEGF receptor antibody (flk-1) (Figure 4A) that is specific for endothelial cells. As observed in the chick, expression of the kinase-deleted Src 251 cDNA blocked VEGF-induced angiogenesis in this murine model while having no effect on bFGF-induced angiogenesis (Figure 4B). To establish the role of endogenous Src in this model, tissues were infected with a retrovirus expressing Csk that inhibits endogenous Src activity by phosphorylation of the C-terminal regulatory site (Nada et al., 1991). Expression of Csk blocked VEGF-, but not bFGF-, induced angiogenesis (Figure 4), confirming a role for endogenous Src activity in VEGF-mediated angiogenesis. Neovascularization of these virus-infected VEGF-stimulated tissues was confirmed by direct immunofluorescence with a FITC-conjugated anti-CD34 antibody (Figure 4) or an anti-flk-1 antibody (data not shown) and quantitated by enumerating the number of positively stained CD34 blood vessels in each cryosection (Figure 4C).

The Effect of Intradermal Expression of VEGF in *src*$^{-/-}$ or *src*$^{+/-}$ Mice Ears

To extend the observations made in the chicken and mouse angiogenesis models, a direct genetic approach was employed to examine intradermal VEGF-induced angiogenesis in *src*$^{-/-}$ mice. We also considered the fact that VEGF both initiates new blood vessel growth and can promote vascular permeability (Senger et al., 1983; Ferrara and Davis-Smyth, 1997). Intradermal injections of adenovirus expressing a human VEGF cDNA were performed in the ear of *src*$^{+/-}$ and *src*$^{-/-}$, while control β-galactosidase expressing adenovirus was injected into the opposite ear of each mouse. VEGF-dependent

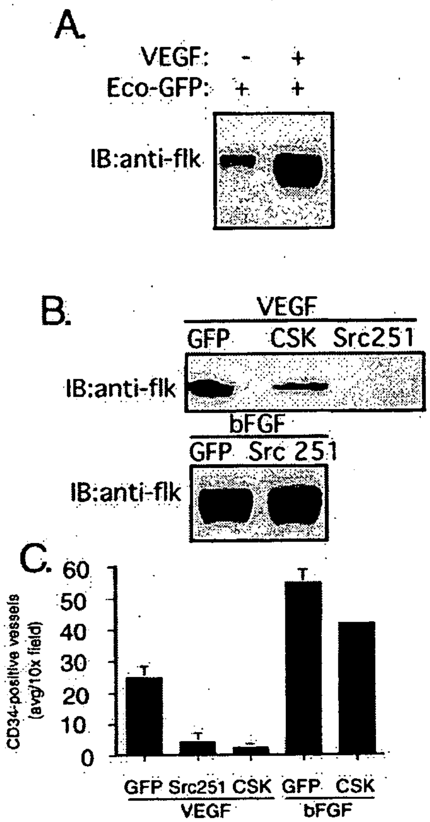

Figure 4. Retroviral Delivery of Src 251 and Csk in a Subcutaneous Murine Angiogenesis Model

(A) Angiogenesis was induced by a subcutaneous injection of growth factor-depleted Matrigel containing saline or VEGF (400 ng/ml) with 2×10^6 ecotropic packaging cells expressing GFP retrovirus in the flank of athymic wehi (nu/nu) mice and analyzed after 5 days of incubation. The neovascularization was quantitated by immunoblotting with a VEGF receptor antibody (flk-1) that is specific for endothelial cells.

(B) The effects of kinase-deleted Src 251, Csk, or GFP retrovirus on VEGF- (400 ng/ml) or bFGF- (400 ng/ml) induced angiogenesis was analyzed by immunoblotting the tissue lysates with an anti-flk-1 antibody.

(C) The effect of the Src 251– and Csk-expressing retroviruses on VEGF-induced neovascularization was quantified by enumerating the number of CD34 positive vessels in tissue cross sections by indirect immunofluorescence in triplicate random fields at 20× as described in the Experimental Procedures.

new blood vessel growth in $src^{+/-}$ ears was first detectable within 48 hr, and neovascularization was analyzed after 5 days (Figure 5A). There were identical viral expression levels in $src^{+/-}$ and $src^{-/-}$ as determined by X-gal staining of β-galactosidase-adenovirus injected ears (data not shown). In VEGF-injected $src^{-/-}$ ears, there was no significant decrease in angiogenesis (data not shown) as measured by counting branch points ($p < 0.05$). However, the most apparent phenotype in these animals was the complete blockade in the vascular leakage compared to the VEGF-injected $src^{+/-}$ ears. Representative ears injected with VEGF are shown in Figure 5A, which confirms the extent of the vascular leakage in $src^{+/-}$ mice that is essentially absent in the $src^{-/-}$ mice. The vascular leakage in these animals suggested that the VP activity, which has been associated with angiogenesis in vivo (Dvorak et al., 1995), could be selectively disrupted in pp60$^{c\text{-}src}$-deficient mice.

VEGF Fails to Compromise the Blood–Brain Barrier in Mice Lacking pp60$^{c\text{-}src}$

The brain vasculature is characterized by a highly restrictive blood–brain barrier that prohibits small molecules from extravasating into the surrounding brain tissue. Tumor growth within the brain can compromise this barrier due in part to the production of angiogenic growth factors such as VEGF. Therefore, we examined the nature of the blood–brain barrier in $src^{+/-}$ or $src^{-/-}$ mice. In this case, VEGF or saline was stereotactically injected into the right or left hemisphere of the brain, respectively. All mice received systemic injections of Evan's blue to monitor VP activity. As shown in Figure 5B, vascular leakage of blood was localized to the VEGF-injected hemisphere in $src^{+/-}$ mice, but there a complete absence of vascular leakage in $src^{-/-}$ mice. This was also the case when examining the VP by measuring the accumulation of Evan's blue dye as detected by epifluorescence analysis of cryostat sections of these brains (Figure 5C). Thus, VEGF compromises the blood–brain barrier in a manner that depends on pp60$^{c\text{-}src}$.

VEGF-Mediated VP, but Not Inflammation-Associated VP, Depends on pp60$^{c\text{-}src}$

To further analyze and quantitate the effect of VEGF as a VP factor in $src^{+/-}$ or $src^{-/-}$ mice, we used the Miles assay (Miles and Miles, 1952) to quantitatively measure the vascular permeability in the skin of these animals. VEGF was injected intradermally in $src^{+/-}$ or $src^{-/-}$ mice that had received an intravenous systemic administration of Evan's blue dye. Within 15 min after injection of VEGF, there was a 3-fold increase in VP in $src^{+/-}$. However, in $src^{-/-}$ mice, we observed no detectable VP activity (Figures 6A and 6B). Dye elution of the injected skin patches was quantitated and compared with control saline and bFGF (Figure 6B, left panel). bFGF or saline controls injected adjacent to the VEGF showed no significant increase in VP.

Vascular leakage/permeability is also known to occur during inflammation, which allows for the accumulation of serum-associated adhesive protein and inflammatory cells in tissues. In fact, inflammatory mediators themselves directly promote vascular leakage. Therefore, we tested one such inflammatory mediator, allyl isothiocyanate, also known as mustard oil (Inoue et al., 1997), in $src^{+/-}$ or $src^{-/-}$ mice for its capacity to produce VP. Unlike that observed in VEGF-stimulated $src^{-/-}$ animals, we detected no decrease in the VP produced by injection of the inflammatory mediator allyl isothiocyanate (Figure 6B, right panel). Thus, we conclude that Src plays a selective role in the VP activity induced with VEGF and does not influence VP associated with the inflammatory process.

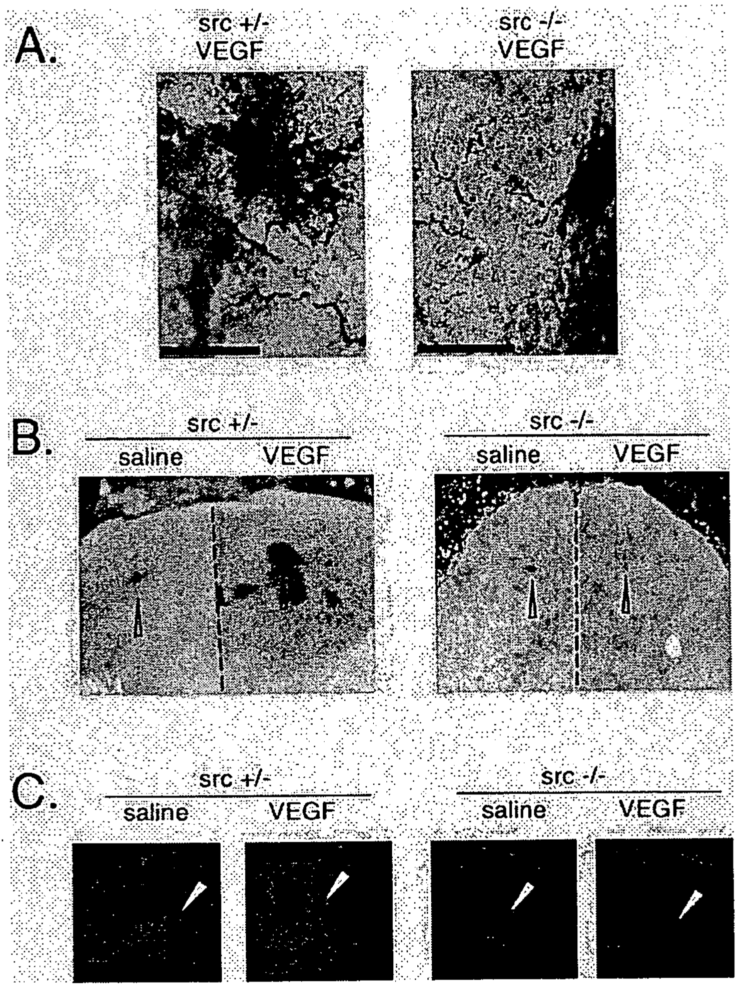

Figure 5. The Effect of VEGF-Induced Vascular Leakage in the Ears and Brains of $src^{-/-}$ and $src^{+/-}$ Mice

(A) Gene delivery of the human VEGF cDNA in an adenovirus vector was injected intradermally in the right ear of $src^{+/-}$ or $src^{-/-}$ mice, and the neovascularization of the ears were photographed after 5 days of expression. Adenovirus expressing β-galactosidase was injected into the left ears as a negative control. Staining for β-galactosidase in these ears confirmed similar adenovirus expression in each genetic background. Scale bar, 1 mm; n = 4.

(B) VEGF or saline was stereotactically injected into the left or right frontal lobes, respectively, of $src^{+/-}$ or $src^{-/-}$. After injection with Evan's blue and perfusion, the brains were removed and photographed with a stereoscope (6×, final magnification; arrowhead, injection site).

(C) Cross sections of the above VEGF- or saline-injected brains from $src^{+/-}$ or $src^{-/-}$ mice were prepared and analyzed for VEGF-induced VP by confocal microscopy to visualize the fluorescence of the extravasated Evan's blue (6×, final magnification; arrowhead, injection site).

VEGF-Mediated VP Activity Depends on Src and Yes but Not Fyn

We next tested the specificity of the Src requirement for VP by examining the VEGF-induced VP activity associated with SFKs such as Fyn or Yes, which, like Src, are known to be expressed in endothelial cells (Bull et al., 1994; Kiefer et al., 1994). In fact, we confirmed that these three SFKs were expressed equivalently in the aortas of wild-type mice (data not shown). Like $src^{-/-}$ mice, animals deficient in Yes were also defective in VEGF-induced VP (Figure 6C). However, to our surprise, mice lacking Fyn retained a high VP in response to VEGF that was not significantly different from control animals (Figure 6C). The disruption of VEGF-induced vascular permeability in $src^{-/-}$ or $yes^{-/-}$ mice demonstrates that the kinase activity of specific SFKs is essential for VEGF-mediated signaling event leading to VP activity but not angiogenesis.

Discussion

While multiple growth factors and adhesion events can promote angiogenesis, little is known regarding the signaling events required for the growth of new blood vessels. In this report, evidence is provided that two angiogenic growth factors, bFGF and VEGF, initiate signaling pathways that can be distinguished based on their requirement for Src kinase activity. Even though both bFGF and VEGF led to increased Src activity in angiogenic tissues, only VEGF-induced angiogenesis depended on it. This was based on studies where kinase-deleted Src or Csk was retrovirally delivered to stimulated blood vessels. The use of intact Csk was important as it blocks the activity of endogenous Src rather than acting as a dominant-negative mutant like Src 251. Src activity was found to be required for the survival of VEGF-stimulated endothelial cells in vivo.

VEGF was originally described as a vascular permeability factor secreted by tumor cells (Senger et al., 1983). Using mice deficient for specific SFKs, we demonstrated that $pp60^{c\text{-}src}$ or $pp62^{c\text{-}yes}$ are essential for VEGF-induced VP, while its angiogenic activity was not significantly influenced in these animals. Moreover, animals deficient in Fyn show no loss of VP activity demonstrating that only certain SFKs are required to regulate VEGF-mediated VP activity. Importantly, all three of

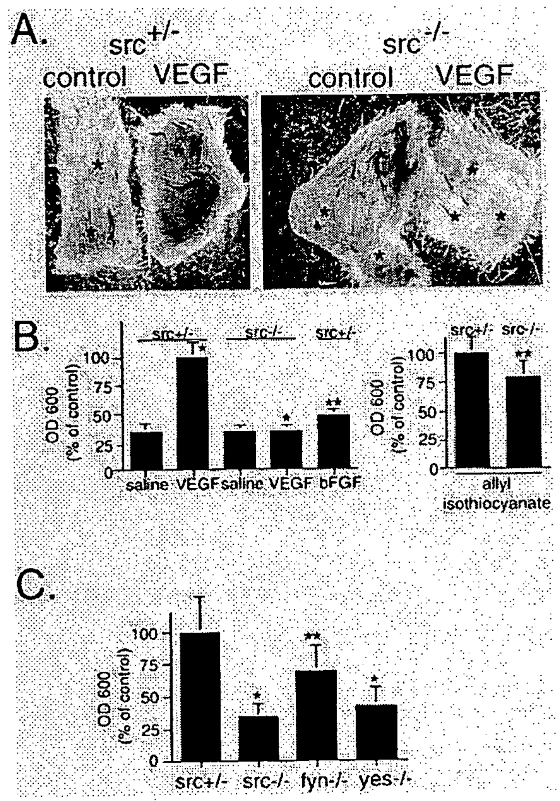

Figure 6. Miles Assay for Vascular Permeability of VEGF in the Skin of Mice Deficient in Src, Fyn, or Yes

(A) The vascular permeability properties of VEGF in the skin of $src^{+/-}$ (upper) or $src^{-/-}$ (lower) mice was determined by intradermal injection of saline or VEGF (400 ng) into mice that have been intravenously injected with Evan's blue dye. After 15 min, skin patches were photographed (scale bar, 1 mm). Arrowheads indicate the injection sites.
(B) The regions surrounding the injection sites of the VEGF, bFGF, or saline were dissected, and the permeability quantitated by elution of the Evan's blue in formamide at 56°C for 24 hr, and the absorbance measured at 600 nm (left). The ability of an inflammation mediator (allyl isothiocyanate), known to induce inflammation-related VP, was tested in $src^{+/-}$ or $src^{-/-}$ mice (right).
(C) The ability of VEGF to induce VP was compared in $src^{-/-}$, $fyn^{-/-}$, or $yes^{-/-}$ mice in the Miles assay. Data for each of the Miles assays are expressed as the mean ± SD of triplicate animals. $src^{-/-}$ and $yes^{-/-}$ VP defects compared to control animals were statistically significant (*$p < 0.05$, paired t test), whereas the VP defects in neither the VEGF-treated $fyn^{-/-}$ mice nor the allyl isothiocyanate–treated $src^{-/-}$ mice were statistically significant (**$p < 0.05$).

these SFKs were shown to be equivalently expressed in the aortas, skin, and brain of wild-type mice and are known to be expressed in endothelial cells (Bull et al., 1994; Kiefer et al., 1994). To our surprise, inflammation-induced VP was shown to be independent of Src kinase in these mice, suggesting that the VP activity induced during inflammation and that induced upon VEGF stimulation are regulated by distinct signaling pathways.

Mice lacking $pp60^{c\text{-}src}$ and $pp62^{c\text{-}yes}$ show apparently normal vascular development, even though mice lacking VEGF or its receptor die during development. Thus, VEGF-induced VP activity is not required for development. However, it may play a role in wound repair or other postnatal process. Interestingly, mice lacking the combination of Src, Yes, and Fyn or the VEGF receptor show embryonic lethality by day 9.5, a time during development that is characterized by active vasculogenesis (Fong et al., 1995; Shalaby et al., 1995). This, together with the fact that mice lacking individual SFKs develop normal appearing blood vessels, suggests that compensation can take place among these SFKs. This is supported by our observation that suppression of Src kinase activity in general by Csk or Src251 suppressed neovascularization in mice or chick embryos in response to VEGF while individual SFK knockouts develop normally.

Evidence provided in this study demonstrates that VEGF and bFGF potentiate somewhat different biological and biochemical effects during the early stages of angiogenesis. There may be a physiological rationale for the existence of two angiogenic pathways. For example, blood vessels in various organs may differ with respect to distinct ECM-associated adhesive proteins and/or growth factors. Neovascularization in the retina has been linked to VEGF expression (D'Amore, 1994; Miller et al., 1994), while that induced during cutaneous wound repair has been associated with bFGF (Takenaka et al., 1997). This may allow endothelial cells to meet the specific needs of a given tissue depending on local requirements for nutrients, oxygen, or waste elimination. After hypoxic injury, VEGF levels are known to rise immediately (reviewed in Ferrara and Davis-Smyth, 1997). Perhaps this hypoxic response facilitates an immediate increased oxygenation by providing local vascular leakage prior to the actual formation of a new vascular network. This would predict that adult $pp60^{c\text{-}src}$- or $pp62^{c\text{-}yes}$-deficient mice may be less capable of restoring oxygenation to damaged or hypoxic tissue. In fact, we noted that stereotactic injection of VEGF in the brain could compromise the blood–brain barrier in control animals. However, animals deficient in $pp60^{c\text{-}src}$ showed no breakdown of the blood–brain barrier.

VEGF is an angiogenic growth factor in many tumors. In fact, an anti-VEGF antibody (Kim et al., 1993) that blocks tumor growth in mice is being evaluated clinically in patients with late-stage cancer. Given the strong association between VEGF and tumor angiogenesis, our results may provide another approach to disrupt the growth of tumors. Thus, by using an avian-specific retrovirus, we were able to specifically target the chick vasculature of a growing human medulloblastoma. Even though the tumor cells remained uninfected by the retrovirus, we observed suppressed tumor growth demonstrating the potential therapeutic efficacy of this approach.

In a combination of experiments using retrovirally delivered mutant Src and Csk as well as a direct analyses of $src^{-/-}$ mice, we provide evidence that the Src tyrosine kinase family distinguishes two pathways of angiogenesis. During VEGF-induced angiogenesis, SFK activity contributes to endothelial cell survival. Furthermore, the VEGF-induced VP is dependent on SFKs, Src, or Yes, but not Fyn, and the VP response is specific for VEGF in contrast to inflammation-induced VP. Therefore, while SFKs serve compensatory roles during embryogenesis and angiogenesis, VEGF-, but not bFGF-, mediated angiogenesis requires Src kinase activity for endothelial

cell survival, whereas VP activity of VEGF depends on the SFKs, Src, or Yes.

Experimental Procedures

Antibodies and Reagents

A rabbit polyclonal antibody raised against amino acids 3–18 of human Src (N-16; Santa Cruz Biotechnology, Santa Cruz, CA) was used for immunoprecipitation for in vitro kinase assays, and monoclonal antibody against avian pp60^{c-src} (Upstate Biotechnology, Lake Placid, NY) was used for Western blotting as a loading control for the kinase assays. The Src constructs were obtained from Dr. H. Varmus (NIH), FAK–GST fusion protein was from Dr. D. Schlaepfer (The Scripps Research Institute [TSRI]), the DF-1 virus producer cell line was from Dr. D. Foster (Univeristy of Minnesota), the DAOY medulloblastoma cell line from Dr. W. Laug (Children's Hospital, USC, Los Angeles), RCAS-GFP was from Dr. C. Cepko (Harvard), and bFGF was kindly provided by Dr. J. Abraham (Scios, Mountain View, CA). All other reagents and media were from Sigma-Aldrich (St Louis, MO) unless otherwise stated.

Src Constructs and Retroviruses

For the studies in the chick embryo, the replication competent RCASBP(A) (Hughes et al., 1987) retrovirus was used to express mutant Src cDNAs subcloned as NotI–ClaI. These constructs were transfected into the chicken immortalized fibroblast line, DF-1. Viral supernatants were collected from DF-1 producer cell lines in serum-free CLM media. Viral supernatants were concentrated by ultracentrifugation at 4°C for 2 hr at 22,000 rpm, and the pellets were resuspended in 1/100 the original volume in serum-free media with a titer of at least 108 i.u. (infectious units)/ml and stored at −80°C.

For the retrovirus studies in the subcutaneous murine matrigel angiogenesis assay, GFP, kinase-deleted Src 251, and Csk cDNA was subcloned into the replication-defective murine Moloney retrovirus (pLNCX) vector. These constructs were transiently transfected into the ecotropic producer line to generate cell-free titers of 10^5–10^6 i.u./ml. Therefore, to increase the effective titer over the 5 day time course of the angiogenesis assay in the matrigel plug, the virus-packaging cells expressing the appropriate construct were included along in the Matrigel to increase the retrovirus infection levels.

VEGF Adenovirus

Recombinant VEGF adenovirus was generated by cloning the human VEGF cDNA from a human placenta cDNA library into pAd/Cl (J. L., A. Reddy, and D. A. C., unpublished data) and cotransfecting with pJM17 into an E1 transcomplementing 293 cell line as previously described (Bett et al., 1994). High titer virus was isolated, purified, and titered to 10^{11} pfu/ml as previously described (Chang et al., 1995). High titer clones were selected based on their expression of soluble VEGF secreted into the media of COS-7, endothelial cells, and in chick CAMs infected with the VEGF adenovirus (data not shown).

Chick Embryo Treatments

Fertilized chick embryos (standard pathogen free grade; SPAFAS, Preston, CT) were prepared, and the CAM was exposed as previously described (Eliceiri et al., 1998). For growth factor–only experiments, cortisone acetate–soaked filter disks were soaked with 250 ng of bFGF or VEGF for 2 hr before harvest. For virus experiments on the CAM, disks were soaked in 20 μl of viral stock per disk. These disks were applied to the CAM of 9 day chick embryos and incubated at 37°C for 24 hr. Then, either serum-free media or growth factors were added at a concentration of 5 μg/ml to the CAM in 20 μl of the virus stock as an additional boost of virus to the CAM tissue and incubated for an additional 72 hr. CAM assays was quantitated by counting branch points as described previously (Eliceiri et al., 1998) in triplicate samples in a double blind manner.

Immunoprecipitation and Immunoblotting

CAM tissues were homogenized in a RIPA lysis buffer, used for immunoprecipitations or immunoblots as previously described (Eliceiri et al., 1998). Anti-Src and anti-flk1 antibodies used in immunoblots were detected with horseradish peroxidase-conjugated goat anti-mouse secondary antibodies as previously described (Eliceiri et al., 1998).

In Vitro Kinase Assay for Src Kinase

The kinase activity of endogenous Src kinase was assayed by the ability of immunopurified Src to phosphorylate a FAK–GST fusion protein in an in vitro assay. Src was immunoprecipitated as described above and subjected to a kinase assay, and the samples were analyzed by 15% SDS-PAGE and quantitated as described previously (Eliceiri et al., 1998).

Immunostaining and Annexin V Labeling of Apoptotic Cells

Cryosections of CAMs treated with RCAS–GFP or RCAS–Src 251 treated with bFGF or VEGF were analyzed for apoptotic cells using the Apoptag kit (Oncor, Gaithersburg, MD). Sections were also immunostained with a rabbit polyclonal anti-vWF (Biogenix, San Ramon, CA) and counterstained with 1 μg/ml DAPI. Fluorescent images were captured with a cooled CCD camera (Roper, Trenton, NJ), and the fluorescent images were processed and exposure matched between experimental treatments as previously described (Eliceiri et al., 1998).

To measure the apoptotic index of retrovirus-infected CAM tissues, FITC-conjugated annexin V (Clontech, Palo Alto, CA) was used to stain cell suspensions, and the washed cells were analyzed by flow cytometry. Cell suspensions of CAM cells were prepared from mock- or virus-infected CAMs by digestion with 0.1% (w/v) collagenase type IV (Worthington Biochemicals, Lakewood, NJ) in RPMI 1640 of minced CAM tissue rocking for 1 hr at 37°C as previously described (Brooks et al., 1994b) and filtered through 100 μM nylon mesh (Becton Dickinson, Fountain Lakes, NJ). Fluorescence was measured with a FACscan flow cytometer (Becton Dickinson) to count 10,000 cells.

Measurement of vWf staining by FACS was performed with parallel collagenase digested CAM tissue cell preparations, that were fixed in 1.6% paraformaldehyde, permeabilized in 70% ethanol, incubated the anti-vWf antibody, and detected with a FITC-conjugated secondary antibody.

Tumor Growth Assay

The 3 and 6 day DAOY medulloblastoma tumor growth assays were performed in the chick CAM essentially as previously described (Brooks et al., 1994b). DAOY cells (5 × 10^6) were seeded on the CAM of a 10 day embryo. After 7 days, 50 mg tumor fragments were dissected and reseeded on another 10 day embryo and incubated for another 3 or 6 days with the topical application (25 μl) of either control RCAS–GFP retrovirus, RCAS–Src 251, or mock treatment. Tumor resections and weighing were performed in a double blind manner removing only the easily definable solid tumor mass (Brooks et al., 1994b). The wet tumor weights after 3 or 6 days were compared with initial weight, and the percent change of tumor weight was determined for each group.

Immunofluorescence and Microscopy

Cryosections of the plugs were also subjected to immunofluorescent staining with an anti-CD34 antibody or an anti-flk antibody, photographed, and quantitated as described above for the CAM angiogenesis assays.

Whole-mount direct fluorescence of RCAS-GFP-infected tumor fragment was accomplished by dissecting a tumor fragment and imaging the unfixed tissue directly on a slide with a laser confocal microscope (MRC 1024; Bio-Rad, Hercules, CA).

Murine Matrigel Angiogenesis Assay

Growth factor–depleted Matrigel (Becton Dickinson) (400 μl) supplemented with PBS, bFGF (400 ng/ml), or VEGF (400 ng/ml) (Passaniti et al., 1992) and murine-specific ecotropic packaging cells (ϕNX-Eco; G. Nolan, Stanford) producing retrovirus expressing GFP, Src 251, or Csk cDNAs was injected subcutaneously in 6-week-old male athymic wehi (nu/nu) mice. The plugs remained palpable for 5 days, facilitating a direct resection of the plug for further analysis by immunoblotting of plug homogenates or immunostaining of plug cryosections. The accuracy of the quantitative methods was confirmed by spectrophotometric analysis of homogenates of plugs from animals

that had been intravenously injected with FITC-labeled lectin (J. D. H. and D. A. C., unpublished data).

Intradermal Ear Injections and Miles Assay

$pp60^{c-src}$-, $pp59^{c-fyn}$-, and $pp62^{c-yes}$-deficient mice (129/Sv/Ev × C57Bl6/J) were generated as previously described (Soriano et al., 1991) and were the generous gift of Drs. P. Soriano and P. Stein. Additional stocks were obtained from Jackson Labs. Mouse ears were injected intradermally (Eriksson et al., 1980) with 5 μl of adenovirus expressing either VEGF or β-galactosidase and the ears photographed after 5 days with a stereoscope.

The Miles assay (Miles and Miles, 1952) was adapted for mice by injecting 10 μl of VEGF (400 ng/ml), allyl isothiocyanate (mustard oil, 20% v/v in mineral oil), or saline intradermally into mice that had previously been intravenously injected with 100 μl of 0.5% Evan's blue. After 15 min, the skin patches were dissected, photographed, and eluted at 56°C with formalin and quantitated with a spectrophotometer (OD_{600}).

Intracerebral Injection and Determination of Blood–Brain Barrier Disruption

Saline or VEGF (200 ng in 2 μl) was injected stereotactically into the left or right frontal lobe 92 mm to the left/right of the midline, 0.5 mm rostral from bregma, and 3 mm in depth from the dura, respectively. The animals received an Evan's blue solution intravenously 30 min after injection, as described above. After an additional 30 min, the mice were perfused and the brains were removed. Evan's blue fluorescence was observed using confocal laser microscopy of fresh unfixed cryosections of the brain.

Acknowledgments

We thank Tessa Brodhag and Catherine Andrews for expert technical assistance and Drs. Harold Varmus, Peter K. Vogt, and Bing Jiang for helpful discussions, Dr. K. Spencer (TSRI) for the anti-vWF immunofluorescence, R. Xiang and C. Dolman for intravenous injections (TSRI), Archana Reddy for the VEGF adenovirus (TSRI), and Ana Venegas (NIH) for assistance with mouse breeding. We also thank Drs. R. Reisfeld (TSRI) and H. Varmus (NIH) for critical reading of this manuscript. Chick CAM and mouse experiments were conducted in accordance with institutional and NIH guidelines. B. P. E. was supported by an NIH NRSA postdoctoral fellowship (1F32HL09435), R. P. by Deutsche Forschungs Gemeinschaft Pa 749/1–1, J. D. H. by an NIH training grant (1T32CA75924), J. L. by an Army Breast Cancer Program (DAMD179616104), and D. A. C. by grants CA50286, CA45726, HL54444, and P01 CA78045 from the NIH. This is manuscript 11851-IMM from The Scripps Research Institute.

Received June 30, 1999; revised September 30, 1999.

References

Bett, A.J., Haddara, W., Prevec, L., and Graham, F.L. (1994). An efficient and flexible system for construction of adenovirus vectors with insertions or deletions in early regions 1 and 3. Proc. Natl. Acad. Sci. USA *91*, 8802–8806.

Brooks, P.C., Clark, R.A., and Cheresh, D.A. (1994a). Requirement of vascular integrin αVβ3 for angiogenesis. Science *264*, 569–571.

Brooks, P.C., Montgomery, A.M., Rosenfeld, M., Reisfeld, R.A., Hu, T., Klier, G., and Cheresh, D.A. (1994b). Integrin αVβ3 antagonists promote tumor regression by inducing apoptosis of angiogenic blood vessels. Cell *79*, 1157–1164.

Broome, M.A., and Hunter, T. (1996). Requirement for c-Src catalytic activity and the SH3 domain in platelet-derived growth factor BB and epidermal growth factor mitogenic signaling. J. Biol. Chem. *271*, 16798–16806.

Bull, H.A., Brickell, P.M., and Dowd, P.M. (1994). Src-related protein tyrosine kinases are physically associated with the surface antigen CD36 in human dermal microvascular endothelial cells. FEBS Lett. *351*, 41–44.

Chang, M.W., Barr, E., Lu, M.M., Barton, K., and Leiden, J.M. (1995). Adenovirus-mediated over-expression of the cyclin/cyclin-dependent kinase inhibitor, p21 inhibits vascular smooth muscle cell proliferation and neointima formation in the rat carotid artery model of balloon angioplasty. J. Clin. Invest. *96*, 2260–2268.

Choi, M.E., and Ballermann, B.J. (1995). Inhibition of capillary morphogenesis and associated apoptosis by dominant negative mutant transforming growth factor-β receptors. J. Biol. Chem. *270*, 21144–21150.

Connolly, D.T., Heuvelman, D.M., Nelson, R., Olander, J.V., Eppley, B.L., Delfino, J.J., Siegel, N.R., Leimgruber, R.M., and Feder, J. (1989). Tumor vascular permeability factor stimulates endothelial cell growth and angiogenesis. J. Clin. Invest. *84*, 1470–1478.

Courtneidge, S.A., Fumagalli, S., Koegl, M., Superti-Furga, G., and Twamley-Stein, G.M. (1993). The Src family of protein tyrosine kinases: regulation and functions. Dev. Suppl., 57–64.

D'Amore, P.A. (1994). Mechanisms of retinal and choroidal neovascularization. Invest. Ophthalmol. Vis. Sci. *35*, 3974–3979.

Dvorak, H.F., Brown, L.F., Detmar, M., and Dvorak, A.M. (1995). Vascular permeability factor/vascular endothelial growth factor, microvascular hyperpermeability, and angiogenesis. Am. J. Pathol. *146*, 1029–1039.

Eliceiri, B.P., Klemke, R., Stromblad, S., and Cheresh, D.A. (1998). Integrin αvβ3 requirement for sustained mitogen-activated protein kinase activity during angiogenesis. J. Cell. Biol. *140*, 1255–1263.

Eriksson, E., Boykin, J.V., and Pittman, R.N. (1980). Method for in vivo microscopy of the cutaneous microcirculation of the hairless mouse ear. Microvasc. Res. *19*, 374–379.

Folkman, J., and Shing, Y. (1992). Angiogenesis. J. Biol. Chem. *267*, 10931–10934.

Fong, G.H., Rossant, J., Gertsenstein, M., and Breitman, M.L. (1995). Role of the Flt-1 receptor tyrosine kinase in regulating the assembly of vascular endothelium. Nature *376*, 66–70.

Ferrara, N., and Davis-Smyth, T. (1997). The biology of vascular endothelial growth factor. Endocr. Rev. *18*, 4–25.

Friedlander, M., Brooks, P.C., Shaffer, R.W., Kincaid, C.M., Varner, J.A., and Cheresh, D.A. (1995). Definition of two angiogenic pathways by distinct αv integrins. Science *270*, 1500–1502.

Hughes, S.H., Greenhouse, J.J., Petropoulos, C.J., and Sutrave, P. (1987). Adaptor plasmids simplify the insertion of foreign DNA into helper-independent retroviral vectors. J. Virol. *61*, 3004–3012.

Inoue, H., Asaka, T., Nagata, N., and Koshihara, Y. (1997). Mechanism of mustard oil–induced skin inflammation in mice. Eur. J. Pharmacol. *333*, 231–240.

Kaplan, K.B., Bibbins, K.B., Swedlow, J.R., Arnaud, M., Morgan, D.O., and Varmus, H.E. (1994). Association of the amino-terminal half of c-Src with focal adhesions alters their properties and is regulated by phosphorylation of tyrosine 527. EMBO J. *13*, 4745–4756.

Kiefer, F., Anhauser, I., Soriano, P., Aguzzi, A., Courtneidge, S.A., and Wagner, E.F. (1994). Endothelial cell transformation by polyomavirus middle T antigen in mice lacking Src-related kinases. Curr. Biol. *4*, 100–109.

Kim, K.J., Li, B., Winer, J., Armanini, M., Gillett, N., Phillips, H.S., and Ferrara, N. (1993). Inhibition of vascular endothelial growth factor-induced angiogenesis suppresses tumour growth in vivo. Nature *362*, 841–844.

Klinghoffer, R.A., Sachsenmaier, C., Cooper, J.A., and Soriano, P. (1999). Src family kinases are required for integrin but not PDGFR signal transduction. EMBO J. *18*, 2459–2471.

Meredith, J.E., Jr., Fazeli, B., and Schwartz, M.A. (1993). The extracellular matrix as a cell survival factor. Mol. Biol. Cell *4*, 953–961.

Miles, A.A., and Miles, E.M. (1952). Vascular reactions to histamine, histamine-liberator and leukotaxine in the skin of guinea pigs. J. Physiol. *118*, 228–257.

Miller, J.W., Adamis, A.P., Shima, D.T., D'Amore, P.A., Moulton, R.S., O'Reilly, M.S., Folkman, J., Dvorak, H.F., Brown, L.F., Berse, B., et al. (1994). Vascular endothelial growth factor/vascular permeability factor is temporally and spatially correlated with ocular angiogenesis in a primate model. Am. J. Pathol. *145*, 574–584.

Murohara, T., Horowitz, J.R., Silver, M., Tsurumi, Y., Chen, D., Sullivan, A., and Isner, J.M. (1998). Vascular endothelial growth factor/

vascular permeability factor enhances vascular permeability via nitric oxide and prostacyclin. Circulation *97*, 99–107.

Nada, S., Okada, M., MacAuley, A., Cooper, J.A., and Nakagawa, H. (1991). Cloning of a complementary DNA for a protein-tyrosine kinase that specifically phosphorylates a negative regulatory site of $p60^{c\text{-}src}$. Nature *351*, 69–72.

Passaniti, A., Taylor, R.M., Pili, R., Guo, Y., Long, P.V., Haney, J.A., Pauly, R.R., Grant, D.S., and Martin, G.R. (1992). A simple, quantitative method for assessing angiogenesis and antiangiogenic agents using reconstituted basement membrane, heparin, and fibroblast growth factor. Lab. Invest. *67*, 519–528.

Satake, S.M., Kuzuya, M., et al. (1998). Angiogenic stimuli are essential for survival of vascular endothelial cells in three-dimensional collagen lattice. Biochem. Biophys. Res. Comm. *244*, 642–646.

Schwartz, M.A., Schaller, M.D., and Ginsberg, M.H. (1995). Integrins: emerging paradigms of signal transduction. Annu. Rev. Cell. Dev. Biol. *11*, 549–599.

Senger, D.R., Galli, S.J., Dvorak, A.M., Perruzzi, C.A., Harvey, V.S., and Dvorak, H.F. (1983). Tumor cells secrete a vascular permeability factor that promotes accumulation of ascites fluid. Science *219*, 983–985.

Shalaby, F., Rossant, J., Yamaguchi, T.P., Gertsenstein, M., Wu, X.F., Breitman, M.L., and Schuh, A.C. (1995). Failure of blood-island formation and vasculogenesis in Flk-1-deficient mice. Nature *376*, 62–66.

Soriano, P., Montgomery, C., Geske, R., and Bradley, A. (1991). Targeted disruption of the c-src proto-oncogene leads to osteopetrosis in mice. Cell *64*, 693–702.

Stein, P.L., Vogel, H., and Soriano, P. (1994). Combined deficiencies of Src, Fyn, and Yes tyrosine kinases in mutant mice. Genes Dev. *8*, 1999–2007.

Stoker, A.W., Hatier, C., and Bissell, M.J. (1990). The embryonic environment strongly attenuates v-src oncogenesis in mesenchymal and epithelial tissues, but not in endothelia. J. Cell Biol. *111*, 217–228.

Takenaka, H., Kishimoto, S., Tooyama, I., Kimura, H., and Yasuno, H. (1997). Protein expression of fibroblast growth factor receptor–1 in keratinocytes during wound healing in rat skin. J. Invest. Dermatol. *109*, 108–112.

Thomas, S.M., and Brugge, J.S. (1997). Cellular functions regulated by Src family kinases. Annu. Rev. Cell. Dev. Biol. *13*, 513–609.

Twamley-Stein, G.M., Pepperkok, R., Ansorge, W., and Courtneidge, S.A. (1993). The Src family tyrosine kinases are required for platelet-derived growth factor–mediated signal transduction in NIH 3T3 cells. Proc. Natl. Acad. Sci. USA *90*, 7696–7700.

Weidner, N., Semple, J.P., Welch, W.R., and Folkman, J. (1991). Tumor angiogenesis and metastasis—correlation in invasive breast carcinoma. N. Engl. J. Med. *324*, 1–8.

Ziche, M., Morbidelli, L., Choudhuri, R., Zhang, H.T., Donnini, S., Granger, H.J., and Bicknell, R. (1997). Nitric oxide synthase lies downstream from vascular endothelial growth factor–induced but not basic fibroblast growth factor–induced angiogenesis. J. Clin. Invest. *99*, 2625–2634.

CLIN. CHEM. 38/1, 71–75 (1992)

UK

Development of Time-Resolved Immunofluorometric Assay of Vascular Permeability Factor

Kiang-Teck Yeo, Tracy M. Sioussat, James D. Faix, Donald R. Senger, and Tet-Kin Yeo

We describe a two-site time-resolved immunofluorometric assay for guinea pig vascular permeability factor (VPF) for quantifying VPF in different biological fluids. Antibody against the carboxy terminus (C-IgG) is immobilized on microtiter wells, and antibody against the amino terminus (N-IgG) is labeled with Eu^{3+}-chelate. Line 10 tumor culture medium, known to be rich in VPF, is assayed in a two-step incubation. Bound Eu^{3+} is then quantified by dissociation into a fluorescent enhancement solution, with measurement of the time-resolved fluorescence. The analytical sensitivity is 0.35 VPF unit, and the intra-assay CV is about 20%. The assay is specific for VPF, because pre-treatment with the appropriate C- or N-peptide, or pre-extraction of VPF, greatly decreases fluorescence. The VPF immunoassay is highly correlated (r^2 = 0.94) with the Miles permeability assay, the classical bioassay of VPF. In addition, the immunofluorometric assay is about 30-fold more sensitive than the Miles assay.

Additional Keyphrases: *vascular endothelial growth factor · angiogenesis · line 10 tumor culture medium · bioassay compared*

Vascular permeability factor (VPF), which is secreted by various tumor cells, is a highly conserved protein (M_r 34 000–42 000) with potent vascular permeability-enhancing activity that causes accumulation of ascites fluid associated with tumor growth (*1, 2*).[1] In addition, recent studies have shown that VPF is similar or identical to vascular endothelial growth factor (VEGF), a mitogen specific for endothelial cells (*3–7*). Thus, tumor-secreted VPF (VEGF) may promote tumor angiogenesis directly by its mitogenic activity for endothelium. VPF (VEGF) may also elicit angiogenesis indirectly by its vascular permeability effect, which causes extravasation of plasma proteins, including fibrinogen, and deposition of an extravascular fibrin gel, which provokes ingrowth of vascular endothelial cells (*8*). Currently, the precise role of VPF (VEGF) in the pathogenesis of solid tumor growth is an area of intense investigation. Important to this investigation is the development of a simple, sensitive, and specific assay for VPF, preferably one that can be used for assaying VPF in various biological fluids and tissue homogenates.

VPF was first measured by using the Miles assay (*9*), which measures the extravasation of intravenously injected Evans Blue dye into the dermis of guinea pigs in response to intradermal injections of VPF (*1*). The amount of accumulated dye can be quantified by extraction and measuring the absorbance at 620 nm (*10*). The Miles assay has been used widely to detect VPF in cell-free culture medium of tumor cells as well as in tumor ascites fluid (*1, 2*). However, this assay is not specific because it will detect permeability changes in response to other inflammatory mediators besides VPF. Also, fluids from different animal species cannot be used because foreign proteins commonly elicit nonspecific permeability changes, leading to a false-positive Miles test.

We report here a sensitive and specific immunofluorometric assay for detecting VPF. Antibodies raised against the C-terminus of VPF (C-IgG) were immobilized on microtiter wells and served as the "capture" antibody. Antibodies raised against the amino terminus of VPF (N-IgG) were labeled with Eu^{3+}-chelate and served as the "detector" antibody. In the presence of VPF, a "sandwich" configuration is formed. After the final wash step, bound Eu^{3+} is dissociated in the presence of β-diketone, forming a highly fluorescent chelate that can be read in a time-resolved fluorometer. This approach is termed "dissociation enhanced lanthanide fluoroimmunoassay," or DELFIA (*11–14*). The reagents and equipment required are commercially available.

Materials and Methods

Reagents. DELFIA Eu^{3+}-labeling kits were purchased from Pharmacia-LKB Nuclear, Inc. (Gaithersburg, MD). Each kit contained 0.2 mg of labeling reagent [N^1-(*p*-isothiocyanatobenzyl)-diethylenetriamine-N^1,N^2,N^3,N^3-tetraacetate-Eu^{3+}], a 100 nmol/L Eu^{3+} standard, highly purified bovine serum albumin (BSA; 75 g/L in Tris · HCl, pH 7.8 plus, NaN_3, 0.5 g/L) stabilizer, enhancement solution (per liter, 15 μmol of 2-naphthoyltrifluoroacetone, 50 μmol of tri-*n*-octylphosphine oxide, 100 mmol of acetic acid, 6.8 mmol of potassium hydrogen phthalate, and 1.0 g of Triton X-100 detergent), assay buffer (Tris · HCl solution, pH 7.8, containing BSA, bovine gamma globulin, Tween 40, diethylenetriaminepentaacetic acid, and NaN_3, 0.5 g/L), and wash concentrate solution (25-fold concentration of Tris · HCl/NaCl, pH 7.8, plus Tween 20) (*11–14*). PD-10 columns, Sepharose CL-6B, and Sephadex G-50 were from Pharmacia LKB Biotechnology (Piscataway, NJ). Macrosolute concentrators were from Amicon (Danvers, MA). Maxisorp microtiter plates and strips (96-well) were obtained from Nunc

Department of Pathology, Beth Israel Hospital and Harvard Medical School, and Charles A. Dana Research Institute, 330 Brookline Ave., Boston, MA 02215.

[1] Nonstandard abbreviations: VPF, vascular permeability factor; VEGF, vascular endothelial growth factor; C-IgG, antibody against carboxy terminus of VPF; N-IgG, antibody against amino terminus of VPF; ELISA, enzyme-linked immunosorbent assay; and BSA, bovine serum albumin.

Received July 9, 1991; accepted November 14, 1991.

Inc. (Naperville, IL). Serum-free medium (HL-1) was purchased from Ventrex Labs. Inc. (Portland, ME). Hemoglobin crystals were from Sigma Chemical Co. (St. Louis, MO). The GammaGone IgG removal device was from Genex Corp. (Gaithersburg, MD).

Buffers. The labeling buffer was 50 mmol/L $NaHCO_3$, pH 8.5, containing NaCl, 9 g/L. The elution buffer was 50 mmol/L Tris · HCl, pH 7.8, containing 9 g of NaCl and 0.5 g of NaN_3 per liter. The coating buffer contained phosphate-buffered saline, pH 7.0, and the blocking reagent was 30 g/L hemoglobin solution.

Polyclonal antibodies. Polyclonal antibodies were raised against two synthetic peptides that correspond to the N- and C-termini of guinea pig VPF (designated N-IgG, C-IgG, respectively). In the single letter code, the 25-amino acid sequence of the N-terminus is APMAEGEQKPREVVKFMDVYKRSYC (*15*), and the 20-amino acid sequence of the C-terminus is YKARQLELNERTCRCDKPRR (*4*). The C-terminal peptide was synthesized by Multiple Peptide Systems (San Diego, CA), and both peptides were used for generation of antibodies in rabbits as described (*15*), except that the C-terminal peptide was coupled to keyhole limpet hemocyanin with bis-diazo benzidine. The antibodies (N-IgG and C-IgG) were affinity-purified from rabbit antisera by using the respective peptides coupled to CNBr-Sepharose (Pharmacia LKB). Bound antibodies were eluted from Sepharose–peptide columns with 0.1 mol/L glycine, pH 2.5, and the activity against each peptide was determined by an ELISA (*16*). Briefly, we used a 1 g/L solution of peptide in 10 mmol/L NaCl and 10 mmol/L Tris, pH 8.5, to coat a 96-well microtiter plate. After blocking with normal human serum (100 mL/L) in phosphate-buffered saline, we added the respective anti-peptide IgG solution (200-, 2000-, or 10 000-fold dilution). Antibody binding was detected with a peroxidase-labeled goat anti-rabbit antibody (Kirkegaard and Perry Labs. Inc., Gaithersburg, MD) with 2,2′-azino-di-[3-ethylbenzthiazoline sulfonate] as the enzyme substrate. Color development was determined with a THERMOmax microplate reader at 405 nm (Molecular Devices, Menlo Park, CA). All affinity-purified IgG preparations retained strong anti-peptide activities, even at 10 000-fold dilution. Moreover, both N-IgG and C-IgG (when bound to Protein A–Sepharose) adsorbed VPF efficiently from solution, as determined with the Miles vessel permeability assay (T. Sioussat et al., manuscript in preparation).

Eu^{3+}-labeling of N-IgG. We performed Eu^{3+}-labeling of the affinity-purified N-IgG according to the DELFIA kit protocol with some modifications and pooled and concentrated the affinity-purified antisera to ~0.5 g/L, using an Amicon Macrosolute concentrator. The PD-10 column was pre-equilibrated with 40 mL of labeling buffer, and 2 mL of the antisera (0.5 g/L) was loaded on the column. We rinsed the column with labeling buffer, collected 1.0-mL fractions, and measured the absorbance at 280 nm with a Model U-2000 spectrophotometer (Hitachi Instruments Inc., Danbury, CT 06810). Fractions corresponding to peak absorbance were pooled, and concentrated to ~1 mL, which typically contained 1.5 g/L IgG concentration (we used an absorptivity value of 1.34 for 1 g/L of IgG solution to calculate IgG concentration). We added 1.0 mL of the IgG solution to 0.2 mg of labeling reagent (containing the Eu^{3+}-chelate) and mixed it gently on a rotator for 16 h at room temperature.

Purification of Eu^{3+}-labeled IgG. Sepharose CL-6B was poured into a 1.5 × 30 cm column to a height of 18 cm. Next, we added pre-swollen Sephadex G-50 to a height of 28 cm and equilibrated the column with 180 mL of elution buffer. The Eu^{3+}-labeled IgG reaction mixture was added and fractionated on this column. We rinsed the column with elution buffer, collected 60 1-mL fractions, and measured their absorbance at 280 nm. We diluted a small aliquot of each fraction 10 000-fold with enhancement solution and determined the fluorescence with a 1232 DELFIA time-resolved fluorometer (Pharmacia Diagnostics, Fairfield, NJ), in which a pulsed xenon flash at 340 nm and electronic gating were used to detect fluorescence at 613 nm between 400 and 800 μs after the excitation flash.

Characterization of Eu^{3+}-labeled N-IgG. Fractions corresponding to peak IgG absorbance (280 nm) and fluorescence were pooled (usually, fractions 25 to 33) and the resulting absorbance (280 nm) and fluorescence (10 000-fold dilution) were determined. The yield of Eu^{3+}/IgG was calculated as described in the DELFIA kit protocol (typically, 10 Eu^{3+}/IgG). To increase the stability of the Eu^{3+}-labeled N-IgG, purified BSA was added to a final concentration of 1.0 g/L.

Coating of microtiter strips. We added 50 μL of a 50-fold dilution of C-IgG (stock concentration of 0.64 g/L in phosphate-buffered saline) to each well of the microtiter strips, and incubated the plate overnight at 4 °C on a shaker. Thereafter, we washed the wells six times with DELFIA wash buffer, and blocked by incubation with 30 g/L hemoglobin solution at 20 °C for 2 h with gentle shaking. Plates were washed six times with DELFIA wash buffer before use.

Line 10 cell cultures. Line 10 tumor cells from guinea pig were grown as suspension cultures in serum-free defined medium HL-1 as described previously (*17*). Conditioned line 10 medium, which contains large amounts of VPF, was centrifuged and frozen at −70 °C to serve as calibrators.

Immunoassay procedure. We used freshly coated microtiter strips on the same day to assay VPF. We added 50 μL of various dilutions of line 10 conditioned media (using HL-1 medium as the diluent) to each well and incubated at 20 °C for 2 h with gentle shaking. After six washes with wash buffer, we added 50 μL of Eu^{3+}-labeled N-IgG (diluted appropriately in assay buffer), incubated for another 2 h at 20 °C, and again washed six times. Finally, we dispensed 200 μL of enhancement solution into each well, and after 5 min of gentle shaking, read the absorbance of the plate in the 1232 DELFIA fluorometer.

Miles vessel permeability assay. We assayed the bio-

activity of VPF in the line 10 culture medium preparations, using the Miles assay as described previously (*1*, *17*).

Results

Preparation and purification of Eu^{3+}-labeled N-IgG. Eu^{3+} labeling of affinity-purified antibodies directed against the N-terminal region of VPF was performed as described in *Materials and Methods*. The Sepharose 6B/Sephadex G-50 chromatographic profile in Figure 1 shows two distinct peaks. The first peak (I) corresponds to Eu^{3+}-labeled N-IgG, and the second peak (II) represents unreacted Eu^{3+}-chelate. For this reason, we showed in a separate experiment that >90% of the fluorescence associated with peak I could be removed by an IgG-removing device (Gammagone), indicating that peak I comprised mainly Eu^{3+}-labeled N-IgG. We pooled fractions 25–33, corresponding to Eu^{3+}-labeled N-IgG, and determined the corrected protein concentration to be 115 mg/L (using the absorptivity value of 1.34 mentioned above, with corrections for absorbance of the thiourea bonds of ~0.008 *A* per μmol/L). We calculated the specific activity of the Eu^{3+}-labeled N-IgG to be ~10 Eu^{3+}/IgG, using a 1 nmol/L Eu^{3+} standard as described in the DELFIA kit protocol.

Optimization of VPF immunoassay. To determine the optimal dilution of Eu^{3+}-N-IgG, we studied the effect of various amounts of N-IgG on the VPF binding curve. Microtiter plate wells were immobilized with a constant amount (225 ng/well) of C-IgG. Because pure VPF is not available, we used line 10 tumor cell conditioned medium, which is rich in VPF (*17*), to standardize the assay. We used the same lot of line 10 conditioned medium in all experiments. The concentration of VPF was expressed in arbitrary units, i.e., 100 units is defined as the amount of VPF in our batch of undiluted line 10 tumor cell conditioned medium. We arbitrarily defined "signal" as the fluorescence obtained with undiluted line 10 conditioned medium, and "noise" as the nonspecific fluorescence associated with HL-1 medium (0 unit). Thus, the signal-to-noise ratio is defined as $\text{fluorescence}_{100\ \text{units}}/\text{fluorescence}_{0\ \text{unit}}$. The effect of varying the N-IgG dilution (from five- to 50-fold) is shown in Figure 2*A*. We determined that 50-fold diluted N-IgG gave a maximal signal-to-noise ratio of 83 (Figure 2*B*).

In a separate experiment, we studied the effect of varying the C-IgG dilution, keeping Eu^{3+}-N-IgG constant at 115 ng/well. As shown in Figure 3, we obtained a maximal signal-to-noise ratio of 89 with 30-fold diluted C-IgG (1000 ng/well). However, because of our limited supply of C-IgG, we decided to use a 50-fold dilution of C-IgG (640 ng/well) to coat the microtiter wells; at this concentration, the signal-to-noise ratio was close to maximal at 80. For all subsequent experiments, we coated microtiter plate wells with 50-fold dilution of C-IgG, and bound VPF was detected with 50-fold dilution of Eu^{3+}-N-IgG.

Sensitivity and intra-assay CV of VPF immunoassay. To assess the analytical sensitivity of the VPF assay, we prepared line 10 conditioned medium corresponding to 0.25 unit, 0.50 unit, and 1.00 unit by diluting with HL-1 medium, then assayed these 10 times. HL-1 medium devoid of VPF served as the zero standard. The sensitivity or minimal detectable dose (defined as +2 SD above the zero standard), determined by extrapolation from the standard curve, was ~0.35 unit (Figure 4*A*). The intra-assay CV was <20% at 0.50 unit (Figure 4*B*).

Specificity of VPF immunoassay. Because the format of this assay depended on C-IgG as the capture antibody and Eu^{3+}-N-IgG as the detector antibody, we used peptides corresponding to the N- and C-termini of VPF to demonstrate the assay specificity. As shown in Figure 5, inclusion of C-VPF, N-VPF, or both peptides in the assay inhibited the binding of VPF in line 10 medium by ~80%. In addition, when VPF was selectively removed from line 10 conditioned medium (by unlabeled N-IgG followed by incubation with Protein A–Sepharose and

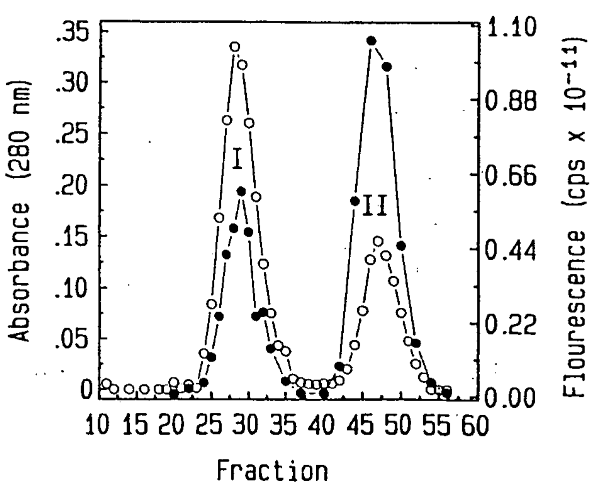

Fig. 1. Chromatographic profile of Eu^{3+}-labeled N-IgG

Absorbance at 280 nm (○) and fluorescence (●) were determined on fractions collected from a Sepharose 6B/Sephadex G-50 column. Each fraction was diluted 10 000-fold before fluorescence measurements, and results were expressed as total counts/s. Peak I denotes the Eu^{3+}-labeled N-IgG and peak II represents the free Eu^{3+}-chelate. Typical labeling yield is ~10 Eu^{3+} per IgG molecule

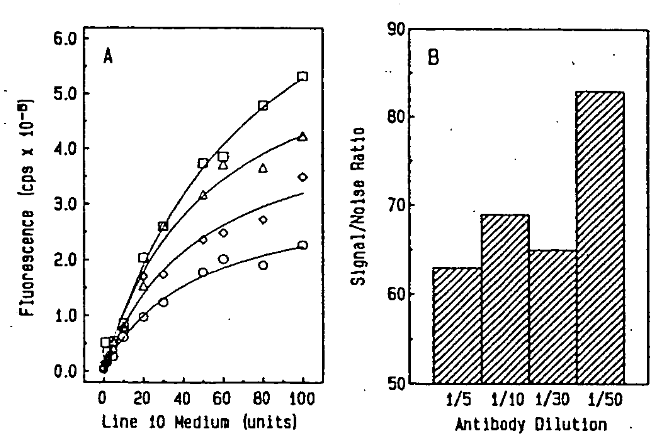

Fig. 2. Optimization of Eu^{3+}-labeled N-IgG

Eu^{3+}-labeled N-IgG was used at various titers (at constant C-IgG) to determine the optimal titer. Signal-to-noise ratio is arbitrarily defined as $\text{fluorescence}_{(100\ \text{units})}/\text{fluorescence}_{(0\ \text{unit})}$. *A:* calibration curves at 50-fold (○), 30-fold (◇), 10-fold (△), and fivefold (□) dilution of N-IgG. *B:* effect of antibody dilutions on the signal-to-noise ratio

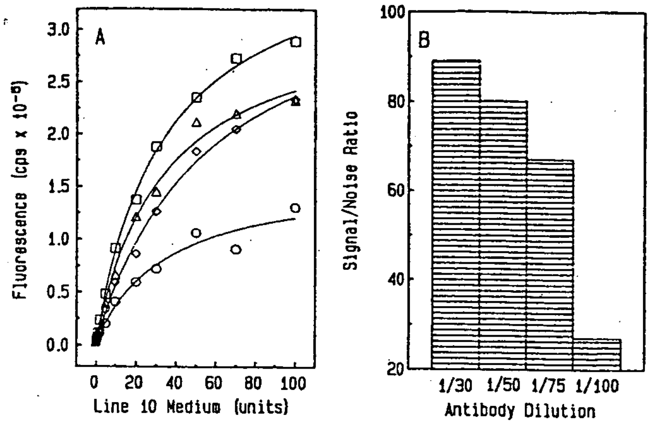

Fig. 3. Optimization of C-IgG

A: C-IgG was coated at 100-fold (○), 75-fold (◇), 50-fold (△), and 30-fold (□) dilution, at constant Eu^{3+}-labeled N-IgG concentration to determine the optimal concentration for the assay. *B:* effect of antibody dilutions on the signal-to-noise ratio

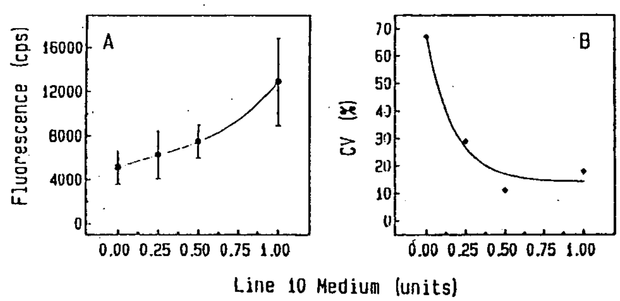

Fig. 4. Sensitivity and intra-assay CV of VPF immunofluorometric assay

Each point in *A* represents the mean of 10 determinations, and the *error bar* represents ±2 SD. *B:* intra-assay CV of VPF as a function of VPF dose

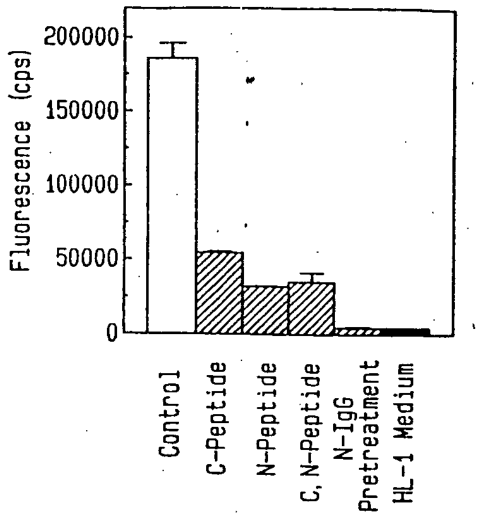

Fig. 5. Specificity of VPF immunofluorometric assay

Line 10 medium was used as the positive control and HL-1 medium was the negative control. C-peptide of VPF (final concentration 80 mg/L) was included during the first incubation with the sample. The N-peptide (final concentration 80 mg/L) was pre-incubated with the Eu^{3+}-labeled N-IgG and added during the second incubation. N-IgG pretreatment refers to line 10 medium that has been pre-extracted for VPF by using the N-IgG. *Error bars* denote ± SEM

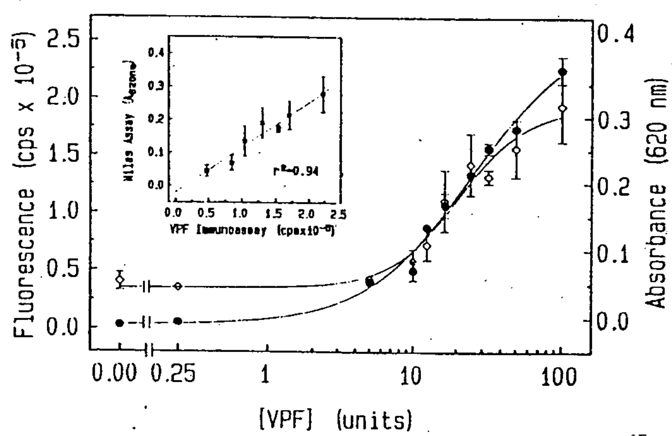

Fig. 6. Correlation of VPF immunoassay and Miles assay

Line 10 conditioned media at various concentrations were prepared for Miles assay (◇) and VPF fluoroimmunoassay (●) by diluting with HL-1 medium. Each point and its respective *error bar* represent the mean ± SEM of duplicate determinations. For the Miles assay, two animals were used to generate each point. *Inset:* correlation of the Miles and the VPF immunoassay at concentrations >10 units

centrifugation), little fluorescent signal remained in the supernatant solution. In addition, when guinea pig serum containing platelet-derived growth factor and other growth factors was assayed, no VPF was detected (data not shown).

Correlation of VPF immunoassay with Miles permeability assay. We prepared and tested various concentrations of VPF from line 10 medium in both the Miles permeability assay and the VPF immunofluorometric assay. For the Miles assay, the amount of local dye development due to VPF permeability-enhancing activity was quantified by absorbance at 620 nm as described earlier (*17*). The VPF immunofluorometric assay was more sensitive than the Miles permeability assay; at a dose of 0.35 unit of VPF, the immunoassay gave values that were markedly different from zero (Figure 4*A*). In contrast, the sensitivity of the Miles permeability assay extended to only ~10 units (Figure 6). There was an excellent linear correlation (r^2 = 0.94) between the Miles permeability assay and the VPF immunoassay at VPF concentrations >10 units (Figure 6, inset).

Confirmed by immuno assay

Discussion

Immunofluorometric assays involving Eu^{3+}-chelate as the label are characterized by low-end sensitivity and wide dynamic range. The principles underlying these advantages have been reviewed recently (*18*). The large Stokes shift of Eu^{3+}-chelate and the time-resolved nature of the fluorometric measurements yield a high signal-to-noise ratio. Because of the longer decay time of the Eu^{3+}-chelate (>500 μs), readings can be determined between 400 and 800 μs to decrease nonspecific fluorescence, which typically has shorter decay times (~0.01 μs). This feature minimizes the endogenous nonspecific fluorescence of various biological specimens, making it especially attractive as a method to measure VPF in both tumor cell culture medium and in biological fluids.

We prepared affinity-purified N- and C-termini antibodies to guinea pig VPF and used the DELFIA approach

to develop a sensitive and specific immunofluorometric assay of VPF. We also demonstrated that our fluoroimmunoassay provides a quantitative measure of VPF in line 10 tumor cell culture medium. Although absolutely pure VPF is unavailable for standardization, we showed good correlation between the VPF immunoassay and the Miles bioassay with line 10 medium, thus confirming that the immunoassay is measuring bioactive VPF. We are confident that the immunoassay is measuring VPF in the physiologically relevant range because the dynamic range correlates well with the dynamic range of the Miles bioassay.

The VPF immunofluorometric assay has a minimal detection limit of 0.35 unit, and is ~30 times more sensitive than the Miles permeability assay. In addition, the immunoassay is much more precise and simpler to perform, is readily automatable, and can measure several specimens rapidly and inexpensively. In a separate study, we used the VPF immunoassay to measure VPF in ascites fluid, serum, and urine to study the potential role of VPF in tumor-elicited ascites fluid accumulation (*19*). We have also currently adapted the VPF immunofluorometric assay to measure VPF in human fluids to study its potential diagnostic utility in the pathogenesis of tumor metastases and the often accompanying fluid accumulation found in pleural and peritoneal cavities (*19*).

We thank Lisa Freter, Cheryl Hart, and the staff of the Clinical Chemistry Laboratory for their technical assistance. We also thank Dr. Harold F. Dvorak for his critical review of this work. This work was supported by USPHS NIH grant nos. CA-28471 and CA-50453 (to H.F.D.), and by grant no. CA-43967 (to D.R.S.) from the National Cancer Institute.

References

1. Senger DR, Galli SJ, Dvorak AM, Perruzzi CA, Harvey VS, Dvorak HF. Tumor cells secrete a vascular permeability factor that promotes accumulation of ascites fluid. Science 1983;219:983–5.
2. Senger DR, Perruzzi CA, Feder J, Dvorak HF. A highly conserved vascular permeability factor secreted by a variety of human and rodent tumor cell lines. Cancer Res 1986;46:5629–32.
3. Leung DW, Cachianes G, Kuang WJ, Goeddel DV, Ferrara N. Vascular endothelial growth factor is a secreted angiogenic mitogen. Science 1989;246:1306–9.
4. Keck PJ, Hauser SD, Krivi G, et al. Vascular permeability factor, an endothelial cell mitogen related to PDGF. Science 1989;246:1309–12.
5. Conn G, Bayne ML, Soderman DD, et al. Amino acid and cDNA sequences of a vascular endothelial cell mitogen that is homologous to platelet-derived growth factor. Proc Natl Acad Sci USA 1990;87:2628–32.
6. Connolly DT, Olander JV, Heuvelman D, et al. Human vascular permeability factor: isolation from U937 cell. J Biol Chem 1989;264:2017–24.
7. Connolly DT, Heuvelman DM, Nelson R, et al. Tumor vascular permeability factor stimulates endothelial growth and angiogenesis. J Clin Invest 1989;84:1470–8.
8. Dvorak HF, Harvey VS, Estrella P, et al. Fibrin containing gels induce angiogenesis. Implications for tumor stroma generation and wound healing. Lab Invest 1987;57:673–86.
9. Miles AA, Miles EM. Vascular reactions to histamine, histamine-liberator, and leukotaxine in the skin of guinea pigs. J Physiol (London) 1952;118:228–57.
10. Udaka K, Takeuchi Y, Movat HZ. Simple method for quantitation of enhanced vascular permeability. Proc Soc Exp Biol Med 1970;133:1384–7.
11. Soini E, Kojola H. Time-resolved fluorometer for lanthanide chelates—a new generation of nonisotopic immunoassays. Clin Chem 1983;29:65–8.
12. Hemmilä I, Dakubu S, Mukkala VM, Siitari H, Lövgren T. Europium as a label in time-resolved immunofluorometric assays. Anal Biochem 1984;137:335–43.
13. Hemmilä I. Fluoroimmunoassays and immunofluorometric assays [Review]. Clin Chem 1985;31:359–70.
14. Soini E, Lövgren T. Time-resolved fluorescence of lanthanide probes and applications in biotechnology. Crit Rev Anal Chem 1987;18:105–54.
15. Senger DR, Connolly DT, Van De Water L, Feder J, Dvorak HF. Purification and NH_2-terminal amino acid sequence of guinea pig tumor-secreted vascular permeability factor. Cancer Res 1990;50:1774–8.
16. Engvall E. Enzyme immunoassay ELISA and EMIT. Methods Enzymol 1980;70:419–39.
17. Yeo TK, Senger DR, Dvorak HF, Freter L, Yeo KT. Glycosylation is required for efficient transport but not for permeability-enhancing activity of vascular permeability factor (vascular endothelial growth factor). Biochem Biophys Res Commun 1991;179:1568–75.
18. Diamandis EP, Christopoulos TK. Europium chelate labels in time-resolved fluorescence immunoassays and DNA hybridization assays [Review]. Anal Chem 1990;62:1149A–57A.
19 Yeo KT, Wang H, Nagy JA, et al. Vascular permeability factor levels in line 1 and line 10 ascites tumors and human fluids [Abstract]. J Cell Biol 1991;115:421A.

Exhibit